Development of an oleophobic woven fabric microfiltration membrane for decentralized sanitation applications

by

Suzanne Akoth Yala

Thesis presented in partial fulfilment
of the requirements for the Degree

of

MASTER OF ENGINEERING
(CHEMICAL ENGINEERING)

in the Faculty of Engineering
at Stellenbosch University

Supervisor
Professor V.L Pillay

December 2020

Declaration

By submitting this thesis electronically, I declare that the entirety of the work contained therein is my own, original work, that I am the sole author thereof (save to the extent explicitly otherwise stated), that reproduction and publication thereof by Stellenbosch University will not infringe any third party rights, and that I have not previously in its entirety or in part submitted it for obtaining any qualification.

Date: December 2020

Abstract

Developing countries are faced with the major challenge of providing safe and adequate sanitation to their citizens. Decentralized sanitation systems have a great potential to address this challenge. The woven fabric immersed membrane bioreactor (WF-IMBR) technology is a promising option for such systems. This technology employs robust woven fabric microfilter (WFMF), developed in South Africa. However, organic fouling poses a major challenge to its application. Fine organics tend to penetrate the membrane, reduce productivity, and make cleaning difficult. Hence, the overall aim of this study was to develop and evaluate an oleophobic WFMF (OWFMF) membrane, which could repel organics.

First, the fouling characteristics of the WFMF membrane were investigated by performing filtration and membrane cleaning experiments on a laboratory filtration unit, using 0.5 g/L of yeast suspensions as synthetic wastewater. From the flux and pressure drop profiles, fouling resistance profiles were generated. The fouling resistance profiles showed that fouling occurred in two stages, namely rapid irreversible fouling followed by progressive cake layer formation. The irreversible fouling occurred within the first five to ten minutes of filtration and could not be removed by water scouring, air scouring or backwashing. The cake layer could easily be removed by these methods. Photomicrographs of the cleaned and fouled membranes revealed that the irreversible foulants settled at the intersections of groups of fibres, where water scouring, and air scouring were unable to reach.

The second phase of the study focused on the development of an OWFMF membrane. The process involved chemically bonding fluorocarbons onto a standard WFMF membrane through a pad-dry-cure process. The process was optimized using a 3^3 full factorial design. The factors considered include fluorocarbon concentration (40 – 80 g/L), padding pressure (0.5 – 3.5 bar) and fabric speed (1 – 3.5 m/min).The optimum conditions were identified as: 80 g/L fluorocarbon concentration; 2 bar padding pressure; and 1 m/min fabric speed at 20 g/L wetting agent concentration, 180˚ curing temperature and 90 seconds curing time. Unlike the standard WFMF which was non-oleophobic, i.e. oil droplets easily penetrated the fabric, the developed OWFMF membrane showed a high oleophobicity with an oil contact angle of 123.5˚.

In the third stage, the OWFMF and the standard WFMF membranes were then compared in terms of pure water fluxes, permeate quality, fouling characteristics and ease of cleaning. This was done on yeast suspensions. Compared with the standard WFMF membrane, the OWFMF membrane

showed a 60% reduction of the irreversible fouling resistance after five cycles of filtration and cleaning. This indicated that the oleophobic surface was very effective at repelling most of the organics; which made the cleaning of the membrane easier. Furthermore, the OWFMF membrane had a slightly enhanced flux when compared to the standard WFMF, and yet still achieved a permeate turbidity of below 1 NTU. In terms of stability, the oleophobic surface was fairly stable and only initial minimal erosion was observed.

With the improved fouling resistance and ease of cleaning, the OWFMF membrane has a great potential for decentralized sanitation applications in developing countries. However, further performance evaluation of the long-term stability and performance on real wastewaters will be necessary.

Opsomming

Ontwikkelende lande staar groot uitdagings in die gesig om veilige en voldoende sanitasie aan hul burgers te verskaf. Gedesentraliseerde sanitasiestelsels het groot potensiaal om hierdie uitdaging aan te spreek. Die geweefde materiaal onderdompelde membraan bioreaktor (WF-IMBR) is ’n belowende opsie vir sulke stelsels. Hierdie tegnologie gebruik ’n robuuste materiaal mikrofilter (WFMF), ontwikkel in Suid-Afrika. Organiese aanpakking is egter ’n groot uitdaging vir die toepassing hiervan. Fyn organiese materiaal neig om deur die materiaal te penetreer, wat produktiwiteit verminder, en die skoonmaak bemoeilik. Daarom was die algehele doel van hierdie studie om ’n oleofobiese WFMF (OWFMF)-membraan te ontwikkel en te evalueer, wat organiese materiaal kan afweer.

Eerstens is die aanpakkingseienskappe van die WFMF-membraan ondersoek deur filtrasie en skoonmaak van die membraan op ’n laboratorium filtrasie-eenheid uit te voer, deur 0.5 g/L gissuspensie as sintetiese afvalwater te gebruik. Vanaf die fluks en drukvalprofiele, is aanpakkingsweerstandprofiele gegenereer. Die aanpakkingsweerstandprofiele het gewys dat aanpakking in twee fases voorkom, naamlik vlugtige onomkeerbare aanpakking gevolg deur progressiewe koeklaagformasie. Die onomkeerbare aanpakking kom voor binne die eerste vyf tot tien minute van filtrasie en kan nie deur waterskuring, lugskuring of terugspoeling verwyder word nie. Die koeklaag kon maklik deur hierdie metodes verwyder word. Fotomikrograwe van die skoongemaakte en aangepakte membrane het getoon dat die onomkeerbare bevuilers afgesak het by die interseksies van groepe van vesels waar waterskuring en lugskuring dit nie kon bereik nie.

Die tweede fase van die studie het op die ontwikkeling van ’n OWFMF-membraan gefokus. Die proses behels die chemiese verbinding van fluoorkoolstowwe op ’n standaard WFMF-membraan deur ’n belaai-droog-nabehandelingsproses. Die proses is geoptimeer deur ’n 3^3 vol faktoriaalontwerp te gebruik. Die faktore oorweeg het fluoorkoolstofkonsentrasie (40 – 80 g/L), drukkingsdruk (0.5 – 3.5 bar) en materiaalspoed (1 – 3.5 m/min) ingesluit. Die optimale kondisies is geïdentifiseer as: 80 g/l van fluoorkoolstofkonsentrasie; 2 bar drukkingsdruk; en 1 m/min materiaalspoed teen 20 g/L benattingsmiddelkonsentrasie, 180 °C nabehandelingstemperatuur en 90 sekondes nabehandelingstyd. Anders as die standaard WFMF wat nie-oleofobies is, i.e. oliedrupples penetreer maklik die materiaal, het die OWFMF-membraan ’n hoë oleofobisiteit getoon met ’n oliekontakhoek van 123.5°.

In die derde fase is die OWFMF- en die standaard WFMF-membrane vergelyk in terme van suiwer water flukse, deurlaatkwaliteit, aanpakkingskarakteristieke en skoonmaakgemak. Dit is gedoen op gissuspensie. In vergelyking met die standaard WFMF-membraan, het die OWFMF-membraan ’n 60% reduksie van die onomkeerbare aanpakkingsweerstand getoon na vyf siklusse van filtrasie en skoonmaak. Dit het aangedui dat die oleofobiese oppervlak baie effektief was met die afwering van meeste van die organiese materiaal; wat die skoonmaak van die membraan vergemaklik. Verder het die OWFMF-membraan ’n effense vergrote fluks gehad in vergelyking met die standaard WFMF, en het tog steeds ’n deurlaattroebelheid van onder 1 NTU bereik. In terme van stabiliteit, was die oleofobiese oppervlak redelik stabiel en is slegs aanvanklike minimale erosie waargeneem.

Met die verbeterde aanpakkingsweerstand en skoonmaakgemak, het die OWFMF-membraan groot potensiaal vir gedesentraliseerde sanitasietoepassing in ontwikkelende lande. Verdere evaluasie op langtermyn stabiliteit en werkverrigting op regte afvalwater is egter nodig.

Dedication

To my mum, who departed so soon.

Forever in my heart.

Acknowledgements

This work was performed under Water Research Commission Project No 2840, 'The development of an oleophobic (low-fouling) membrane for decentralised sanitation applications'. Additional sponsorship was received from Sasol.

I would like to use this opportunity to thank everybody who has contributed to the successful completion of this project.

First of all, I would like to express my profound gratitude to my supervisor Professor VL Pillay for his support, advise and mentorship which has contributed immensely to my thesis and overall research experience. Your confidence in me gave me the strength to forge ahead even when things seemed impossible. From you, I have gained a lot of knowledge not only in the field of membranes, but in general research work. Thank you.

I am also grateful to Mrs Adine Gericke from Polymer department for allowing me to use the various equipment in her laboratory, including the padding machine. Without the padding equipment, I would not have been able to develop the oleophobic WFMF membranes.

A special thanks goes to Dick Kongolo for his practical advice in the textile field. Your pieces of advice contributed greatly to the development of the oleophobic WFMF membrane.

My sincere appreciation to Rudolf Chemicals Ltd (South Africa), who freely provided the materials used in preparing the fluorocarbon liquor, and also for their advice on different fabric coating emulsions.

I also acknowledge the help provided by the technical staff, Mr Jos Weerdenburg and Mr Anton Cordier, in constructing some of the set-ups used in this project.

Special regards go to my dad and my siblings for their unfailing support and encouragement throughout my research work. Your support has motivated me to always aim for the best in whatever I do. I love you.

Most of all, I would like to thank God for this far He has brought me. You are always with me in both my happy and lowest moments. Praise and honour to You.

Table of content

List of figures

List of tables

Nomenclature

Symbols

A	Effective membrane area	(m^2)
C_f	Feed concentration	(g/L)
C_p	Permeate concentration	(g/L)
J	Permeate flux	(L/m^2h/ LMH)
J_0	Pure water flux	(L/m^2h or LMH)
l_e	Length of the stretched membrane	(cm)
l_o	Length of the original membrane	(cm)
ΔP	Pressure difference	(Pa)
P_f	Pressure of the feed	(Pa)
P_p	Pressure on the permeate side	(Pa)
P_r	Pressure of the retentate	(Pa)
Q	Volumetric flowrate	(L/h)
R	Rejection	(%)
R_f	Resistance after physical cleaning	(m^{-1})
R_{ir}	Irreversible fouling resistance	(m^{-1})
R_m	Intrinsic membrane resistance	(m^{-1})
R_r	Reversible fouling resistance	(m^{-1})
R_t	Resistance during/at the end of filtration	(m^{-1})
R_{tf}	Total fouling resistance	(m^{-1})
Tg	Glass transition temperature	(˚)
Δt	Time taken	(h)

μ	Viscosity	(Pa.s)
v	Permeate volume	(L)
wpu	Wet pickup of a fabric	(%)

Acronyms

BSA	Bovine serum albumin
CEB	Chemically enhanced backwash
CIP	Clean-in-place
COD	Chemical oxygen demand
COP	Clean-out-of-place
CW	Chemical wash
EMBR	External membrane bioreactor
EPS	Extracellular polysaccharide substances
FC	Fluorocarbon
FAS	Fluoroalkyl-functional siloxane
HA	Humic acid
HRT	Hydraulic retention time
IMBR	Immersed membrane bioreactor
LMH	Litre/metre^2-hour
MBR	Membrane bioreactor
MLSS	Mixed liquor suspended solids
NTU	Nephelometric turbidity units
OCA	Oil contact angle
OWFMF	Oleophobic woven fabric microfilter
PDC	Pad-dry-cure
PES	Polyethersulfone
PE	Polyethylene

PET	Polyethylene terephthalate
PFTE	Polytetrafluoroethylene
PVC	Polyvinyl chloride
PVDF	Poly(vinylidene) fluoride
PWF	Pure water flux
RMS	Root mean square
SEM	Scanning electron microscope
SMP	Soluble microbial products
SRT	Solid retention time
TMP	Transmembrane pressure
TSS	Total suspended solids
WCA	Water contact angle
WF-IMBR	Woven fabric-immersed membrane bioreactor
WF-IMF	Woven fabric immersed membrane filtration
WFMF	Woven fabric microfilter

Chapter 1.
Introduction

Overview

Background; Objectives; Approach; Brief thesis outline.

1.1. Background

South Africa, as well as most developing economies internationally, is faced with a major challenge of providing safe and adequate sanitation to all its citizens. Urban and peri-urban areas are the most affected (Woltersdorf *et al*., 2017). A report released by the World Health Organization reveals that 2.4 billion people in developing countries lack adequate sanitation, with 756 million being in urban areas alone (WHO & UN Habitat, 2016). This sanitation problem is worsened by the influx of people into peri-urban and urban areas in search of a better living, therefore putting pressure on the available conventional centralized sanitation systems. For these systems to cope with the ever-increasing population in the urban areas, they will have to be expanded. This will require many years of planning and construction before implementation (Larsen *et al.*, 2013). In this instance, therefore, the conventional centralized sanitation systems are not feasible.

An alternative to centralized systems are decentralized sanitation systems. These systems are flexible and less costly in terms of construction. They can be installed on a needs basis and are usually on a small-scale, therefore avoiding the extensive years of planning and costly implementation of centralized systems (Massoud *et al.*, 2008). Thus, decentralized sanitation systems would contribute greatly in addressing the sanitation challenge in the urban and peri-urban areas in developing countries.

Globally, there has been a major shift towards combining biological processes with membrane separation processes to enhance wastewater treatment processes (Teow *et al*., 2018). The most popular example is the Immersed Membrane Bioreactor (IMBR). An IMBR system integrates a membrane in a bioreactor to provide a single unit for wastewater filtration processes (Singhania *et al*., 2012). This gives it an inherent compact design, and thus an attractive option for decentralized sanitation systems (Cecconet *et al.*, 2019). The IMBR system does not only have a small footprint, but also produces a high-quality effluent (Hoinkis *et al.*, 2012; Judd, 2011; Xiao *et al.*, 2019). Furthermore, it can also handle shock loads and high variation in organic loading while still producing an effluent of superior quality.

However, the major obstacles to the implementation of IMBR technology in developing countries are the high costs and lack of robustness of current commercially available membranes, as well as membrane fouling (Chollom *et al.*, 2017; Guo *et al.*, 2012). Commercial membranes are expensive and potentially vulnerable since they cannot handle mechanical abrasion and can experience irreversible damage if allowed to dry out (Chollom *et al.*, 2017). This necessitates frequent replacing of membranes, making IMBR technology potentially expensive. In addition, most commercial membranes are affected by fouling, which adversely affects their productivity and increases the operational cost of the system (Lin *et al.*, 2014). The increase in the operational cost is usually as a result of the defouling processes that are incorporated in the system. It is also caused by the constant replacing of membranes damaged due to frequent chemical cleaning. All these challenges limit the implementation of the IMBR technology in numerous countries. As a result, there is a need to develop a more robust and inexpensive membrane that can overcome these problems and therefore accelerate IMBR implementation in developing countries.

In recent years, a novel microfiltration technology was developed in South Africa. Termed the woven fibre microfilter (WFMF), the technology is based on a very robust woven polyester filtration fabric. Previous studies have shown that the WFMF membrane is more robust than most commercial membranes being employed currently. The advantage of this membrane is that it can be left out to dry, as well as withstand mechanical abrasion without getting destroyed (Chollom *et al.*, 2017). In addition, the membrane is produced locally thus making it relatively inexpensive (Pillay, 2009). Hence, the integration of this membrane in an IMBR system could result in a system that is sustainable and relatively inexpensive. This could accelerate the implementation of IMBR technology in developing countries such as South Africa to provide decentralized sanitation services.

Previously, investigations were done to explore the use of the woven fabric membrane in a membrane bioreactor aimed at decentralized sanitation. The results were promising. The system produced a very good product quality, comparable with that of current commercially available IMBRs, and operated at a relatively low energy. It was reported that the system successfully achieved a permeate turbidity of below 1 Nephelometric Turbidity Unit (NTU) and a 95 % Chemical Oxygen Demand (COD) removal (Pillay *et al.*, 2016). Hence, the incorporation of the WFMF membrane in an IMBR system is a potential technology for sanitation applications.

However, just as in commercial IMBR systems, membrane fouling was a major operational challenge. Pillay *et al.* reported that membrane fouling occurred even when the membranes were

operated at 'subcritical flux' conditions, an operating regime where theoretically fouling should not occur (Pillay *et al.*, 2016). A common way of minimizing fouling in IMBRs, is to continuously air-scour the membranes. However, this strategy also did not assist in attenuating fouling in the WFMF system. Indeed, it appeared that air scouring caused the rate of fouling to increase, contradicting all previous studies on air scouring in IMBRs (Melidis *et al*., 2016; Meng *et al*., 2008; Nywening & Zhou, 2009; Tian *et al.*, 2010). Pillay *et al* also reported that seemingly a gel-like layer formed on the membrane, which could not be removed by air-scouring. This gel fouling layer resulted in a significant decrease in permeate flux, as well as a rapid increase in pressure drop, within a short time after start-up.

The investigation of Pillay *et al.* postulated that:- the mechanism of fouling in WFMF systems may be different from that of commercial microfiltration membranes; that fouling was possibly controlled by the irreversible penetration of fine organics into the membrane structure; and hence that an oleophobic WFMF membrane, that is able to repel organics, would probably exhibit superior resistance to fouling than the standard WFMF membrane.

This project is a contribution towards the further development of the WFMF technology, and it addresses three issues:- an investigation into the fouling characteristics of WFMF membranes; the development of a more oleophobic WFMF membrane; and the comparative evaluation between the oleophobic membrane to be developed and the standard WFMF membrane.

1.2. Objectives

The main aim of this study was to develop a woven fabric microfiltration (WFMF) membrane with an improved fouling resistance. To address this aim, three objectives were formulated:

i) **To investigate the fouling characteristics of woven fabric microfiltration (WFMF) membranes:** This objective focused on:- investigating the fouling characteristics of WFMF membranes, comparing it to the fouling characteristics of standard membranes, and establishing whether they share similar characteristics.

ii) **To develop and characterize oleophobic woven fabric microfiltration (OWFMF) membranes:** It involved:- developing oleophobic WFMF membranes that are able to repel organics, characterizing them in terms of oleophobicity and morphology, and finally comparing their characteristics to that of standard WFMF membranes.

iii) **To evaluate the performance of the oleophobic woven fabric membranes in comparison to the standard WFMF membranes:**

In this objective, the focus was on:- evaluating the performance of OWFMF membranes relative to the standard WFMF membranes in treating feeds that contain organics in terms of fluxes, resultant membrane product quality, fouling resistance characteristics and ease of cleaning the fouled membranes; evaluating the stability of the oleophobic characteristics on the developed membranes.

1.3. Approach

The approach employed during this study has been briefly described as per each objective;

1.3.1. Establishing the fouling characteristics of WFMF membranes

The fouling characteristics of the WFMF membranes was evaluated on a laboratory scale using a woven fabric immersed membrane filtration (WF-IMF) rig. This was achieved by performing two major investigations, namely: the evaluation of the effectiveness of air scouring, backwash and water scouring in the restoration of WFMF membranes; and the establishment of the nature of fouling of the WFMF membranes.

The effectiveness of air scouring, backwash and water scouring was evaluated in three main stages. First, pure water flux (PWF) experiments were performed using the WF-IMF rig. This involved filtering distilled water at increasing pump settings of between 100 and 300 rev/min at intervals of 50 rev/min. The PWF experiments were followed by a 1-hour filtration of synthetic wastewater. Thereafter, the membranes were cleaned using one of the aforementioned cleaning methods in separate runs. During the cleaning process, the effect of the different air scouring, and backwash parameters on minimizing fouling on WFMF membrane were evaluated. The parameters included: air scouring flowrate, air scouring duration, air scouring frequency, and backwash heights. Finally, the PWF experiments were repeated with the cleaned membranes. The fluxes and the drop in pressure across the membranes (ΔP) were measured and recorded during the PWF experiments and the filtration process. These results were used to generate pure water flux curves and resistance profiles; which were used to evaluate the effectiveness of air scouring, backwash, and water scouring on minimizing fouling on WFMF membranes.

The next investigation involved establishing the nature of fouling of the WFMF membranes. This involved: pure water flux experiments; followed by the filtration of synthetic wastewater for 10, 20,

30, 60 and 90 minutes in separate runs; the membranes were then water scoured; and finally, the PWF experiments repeated with the water scoured membranes. The fluxes and ΔPs measured during the PWF and filtration experiments were then used to calculate resistances of the initial, fouled, and water scoured membranes. From these calculated data, resistance profiles were generated to indicate the nature of fouling of the WFMF membranes.

In addition to the resistance profiles, membrane photomicrographs were also used to establish the nature of fouling on WFMF membranes. Images of membranes before and after the filtration process, and also after the water scouring process, were taken under a stereo microscope. These images provided additional information on the mechanism of fouling that occurs on the WFMF membranes during filtration processes.

1.3.2. Development and characterization of the oleophobic WFMF membranes

To develop an oleophobic membrane, the standard WFMF membrane was impregnated with fluorocarbon in a process that is known as padding process. This is a process used in the textile industry to chemically bond surface coatings onto fabrics. The fabrics were then dried and cured in an oven. The drying process was to remove water from the fabric, while the curing process was to initiate the chemical reaction between the fluorocarbon and the fabric. Thereafter, the oleophobicity of the membranes was characterized through the measurement of their oil contact angles. During the fluorocarbon application process, various padding process parameters including fluorocarbon concentration, padding pressure and fabric speed were optimized using a 3-factor, 3-level full factorial design. Optimum values of other variables such as wetting agent concentration, curing temperature and curing time were determined through screening experiments. The membrane's oil contact angle acted as the response variable for the optimization process. After the fluorocarbon application process, the response surface methodology (RSM) was conducted for the experimental results using the *Statistica* software to obtain surface and contour plots. Additionally, a desirability analysis of the experimental data was also done. Optimum conditions for developing an oleophobic WFMF membrane were then identified from the surface plots and the desirability analysis plots. A regression model was also generated from the analysis of the results. This model is useful in predicting future response variables in the development the OWFMF membrane through padding process. Using the optimum conditions, more OWFMF membranes were produced for the performance evaluation.

The OWFMF membranes that were developed at the optimum conditions were then characterized. First, the wetting properties of the membrane were analysed through the measurement of both the oil and water contact angles. In addition, the surface structure of the developed membranes was also evaluated using a Scanning Electron Microscope (SEM). All these results were then compared to that of the standard WFMF membrane.

1.3.3. Performance evaluation of the OWFMF membranes

The performance of the OWFMF membranes was evaluated using the laboratory WF-IMF rig. Filtration on organic-containing feed was carried out, and permeate turbidity, volumetric flow rate and ΔP were measured at different time intervals. The results were then used to generate time profiles of permeate turbidities, fluxes, ΔPs, and resistances. The profiles of the OWFMF membranes were then compared to those of the standard WFMF membranes. These plots were used to illustrate the performance of the OWFMF membranes relative to that of the standard WFMF membranes.

In addition, repeated fouling and cleaning runs were also carried out to evaluate the antifouling property and the ease of cleaning the OWFMF membranes. One complete fouling and cleaning run was referred to as a cycle. Each cycle involved a fresh yeast filtration process using the WF-IMF rig, followed by a simple water scouring process. Both the standard WFMF and the OWFMF membranes underwent five fouling and cleaning cycle. During the experiments, the flux and the ΔP were measured and recorded, and then used in generating resistance profiles and graphs for each cycle. These plots aided in analysing the effectiveness of the oleophobic surface in resisting fouling and also the ease of cleaning the OWFMF membranes compared to the standard WFMF membranes.

Lastly, the performance of the OWFMF membranes was evaluated in terms of the stability of the oleophobic characteristic. This was done through the measurement of the oil contact angles of the OWFMF membranes before and after a certain number of filtration and cleaning cycles. Different membrane samples were used for different number of filtration and cleaning cycles. Their oil contact angle before and after the cycles were plotted on a graph and compared. From these results, the change in the oil contact angle with increasing filtration and cleaning cycles was analysed.

1.4. Brief thesis outline

This thesis comprises six chapters. A brief overview of each chapter is highlighted below;

Chapter 1 provides the Background to the study, states the Objectives and the Approach adopted, and indicates the Structure of this thesis.

Chapter 2 presents a brief overview of Membrane technology, along with a short introduction of the WFMF membrane technology. Thereafter, a detailed outline of Membrane fouling together with its mitigation techniques are discussed. This is followed by an Overview of Immersed membrane bioreactors. Afterwards, the Woven Fabric Immersed MBR technology is introduced, where its performance, past investigations, and operational challenges such as fouling, are presented. This chapter concludes by outlining Membrane surface modification as a technique for mitigating membrane fouling, with an emphasis on the fluorocarbon application using padding process, as an option of modifying WFMF membranes.

In Chapter 3, the focus is on establishing the nature of fouling in WFMF membranes. It outlines the experimental steps taken to meet this objective and the outcome of the investigation. Finally, the findings of the investigation are discussed, and conclusions given.

Chapter 4 is based on the development and characterization of the OWFMF membrane. It focuses on the second objective. The development process of the OWFMF membrane on a laboratory scale, the optimization of the parameters involved, and the characterization of the developed membrane is outlined.

In Chapter 5, the focus shifts to evaluating the performance of the developed membrane, in comparison to the standard WFMF. Firstly, the methodology applied in evaluating both the standard WFMF and the OWFMF membrane is outlined. This is followed by a presentation of the results, a comprehensive discussion and finally, a conclusion is made.

Chapter 6 outlines the conclusions drawn from the whole research project, and further gives recommendations for future studies.

Chapter 2.
Literature review

Overview

Overview of membrane technology; Membrane fouling; Immersed membrane bioreactor; Woven-fabric immersed membrane bioreactors; Membrane surface modification.

2.1. Overview of membrane technology

2.1.1. Introduction

A membrane is a material that allows some physical or chemical components to pass through more readily than others, because of its semi-permeable properties (Judd, 2011). Membrane technology can be defined as the process of separating entities based on different abilities to pass through a selective membrane.

Membrane technology is one of the most promising separation technologies in this century (Gao, 2016). It is an emerging technology, and because of its multi-disciplinary character, it can be used in many separation processes. As an established water treatment process, membrane processes have attracted a lot of interest because they reduce the number of unit operations, and are able to recycle process water as well as recover valuable products in various applications (Guo *et al.*, 2012). Unlike the conventional water treatment systems, membrane technology requires a small footprint and purifies water usually without chemical additives (Gao, 2016).

However, membrane technology has experienced various operational problems which tend to hinder the growth of membrane applications in the separation industries, most especially in the water treatment industry (Judd, 2011). The major disadvantage that has been associated with the use of membranes is fouling. Fouling results in a rapid decline of the permeate flux, as well as reduction in the membrane life span after a long period of accumulation of irrecoverable foulants (Meng *et al*., 2017; Gkotsis *et al*., 2014), thus increasing the operational cost in membrane application. Therefore, for the membrane separation process to be efficient, fouling must be minimized. This is the focus of this investigation.

2.1.2. Types of membranes

Membranes can be classified according to their nominal pore size (Judd, 2011). Nominal pore size is defined as the average equivalent perfect cylindrical pore size for a membrane. There are different

application ranges for the different types of membranes, namely, conventional filtration, microfiltration, ultrafiltration, nanofiltration and reverse osmosis. Figure 2-1 indicates a generalized membrane pore size cut-off range used to classify the membranes into their various types. It also indicates the various materials they can exclude based on the size of their pores.

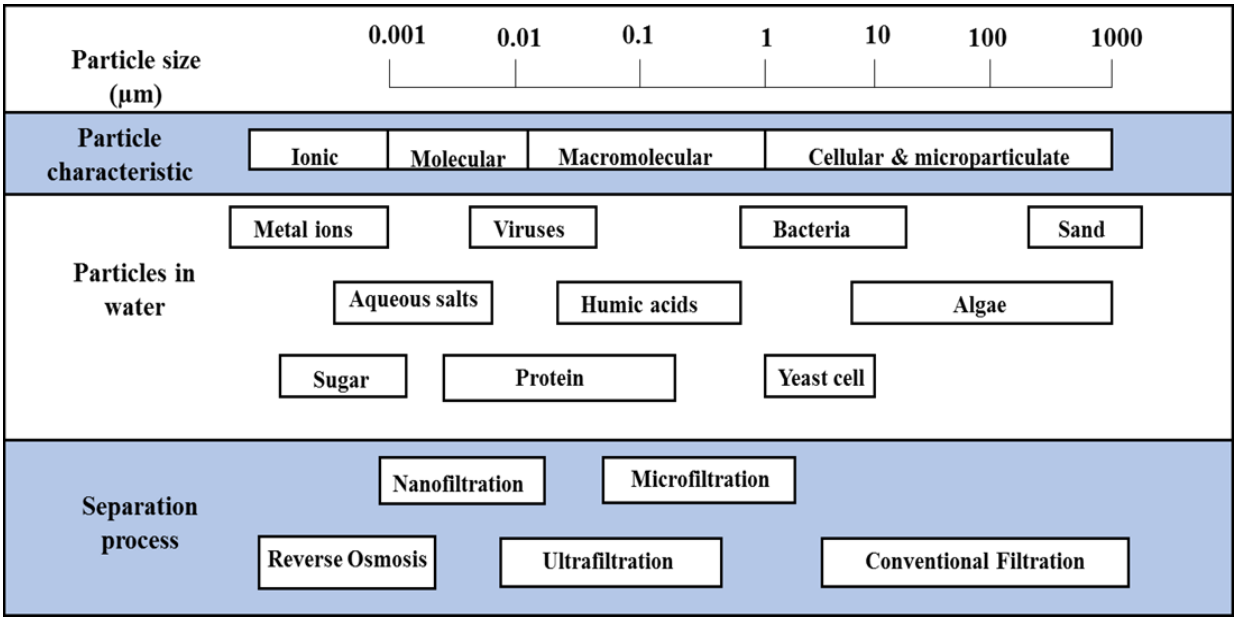

Figure 2-1: Membrane Classification and Application adapted from (Lai *et al.*, 2014)

Microfiltration and ultrafiltration membranes use the separation mechanism of sieving, while nanofiltration and reverse osmosis employ the solution adsorption-diffusion mechanism. Furthermore, microfiltration and ultrafiltration are low-pressure driven membranes, and are thus popular in the water treatment industry due to their proven effectiveness in removing particles, colloids and high molecular weight organics (Akhondi *et al.*, 2017). By contrast, nanofiltration and reverse osmosis are commonly used for water purification due to their superior ability to remove viruses and dissolved ions and solids, such as salt (Butts, 2016).

This study employed a microfiltration membrane given that it is efficient in removing particles, colloids and high molecular weight organics from wastewater (Pillay *et al.*, 2016).

2.1.3. Membrane performance characteristics

The performance of a given membrane process is usually represented by both its rejection ability and permeate flux. The rejection ability is usually assessed in terms of the permeate quality, while the permeate flux is sometimes expressed in terms of the permeability index or hydraulic resistance (Gander *et al.*, 2000).

A membrane process involves splitting a feed stream into a retentate and a permeate stream (as shown in Figure 2-2). Pressure-driven membrane processes, such as microfiltration process, use pressure difference between the feed and permeate side as the driving force to transport solvent through the membrane. This driving force is commonly known as the transmembrane pressure (TMP) or the pressure drop (ΔP). Considering the pressure drop along a membrane, it can be calculated as shown in Equation 2-1 (Drews, 2010);

Equation 2-1

$$\boldsymbol{TMP = \Delta P = \frac{P_f + P_r}{2} - P_p}$$

where ΔP is the pressure difference across the membrane (Pa), P_f is the pressure of the feed (Pa), P_r is the pressure of the retentate (Pa) and P_p is the pressure on the permeate side (Pa).

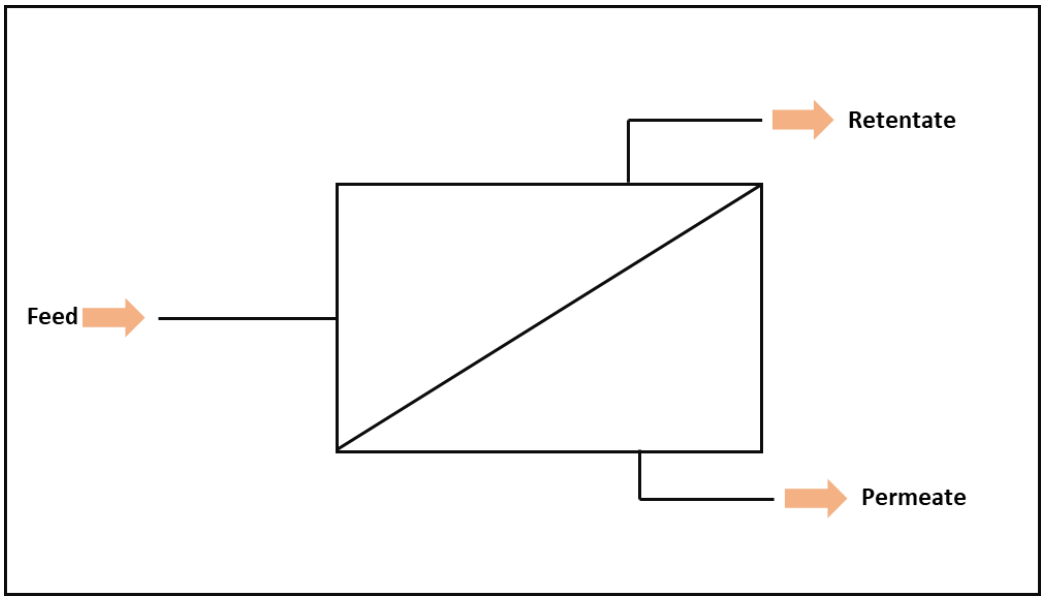

Figure 2-2: Schematic of a membrane filtration process, redrawn from (Judd, 2011)

The volumetric rate at which permeate crosses the membrane per unit area of the membrane surface is referred to as permeate flux. Permeate flux is related to the applied transmembrane pressure divided by the resistance to mass transfer and the permeate viscosity (Miller *et al.*, 2014). It is one of the key parameters used in defining the performance of membrane processes. The flux can be described by expressions presented in Equation 2-2.

Equation 2-2

$$\boldsymbol{J = \frac{Q}{A} = \frac{v}{A\Delta t} = \frac{\Delta P}{\mu R_t} = \frac{\Delta P}{\mu(R_m + R_{tf})}}$$

where J is the flux (L/m^{2}h or LMH), Q is the volumetric flowrate (L/h), A is the effective membrane

area (m^2), v is the permeate volume collected (L), Δt is the time taken to collect the permeate (h), ΔP is the pressure drop across the membrane (Pa), μ is the permeate viscosity (Pa.s), R_t is the total membrane resistance to mass transfer during the filtration process (m^{-1}), R_m is the intrinsic membrane resistance (m^{-1}) and R_{tf} is the total fouling resistance on the membrane (m^{-1}).

In filtering pure water using a membrane, R_m represents the inherent resistance to mass transfer associated with the membrane. The resistance is a function of the membrane structure. When filtering a solution or a suspension the total resistance to mass transfer tends to increase (Miller *et al.*, 2014). This is due to the deposition of soluble and/or particulate materials onto and into the membrane, resulting in additional resistance represented by R_{tf} in Equation 2-2. This deposition phenomenon is referred to as fouling. Fouling usually results in a decline in permeate flux and an increase in TMP, thereby decreasing the performance of the membrane (Le-Clech *et al.*, 2006). It is the major limitation of membrane processes. More details on fouling are presented in section 2.2.

In the case of product quality, the membrane performance is usually expressed in terms of membrane rejection. The rejection indicates the percentage retention of a particular species by the membrane and is based on the selectivity of the membrane to allow materials to pass through the membrane barrier (Bruggen *et al.*, 2003). It is calculated using the expression in Equation 2-3.

Equation 2-3

$$\boldsymbol{R = (1 - \frac{C_p}{C_f}) \times 100\%}$$

where R is rejection (%) , C_p is the permeate concentration (g/L) and C_f is the feed concentration (g/L).

In microfiltration and ultrafiltration membranes, which are known to reject colloids, bacteria and organics, the rejection is generally expressed in terms of various parameters that can be more easily measured. These include turbidity rejection, suspended solids rejection and organic matter rejection (Akhondi *et al.*, 2017; Melidis *et al.*, 2016; Radjenović *et al.*, 2008).

2.1.4. Membrane modules

A membrane module refers to the geometry of the membrane in relation to the flow of the feed and that of the permeate. The geometry can be either planar or cylindrical (Cuperus, 2018). There are various types of modules that are used in membrane processes, including flat sheet modules, hollow fibre modules, multi-tubular modules, spiral wound modules and capillary modules (Judd,

2011). The representation of the flow in the various configuration is illustrated in Figure 2-3.

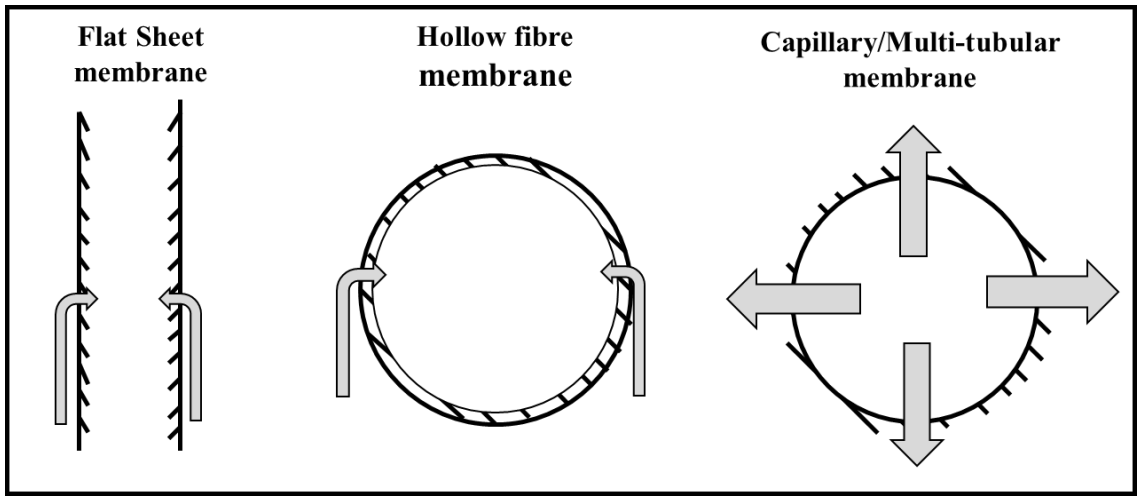

Figure 2-3: Membrane flow orientation for different membrane configurations redrawn from (Judd, 2011).

The different membrane module configurations offer various benefits and limitations, depending on the field of application. Hollow fibre and spiral wound modules have a high packing density and are therefore suitable for large scale applications, while the flat sheet and tubular modules pose low packing density and hence are mostly applied in small scale applications like decentralized sanitation systems (Jeon *et al.*, 2016). Due to their open channel design, tubular modules perform better in terms of minimizing fouling and blockages (Zhang *et al.*, 2015). In the case of ease of cleaning, the flat sheets are the most preferred modules. On the other hand, hollow fibre modules seem to have a major challenge when it comes to cleaning (Judd, 2011). Flat sheet modules were employed in this study.

2.1.5. Membrane materials

2.1.5.1. Current commercial membranes

Membranes are usually designed to have a high surface porosity and narrow pore size distribution, so as to provide as high a throughput and a selectivity as possible (Judd, 2011). Furthermore, the membranes should be resistant to chemical and thermal attack such as extreme temperature and pH, that often occur during chemical cleaning (Murić *et al.*, 2014). Therefore, in choosing a membrane material these characteristics need to be considered.

There are two types of membrane materials that are commonly used in fabricating commercial membranes, viz. ceramic and polymeric materials. These materials have both limitations and benefits, which have been indicated in Table 2-1.

Table 2-1: Advantages and disadvantages of two different membrane materials

Ceramic material[a,b,]	Polymeric material[a,b,c,d]
Advantages • They have a relatively narrow pore size distribution and high porosity, resulting in better separation and a high flux. • They have a high mechanical stability and therefore can withstand high pressure. • They are chemically and thermally stable resulting in longer membrane life span. **Disadvantages** • They are costly • They are prone to breakage **Examples** Inorganic materials such as titania, zirconia, and alumina	**Advantages** • They are flexible and relatively inexpensive **Disadvantages** • Most are chemically, thermally, and mechanically unstable • Most of them are hydrophobic, thus they get easily fouled. **Examples** • They include: polyvinylidene difluoride (PVDF), polyethersulfone (PES), polyethylene (PE)

[a](Murić *et al.*, 2014) [b](Hofs *et al.*, 2011) [c](Basile *et al.*, 2015) [d](Judd, 2011)

The woven fabric microfiltration (WFMF) membrane employed in this investigation is a polymeric membrane. More details of the WFMF membrane are presented in the next section.

2.1.5.2. Woven fabric microfiltration (WFMF) membranes

The membrane employed in this study is a woven fabric microfilter developed in South Africa. The membrane does not have pores as in the commonly known polymeric and ceramic membranes. Instead, it has fibres which are tightly woven to form a surface filter (Pillay *et al.*, 2016). Attempts were made to quantify its pore size by modified exclusion method, and it was found to be 1-2 µm (Chollom *et al.*, 2017). This pore size classifies the woven fabric as a microfilter. WFMF is able to remove suspended solids, colloids, bacteria and protozoa (Chollom *et al.*, 2017), making it suitable for wastewater treatment. A scanning electron microscope (SEM) image of the WFMF is shown in Figure 2-4.

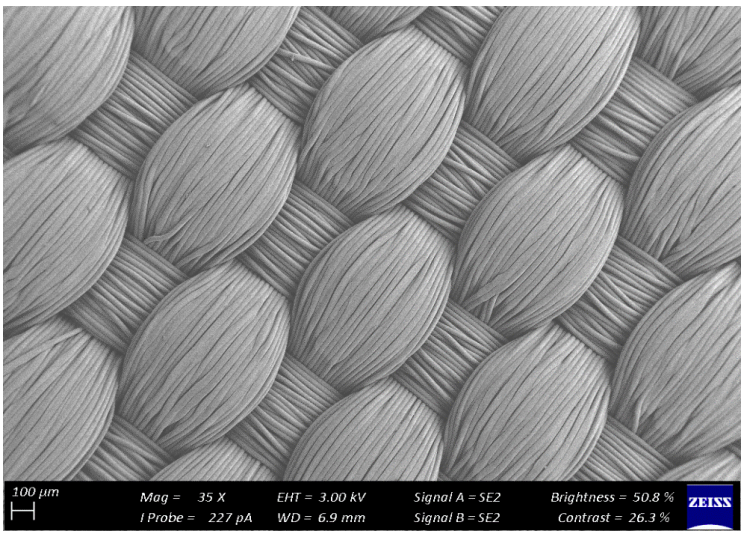

Figure 2-4: Image of a woven fabric microfiltration membrane (produced during this study)

Recent studies on this membrane have shown that this type of membrane has a good potential in the water treatment industry (Cele *et al.*, 2010; Chollom *et al.*, 2017; Pillay *et al.*, 2016). It offers a wide range of benefits over the currently available inversion-cast flat sheet membranes. The advantages of the WFMF membrane over the commercially available membranes include: - robustness (the membrane can dry out as well as withstand mechanical abrasion without any damage); high chemical resistance; can easily be cleaned; and lastly, it requires less chemical to clean (Cele *et al.*, 2010; Chollom *et al.*, 2017; Deelie, 2017).

2.1.6. Membrane characterization

Membrane characteristics play a fundamental role in membrane processes. They affect the membrane flux, membrane rejection capacity and fouling. As such, in order to understand the interaction between the membranes and the foulants, or when developing improved membranes, characterization of the relevant membrane surface properties is very important (Johnson *et al.*, 2018). Membranes are generally characterized by measuring their various properties. These properties include morphology, roughness, hydrophilicity and oleophobicity. Since the focus of this study is on oleophobic membranes and fouling, only the membrane morphology and oleophobicity will be considered.

2.1.6.1. Membrane morphology

Membrane morphology is the study of the size, structure, and shape of the membrane (Sanaei & Cummings, 2017). It can be used to determine the pore size, the topography, the pore density, and the chemical selectivity of the membrane. Various investigations have shown that membrane morphology is a very key parameter in determining the separation efficiency and the fouling

characteristics of a membrane filter. For example, a membrane with smaller pore sizes would not get fouled easily with feed containing large particles. Similarly, a membrane with smoother surface is less likely to be fouled compared to one with a rough surface (Sanaei & Cummings, 2017; Mahady *et al.*, 2015; Zydney & Ho, 2003). Therefore, characterizing the surface properties of a membrane is very crucial to obtaining the desired membrane performance.

One of the simplest and widely used techniques of examining morphology of materials is through optical microscopy (Chen *et al.*, 2004; Gómez *et al.*, 2009; Osterlund & Vingsbo, 1979). This is because it can be performed rapidly, as it often requires no sample preparation. In addition, the optical microscopy technique is frequently non-destructive; and it utilizes relatively inexpensive equipment (Ebnesajjad, 2011). An example of this technique is the use of stereo microscopes. A typical stereo microscope image is shown in Figure 2-5 (A).

However, the images produced by this technique are often not clear. This is because the microscopes used in this technique generally have a low resolution. Hence, it is not suitable for analysis that requires in-depth details of the material's morphology.

The Scanning Electron Microscopy (SEM) technique is another widely employed method for morphology evaluation (Breite *et al.*, 2015; Kishimoto, Wang *et al.*, 2007; Li *et al.*, 2002). This technique gives high quality and high resolution images, though it is destructive (Johnson *et al.*, 2018). An example of a SEM image is shown in Figure 2-5 (B).

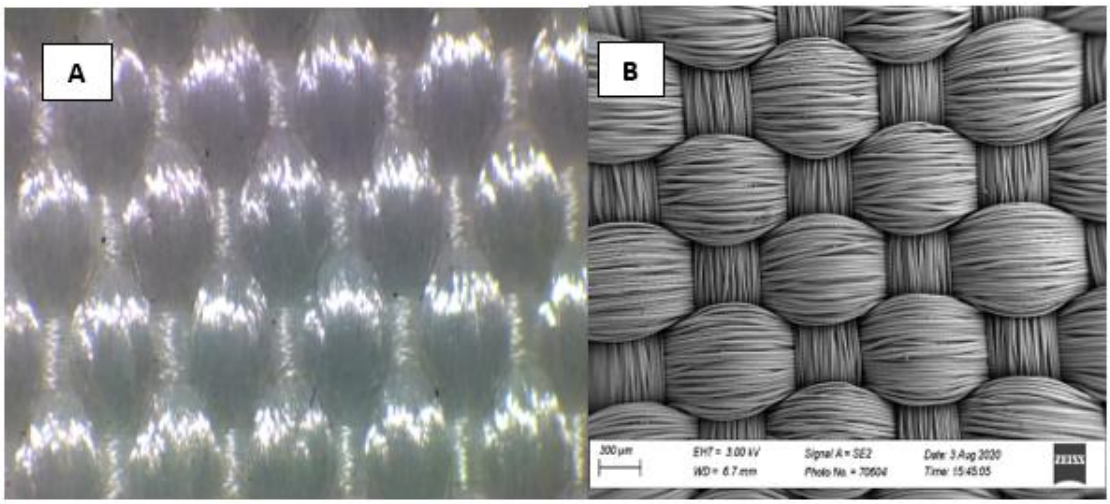

Figure 2-5: WFMF images taken under a: (A) stereo microscope (20x) and (B) scanning electron microscope (37x), (produced during this study)

This study employed the optical microscopy technique for general observation of the membrane morphology and for the analyses that do not require destruction of the membrane samples. The

SEM technique was used in cases where in-depth detail of the membrane morphology is required.

2.1.6.2. Membrane oleophobicity

Oleophobicity refers to the ability of membranes to resist low surface tension liquids and materials such as oils, gel-like materials, among others (Shen *et al.*, 2019; Zhu *et al.*, 2013). This ability prevents the penetration of such foulants into membranes.

The oleophobicity of a membrane is determined by measuring the contact angle a drop of oil makes with the membrane surfaces. A contact angle closer to or greater than 90˚ indicates that the membrane is oleophobic, while it is oleophilic if otherwise. This contact angle can be measured using the Sessile Drop Method (Zhu *et al.*, 2013) or the Captive Bubble Method (Yang *et al.*, 2015). The illustration of an oleophobic membrane surface and how the contact angle is measured is as shown in Figure 2-6.

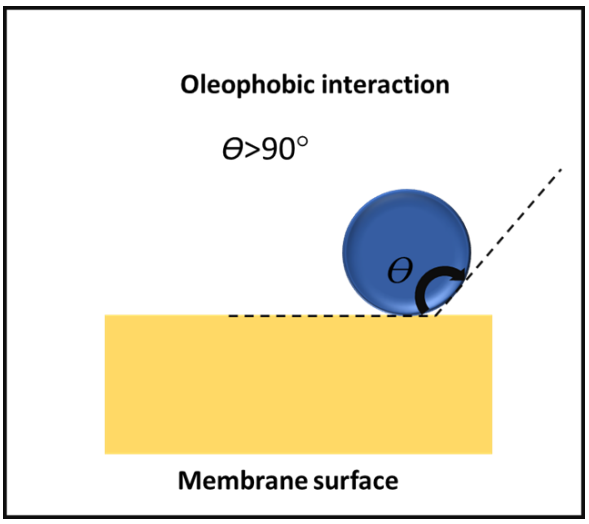

Figure 2-6: Illustration of contact angle measurement of an oleophobic membrane surface

The oleophobic or oleophilic nature of a membrane affects the attachment of organic foulants onto a membrane surface. This in turn affects the degree of fouling of a membrane; which ultimately affects the ease of membrane cleaning.

2.2. Membrane fouling

2.2.1. Overview

Membrane fouling is a major impediment in the application of membranes in separation processes. It is characterized by the accumulation of feed stream components onto the surface, or within the pores of the membrane, thus resulting in an increase in hydraulic resistance, accompanied by a

decrease in permeate flux. This in turn leads to a reduction in separation efficiency, high operational cost needed for cleaning and maintenance, as well as membrane replacement in the long run (Gkotsis *et al.*, 2014; Mohammad *et al*., 2012). Therefore, for a membrane separation process to be efficient, the fouling should be minimized as much as possible (Nguyen *et al.*, 2010). This project is focused on establishing a better understanding of the membrane fouling mechanisms on WFMF membranes and to develop a corrective measure aimed at minimizing the fouling through the modification of the membrane surface characteristic.

2.2.2. Types of membrane fouling

Membrane fouling can be classified according to the physical adhesion of the foulant to the membrane or chemical and biological characteristics of the foulant (Wang *et al.,* 2014; Malaeb *et al.,* 2013). The first category includes reversible, irreversible, and irrecoverable fouling, while the second includes biofouling, organic fouling, and inorganic fouling. Figure 2-7 gives an overview of the different types of membrane fouling during filtration.

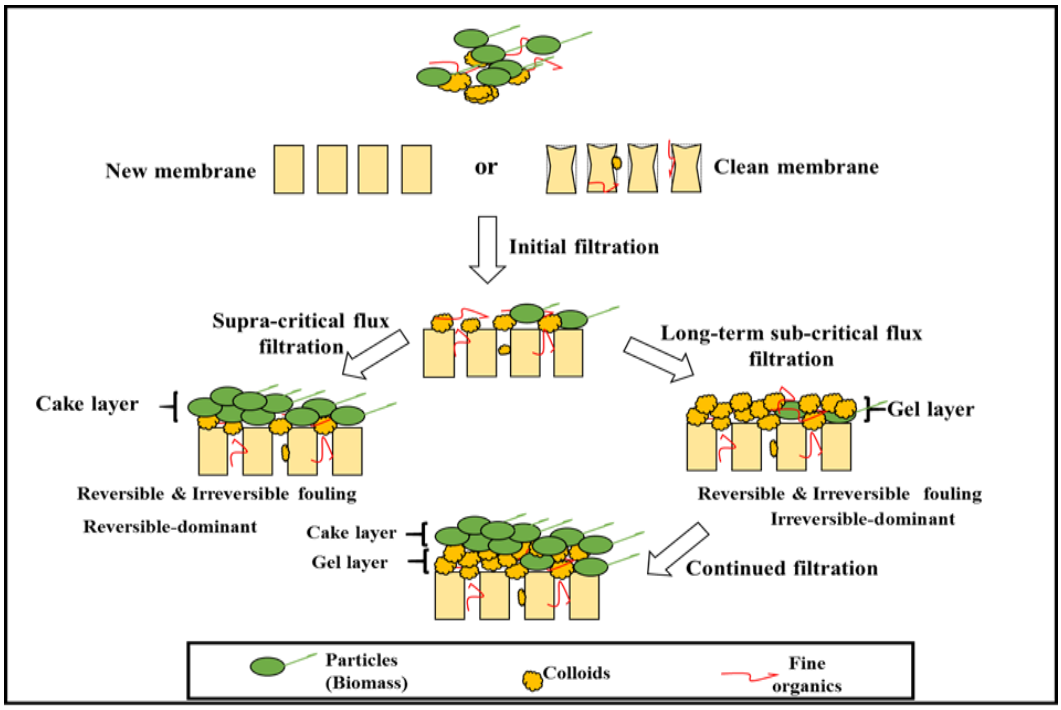

Figure 2-7: Overview of different types of membrane fouling during filtration, modified from (Wang *et al.*, 2014)

2.2.2.1. Reversible, irreversible, and irrecoverable fouling

These three types of fouling are defined based on the attachment strength of fouling materials to the membrane surfaces, or the methods used to recover the initial permeability of the membranes.

i) Reversible fouling

This type of fouling results from the loose attachment of foulants to membrane surfaces. It can be removed by physical cleaning methods such as relaxation, strong shear force, or backflush. Reversible fouling can also be referred to as 'removable' or 'temporary' fouling. This type of fouling is attributed to cake layer formation (Meng *et al.*, 2009).

ii) Irreversible fouling

The formation of a strong matrix of fouling layer with solutes during continuous filtration usually results in a reversible fouling changing into an irreversible fouling layer (Wang *et al.*, 2014). An example of this is the formation of a gel layer under a long-term subcritical flux operation. The deposition of foulants within the membrane pores is also regarded as another kind of irreversible fouling (Wang *et al.*, 2014). This type of fouling results in pore blocking. Irreversible foulants cannot be easily removed by physical cleaning methods (Tsuyuhara *et al.*, 2010) but can be washed out by chemical cleaning.

iii) Irrecoverable fouling

Once a membrane is fouled during a long-term operation, the original membrane permeability is usually never fully recovered (Wang *et al.*, 2014). This is referred to as irrecoverable fouling, also known as permanent fouling, which ultimately determines the life-span of membranes (Judd, 2011).

2.2.2.2. Biofouling, organic and inorganic fouling

i) Biofouling

This is formed due to the deposition and growth of micro-organisms on membrane surfaces. Biofouling is attributed to biofilming or biocaking (Wang *et al.*, 2014). The dominant foulants of biofouling are biosolids but also include part of the organic matter. This type of fouling is only a problem with membranes that are operated on feeds with high organic matter concentrations. The biofouling layer, if well maintained, acts as an additional membrane layer often improving the water quality in membrane filtration processes (Malaeb *et al.*, 2013). The difficulty with this layer lies in managing the thickness, as it affects the membrane flow capability.

ii) Organic fouling

Organic fouling is caused by the deposition of proteins, polysaccharides, humic acids and other organic substances originating from feed water or microbial secretions. This type of fouling, if continuous, results in the formation of a gel layer on the membrane (Wang *et al.*, 2014). Extra-

cellular polysaccharides substances (EPS) and Soluble microbial products (SMP) are regarded as key organic foulants in membrane processes. In addition to the molecular size, the deposition of EPS or SMP on membranes strongly depends on their affinity with the membranes (Meng *et al.*, 2009).

iii) Inorganic fouling

This is also referred to as *scaling*. Inorganic fouling results from chemical precipitation of inorganic crystals and/or biological precipitation of organic-inorganic complexes. This occurs if their saturation concentrations are exceeded on the membrane surfaces. In addition, the inorganic particulates existing in a bioreactor can also attach onto membrane surfaces or block membrane pores thus causing inorganic fouling (Wang *et al.*, 2014).

2.2.3. Membrane fouling mechanisms

It is important to identify the dominant fouling mechanism that occur during the membrane filtration process when choosing ways of minimizing membrane fouling and restoration methods (Kim *et al.*, 2013). This has been discussed by (Lim & Bai, 2003), where they first had to identify the prevalent fouling mechanism in a system that comprised of a microfiltration membrane before evaluating the best cleaning method for the membrane. A mini review of membrane fouling by (Guo *et al.*, 2012) also concluded that in order to minimize fouling using pretreatment process, a better understanding of the fouling mechanism is required. Therefore, it is necessary to investigate the fouling mechanisms that commonly occur on membranes during the separation process.

There are four common types of models used in describing membrane fouling mechanisms, namely, complete pore blocking, intermediate blocking, cake filtration and standard blocking mechanisms (Kim *et al.*, 2013). According to (Judd, 2011), these models have their origin in early filtration studies.

2.2.3.1. Complete pore blocking

This is a mechanism where each feed particle reaching the membrane, blocks a pore without lying on other particles during the separation process as illustrated in Figure 2-8 (a) (Wang & Tarabara, 2008). This occurs on the membrane surface, and thus it is a model associated with external fouling.

2.2.3.2. Standard blocking

This is sometimes referred to as internal pore blocking (Zheng *et al.*, 2018). Standard blocking mechanism involves deposition of small feed particles within the pores as shown by Figure 2-8 (b). This results in pore constriction, and the pore volume reduces with increase in particles deposited

within the membrane pore (Wang & Tarabara, 2008). Unlike the complete pore blocking model, this is associated with internal fouling, since the particles are deposited within the pores. It is reported to occur in microfiltration membranes during the early stages of wastewater treatment (Nguyen *et al.*, 2010; Blanpain *et al.,* 1999).

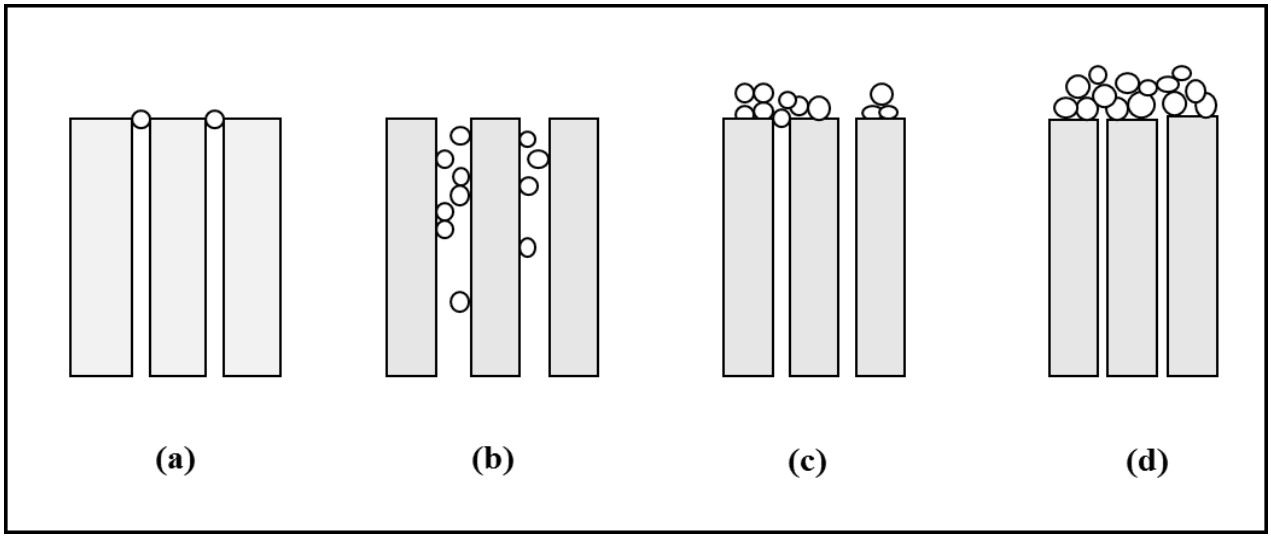

Figure 2-8: Membrane fouling mechanisms: (a) Complete pore blocking (b) Standard blocking (c) Intermediate blocking (d) Cake filtration, redrawn from (Judd, 2011)

2.2.3.3. Intermediate blocking

Intermediate blocking comprises of both complete pore blocking and cake filtration mechanism. In this mechanism, particles do not only block the membrane pores but also deposit on other particles on the membrane surfaces (Zheng *et al.*, 2018; Wang & Tarabara, 2008). This mechanism is dominant in reverse osmosis and ultrafiltration membranes during the initial stages of separation processes (Wang & Tarabara, 2008).

2.2.3.4. Cake filtration

In the formation of a cake layer, there is often particle deposition on the membrane surface and on other particles. This is always so because the pores are already blocked, or the membrane has no pores due to its dense nature (Zheng *et al.*, 2018; Wang & Tarabara, 2008). This can be seen in Figure 2-8 (d). Cake filtration occurs in the late stages of most membrane separation processes including microfiltration membrane processes (Blanpain-Avet *et al.*, 1999; Wang and Tarabara, 2008; Nguyen *et al.*, 2010). It has been reported to be the dominant mechanism that contributes to fouling in microfiltration membranes. It is largely reversible as it can usually be washed off easily by physical cleaning methods.

2.2.4. Quantification of fouling

Membrane fouling is often quantified by either a decline in flux or an increase in pressure drop depending on the operation mode of the filtration process (Le Clech *et al.*, 2003; Miller *et al.*, 2014). Filtration processes generally aim to operate either under constant pressure or constant flux conditions. Hence, in this section, the quantification of fouling in these two operation modes will be outlined and their limitations pointed out.

2.2.4.1. Constant pressure operations

Most laboratory-based membrane fouling studies are often done using constant pressure set-ups (Buetehorn *et al.*, 2010; Dagnew *et al.*, 2012; Louie *et al.*, 2006; Rezaei *et al.*, 2011; Xiao *et al.*, 2013). This is because they are easier and simpler to operate relative to the constant flux rigs (Kraume *et al.*, 2009). The constant pressure mode of operation involves fixing the pressure drop (ΔP) at a constant value, while monitoring permeate flux over time. In this operation, fouling is indicated by the decline in permeate flux, as shown in Figure 2-9.

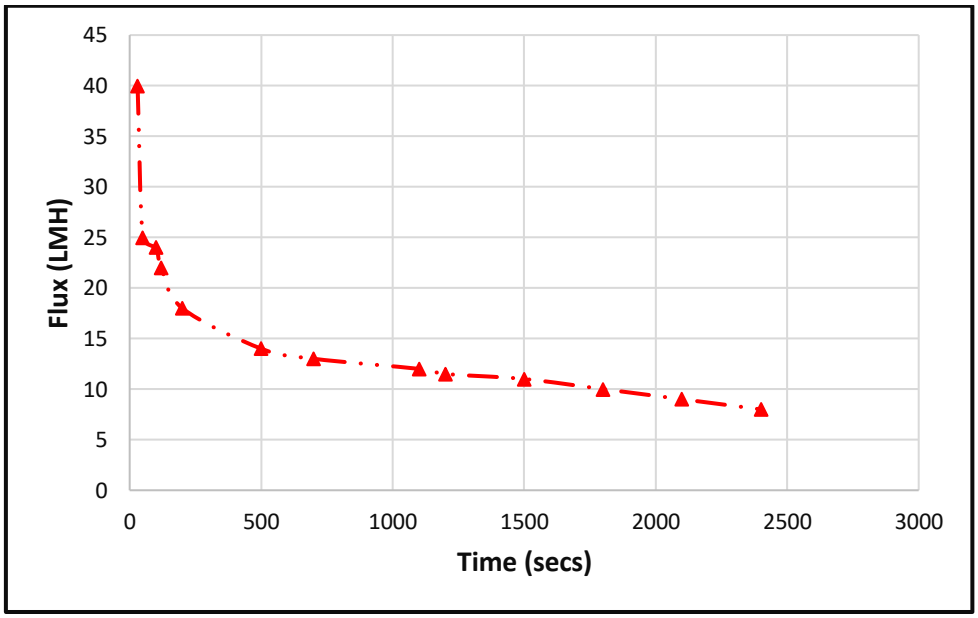

Figure 2-9: A typical flux profile that is used to indicate fouling in a constant pressure filtration operation mode (ΔP = 2 bar), extracted from (Rezaei *et al.*, 2011)

However, as the flux varies in the constant pressure operation, so does the hydrodynamic conditions at the membrane surfaces (Chan & Chen, 2001; Miller *et al.*, 2013). This implies that the observed fouling behaviour, indicated by the flux decline plot, is not solely as a result of membrane-foulant interactions, but also hydrodynamic conditions. Therefore, flux profiles do not accurately indicate fouling in membrane processes. Hence, to address this limitation, some authors studied membrane fouling at constant flux conditions.

2.2.4.2. Constant flux operations

This operation involves fixing the flux at a constant value, while the pressure drop (ΔP) varies with time (Chan & Chen, 2001; Miller *et al.*, 2013). Fouling is then indicated by an increase in the pressure drop as shown in Figure 2-10.

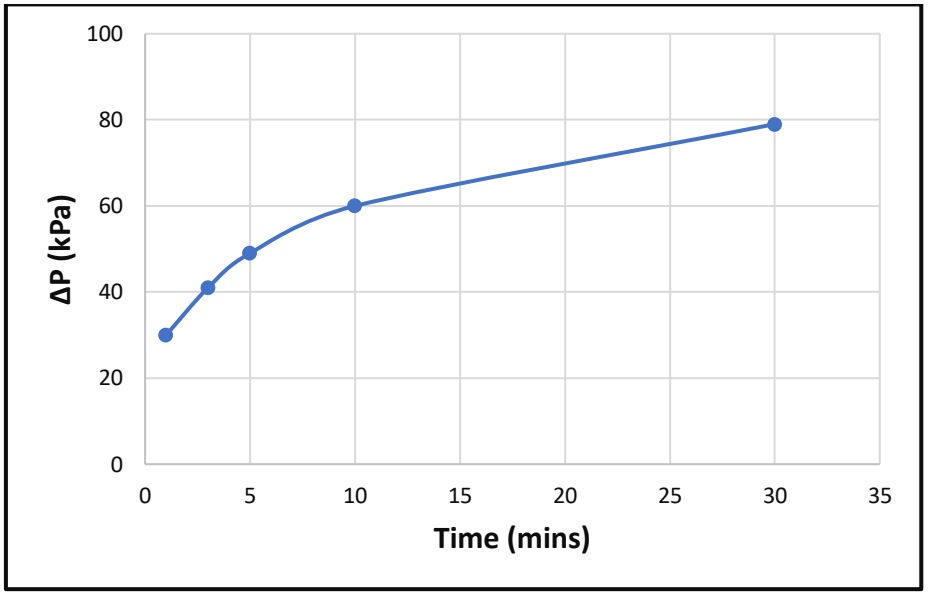

Figure 2-10: A typical ΔP profile that is used to quantify fouling in a constant flux operation (flux = 30 LMH), adapted from (Dagnew *et al.*, 2012)

The constant flux operation is the most commonly used operation mode in industrial applications (Drews, 2010; Miller *et al.*, 2014). It is preferred over the constant pressure operation since it provides better control of the flow of material deposition on the membrane surface, as the convective flow of material towards the membrane is constant during the filtration process (Le Clech *et al.*, 2003). Thus, it is considered most reliable when quantifying fouling.

Additionally, operating at a constant flux helps in minimizing fouling during filtration processes. The severe fouling observed at the initial stages of a constant pressure filtration process, which occurs because of often very high initial flux, is reduced by imposing a constant and a much lower flux in constant flux operations (Miller *et al.*, 2014). However, it is worth noting that in practical operations, there will always be an inevitable decrease in flux, which results from an increase in mass resistance on the membrane surface (Visvanathan *et al.*, 2000). Therefore, regardless of which operation is used, both flux and ΔP should be measured and used to quantify fouling during membrane filtration processes.

2.2.4.3. Real cases in filtration processes

The changes in both ΔP and flux, during membrane separation processes are generally captured in

terms of a *resistance* (Bella & Trapani, 2019; Miller *et al.*, 2014). The deposition of foulants on membranes usually causes an additional hydraulic resistance for the passage of permeate, which decreases the overall permeability of the membrane. Additionally, the increase in hydraulic resistance results in an in increase in pressure drop across the membrane. As a result, fouling in membranes can be represented in terms of a resistance. In estimating fouling resistance, Equation 2-2 can re-written as;

Equation 2-4

$$R_f = \frac{\Delta P}{\mu J} - R_m$$

The permeate flux and ΔP in Equation 2-4 corresponds to data collected during the membrane filtration process. From the calculated resistance data, a resistance profile is usually plotted to represent the fouling behaviour of membranes during the filtration process. A typical resistance plot is shown in Figure 2-11.

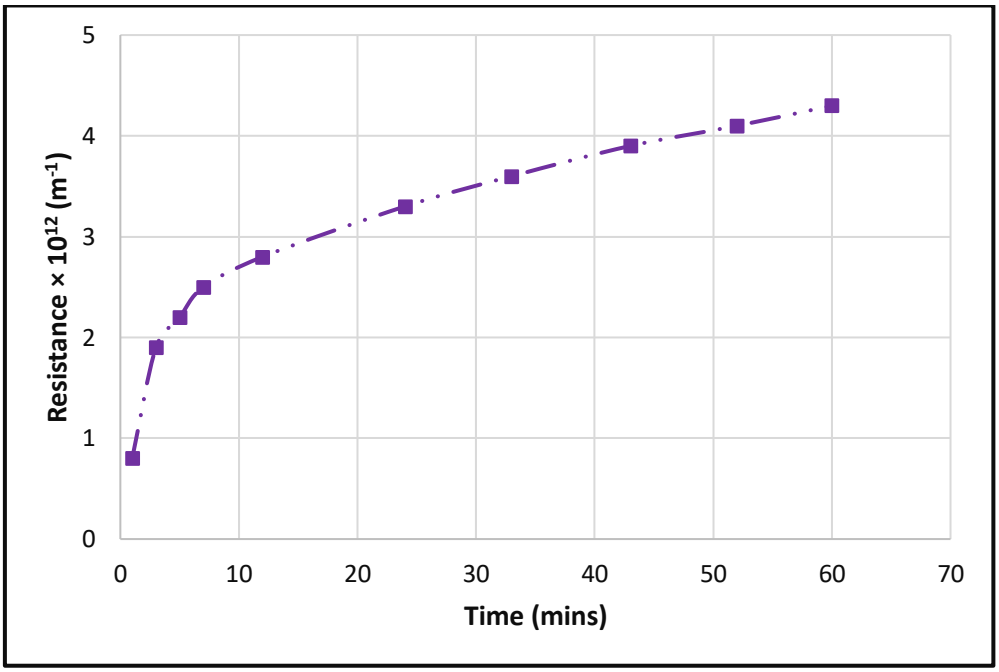

Figure 2-11: A typical resistance profile representing fouling in a membrane filtration process, adapted and modified from (Kong *et al.*, 2017)

The total resistance to mass transfer in membrane process is often described by the resistance-in-series model (Bella & Trapani, 2019; Kong *et al.*, 2016; Miller *et al.*, 2014). In this approach, the individual resistances that contribute to the total resistance are quantified. As discussed in subsection 2.2.1.1, these individual resistances include: reversible, irreversible, and irrecoverable fouling resistances. Figure 2-12 shows a graphical representation of the various types of fouling resistances.

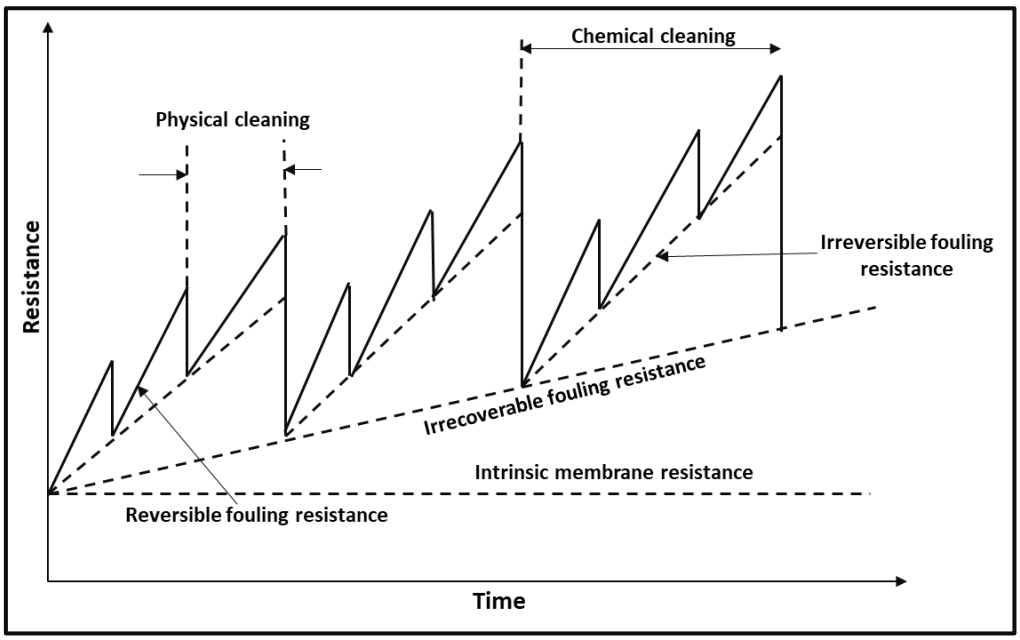

Figure 2-12: Membrane fouling characterization using resistance data, adapted and modified from (Drews, 2010; Kraume *et al.*, 2009)

2.2.5. Membrane fouling mitigation

In order to make membrane separation processes economical, membrane fouling must be minimized. Various ways of minimizing fouling in membranes have been proposed and evaluated (Gkotsis *et al.*, 2014; Miller *et al.*, 2013). This is illustrated in Figure 2-13.

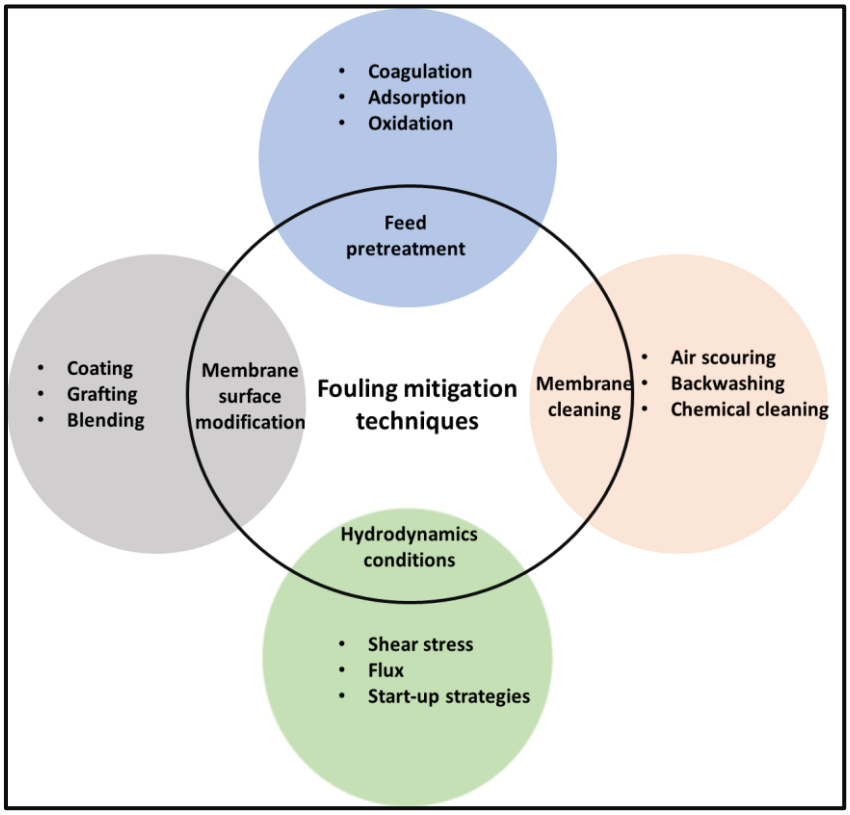

Figure 2-13: Techniques of minimizing membrane fouling

2.2.5.1. Feed pretreatment

Feed pretreatment helps in minimizing fouling by reducing accumulation of foulants on membrane surfaces, as well as modifying the interaction between the foulants and the membranes. Furthermore, it increases the efficiency of separation processes. Pretreatment processes include coagulation, activated carbon adsorption and ozone oxidation (Sun *et al.*, 2013).

i) Coagulation

Coagulation is a process that has been widely employed for a long time in the water treatment sector. This is due to its inexpensive nature and ease of operation. In membrane processes, it can reduce reversible fouling by complexing together organics of high molecular weight, thus making them easier to sediment out. However, its ability to eliminate organics is limited. It has been reported that coagulation cannot eliminate small organics molecules like polysaccharides and proteins, which are the major contributors to irreversible fouling (Sun *et al.*, 2013; Kimura *et al* 2005).

ii) Adsorption

This pretreatment process involves incorporating activated carbon powder on low pressure membranes such microfiltration membranes. The activated carbon powder helps in minimizing fouling by adsorbing foulants. The powder can adsorb small organic molecules which a coagulation process cannot get rid of, as well as improve the water treatment efficiency. Nonetheless, the adsorption of macromolecular organics is very poor (Sun *et al.*, 2013). Thus, it is not highly efficient in minimizing fouling. Furthermore, the active sites get saturated with time, and thus a constant replacement of the powder would be required (Ng *et al.*, 2006).

iii) Oxidation

The molecular weight distribution of organic foulants have a major impact on membrane fouling. Oxidation processes minimizes fouling by breaking down macromolecules into small molecules and further into inorganic compounds using ozone. This decreases the concentration of organic foulants in the feed, and subsequently decreases membrane fouling (Sun *et al.*, 2013). Notwithstanding its benefits, ozone being a strong oxidant can corrode and oxidise membranes. Hence, although it is a viable option, its ability to corrode membranes needs to be investigated before being incorporated.

2.2.5.2. Membrane cleaning

Membrane cleaning can generally be classified as a physical or a chemical cleaning method, based

on the fouling removal mechanism. Physical cleaning methods include hydraulic, pneumatic and sonication methods (Lin *et al.*, 2010). Additionally, mechanical cleaning such as the use of a brush can be classified as a physical method. Chemical cleaning involves the use of chemical reagents. Membrane cleaning can either be *in-situ* or *ex-situ* (Wang *et al*., 2014).

A. Physical cleaning methods

i) Membrane relaxation

Membrane relaxation is a process whereby a period of filtration is followed by a period of non-filtration. During the non-filtration duration, the permeate suction pump is switched off and the transmembrane pressure drops to zero. This enhances the back transport of loosely attached foulants from the membrane surface back to the bulk solution (Lin *et al.*, 2010), which in turn reduces the amount of foulants on the membrane surface.

In addition, during the non-filtration period, the process of air scouring is usually allowed to continue (Radjenović *et al.*, 2008). This increases the shear stress on the membrane surface, which in turn increases the rate of foulants being dislodged from the membranes. Thus, the combination of non-filtration and air scouring makes it easier for the foulants to be removed from the membrane surface. More details on air scouring are presented further in this chapter.

ii) Water scouring

Water scouring is one of the simplest membrane cleaning methods. Its cleaning effect is usually provided by the shear effect and the power of water as a universal solvent (Bansal *et al.*, 2006; Cabero *et al.*, 1999). This method involves rinsing of membranes with water at a high velocity and pressure (Bansal *et al.*, 2006; Cabero *et al.*, 1999; Kong *et al.*, 2016). An example involves rinsing fouled membranes with running water from a tap or a hose pipe. The flow of water creates the shearing effect, which in turn scours the membrane surface. In addition, water scouring can clean the membranes through the dissolution of the deposited foulants (Bansal *et al.*, 2006).

It is worth noting that this method is often used as a preliminary step in combination with other cleaning methods, and is the first cleaning step performed immediately after a filtration run (Cabero *et al.*, 1999; Kong *et al.*, 2016; Wang *et al.*, 2010). Generally, the main aim of the water scouring technique is to remove as many foulants as possible from the membrane surface in order to prepare the membrane for the next cleaning step. Water scouring alone, even at the best operating conditions, cannot clean membranes satisfactorily (Cabero *et al.*, 1999; Mohammadi *et al.*, 2002).

iii) Hydraulic methods

Hydraulic methods which include backwashing and back pulsing are the most common methods used for membrane cleaning (Lin *et al.*, 2010).

- Backwashing - is a process of reversing the flow of permeate through the membrane to dislodge the particles entrained within the membrane pores. A more intensive backwash can more readily reduce reversible fouling in membrane filtration systems.
- Back pulsing - it is also referred to as back shocking. This method is a more rapid backwash with a forward filtration step and then followed by a reversed filtration step. Rapid back pulsing (< 0.1s) can effectively remove non-adhesive foulants from membranes.

iv) Pneumatic method

This is also termed air scouring or air sparging. Air is applied for direct cleaning, or to enhance flux during the filtration process (Lin *et al.*, 2010). It is a method commonly used in membrane filtration systems for the removal of any biofilm layer on the membrane surface. An air stream is used to create a two-phase fluid flow over the membrane surface. The two-phase fluid flow is as a result of the upward airstream entraining fluid as it moves upward within the membrane vessel (Ducom *et al.*, 2002). The two-phase fluid stream applies a shear force to the fouling layer. However, the disadvantage of air scouring is the limited cleaning effectiveness and the high energy cost.

v) Sonification method

This is another effective physical cleaning method, but has received comparatively little attention in the literature. It is also termed ultrasound irradiation. Ultrasound waves produce cavitation and induce acoustic streaming, which provides vigorous mixing that breaks the concentration polarization and the cake layer on the membrane surface (Kyllönen *et al.*, 2006). However, it can influence the intrinsic permeability of the membranes.

B. Chemical cleaning methods

Though physical cleaning methods show great potential in attenuating membrane fouling, they cannot be effective if the foulants have a strong chemical interaction with the membranes. Chemical cleaning is the most common method for removing irreversible fouling (Tijing *et al.*, 2015). It removes the irreversible fouling layer using chemical reagents, which include bases (caustic soda); acids (hydrochloric, sulfuric, citric, oxalic); and oxidants (hypochlorite and hydrogen peroxide) (Wang *et al.*, 2014). It is the mostly widely employed method in restoring and maintaining the

'expected' permeability and selectivity in most membrane processes (Lin *et al.*, 2010).

Chemical cleaning can be carried out in various ways listed below:

- directly immersing the fouled membranes in the chemicals, referred to as clean-in-place (CIP).
- soaking in a separate tank with high concentration cleaning agents known as 'clean-out-off-place (COP).
- adding chemicals in the feed stream referred to as chemical wash (CW).
- cleaning in conjunction with the physical cleaning step termed as chemically enhanced backwash (CEB).

Although chemical cleaning is effective in restoring membrane permeability after fouling, its effect in decreasing the membrane lifespan is a major point of concern. The shortening of membranes' lifespan may be caused by frequent cleaning, high concentration of chemicals, and a long exposure time to chemicals.

2.2.5.3. Hydrodynamic conditions

Favourable hydrodynamic conditions are essential in minimizing membrane fouling. Hydrodynamic conditions in membrane technology defines the different hydrodynamic phenomena that are experienced close to the membrane surfaces during filtration processes. These phenomena include concentration polarization and back-transport. Concentration polarization describes the tendency of materials to accumulate near the membrane surfaces and it the driving force for this is the permeate flow. Back-transport describe the removal of retained materials from near the membrane surfaces back to the bulk solution. If the convection of material towards the membrane by the permeate flow is greater than the back transport, then material will be deposited on the membrane surface resulting in high fouling rate. Conversely, when the back-transport is greater than the convection towards the membrane, the likelihood of material being deposited on the membrane surface is minimal. Hydrodynamic conditions that increase back-transport are facilitated by various factors including shear stress, permeate flux, and start-up strategy (Lin *et al.*, 2013; Zhang, *et al.*, 2015).

i) Shear stress

Shear stresses facilitates back-transport mechanisms. An increase in shear stress facilitates the removal of materials near the membrane surfaces back to the bulk suspension, hence, minimizing

the deposition of foulants (Böhm *et al.*, 2012; Zhang, *et al.*, 2015). Shear stress in membrane processes is usually achieved either by an increase in the cross-flow velocity or the air scouring rate (Khan & Visvanathan, 2008). The cross-flow velocity method is mainly applicable to side-stream membrane bioreactor processes, while air scouring has been the strategy of choice in submerged membrane bioreactor systems. A detailed discussion on membrane bioreactor processes is presented in section 2.3.

While improving shear stress near membrane surfaces can certainly minimize membrane fouling, it also has its downsides. This approach results in an increase in energy consumption, which increases the operational cost of membrane processes (Buer & Cumin, 2010). In addition, an increase in cross-flow velocity or aeration rate also disrupts sludge flocs, producing small-size particles and releasing more organics which negatively impact membrane fouling (Ding *et al.*, 2016; Lin *et al.*, 2013). Therefore, it is essential to optimize the cross-flow velocity and the aeration rate in order to achieve satisfactory results.

ii) Flux

Permeate flux plays an important role in membrane fouling. A high initial flux usually results in a high permeate volume and a greater hydrodynamic permeate drag towards the membrane surface, causing adsorption of foulants on the membrane (Zhang *et al.*, 2015). Conversely, a low initial flux results in lesser deposition of foulants on the membrane.

On this basis, Field *et al*. introduced the concept of sub-critical operation as a strategy for minimizing membrane fouling. They defined the critical flux as the flux below which an increase of TMP with time under constant flux does not occur; however, above it a rapid increase in ΔP occurs (Field *et al.*, 1995).

This is illustrated in Figure 2-14 where ΔP was measured at each fixed flux for a duration of 15 minutes. From the graph, it can be seen that no change in ΔP was witnessed until a flux of around 17.5 LMH was reached. This flux is referred to as the critical flux. The region below this flux is known as the subcritical flux region, where no significant fouling occurs. Whereas operating above the critical flux is known to cause severe fouling as shown by the rapid increase in ΔP in Figure 2-14 (Chu *et al.*, 2014). Hence, operation at a subcritical flux has been extensively employed as one of the ways of minimizing fouling in membrane processes (Chu *et al.*, 2014; Field *et al.*, 1995; Wang *et al.*, 2008).

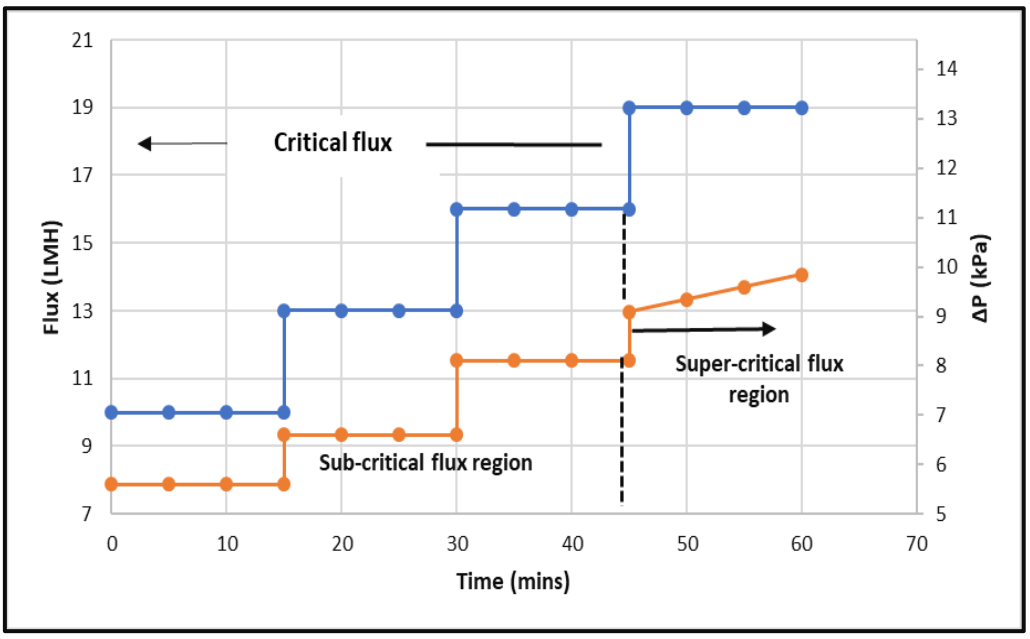

Figure 2-14: Illustration of the subcritical flux region during a membrane filtration process, redrawn from (Wu *et al.*, 2008)

iii) Start-up strategies

Filtration start-up strategies can also affect membrane fouling. Chen *et al* evaluated different start-up strategies and their effect on membrane fouling (Chen *et al.*, 1997). The gradual start-up which involved increasing the flux gradually from a low value to a high value had a lower fouling rate compared to direct increase to a high flux value. This was due to the fact that the driving forces near the membrane surfaces were predominantly back transport during the gradual start-up, thereby resulting in less deposition of materials on the membrane surface. However, this strategy does not apply to all filtration processes. It is dependent on the dominant fouling mechanism in a particular filtration process (Zhang, *et al.*, 2015).

2.2.5.4. Membrane surface modification

Membrane surface modification is one of the methods of mitigating fouling as it helps in maintaining a high level of water production. It reduces the frequency of employing other mitigation strategies by making the membrane less susceptible to fouling (Miller *et al.*, 2017). This technique involves altering certain surface properties of the membranes such as the surface charge, hydrophilicity, and oleophobicity, thus minimizing the adhesion or adsorption of foulants onto the membrane surface or within its pores (Ayyavoo *et al.*, 2016). Surface modification can be done through surface coating, surface grafting, blending or even use of nanocomposites. This will depend on whether this is carried out during new membrane fabrication, or post modification.

Several positive effects of membrane modification in the minimization of membrane fouling have

been reported in various studies. Zhu *et al*. modified Polyvinylidene fluoride (PVDF) membranes by blending them with an additive polymer that contained both hydrophilic and oleophobic segment and used them for the filtration of protein and humic acid solution. The modified membranes showed enhanced water flux and reduced organic fouling (Zhu *et al*., 2013). In another study, significant enhancement of antifouling property was observed with a modified polypropylene microporous membrane. The membrane was modified by adsorption of Tween 20 surfactant and then used in the treatment of synthetic wastewater in a membrane bioreactor. The monolayer adsorption of surfactant enhanced the membrane's intrinsic property (XIE *et al.*, 2007). From these few examples, it can be concluded that membrane modification is one of the most effective way of mitigating membrane fouling.

2.3. Immersed membrane bioreactors

2.3.1. Overview

Membrane bioreactors (MBRs) are increasingly being applied in wastewater treatment plants especially where high effluent quality is required (Ding *et al*., 2016). This technology involves integrating together the membrane separation process and the biological treatment process, thus, replacing the need for a second clarifier (Ndinisa *et al*., 2006). In addition to the effluent quality, MBRs offer benefits in terms of small footprint, low sludge production, high volumetric loading, and modular design (Wu *et al*., 2008; Singhania *et al*., 2012; Ding *et al*., 2016; Melidis *et al*., 2016). Consequently, there has been an increase in MBR adoption and installation worldwide (Singhania *et al*., 2012).

MBR systems are implemented based on two configurations, viz. the *side-stream* configuration and the *submerged* configuration. In a side-stream MBR, also referred to as external MBR (EMBR), the membrane is a separate unit process requiring an intermediate pumping step. In a submerged MBR, the membranes are immersed in the biological reactor, and hence this is also known as an immersed membrane bioreactor (IMBR). The EMBR and IMBR configurations are shown in Figure 2-15.

Between the two configurations, the IMBR is the most commercially employed configuration, the reason being that the submerged configuration operates more cost effectively as compared to the side-stream MBR in terms of energy consumption (Gander *et al.*, 2000). The additional energy consumption in the side-stream MBR is mostly due to the pumping required in the recycle stream (Ndinisa *et al.*, 2006; Singhania *et al.*, 2012). Furthermore, the IMBR system has a relatively smaller

footprint due to its compact design (Hoinkis *et al.*, 2012; Judd, 2011), has less sludge to handle due to its low permeation rate, and lastly, it requires less operator input (Singhania *et al.*, 2012).

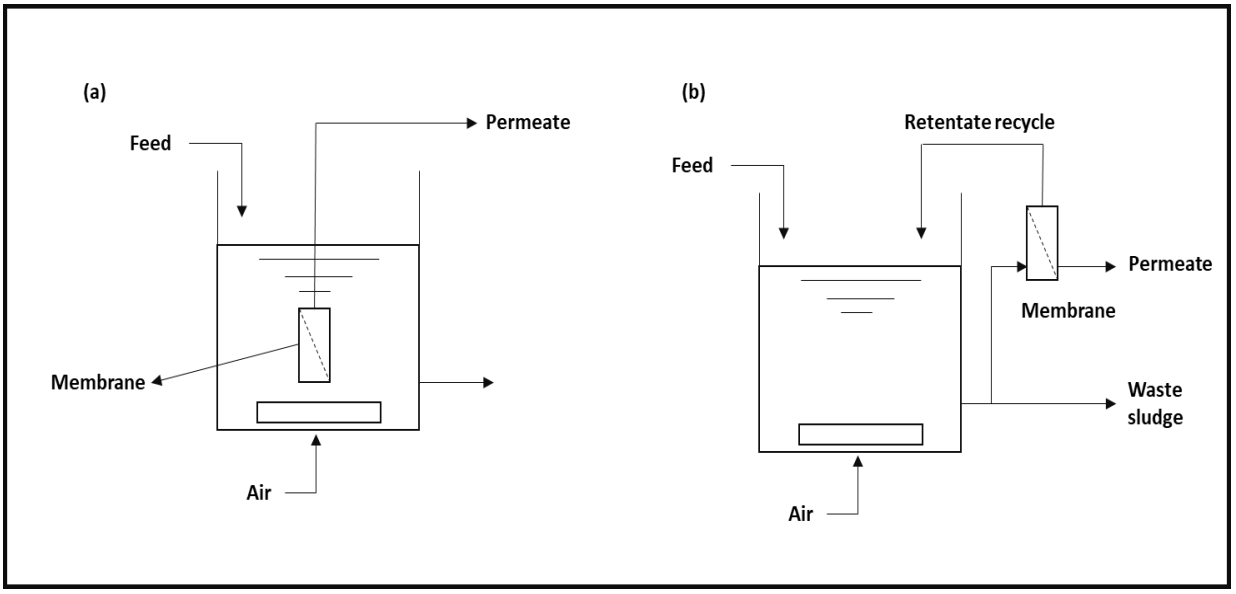

Figure 2-15: MBR configurations: (a) Immersed and (b) side-stream adapted from (Judd, 2008)

Owing to its compact design, the IMBR configuration has become a very attractive and popular option for decentralized systems (Cecconet *et al.*, 2019). An IMBR needs a very small land area and the management of the installations in this configuration is also easy. Hence, it can be installed very near to residential buildings (Singhania *et al.*, 2012). The application of the IMBR configuration has been employed in different decentralized applications such as in complete separation of liquid and solids (Kim *et al.*, 2008), in bathing wastewater treatment where high rate removal of COD was reported (Xia *et al.*, 2008), and in drinking water purification (Yamamura *et al.*, 2007). From these few examples, it can be concluded that the IMBR technology could certainly be an attractive option for decentralized sanitation systems.

2.3.2. Historical background

The MBR technology was first introduced in the late 1960s by Dorr-Olivier Inc. (Benedek & Côté, 2006; Le-Clech *et al.*, 2006; Radjenović *et al.*, 2008). They combined the use of an activated sludge bioreactor with a crossflow membrane filtration loop. Although the idea of replacing the clarifier of the conventional water treatment process was attractive, it did not gain much interest. It was difficult to justify the use of this process due to the high cost of membranes, low economic value of the product (tertiary effluent), and rapid loss of system performance due to fouling. The focus, therefore, shifted to attaining high fluxes and reduce fouling in the system through pumping the mixed liquor suspended at a high crossflow velocity. This resulted to high energy cost, thus leading

to the next stage of MBR development.

The breakthrough in the MBR technology came in 1989 with the idea of Yamamoto and his co-workers to immerse the membranes in a bioreactor (Benedek & Côté, 2006). This gave rise to the immersed membrane bioreactors (IMBRs), which had reduced energy consumption. The concept was picked up by Japanese companies Kubota and Mitsubishi Rayon who continued the research and development, and then commercialized the technology. Kubota developed the first flat sheet modules, while Mitsubishi focused on fine hollow fibres (Singhania *et al.*, 2012).

2.3.3. Performance of IMBRs

Operations of MBR systems are largely characterized by hydraulic and purification performance. The purification performance of MBRs is mainly presented in terms of chemical oxygen demand (COD), total suspended solids (TSS), and turbidity reductions. Permeate fluxes and fouling, which are related to hydraulic retention time, sludge retention time (SRT) and feed characteristics, are used to represent the hydraulic performance of the MBR systems.

Due to their improved design, IMBRs have been reported to have improved performance compared to other MBR systems. While early MBR systems were operated at a high SRT of around 100 days with mixed liquor suspended solids (MLSS) level of 30 g/L, the IMBRs apply lower SRT of around 10-20 days, resulting in more manageable MLSS levels of 10-15 g/L. Details of other operating parameters that characterizes the performance of IMBR systems are presented in Table 2-2.

Table 2-2: Performance characteristics of an IMBR system

Parameter	Value ranges	References
MLSS	10-15 g/L	(Le-Clech *et al.*, 2006; Singhania *et al.*, 2012)
Hydraulic retention time (HRT)	3-10 hours	(Judd, 2011; Singhania *et al.*, 2012)
SRT	10-20 days	(Le-Clech *et al.*, 2006; Singhania *et al.*, 2012)
Flux	20-50 LMH	(Böhm *et al.*, 2012; Chang, 2011)
COD removal	>95%	(Al-malack, 2007; Campo *et al.*, 2017)
TSS removal	100%	(Ivanovic *et al.*, 2008; Le-Clech *et al.*, 2006)
E.coli removal	99.99%	(Ueda & Hata, 1999)
Turbidity	<1 NTU	(Gander *et al.*, 2000)

2.3.4. Fouling and fouling mitigation in IMBRs

Membrane fouling is a major obstacle in the wider application of immersed membrane bioreactors as it results in the deterioration of the permeate flux and an increase in the operational cost. The fouling in immersed membrane bioreactors (IMBRs) is as a result of the interaction between the sludge suspension and the membrane modules. The suspended sludge is usually composed of varied salts, organics substances, colloids, microbial cells and sludge flocs, which are all potential foulants that are responsible for membrane fouling (Lin *et al.*, 2014; Singhania *et al.*, 2012).

Among these potential foulants, Extracellular polymeric substances (EPS) are seen as the key substances which have complex interactions with other foulants and fouling mechanisms in IMBRs. They can block membrane pores, adhere to membrane surfaces, affect cake structure and induce osmotic effects, thereby having a profound effect on the performance of the membranes (Lin *et al.*, 2014). Furthermore, EPS poses complex characteristics such as surface charge, adhesive properties and hydrophobicity, which play crucial roles in flocculation, stability and dewatering behaviour of sludge flocs (Campo *et al.*, 2017). Thus, EPS play a big role in membrane fouling in IMBR systems.

In order to maintain sustainable operations in immersed MBRs, membrane fouling must be controlled. There are various methods that have been investigated and adapted in IMBR systems to minimize fouling. The two most important methods include operation at subcritical flux conditions (Gander *et al.*, 2000; Wang *et al.*, 2008; Li *et al.*, 2013), and intensive air-scouring of membranes (Judd, 2008; Meng *et al.*, 2009; Ndinisa *et al.*, 2006; Tian *et al.*, 2010). These two methods will be discussed further in the following subsections.

2.3.4.1. Operation at subcritical flux

As it was discussed in subsection 2.2.5.3, operating at a subcritical flux condition is one of the techniques used in membrane processes to minimize fouling. This technique has been extensively employed as one of the ways of minimizing fouling in IMBR systems (Chu *et al.*, 2014; Field *et al.*, 1995; Wang *et al.*, 2008). In one study (Melidis *et al.*, 2016) where a pilot scale immersed MBR was used to treat municipal wastewater, operation at a subcritical flux condition was used to minimize fouling for more than one hour, and no increase in ΔP was observed throughout the run. Guglielmi *et al*., also observed a similar phenomenon when using an IMBR for municipal wastewater treatment (Guglielmi *et al.*, 2007). It is important to note that this only applies to short-term operation of membrane filtration processes (Meng *et al.*, 2009).

However, for long-term operation of filtration processes, it has been reported by a number of researchers that even at very low fluxes, an increase in ΔP normally takes place with time (Hwang *et al.*, 2008; Wang *et al.*, 2008; Li *et al.*, 2013). Hwang *et al* noted that for an IMBR, a period of relatively slow increase in ΔP was followed by a sudden rise in the ΔP (Hwang *et al.*, 2008). It has been widely accepted that this subcritical fouling is caused by organic macromolecules such as EPS, soluble microbial products (SMP) and possibly other substances that are released during cell lysis (Pollice *et al.,* 2005; Wang *et al.*, 2008). This prompted the introduction of a flux known as sustainable flux.

The sustainable flux is a flux at which the fouling rate is operationally and economically acceptable for IMBR operations (Wang *et al.*, 2008). It is usually characterized by two-stage increase in ΔP, that is, an initial slow and gradual increase followed by an abrupt rise in the ΔP (Hwang *et al.*, 2008). Figure 2-16, which was adapted from Hwang *et al,* illustrates this concept.

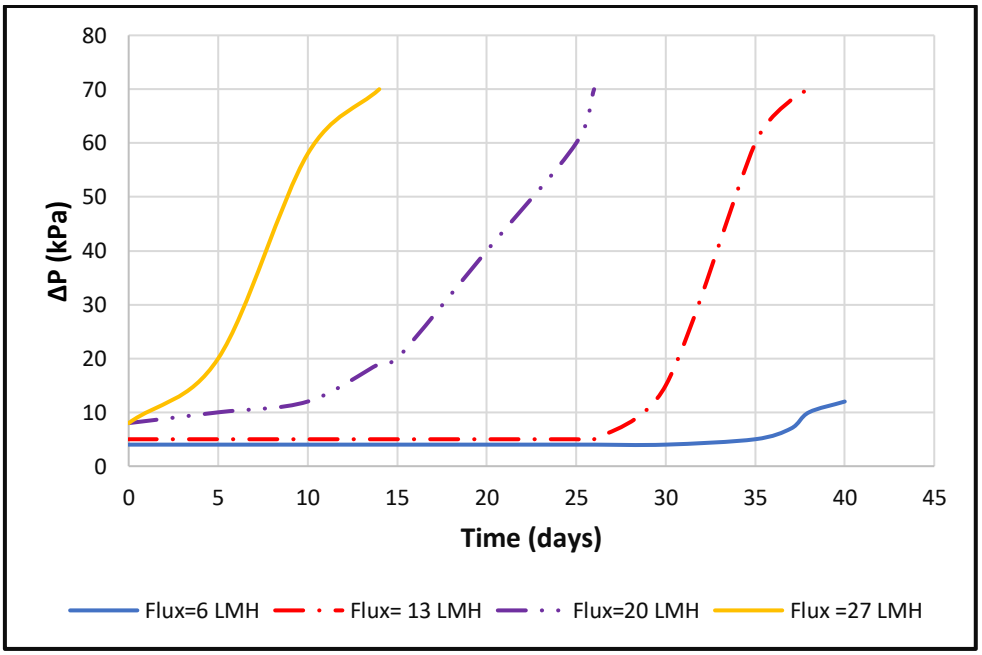

Figure 2-16: ΔP profiles for filtration runs with different fluxes, redrawn from (Hwang, *et al.*, 2008)

Hwang *et al.,* estimated the critical flux to be around 14 LMH, and carried out a filtration process of synthetic wastewater at fluxes below and above the critical flux. From Figure 2-15, it could be seen that when the IMBR system was operated at sub-critical fluxes of 6 and 13 LMH, there was a minimal increase in the ΔP in the first 35 and 30 days, respectively. This was then followed by an abrupt rise in the ΔP in the following days. However, at fluxes higher than 14 LMH, the increase in ΔP occurred within the first early days. This made operating above the critical flux unsustainable and uneconomical, as a rapid increase in ΔP always corresponds to a faster decrease in permeate

production and a rapid increase in fouling. Therefore, in order to minimize fouling, it is economical to operate an IMBR system at a sustainable flux.

2.3.4.2. Air scouring of membranes

Air scouring is one of the fundamental strategies that has been extensively applied to mitigate membrane fouling in submerged MBR systems (Judd, 2008; Tian *et al.*, 2010). During the aeration process, a shear stress is created near the membrane surface (Meng *et al.*, 2008). This facilitates the back transport of foulants from the membrane, thus minimizing fouling.

It has been reported that for immersed MBRs (IMBR), increasing the aeration rate is an effective strategy for membrane fouling retardation. In one investigation, Nywening and Zhou reported that the fouling rate decreased exponentially with an increase in air scouring intensity (Nywening & Zhou, 2009). The effect of aeration rate on membrane fouling was revealed in an investigation by Ibrahim, where he evaluated air-scouring as a means of mitigating fouling in a submerged MBR (Ibrahim, 2018).

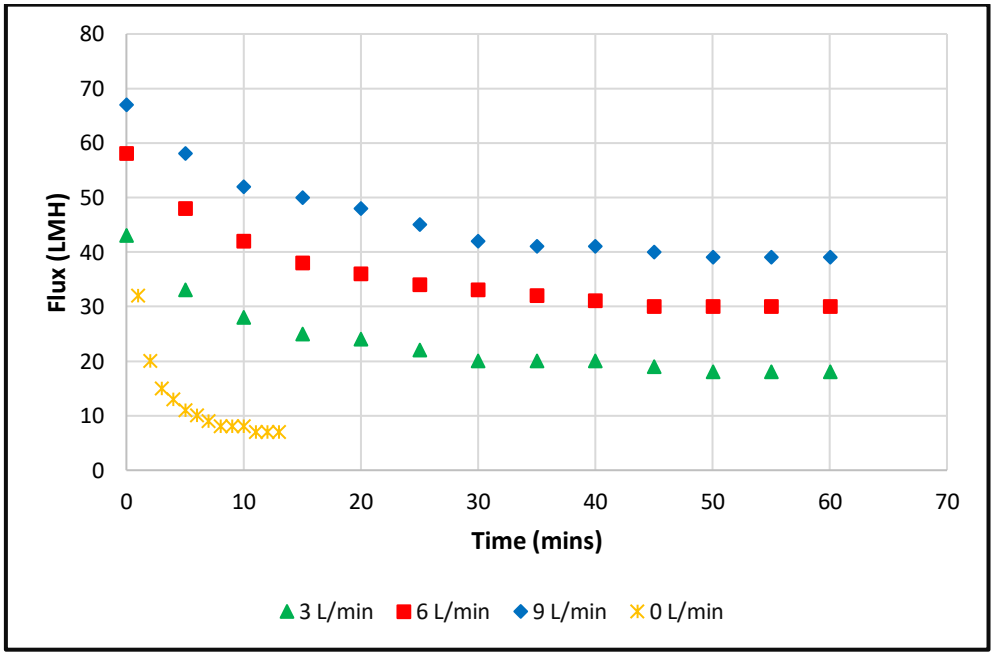

Figure 2-17: Flux profiles at different air scoring rates for membranes in an IMBR system, redrawn from (Ibrahim, 2018)

From Ibrahim's findings shown in Figure 2-17, it was concluded that the higher the aeration rate, the higher the permeate flux. The high flux values at high aeration rate are attributed to the high shearing stress produced by high intensity air bubbles that sweep foulants away and results in low fouling. This in turn increases the membranes' permeability (Trussell *et al.*, 2007). Therefore, air-scouring is essential in minimizing fouling in IMBR systems.

However, as reported by Ding *et al*., aeration intensity has an impact on the mixed liquor organic matter fraction and correspondingly influences the fouling rate (Ding *et al.*, 2016). Therefore, an optimum aeration intensity coupled with other membrane cleaning methods such as backwashing are usually employed in the immersed MBR systems.

2.4. Woven fabric immersed membrane bioreactors

2.4.1. Overview

The woven fabric immersed MBR (WF-IMBR) is a relatively new technology that integrates the WFMF technology with the immersed MBR for applications in wastewater treatment. The motivation behind its inception was the need for an immersed MBR system that is suitable for applications in developing countries. This involved using a membrane such WFMF membrane that is robust in nature, as well as less costly compared to the commercial membranes (Cele, 2014; Pillay & Jacobs, 2008). Hence, the development of the WF-IMBR system. Since its inception, very few investigations have been reported on the WF-IMBR technology. A summary of these studies is listed in Table 2-3.

Table 2-3: A summary of previous investigations on the WF-IMBR technology

Configuration	Feed characteristics	Operation conditions	Performance	References
WF-IMBR system with 20 flat sheet modules and membrane area of 7.14 m^2 on a pilot scale	**Type**- real activated sludge **MLSS**- 4-16 g/L	**Flux**-30 LMH SRT-30 days **HRT**-24 h **Membrane cleaning** – air scouring (10 L/min) rate	**Permeate turbidity**-<1NTU **MLSS removal**- 100% **COD removal** -95%	(Cele & Pillay, 2010)
WF-IMBR system with 5 flat sheet modules and membrane area of 1 m^2 on a pilot scale	**Type**- domestic wastewater **MLSS**-8 g/L	**Flux**-6.7-7.6 LMH **HRT**- 10-15 h Membrane cleaning-brushing, solar drying, chemical cleaning	**Permeate turbidity**-0.01 NTU **COD removal**-88-91.2% **Nitrogen removal**-88-99.1%	(Vongsayalath, 2015)
WF-IMBR system with 19 flat sheet modules and membrane area of 5.12 m^2 on a pilot scale	**Type**- raw sewage feed or activated sludge **MLSS**-9-14 g/L	**Flux**-<25 LMH **HRT**-4-7 h **Membrane cleaning**-air scouring (7.5-12.5 L/min)	**Permeate turbidity**-<1 NTU **COD removal** – 96%	(Pillay *et al.*, 2016)

2.4.2. Performance of WF-IMBR systems

The WF-IMBR system has been reported to perform well in terms of permeate quality in wastewater treatment applications. This can be seen from Table 2-4 where the permeate quality from the WF-IMBR system seems to compare well with that of the various commercial immersed MBR systems including those from Kubota and Zenon. In terms of the flux, the latest design of WF-IMBR system was found to have a critical flux of around 25 LMH (Pillay *et al.*, 2016). This flux is within the estimated range of current commercial membranes (Böhm *et al.*, 2012; Chang, 2011).

Table 2-4: Performance comparison of the WF-IMBR system to other commercial IMBRs, in terms of permeate quality

Parameter	Type of MBR system		
	Kubota[a, b, c]	Zenon[d, e]	WF-IMBR[f, g]
COD removal %	>94	>94	>95
BOD removal %	>97	>98	-
TSS removal %	100	100	100
Coliform bacteria removal %	99.99	-	99.9
Turbidity (NTU)	<1	<1	<1

[a](Ueda & Hata, 1999) [b](Hu & Stuckey, 2006) [c](Hoinkis *et al.*, 2012) [d](Ivanovic *et al.*, 2008) [e](Campo *et al.*, 2017) [f](Cele, 2014) [g](Pillay *et al.*, 2016)

However, in the investigation of Pillay *et al.* on wastewater treatment, it was found that the system could not operate stably at sub-critical flux conditions (Pillay *et al.*, 2016). They reported that the TMP increased immediately the filtration process was started and doubled within six hours. This was attributed to the fouling of the membranes. Hence, fouling posed a challenge in the operation of the WF-IMBR system in wastewater treatment. More detail on fouling in WF-IMBR system is discussed in the next section.

2.4.3. Fouling in WF-IMBR systems

In principle, an immersed MBR (IMBR) needs to be operated under hydrodynamic conditions where fouling of membranes is minimized. As discussed in subsection 2.3.4, this is commonly done through subcritical flux operations and air scouring of membranes. Hence, a recent investigation on WF-IMBR operated the system under these conditions evaluated its performance (Pillay *et al.*, 2016).

2.4.3.1. Latest investigation

In their effort to ensure that minimum fouling occurs in the system during wastewater treatment, Pillay *et al.* operated the WF-IMBR system at subcritical flux conditions. First, the critical flux of the modified system was investigated and found to be around 25 LMH. They then proceeded to conduct the first subcritical operation trial at an initial flux of 15 LMH, where the permeate flux and ΔP were measured and recorded at different time intervals. The results are shown in Figure 2-18.

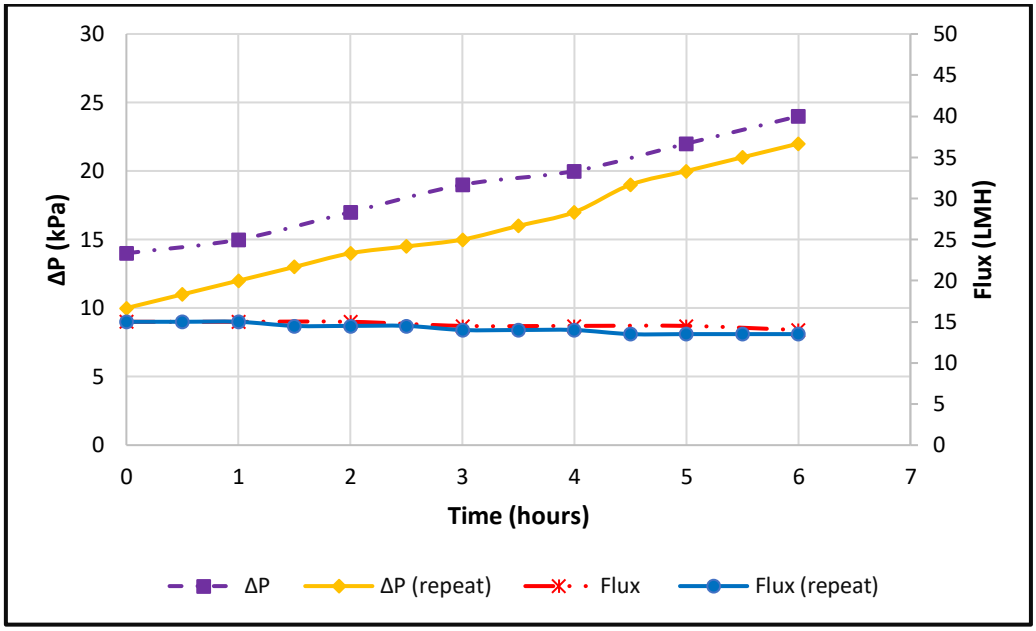

Figure 2-18: Flux and ΔP profiles at a flux of 15 LMH, for a system with an estimated critical flux of 25 LMH, redrawn from (Pillay *et al.*,2016)

During the run, the membrane modules were air-scoured at a rate of 7.9 L/min per module. Within an hour of commencement of the filtration process, the ΔP began increasing and doubled within six hours. Similar results were reported when the experiment was repeated. From these results, it was clear that the system was not stable at subcritical flux conditions.

The runs were then repeated at two lower fluxes of 10 and 5 LMH. The earlier reported trend was again observed for both fluxes. It was therefore clear that it is not possible to operate the WF-IMBR system at stable subcritical conditions, even at very low fluxes (Pillay *et al.*, 2016).

Pillay *et al.* went further to explore the second strategy of minimizing fouling in IMBR systems. They investigated the efficiency of air-scouring at minimizing fouling in the WF-IMBR system. Given that the 7.9 L/min per module air-scouring rate was not sufficient in minimizing fouling in the previous runs, they decided to increase the rate and also evaluate its effect on fouling rate. Aeration rates of 0 L/min, 7.5 L/min, 10 L/min and 12.5 L/min at two subcritical fluxes of 20 LMH and 11 LMH were

investigated. The effect of aeration rate on membrane fouling was presented in terms of resistance profiles. One of the findings is shown in Figure 2-19.

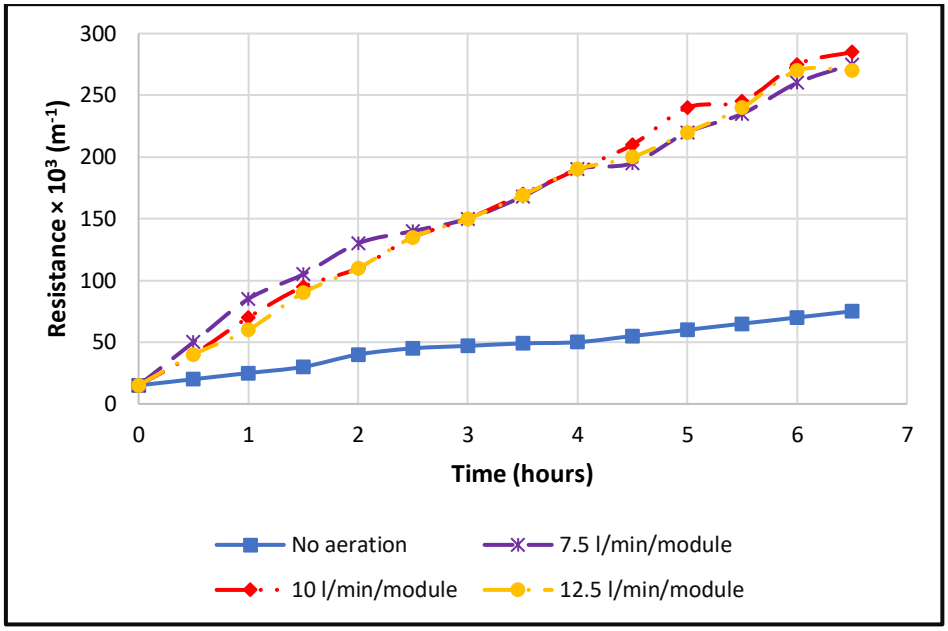

Figure 2-19: Resistance profiles for filtration runs with a starting flux of 20 LMH at different air scouring rates, redrawn from (Pillay *et al.*,2016)

From Figure 2-19, it can be observed that the aeration rate over the investigated range had little effect on the increase in fouling resistance. Regardless of the aeration rate, the same fouling resistance was eventually reached after approximately six hours. These reported results do not correlate with what has been described in subsection 2.3.4.2 about the effect of air scouring rate on fouling in conventional submerged MBR systems (Pillay *et al.*, 2016).

However, the contradicting results emerging from Pillay *et al.*'s investigation is that the lowest growth of filtration resistance was obtained with no aeration. These findings imply that operating an IMBR system without air scouring the membranes would give a better permeate production relative to operating the IMBR with aeration. This completely contradicts the whole design concept of an IMBR system as discussed in subsection 2.3.4.2, and all the major findings from literature on IMBR to date. The literature suggests the opposite, i.e. that high scouring rates result in low fouling rates.

Pillay *et al.* also reported that cleaning of the fouled WFMF membranes posed a major challenge. The membranes' permeability could neither be restored by brushing nor by backwash (Pillay *et al.*, 2016). But after a sodium hypochlorite soak followed by backwash, the membranes' managed to return to their original permeability. This gave an indication of organic fouling that had deeply penetrated into the membranes (Chollom *et al.*, 2017). Sodium hypochlorite is mostly used to

oxidize organic and biological foulants, and thus facilitate their removal from membrane surfaces (Guan *et al.*, 2018; Meng *et al.*, 2017). Furthermore, the additional use of backwash to dislodge foulants shows that the organics had penetrated deep into the membranes.

2.4.3.2. Postulation on the anomalous findings

The investigation of Pillay *et al.* postulated that these findings could be due to high content of EPS in the feed samples. It has been reported that the content of EPS in activated sludge is usually high when the bacteria are stressed (McAdam *et al.*, 2011). Pillay *et al.* therefore assumed that when the WF-IMBR system was operated with high aeration rates, all the bacteria seem to have been swept away from the membrane surfaces which allowed the EPS to easily penetrate the membrane surfaces. On the other hand, when the system was operated without aeration, the bacteria seemed to have formed a layer, which prevented EPS from reaching the membrane surfaces. (Deelie, 2017; Pillay *et al.*, 2016). This is due to the fact that the bacteria are relatively 'large' (2 µm to 5 µm), easy to filter and have a low fouling propensity. Conversely EPS forms a gel-like structure, and easily penetrate the membranes. In addition, the study also suggested that the anomalous findings may also be due to the different fouling characteristics of the WFMF membranes compared to the normal membranes.

2.4.3.3. Research gap

From Pillay *et al*. investigation on the performance of WFMF membranes on wastewater treatment, the following problems were reported:

- It was not possible to operate the WF-IMBR system at stable subcritical conditions as other IMBR systems. It was reported that the TMP increased shortly after the commencement of the filtration process even at low fluxes.
- Increase in the air-scouring rate was not able to minimize the membrane fouling. Surprisingly, low growth of the filtration resistance was experienced without any aeration compared to that with aeration at relatively higher rates.
- The membranes were difficult to clean and required both a soak in hypochlorite and a backwash to restore their original permeability.

It was reported that all of the above findings point to significant organic fouling of the membranes, that could not be removed by either brushing or both brushing and soaking techniques used previously. Following these contradicting findings about air-scouring in minimizing fouling in the

WF-IMBR system, this study proposed to investigate the fouling characteristics in WFMF membranes, with a view to establish the best strategy of minimizing fouling. Furthermore, it sought to develop an oleophobic WFMF membrane that will be able to repel organics such EPS from the membranes' surfaces, in order improve the performance and cleanability of the membranes.

2.4.4. Restoration of fouled WFMF membranes

As discussed in the previous sections, fouling of membranes during filtration processes remains a major operational challenge. As a result, cleaning of the fouled membranes to restore their original performance is very essential.

Various potential methods for restoring fouled WFMF membranes have been evaluated. They include: water scouring, air scouring, backwash, sodium hypochlorite soak and brushing (Alfa *et al.*, 2016; Chollom *et al.*, 2017; Pillay, 2009; Pillay *et al.*, 2016). The efficiency of some of the above-mentioned methods in restoring the original permeability of the WFMF membranes are illustrated in Figure 2-20. These results are from preliminary experiments carried out during this study.

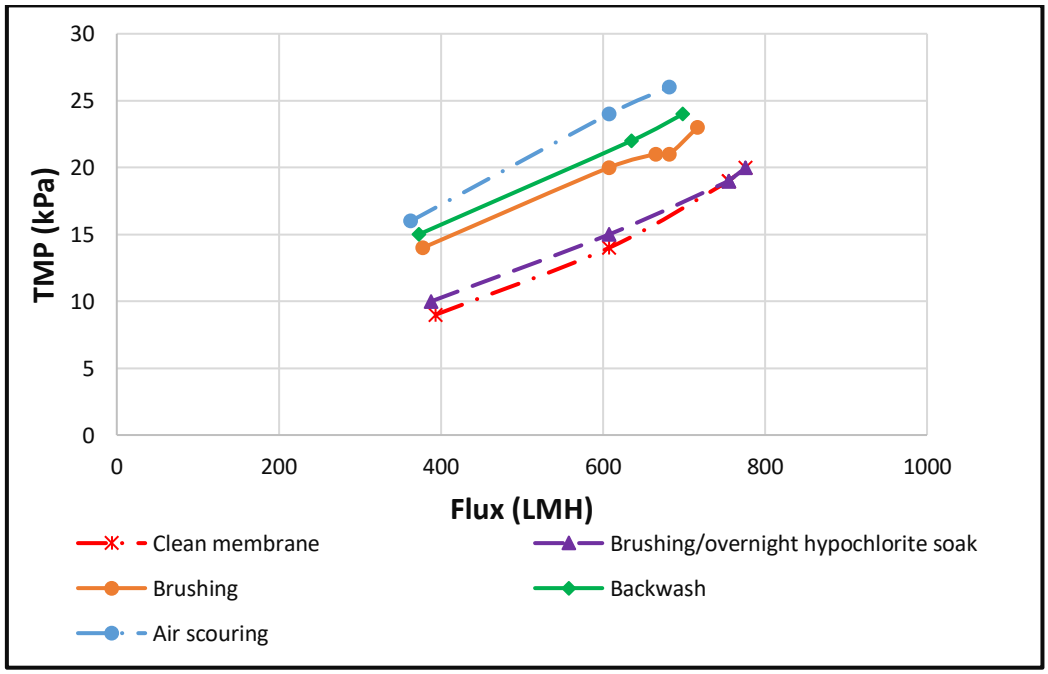

Figure 2-20: Pure water flux results for WFMF membranes after being restored using various cleaning methods (The data was obtained from preliminary runs done in this study)

With respect to the cleaning efficiency, a sodium hypochlorite soak and brushing are considered to be at the top of the hierarchy. This is because a cleaning strategy involving a sodium hypochlorite soak followed by brushing completely restores the fouled WFMF membranes (Alfa *et al.*, 2016; Chollom *et al.*, 2017). The hypochlorite soak is reported to oxidize and remove organic foulants

within the membrane matrix, while the action of brushing can remove foulants in between the membrane fibres.

2.5. Membrane surface modification

2.5.1. Membrane surface characteristics

Various surface characteristics such as surface charge, surface roughness, hydrophilicity, and oleophobicity play important roles in the degree of membrane fouling. This is because they determine the interaction between the membranes and the foulants (Gkotsis *et al.*, 2014; Nady *et al.,* 2011). Therefore, a brief understanding of the various membrane surface characteristics and their relationship to fouling is important. This would help in understanding how to modify the membrane surfaces in order to minimize fouling.

2.5.1.1. Surface charge

This is the electrostatic attraction or repulsion of the membrane surface. This property of the membrane has an antifouling effect depending on the charge of the contaminants in the feed being filtered through it (Breite *et al.*, 2015). If the membrane surface has similar charges as the foulants, the surface will repel them and prevent deposition of the materials, thus subsequently reducing fouling, as shown in Figure 2-21 (Gkotsis *et al.*, 2014).

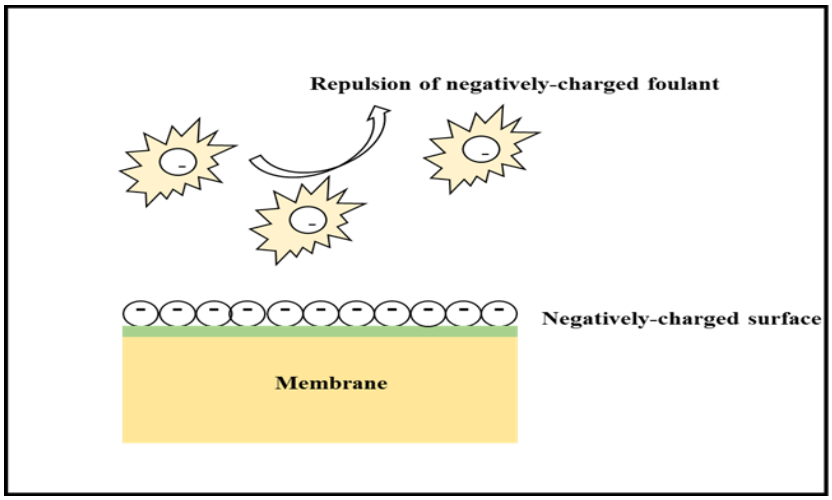

Figure 2-21: Illustration of fouling mitigation through modification of membrane surface charge redrawn from (Kochkodan *et al.*, 2014)

Therefore, the membrane surface charge is modified according to the feed that will be filtered through it. The surface charge can be tailored by anchoring either anionic or cationic groups on the membrane surface (Kumar & Ulbricht, 2014). Surface charge can be quantified by measuring the Zeta potential of the membrane surface.

2.5.1.2. Surface roughness

Surface roughness influences fouling depending on the particle size of the foulants in the wastewater and whether the foulants are soluble. For soluble foulants like organics, an increase in the surface roughness increases the interacting surface between the membrane and the foulants, thus increasing fouling. But when the foulants particles are larger, the surface roughness does not affect the membrane fouling (Zhang *et al*., 2015). This has been illustrated by Figure 2-22.

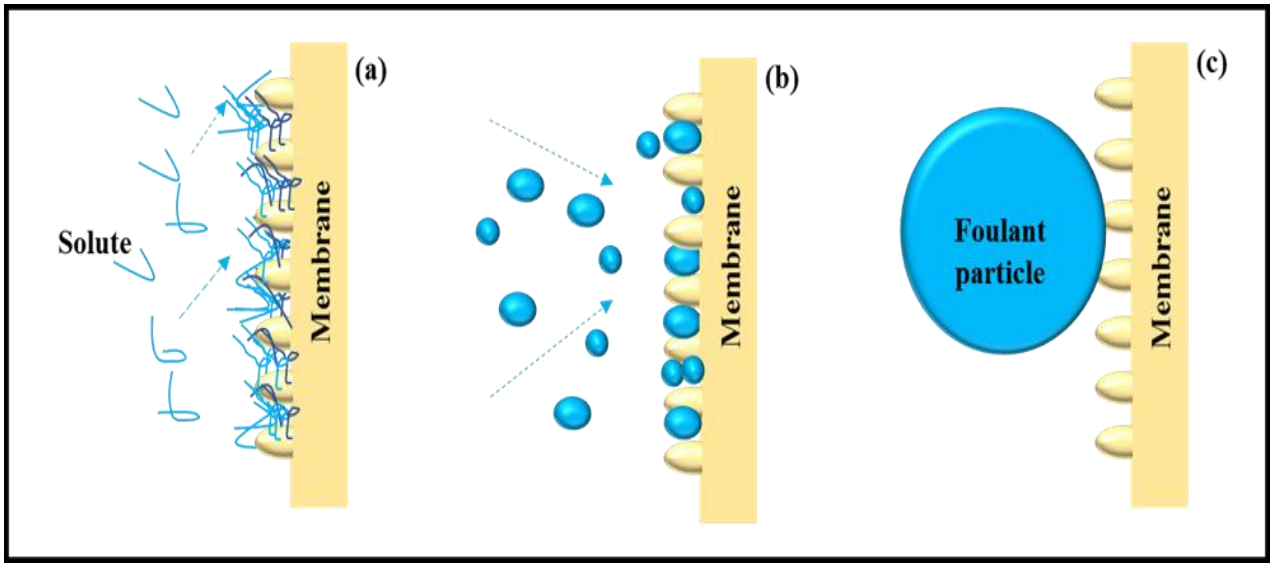

Figure 2-22: Foulant interaction with rough membrane surface associated with: (a) solute (b) small size foulant particles (c) large size foulant particles redrawn from (Zhang *et al.*, 2015)

2.5.1.3. Hydrophobicity/hydrophilicity

Membrane hydrophobicity and hydrophilicity describe the water wetting characteristics of a membrane surface. Hydrophobic membranes have low affinity to water while the hydrophilic membranes have high affinity for water. Thus, hydrophilic membranes allow water to pass through them more easily, unlike membranes with hydrophobic surfaces. This gives the hydrophilic membranes the tendency to have better filtration performance due to their high water permeability properties (Zhu *et al.*, 2013).

Furthermore, hydrophilic membranes perform better than hydrophobic ones in minimizing biological and organic fouling. The antifouling mechanism has been attributed to the formation of a tight bound layer of water. This minimizes the adhesion of foulants brought to the vicinity of the membrane surface by the convective flow (Miller *et al,*, 2017) as illustrated in Figure 2-23. Therefore, hydrophilic membranes are more preferred in the wastewater treatment industry than

the hydrophobic ones. The woven fabric membrane being used in this study is slightly hydrophilic with a water contact angle of 76˚ (Mecha & Pillay, 2014).

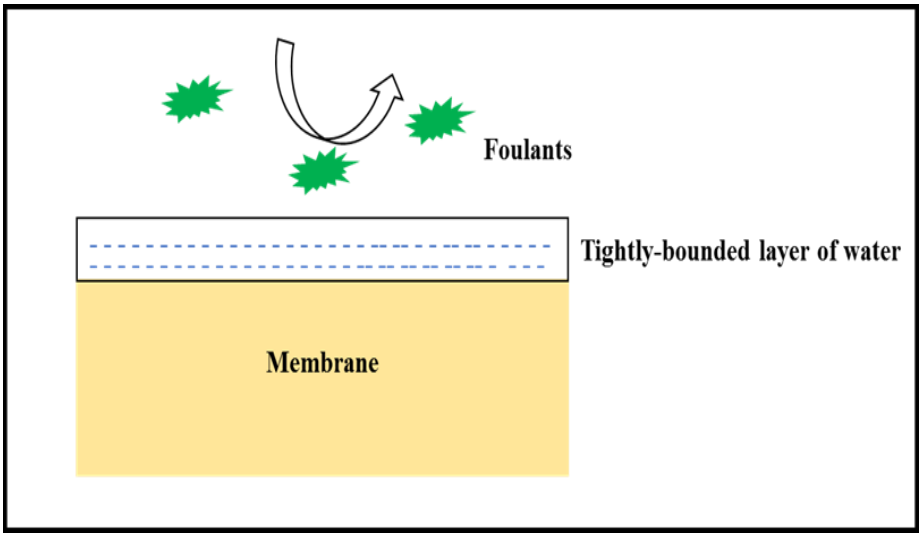

Figure 2-23: Illustration of fouling mitigation by a hydrophilic membrane surface redrawn from (Kochkodan *et al.*, 2014)

Despite the desirable characteristics of these type of membranes, it has been reported that some hydrophilic membranes still get fouled. This is because the hydration layer may be broken by the drag force exerted as result of filtration pressure. Furthermore, the forces of interaction between the foulants and the membranes may be greater than that between the foulants and the water. Thus, the foulants tend to be attracted towards the membrane surfaces (Zhu *et al.*, 2013). This was also witnessed on the woven fabric microfiltration (WFMF) membrane during a previous investigation (Pillay *et al*, 2016). Therefore, hydrophilic characteristic may not be sufficient minimize fouling to a large extent.

2.5.1.4. Oleophobicity

Oleophobicity is the tendency of a surface to be oil-repellent because of its lower surface energy compared to the surface tension of oil, which is in the range of 10-20 mN/m (Jain *et al.*, 2019). The lower energy of the oleophobic surface causes it to have minimal cohesive interaction with oil or any other substance with a higher surface tension than oil. Thus, oleophobic surface can be expected to be more effective in repelling most organic foulants whose surface energy is greater than that of oil (Zhu *et al.*, 2013). Figure 2-24 illustrates how this principle works in an oleophobic membrane to minimize fouling.

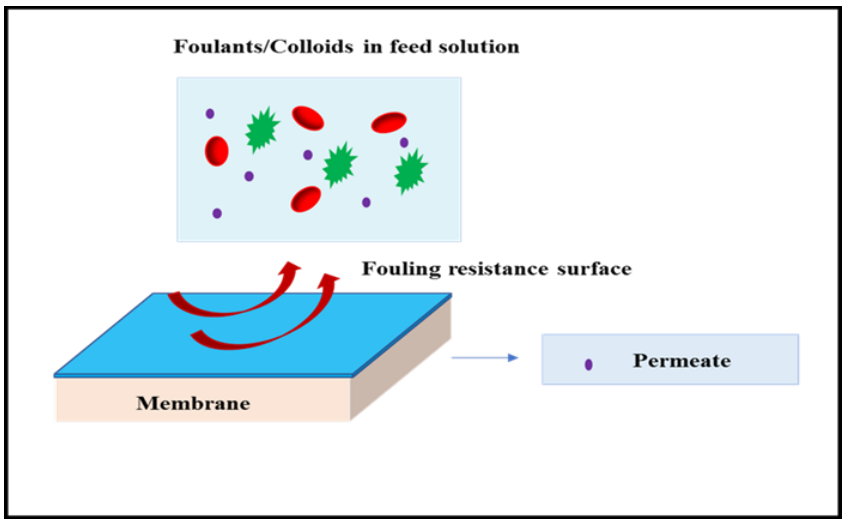

Figure 2-24: Illustration of fouling mitigation by an oleophobic membrane surface redrawn from (Ayyavoo *et al.*, 2016)

Fluorocarbon compounds are commonly used to achieve oleophobic surfaces in industries. This is because the CF_3 alignments in these compounds have a very low surface free energy of 6 mJ/m^2 (Yang *et al.*, 2013). The low surface energy helps in repelling substances of high surface energy such as oil and organics. Therefore, oleophobic surfaces have attracted attention in separation industries because of their self-cleaning abilities through the repulsion of oil and organics (Nakashima *et al.*, 2017; Saito *et al.*, 2016; Yang *et al.*, 2013).

However, there is a limitation. Oleophobic surfaces also tends to possess hydrophobic properties too. This is because they have surface energies below that of the surface tension of water which is 73 mJ/m^2 (Jain *et al.*, 2019). This makes oleophobic surfaces water repellent. Hence, membranes with oleophobic surfaces tend to have lower water permeability as compared to oleophilic membranes.

This therefore makes a membrane with both hydrophilic and oleophobic properties the best option for wastewater treatment. The former characteristic would achieve higher water permeability while the latter would provide low interaction strength between the membrane surface and the organic foulants. However, hydrophilicity and oleophobicity are two opposite surface properties which cannot be achieved by a single polymer. Therefore, both characteristics can only be achieved through a layer-by-layer coating method (Zhu *et al.*, 2013). This is when one characteristic is achieved first then the other follows through coating. That is, hydrophilicity then oleophobicity or vice versa.

This research project sought to introduce the oleophobic property onto the slightly hydrophilic woven membrane to achieve a combination of these two properties. This would result into a low

fouling microfiltration membrane.

2.5.2. Membrane modification techniques

The undesirable interaction between foulants and membranes can be reduced through the technique of membrane modification. Membrane modification methods such as coating, blending, functionalization, and grafting have been employed for various polymeric membranes. These techniques can either be done during the membrane manufacturing stage or after they have been fabricated (Ayyavoo *et al*., 2016; Kochkodan *et al*., 2014; Nady *et al*., 2011). Therefore, it is essential to know what each technique entails, as this will assist in selecting the most suitable method for the modification of a membrane. It is also important to identify specific options ideally suitable for the modification of the woven fabric microfiltration (WFMF) membranes.

2.5.2.1. Coating

Coating is a technique where the coating material forms a thin layer that non-covalently binds to the membrane surface (Nady *et al.*, 2011). The coating is usually applied directly on top of the membrane surface, and thus this technique is suitable as a post-modification method (Ayyavoo *et al*., 2016). An investigation by Akbari *et al*., where a polyamide NF membrane was coated with chitosan, is a good example of where this technique was employed in membrane fouling mitigation. The chitosan coating reduced the total resistance from 37.7% to 13.9% (Akbari *et al.*, 2015). This clearly shows the advantageous effect that can be achieved through coating. However the decrease in membrane's permeability and the stability of the coating during the filtration process are points of concern (Ayyavoo *et al*., 2016).

2.5.2.2. Blending

The blending technique is usually employed during membrane preparation and processing stages (Ayyavoo *et al.*, 2016; Miller *et al.*, 2017). It is a technique in which two or more polymers are physically mixed to obtain the required properties (Nady *et al.*, 2011). The proper selection and combination of polymeric components in a precise ratio can result in a blend with favourable properties for antifouling membranes (Ayyavoo *et al.*, 2016).

2.5.2.3. Functionalization with chemical treatment

Chemical treatment is a widely known technique of altering membrane surfaces with different functional group such as sulfone, carboxyl, hydroxyl among others. It can either be a pre-

modification or a post-modification technique. The main methods involved in chemical treatment include hydrolysis, substitution, oxidation, and addition. During these processes, the different functional groups get attached to the polymer or membrane surface thereby forming superior properties such as antifouling characteristics (Ayyavoo *et al*., 2016).

2.5.2.4. Grafting

This is a technique where monomers are covalently bonded onto the membrane. It can be initiated either by chemicals, high energy radiation, plasma, or enzymes. The choice of a specific initiator depends on the chemical structure of the membrane and the desired characteristic after the modification process (Nady *et al.*, 2011).

2.5.2.5. Combined technique

Recently, combined techniques have been used in modifying membranes. This involves using two or more methods in the alteration of membrane surface properties (Miller *et al.*, 2017; Nady *et al.*, 2011).

2.5.3. Options available for developing an oleophobic WFMF membrane

Having discussed the various modification techniques, as well as understanding oleophobicity and how it can attenuate membrane fouling, this subsection will discuss various options available for imparting oleophobic property to the WFMF membrane.

The membrane surface modification techniques discussed in subsection 2.5.2 are general methods and are not specific to particular membranes. In order to identify a suitable method for modifying a specific membrane, a survey of the various options presently available for modifying that specific membrane must be carried out. Since the WFMF membrane is a textile product, this subsection will examine specific modification options available in the textile industry for the development of an oleophobic WFMF membrane.

2.5.3.1. Functionalization of the membrane

As described in subsection 2.5.2.3, this option involves attaching functional groups onto the membrane. Chemical modification of the polyester chains that make up fibres in the WFMF membrane is possible. Assuming that the right chemicals are chosen, the end results will be a more oleophobic membrane. In one study (Demir, 2015), fluorinated polyesters possessing different end groups were synthesized using the Schotten-Baumann reaction. Three of such polyesters were

produced, namely, fluorinated isophthaloic acid polyester containing -OH and -COOH groups, fluorinated isophthaloyl polyester containing -OH and -CF_3 groups, and fluorinated diester isophthaloyl polyester containing only -CF_3. These modified polyesters were then blended with standard polyethylene terephthalate (PET) and their wetting characteristic measured using hexadecane. From the oil contact angle results, they all recorded an improvement in their oleophobic characteristic, with the greatest improvement being observed with the third polyester that contained fluoro groups. Therefore, functionalization might be an option in acquiring a more oleophobic WMFM membrane.

However, considering the complexities involved in functionalization, this option might take a long time. First, the right chemical treatment to be used must be found. Apart from this, an appropriate company will have to be contracted to do the conversion from a standard WFMF to a modified WFMF membrane. Furthermore, the modified yarn might behave differently from the original yarn thus affecting the WFMF membrane production process. If the attachment of the functional group to the membrane is done at a post-production stage, this might as well affect the macroscopic fabric performance. It was therefore imperative to explore other available options.

2.5.3.2. Changing the membrane composition

A second option of creating an oleophobic membrane is to change the fibre composition used in the WFMF membrane from polyester to a polymer which is inherently oleophobic. If an industrially available option is chosen, it will remove the need of modifying the chemical structure of polyester. This reduces the number of steps required to get from the current WFMF membrane to an oleophobic type by simply substituting the polymer yarn used during manufacturing process. Care must be taken to ensure that the yarns have the required weaving and further processing characteristics. This will ensure a direct substitution as far as possible, so that similar filtration performance is achieved when comparing the current WFMF membrane with the new oleophobic type.

Halogen containing polymers especially fluoropolymers and more specifically thermoplastic polyfluoroolefins, would be well suited for filtration due to their oleophobic properties (Wei, 2019). They are inert and chemically stable, ensuring no toxic substance will leach into the filtrate during filtration. Some industrially available options include polytetrafluoroethylene, polyvinylidene fluoride, polychlorotrifluoroethylene, ethylene tetrafluoroethylene, polyfluoroalkoxy alkane, ethylene chlorotrifluoroethylene, and fluorinated ethylene propylene (Gardiner, 2015). Among

industrially available fluoropolymers, polytetrafluoroethylene (PFTE) is the most widely studied as well as most widely available fluoropolymer (Li *et al.*, 2019; Nittami *et al.*, 2012; Zhao *et al.*, 2019). Therefore, it would be the recommended fabric of choice. It can be procured as either 100% PFTE or as a PFTE coated fiberglass. However, PFTE membranes are costly (Wei, 2019) and therefore will result in an expensive oleophobic WFMF compared to the current WFMF.

2.5.3.3. Changing the membrane surface structure

The manipulation of the membrane can be done by coating the entire surface of the membrane with an oleophobic layer. A study by Vasiljević *et al*. shows how a fluoroalkyl-functional siloxane (FAS) can be applied to polyester fabric's surface using a sol-gel coating process (Vasiljević *et al.*, 2013). The FAS once attached to the polyester via standard textile pad-dry-cure process, exhibited both hydrophobic as well as oleophobic character. A myriad of similar products for topical oleophobic are available commercially. Therefore, this option is direct and can easily be implemented both on a laboratory and industrial scale.

However, it is important to ensure that the oleophobic coating employed on the fabric surface does not form a continuous film that will block the pores. If the interstice where the yarn cross over as well as between the fibres are blocked, the filtrate will not be able to pass through. The imparted oleophobic properties will then be at the expense of the filtration capability of the WFMF membrane. This problem can be avoided by controlling the amount oleophobic coating to be applied on the membrane surface (Schindler & Hauser, 2004).

2.5.3.4. Summary of options

From the literature survey, the available options for developing an oleophobic WFMF membrane include functionalization of the standard WFMF membrane, changing the membrane composition of the WFMF membrane, and lastly modifying the surface of the standard WMF membrane. However, the option of functionalizing the standard WFMF membrane is considered complex and would take a long time to be realized on an industrial scale. The option of changing the membrane's composition was found to be expensive. This is because inherently available oleophobic materials such as PFTE are expensive. Hence, among the three options, the most feasible method that can be employed commercially; is the modification of the surface of the standard WFMF membrane. As discussed in subsection 2.5.3.3, this method is relatively simple and direct, and can easily be implemented on both laboratory and industrial scales.

2.5.3.5. Selection of an option

The previous subsection identified the option of modifying the standard WFMF membrane's surface as the best available option for developing the oleophobic WFMF membrane. Based on what is reported in literature, and advice from experts in the textile industry, the surface modification of the standard WFMF membrane can be best achieved through fluorocarbon application. This is due to the following reasons:

- Fluorocarbons can be used to impart oleophobic properties on surfaces (Dasdemir & Ibili, 2017; Yang *et al.*, 2013). In textile industries, they are the most preferred materials for achieving oleophobic properties in fabrics (Dasdemir & Ibili, 2017; Saffari *et al.*, 2015). This is due to their excellent ability of minimizing the surface energy of fabrics.
- It has already been proven that fluorocarbons can get attach to polyesters (Audenaert *et al.*, 1999; Demir, 2015).
- This option can be implemented industrially. This is because there are already available commercial fluorocarbon emulsions that are being used by the textile industry to impart oleophobic properties onto fabrics (Audenaert *et al.*, 1999; Dasdemir & Ibili, 2017; Saffari *et al.*, 2015).
- There is an already established process for applying fluorocarbon compounds onto fabrics. The process is known as the padding process (Sayed & Dabhi, 2014; Schindler & Hauser, 2004). More details about the padding process will be presented in the next section.

Owing to the abovementioned reasons, the application of fluorocarbon onto the standard WFMF membrane using a padding process was considered as the best option for developing an oleophobic WFMF membrane.

2.5.4. The padding process

2.5.4.1. Overview

The padding process is one of the major processes used in the textile industry for applying finishes onto fabrics. It is mostly used for chemicals that do not have affinity for fibres, such as fluorocarbon (FC). Basically, the process involves two steps, viz. immersion of the fabric in a pad liquor, followed by the squeezing-off process done using rollers. The amount of liquor taken up by the fabric is mostly related to the capillary effect between the fibres. This is facilitated by the pressure applied by the rollers during the squeezing-off process, where the liquor on the fabric is brought into closer contact

with the individual fibres for liquor uptake (Rouette & Kittan, 1991). Furthermore, the pressure of the rolls forces the liquor into the interstices and the fibres of the fabric (Huang & Liu, 2006). After the padding process, the fabric is taken through an oven to dry out the chemical and then cure it. The physical set-up and the block diagram of the pad-dry-cure (PDC) process are shown in Figures 2-25 and 2-26, respectively.

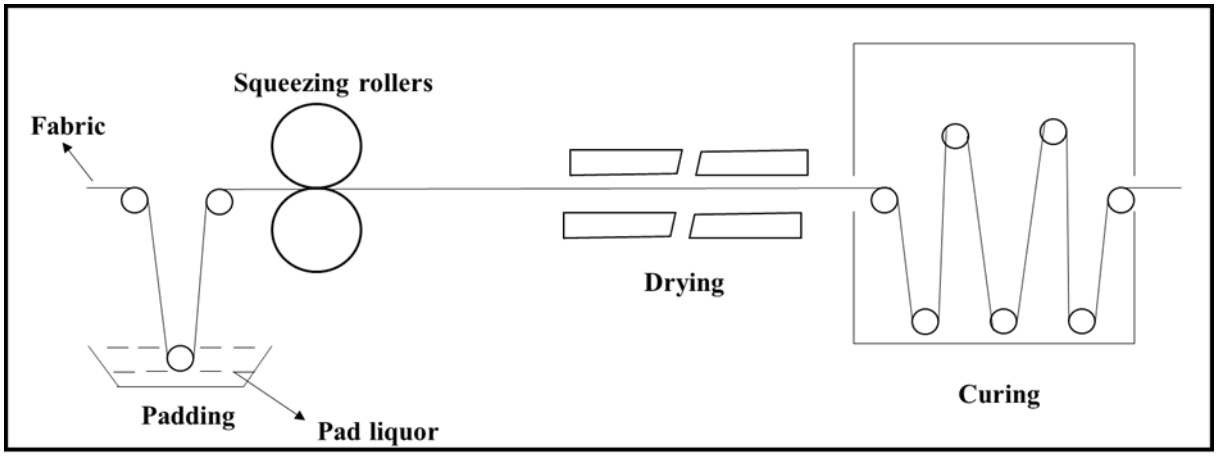

Figure 2-25: A schematic diagram of the pad-dry-cure process adapted from (Schindler & Hauser, 2004)

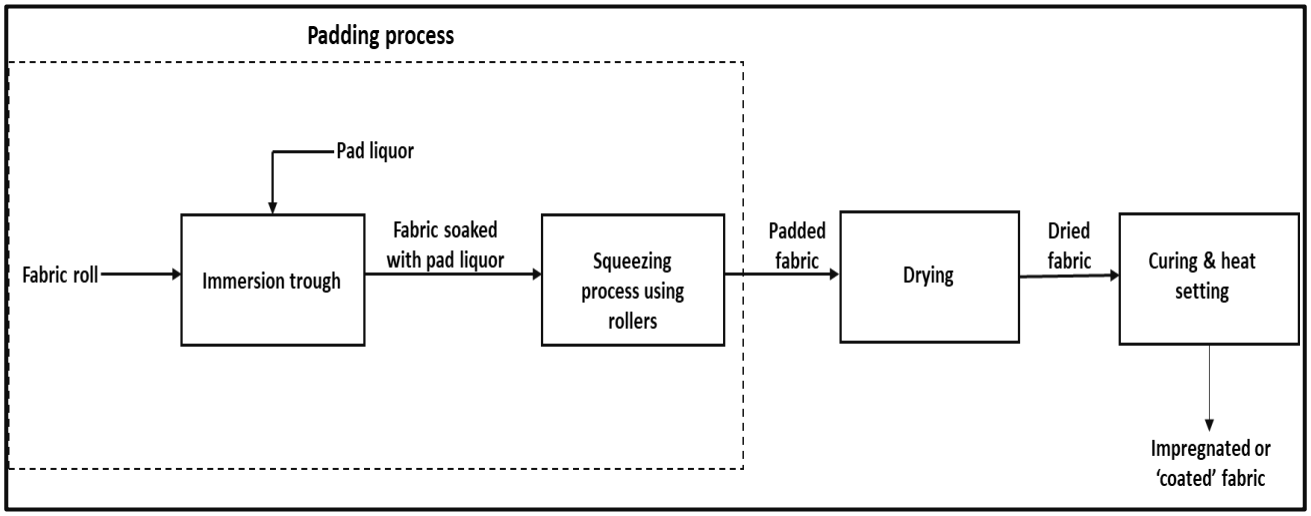

Figure 2-26: A block diagram of the pad-dry-cure process

Most fluorocarbon compounds on fabrics are padded, dried, and cured. During the curing processes, the perfluoro side chains orient to almost crystalline structures. Furthermore, the blocked isocyanate in the FC dispersion gets activated and crosslinks with the functional group of fluorocarbons, the fibre and itself. This makes the fluorocarbon bonding to the fibre permanent. The final fibre surface will be as shown in Figure 2-27, where the dense CF_3 is oriented on the outer surface for maximum repellence (Schindler & Hauser, 2004).

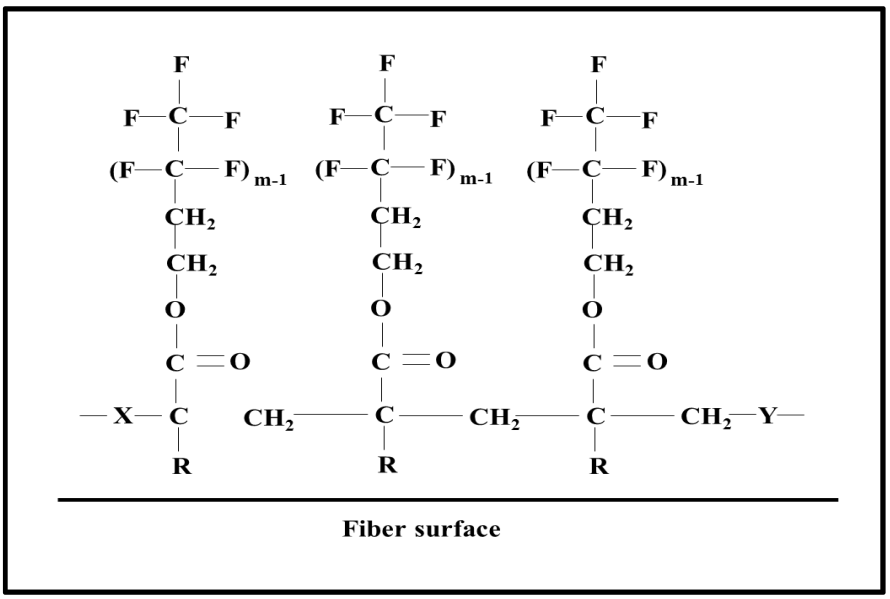

Figure 2-27: Fluorocarbon repellent on a fibre surface, redrawn from (Sayed & Dabhi, 2014)

The amount of finishing solution or emulsion applied on a fabric is usually expressed as a wet pickup percent, as shown in Equation 2-5. The wet pickup of a solution in a pad mangle is affected by various processes parameters. These include the concentration of the pad liquor, temperature of the pad liquor, pad mangle pressure, and the fabric speed (Schindler & Hauser, 2004).

Equation 2-5

$$wpu = \frac{wt\ of\ solution\ applied\ \times 100\%}{wt\ of\ dry\ fabric}$$

where *wpu* is the wet pickup of a fabric (%), *wt. of solution applied* is the difference between the weight of the impregnated fabric (g) and the weight of the dry fabric (g).

This study aims to modify a woven fabric microfiltration membrane by impregnating it with a fluorocarbon emulsion. This will be done using a laboratory scale padding machine where the various process parameters will be varied in order to apply an optimum amount of fluorocarbon on the membrane. Therefore, a brief discussion on how the various process parameters affect the impregnation of fabric with fluorocarbon using the pad-dry-cure process will be presented. In this study the amount of fluorocarbon applied to the WFMF membrane will be measured in terms of oil contact angles, instead of using the wpu.

2.5.4.2. Factors affecting fabric impregnation by PDC

The application of fluorocarbon on a fabric using the pad-dry-cure process is affected by the following parameters: pad liquor concentration and temperature; wettability; pressure of the squeeze rolls; fabric speed; curing temperature; and curing time (Hashem *et al.*, 2009; Schindler & Hauser, 2004).

i) Pad liquor concentration

The concentration of the liquor affects the add-on of the chemical onto the fabric. For example, an increase in the concentration of fluorocarbon solution increases the amount of fluorocarbon that is applied on membrane fabric until the fabric is saturated (Dasdemir & Ibili, 2017; Thilagavathi & Kannaian, 2008). Therefore, pad liquor concentration affects the fabric impregnation process.

ii) Pad liquor temperature

The pad liquor application is normally done at room temperature. However, hot impregnation may be necessary to achieve quick turnaround, uniform wetting-out and high pick-up (Choudhury, 2006). Temperature decreases the viscosity of a solution while increasing its surface tension. Similarly, during padding, an increase in pad liquor temperature decreases both its viscosity and surface tension. This increases the liquor penetration efficiency into the fabric's interstices, resulting in an increase in the fabric's wet pickup. Therefore, an increase in pad liquor temperature increases the amount of liquor picked up by the fabric (Wang, 2006; Schindler & Hauser, 2004).

iii) Wettability

This refers to how easily a surface can be made wet by a liquor. The wettability of a fabric in the padding process is enhanced by the presence of a wetting agent. The wetting agent decreases the marginal interfacial tension between the fibres and the liquor, and thus the fabric becomes saturated with liquor faster. Hence, it is essential that a wetting agent is included during the padding process to enhance the fabric impregnation process (Rouette & Kittan, 1991).

iv) Pressure of the squeeze rollers

The fabric is usually passed between rollers after immersion to squeeze out air, and to force the pad liquor into the fabric. But it also results in the squeezing out of some liquor from the fabric. The liquor retained is what is expressed as a pickup percentage. An increase in pressure exerted by the roller results in a low pickup, but at the same time, a better penetration of the liquor into the fabric (Choudhury, 2006). Therefore, a balance must be found between the pickup and the penetration during the padding process.

v) Fabric speed

The fabric speed affects the fabric immersion time in the padding liquor, as well as its squeezing time. An increase in the fabric speed decreases the time of immersion of the fabric, thus decreasing the impregnation process. Additionally, an increase in fabric speed decreases the squeezing time and hence the complete penetration of the pad liquor may not be achieved (Speke, 1954). But the effectiveness of the penetration also depends on the interaction between the fabric speed and the padding pressure. A balance has to be found between these two parameters.

vi) Curing temperature

The curing step is the fixation stage where a chemical reaction is initiated between a chemical solution, a cross-linking agent, and the fabric (Paul, 2015). A study revealed that an increase in the curing temperature increases the chemical reaction between the chemicals and the fabric, which in turn accelerates the fixation of the finishing chemical onto the fabric until all the chemical additives present have been exhausted (Aly *et al.*, 2004). However, in the case of fluorochemicals, the temperature is normally increased but kept in the range of 150-180^{o} C (Sayed & Dabhi, 2014).

Thermoplastic polymer materials such as polyester shrink when exposed to heat. This results in yarn distortion in fabrics (Perera & Lanarolle, 2020). Curing being a heat-based process can result in the misalignment of fibres in the WFMF membrane. A correctional measure will thus be required to avoid this undesirable outcome.

vii) Curing time

An increase in the curing time increases the amount of finishing chemicals fixed on the fabric. This is because a longer time provides a good opportunity for crosslinking between the reactants and thus, a higher level of fixation (Hashem *et al.*, 2009). On the other hand, the curing time is related to curing temperature. When curing temperature is increased, the required fixation time is shortened (Sayed & Dabhi, 2014).

2.5.4.3. Heat setting

In section 2.5.4.2, a reference was made to the fact that curing can cause shrinkage in the WFMF membrane. The exposure of a fabric to heat can cause fibre pattern distortion within it (Huang & Liang, 1996). This is due to the fact that above its glass transition temperature, the polymer chains within the fabric become mobile and begin to vibrate. This causes the fibres in the fabric to become disoriented. Therefore, maintaining the dimensional stability of the fabric during curing is very essential and this is usually achieved through heat setting.

The heat setting process is usually done at temperatures above the glass transition temperature (Tg). Thus, the Tg is an important parameter when it comes to exposing a material to a high temperature (Haar, 2011). A glass transition temperature is a temperature below which the physical properties of polymer and plastic change to those of glassy or crystalline state, but above this temperature they behave like rubbery materials (Ebnesajjad, 2016). At temperatures above Tg, bond rotation occurs spontaneously, and oriented polymer molecules tend to return to their most probable configuration. This behaviour of polymer with the Tg above the ambient temperature is known as thermal shrinkage. Therefore, fabrics produced from synthetic fibre such as polyester are normally subjected to heat setting to impart dimensional stability at elevated temperature (Perera *et al.*, 2019).

Basically, a heat setting process involves an interaction between time and temperature, with the influence of temperature being much higher than that of time. It involves exposure of a fabric under tension to a temperature above its glass transition temperature for a certain period. Thereafter, the fabric gets back to its normal dimensions upon cooling (Ertekin & Marmarali, 2016; Gacén *et al.*, 2002). The heat setting process introduces enhanced dimensional stability to fabrics and this results in improved fibre orientations (Idumah & Nwachukwu, 2013).

The WFMF membrane is made of a polyester fabric and different researchers propose different heat setting conditions for this fabric. According to Gacén *et al.,* polyester fabric is usually heat set at temperatures between 160 and 220° within a time range of 30 -120 seconds (Gacén *et al.*, 2002). In another investigation, it was stated that the heat setting of polyester fabric occurs at 130 – 140° in steam or 190 - 220° in dry air in the presence of some tension (Idumah & Nwachukwu, 2013). These temperature ranges are above the glass transition temperature of polyester fabrics, which is usually 80° and they allow dimensional stability to be achieved.

Furthermore, as seen in the mentioned examples, different methods are usually used in the heat setting process. The standard method for heat setting synthetic materials such as polyester is normally through the use of stenter frames. This method uses hot air to heat set fabrics that are tightly held onto the stenter frames (Besler *et al.*, 2016). The action of holding the fabrics tightly onto the frames ensures that the dimensional stability of the fabrics is maintained during the curing process. Hence, this study will employ the stenter frame method to heat set the WFMF membranes.

Chapter 3.
Fouling characteristics of woven fabric microfiltration membranes

Overview

Introduction; Effectiveness of air scouring, backwash, water scouring in membrane restoration; Nature of fouling; Impact of irreversible fouling resistance on the performance of the WFMF membranes; General outcomes of the investigations; Summary.

3.1. Introduction

In the previous chapter (see section 2.4.3.1), it was reported that prior studies on WFMF membranes seemingly indicated anomalous fouling behaviours. This led to the postulation that WFMF membrane may exhibit different fouling characteristics compared to the current commercial membranes.

This chapter presents an investigation into the fouling characteristics of WFMF membranes and compares it to that of other commercial membranes. First, the effects of various air-scouring and backwash regimes on the fouling characteristics of the standard WFMF membranes were evaluated. The efficiency of air scouring, backwash, and water scouring on minimizing fouling on WFMF membranes was then investigated. Finally, the kinetics of fouling layer formation on WFMF membranes was established.

3.2. Effectiveness of air scouring, backwash, and water scouring in membrane restoration

The effectiveness of a membrane cleaning method is usually assessed indirectly by evaluating either the pure water flux of the cleaned membrane, or the permeate flux of the membrane during a subsequent filtration run (Middlewood & Carson, 2012). The most common technique is to measure the pure water flux before the filtration process and compare it to the pure water flux after the membrane has been cleaned. This investigation employed this approach in assessing the effectiveness of air scouring, backwash, and water scouring in restoring the permeability of WFMF membranes.

3.2.1. Experimental set-ups

3.2.1.1. Woven fabric immersed membrane filtration (WF-IMF) unit

The pure water flux and fouling experiments were performed using a laboratory woven fabric immersed membrane filtration (WF-IMF) unit shown in Figure 3-1. The set-up was adapted from previous studies with a few modifications (Asquith, 2017; Pillay *et al.*, 2016).

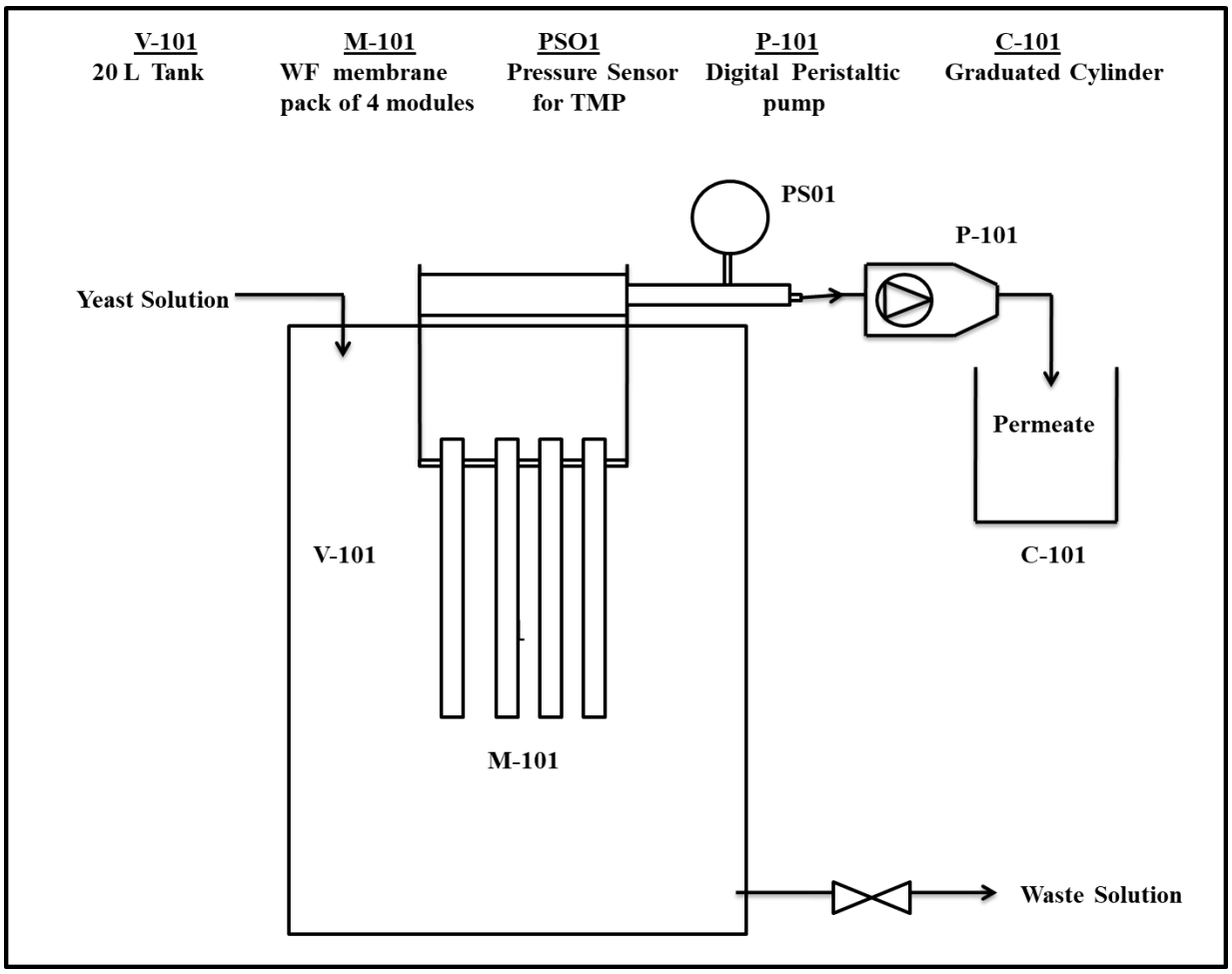

Figure 3-1: A schematic diagram of the laboratory WF-IMF unit

The rig used in this investigation consisted of a 20 L tank for holding the feed, four flat sheet WFMF membrane modules (each with an effective area of 0.0161 m^2), and a pressure gauge for measuring the pressure drop across the membrane. A peristaltic pump was used for the withdrawal of permeate and a graduated cylinder for collecting the permeate. A turbidity meter was used for measuring both the feed and permeate turbidities, and a stopwatch for timing the permeate flow and the filtration process.

3.2.1.2. Woven fabric membrane module

The woven fabric modules used in this project were flat sheet modules. They consisted of four elements: a PVC frame, a permeate outlet which allows permeate to flow out of the module, two sheets of WF membrane glued to either side of the frame, and two spacers between the sheets of fabric to keep the two membranes apart and allow fluid to flow into the module. The module dimensions were 15 cm by 10.5 cm, and the effective surface area of a single module was 0.0161 m^2. The construction of the WF modules was adapted from previous studies (Asquith, 2017; Cele, 2014; Pillay *et al.*, 2016). An image of a single WF module and its components is shown in Figure 3-2.

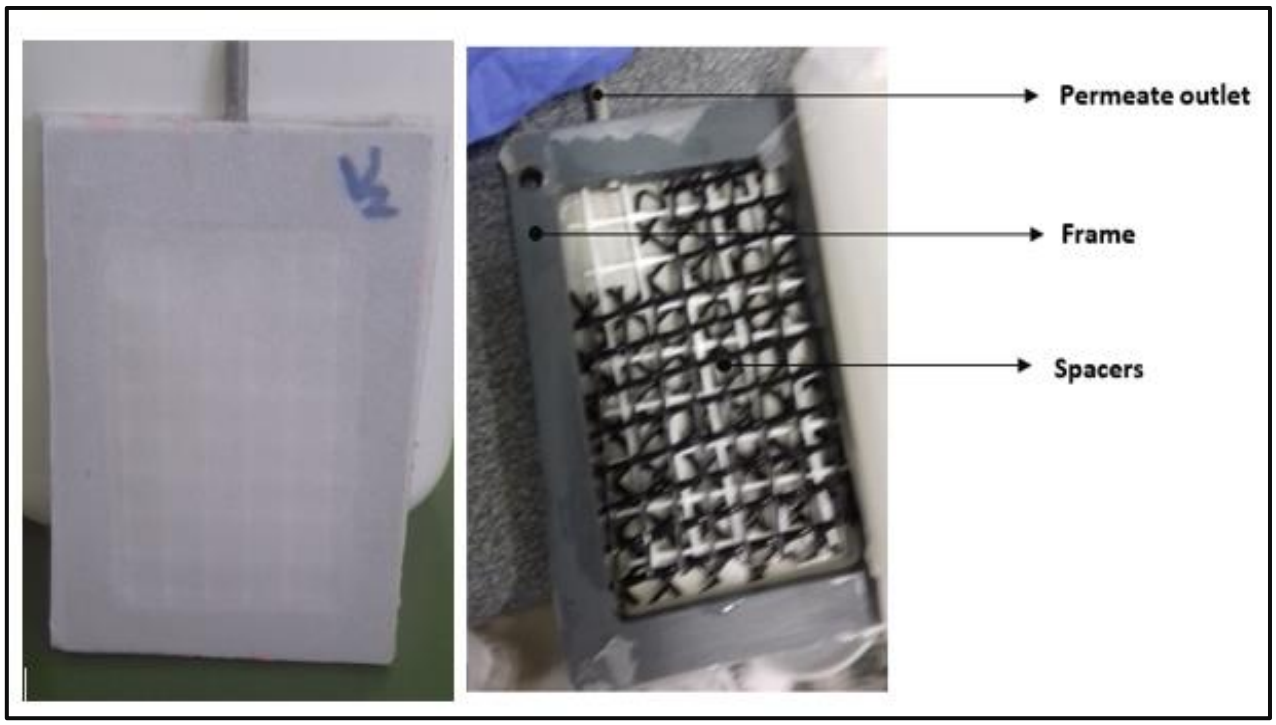

Figure 3-2: An image of a single woven fabric microfiltration membrane module and its components

3.2.1.3. Membrane cleaning set-up

The laboratory set-up shown in Figure 3-3 was used for air scouring and backwashing. The air scouring process was done in a separate glass vessel. Air for scouring the membranes was introduced 7 cm beneath the membrane pack via a rectangular diffuser. The diffuser had 1 mm holes drilled all over its upper surface. An air compressor capable of delivering up to 60 L/min of air was used to supply the air. The setup described above was adapted from Ndinisa *et al.,* with some modifications (Ndinisa *et al.*, 2007).

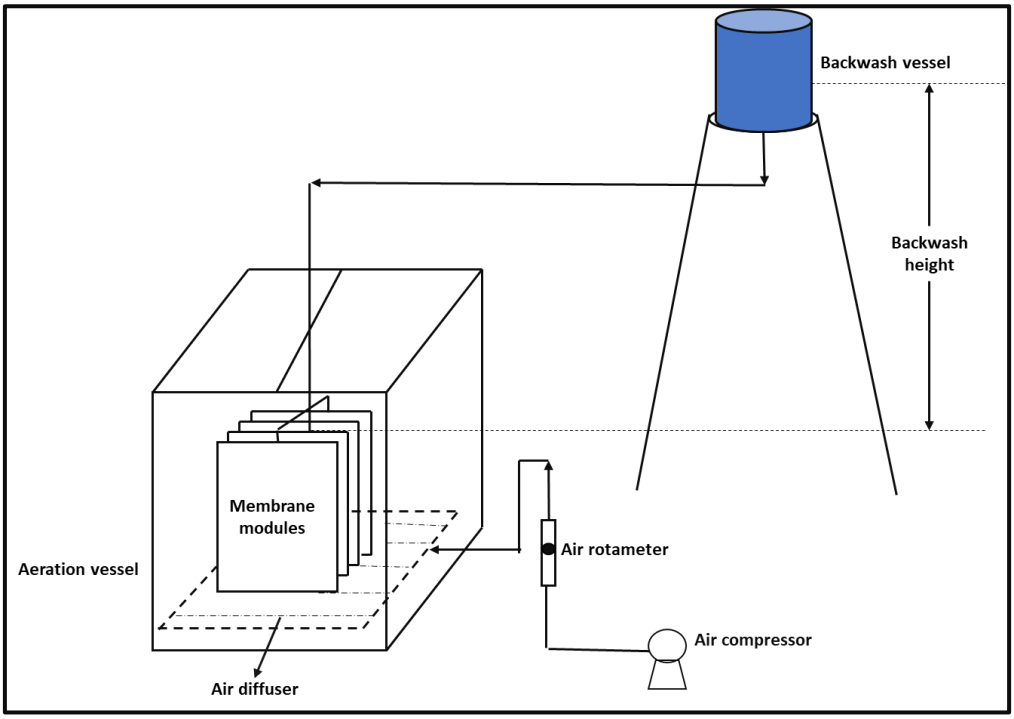

Figure 3-3: A schematic diagram of the membrane cleaning set-up

In addition to air scouring, the membrane cleaning set-up was also used for the backwash regime. Water from the elevated backwash vessel was used to create the pressure for dislodging foulants from the membranes. More details on the backwash process are presented in section 3.2.2.3.

3.2.2. Experimental procedures

3.2.2.1. Pure water flux experiments

Pure water flux (PWF) experiments are often used to characterize the initial, fouled, and cleaned membrane resistances (Ogunbiyi *et al*, 2008). During PWF experiments, the flux increases with the increase in pressure drop (ΔP), resulting in a linear relationship between flux and ΔP.

This study adapted a protocol from a previous investigation in carrying out the pure water flux experiments (Deelie, 2017). The experiments involved filtering distilled water using the WF-IMT rig shown in Figure 3-1. The pump settings were varied from 100 to 300 rev/min at intervals of 50 rev/min during the PWF experiments. At each pump setting, the ΔP and the time taken to fill a 500 ml cylinder were recorded. The pure water fluxes of the membranes were calculated using Equation 3-1.

Equation 3-1

$$J_O = \frac{v}{A \times \Delta t}$$

where J_O is the pure water flux (L/m^{2}h or LMH), v is the volume of water collected (L), A is the

effective area of the membranes (m^2), and Δt is the time taken to collect the water (h).

Pure water curves were then plotted using the calculated flux and the ΔP. Three runs were performed for each pure water flux experiment to ensure reproducibility of the results.

The pure water flux results were also used to calculate the intrinsic membrane resistance. Equation 3-2 shows an expression used to calculate this resistance.

Equation 3-2

$$R_m = \frac{\Delta P}{\mu J_O}$$

where R_m is the intrinsic membrane resistance (m^{-1}), ΔP is the pressure drop across the membrane during water filtration (Pa), μ is the water viscosity (Pa.s) and J_O is the pure water flux.

After every experimental run, the intrinsic membrane resistance (resistance of a clean/initial membrane) was always fully restored through brushing and an overnight hypochlorite soak (see Chapter 2, subsection 2.4.4). This ensured that the integrity of subsequent experiments was maintained.

3.2.2.2. Fouling experiments

i) Test feed

This investigation was focused on fouling and restoration of the WFMF membranes in wastewater treatment. Therefore, the most suitable feed in this study would have been activated sewage sludge. However, the temporal variability of the sewage sludge quality from day to day and hour to hour is quite significant. Hence, the evaluation results would not have been reproducible. This investigation, therefore, chose a synthetic wastewater over real wastewater due to its reproducibility and ease of use under laboratory conditions (Ndinisa *et al.*, 2007).

Potential synthetic feeds were identified after conducting a literature survey. They included sodium alginate, humic acid, bovine serum albumin, and yeast (Aslan & Kapdan, 2006; Ma *et al.*, 2019; Ogunbiyi *et al.*, 2008; Rodgers *et al.*, 2008; Zhang *et al.*, 2015). Sodium alginate is often used to represent polysaccharides in wastewater, while bovine serum albumin (BSA) usually acts as a protein model foulant (Ma *et al.*, 2019). On the hand, humic acid (HA) and yeast are commonly employed to represent organic matter in wastewater (Ogunbiyi *et al.*, 2008; Zhu *et al.*, 2013). All the four feeds were suitable for use in this investigation. This is because previous study showed that the major foulants on the WFMF membrane surfaces were organic matters such as polysaccharides and

proteins (Pillay *et al.*, 2016). However, sodium alginate, BSA and HA are relatively expensive. Hence, in this work, a yeast suspension was chosen as the test feed.

Yeast suspensions of 0.5 g/L were employed in all the fouling experiments. The suspensions were made out of granular dried baker's yeast and water. First, the yeast granules were added to a vessel containing distilled water. Thereafter, the content in the vessel was thoroughly mixed with a laboratory mixer to produce the yeast suspensions.

ii) Fouling procedure

The fouling experiments involved dead-end filtration of 0.5 g/L of yeast suspension using the laboratory WF-IMF rig shown in Figure 3-1. Before the fouling experiment, the pure water flux of the unused membranes was determined. The membrane modules were then transferred to a tank containing the yeast suspension. This was followed by a 1-hour filtration of yeast suspension at a constant pump setting of 100 rev/min, which corresponded to a flux of around 380 LMH. It should be noted that this study employed a high initial fouling flux compared to the fluxes used in previous investigations, and also in commercial IMBRs. This is because the previously used fluxes were too low to be maintained on the laboratory scale rig. Throughout the filtration process, the yeast suspension was continuously added to the tank in order to maintain a constant feed level. The permeate turbidity, permeate volume and ΔP were measured and recorded at a 5-minute interval. The permeate quality was monitored to ensure that the integrity of the membranes was maintained throughout the experiment. This experiment was repeated 3 times, in order to ensure repeatability.

The permeate volume and ΔP results were thereafter used to calculate filtration fluxes and resistances. The filtration fluxes and resistances at pre-defined intervals were calculated using Equation 3-3 and Equation 3-4, respectively. Thereafter, fouling resistance profiles were generated.

Equation 3-3

$$J = \frac{v}{A \times \Delta t}$$

where J is the permeate flux (LMH), v is the volume of permeate collected (L), A is the effective area of the membrane (m^2), and Δt is the time taken to collect the permeate (h).

Equation 3-4

$$R_t = \frac{\Delta P}{\mu J}$$

where R_t is the membrane resistance during the filtration process (m^{-1}), ΔP is the pressure drop across the membrane during filtration process (Pa), μ is the permeate viscosity (Pa.s), and J is the

permeate flux (LMH).

3.2.2.3. Cleaning processes

The essence of membrane cleaning is to restore the flux of a fouled membrane to its original permeability. This section evaluated two cleaning methods namely: air scouring and backwashing. The fouled membranes were first water scoured, i.e. simply rinsed under a tap, and then cleaned using either air scouring or a combination of air scouring and backwash during which different process parameters were evaluated. The laboratory set-up shown in Figure 3-3 was used for the air scouring and backwashing process.

i) Air scouring

In this investigation, the effectiveness of air scouring on the restoration of fouled membrane was assessed. This was done by evaluating different combinations of air scouring parameters. These parameters included air scouring duration, air flowrate, and air scouring frequency. A combination of the three factors resulted in six cleaning regimes. The regimes were as follows:

- Air scouring at 20 L/min for 5 minutes;
- Air scouring at 20 L/min for 15 minutes;
- Air scouring at 30 L/min for 5 minutes;
- Air scouring at 30 L/min for 15 minutes;
- Intermittent air scouring at 20 L/min for 15 minutes;
- Intermittent air scouring 30 L/min for 15 minutes.

During the intermittent air-scouring, there was a 1-minute stop after every 5 minutes. The air scouring duration and air flowrate ranges used in this study were chosen based on preliminary scanning experiments performed on the yeast suspension.

ii) Backwash process

In standard IMBR systems, the backwash process is often done by reversing the flux of permeate. This creates a back pressure that lifts foulants off the membrane surface and removes foulants from the membrane pores. The backwash intensity has to be controlled by varying the backwash flux or backwash pressure (Chang *et al.*, 2017; Yang *et al.*, 2011; Yigit *et al.*, 2009). In this work, the backwash process was driven by gravity. Hence, its intensity was varied by increasing the differential height between the level of water in the backwash vessel and the aeration vessel. An increase in the differential height resulted into an increase in the backwash pressure, and vice versa. The backwash

process was done by slowly allowing water to flow from the elevated backwash vessel into the membrane modules through the permeate outlets; at different backwash heights.

A regime combining air-scouring and backwash was investigated. The air scouring conditions were kept constant at the best-chosen regime from the earlier evaluated parameters. While the backwash intensity was varied by changing the backwash height. Three backwash heights were evaluated namely: 40 cm, 60 cm, and 75 cm. These heights translated to backwash pressures of 3.9 kPa, 5.9 kPa and 7.4 kPa, respectively. Trial runs indicated that the WF modules could not withstand a backwash pressure of around 7.5 kPa and above. A backwash pressure above 7.5 kPa resulted in a failure of the bond between the WF membrane and the PVC frame. Hence, an upper limit of 7.4 kPa backwash pressure was chosen.

3.2.2.4. Air scouring/backwash efficiency

Pure water flux curves were used to evaluate the air scouring and backwash efficiency. The pure water flux curves of the membranes after different air scouring and backwash regimes were compared to that of the initial membranes. From this comparison, a conclusion was drawn on whether the cleaning process was able to restore the membrane to its original permeability.

To further establish the efficiency of the air scouring and backwash regimes, resistance profiles were also generated. First, the best cleaning regime out of the evaluated regimes was identified. The resistance of the membrane cleaned with this regime was then calculated using Equation 3-5. A graph with the initial membrane resistance, resistance after the cleaning process, and resistance during fouling was thereafter plotted.

Equation 3-5

$$R_f = R_t - R_m$$

where R_f is the resistance of the membrane after the cleaning process (m^{-1}), R_t is the total membrane resistance at the end of the filtration process (m^{-1}), and R_m is the intrinsic membrane resistance (m^{-1}).

3.2.3. Results and discussion

The main objective of this section was to assess the effectiveness of air scouring and backwash in restoring the original permeability of the WFMF membranes. Different air scouring and backwash regimes were evaluated. The PWF data for the membranes before the filtration process, and after being cleaned under the different regimes are shown in Figures 3-4, 3-5 and 3-6.

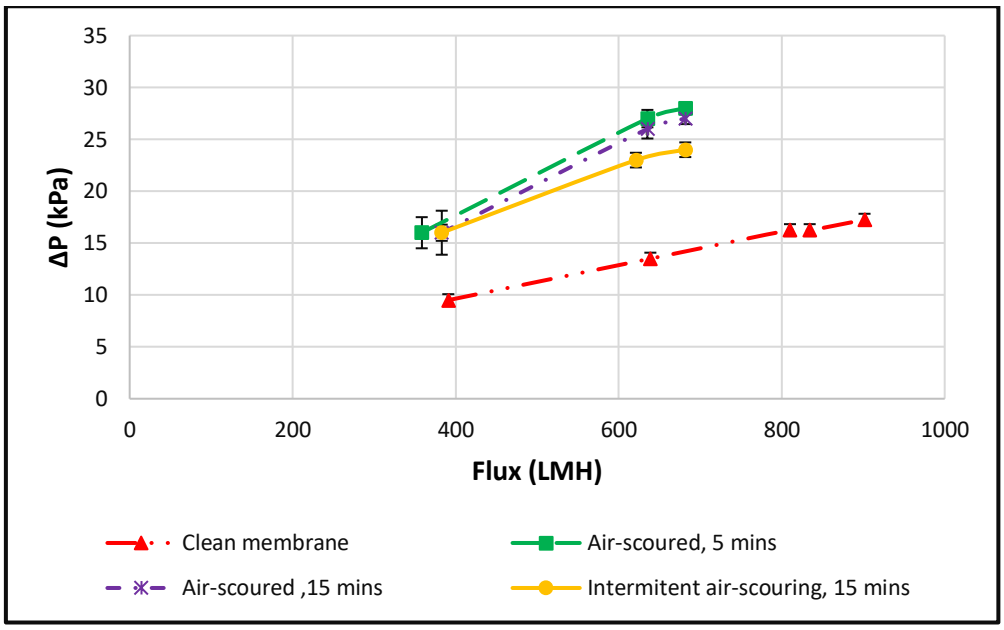

Figure 3-4: PWF results for membranes air scoured at 20 L/min for different duration and frequency

(Three repeat runs, average presented with error bars)

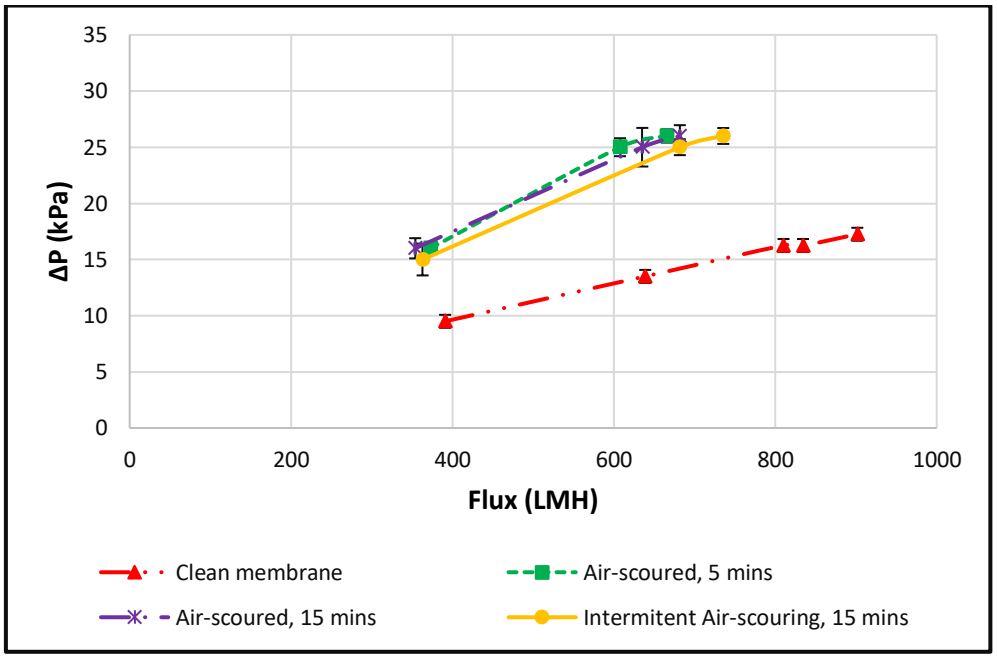

Figure 3-5: PWF results for membranes air scoured at 30 L/min for different duration and frequency

(Three repeat runs, average presented with error bars)

From Figure 3-4 and 3-5, it is clear that an increase in filtration duration, as well as change of frequency from continuous to intermittent slightly increased the efficiency of air-scouring in restoring the membranes. However, the membranes were not restored to their original permeability. This trend was observed for both 20 L/min and 30 L/min air scouring rate. This implies

that there was always a residual fouling resistance that remained on the membranes despite changes made in the air scouring parameters (Rezaei *et al.*, 2014). The lack of success of air scouring to fully restore the membrane was attributed to the fact that the air scouring bubbles were not strong enough to remove all foulants from the WFMF membranes (Chollom *et al.*, 2017).

Hence, a combination of air-scouring and backwash regimes were further investigated. The pure water flux data for the membranes cleaned using these regimes are shown in Figure 3-6.

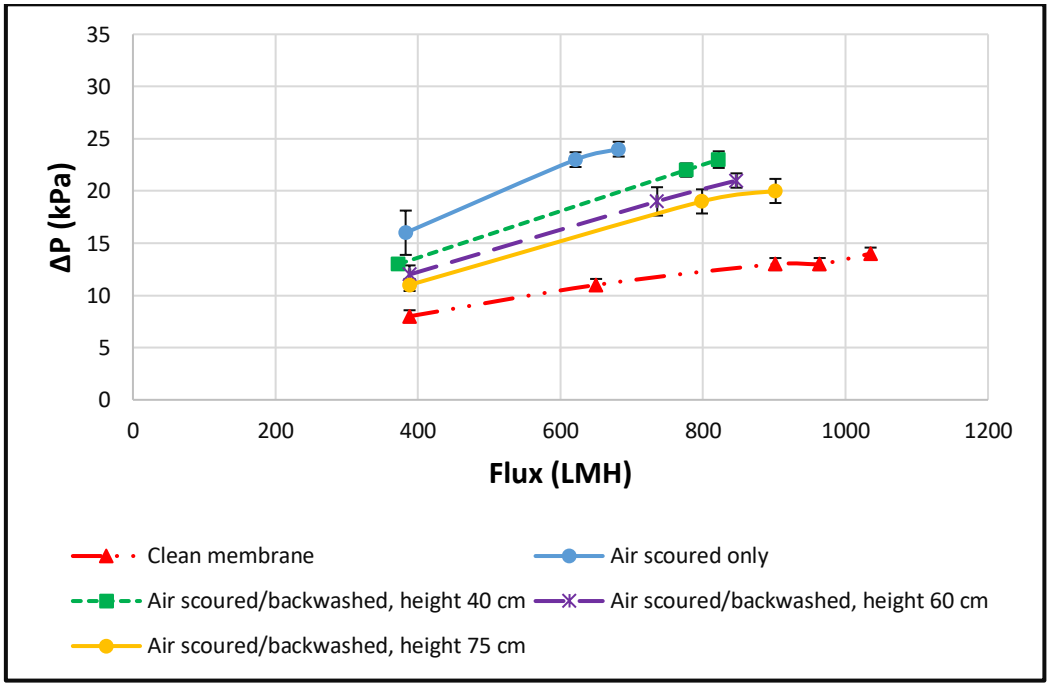

Figure 3-6: PWF results for membranes intermittently air scoured and backwashed at different heights

(Three repeat runs, average presented with error bars)

It is observed from Figure 3-6 that the combination of air scouring, and backwash increased the degree to which the WFMF membranes were restored, with a backwash height of 75 cm giving the best restoration results. The increase in the degree of membrane restoration is attributed to the backwash force which dislodged more of the foulants which had adsorbed onto, or deposited in, membrane pores or on membrane surfaces (Chang *et al.*, 2017; Chollom *et al.*, 2017). An increase in the backwash height increased the dislodging force, thus, resulting in a further increase in the cleaning efficiency. However, the integration of backwashing with the air scouring process also did not restore the WFMF membranes to their original permeability. This prompted an analysis of the extent to which the combination of air scouring, and backwash was able to restore the WFMF membranes to their original permeability. The resistance profiles for the initial clean membranes before filtration, the membranes fouled and then cleaned via air scour and backwash, and the

membranes during the filtration process are presented in Figure 3-7.

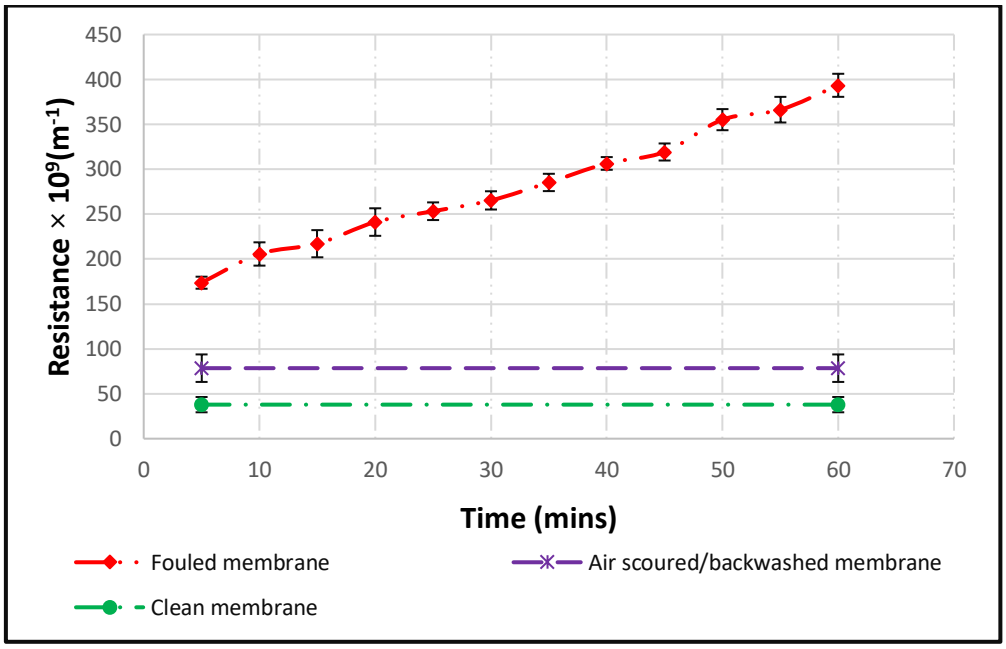

Figure 3-7: Resistance profiles for fouled membranes, air scoured/backwashed membranes and clean membranes

(Three repeat runs, average presented with error bars)

From the Figure 3-7, it can be seen that the combination of air scouring, and backwash reduced the total resistance from around 393 × 10^9 m $^{-1}$ to around 79 × 10^9 m^{-1}. The reduction in the resistance represents 89% of the original fouling resistance. The fouling layer that was washed away by air scouring and backwash is commonly known as reversible fouling resistance. This layer is loosely attached to the membranes and can easily be washed away by physical cleaning processes such as air scouring and backwash (Meng *et al.*, 2009; Rezaei *et al.*, 2014; Wang *et al.*, 2014). However, there was a small portion of the fouling layer that still remained attached to the membrane. This is referred to as irreversible fouling resistance (Kimura *et al.*, 2008; Tsuyuhara *et al.*, 2010). From Figure 3-7, this represents around 11% of the total fouling resistance. Similar percentages of the various resistances have been reported in another study that evaluated fouling resistance in a submerged MBR system (Hwang *et al.*, 2008). The persistent occurrence of the irreversible fouling layer after each air scouring regime was also observed by Ding *et al* (Ding *et al.*, 2016). Ding *et al* reported that air scouring removed majority of the fouling layer but there was always a residual layer after every air-scouring process.

Hence, it can be concluded that a combination of water scouring, air-scouring and backwash can restore the WFMF membranes' permeability close to their initial state, but there is always a residual resistance. An increase in either the air-scouring duration, air flowrate or backwash height achieved

a marginal increase in the degree of fouling resistance removal but failed to get the WFMF membranes restored to their original permeability. Therefore, an investigation into the kinetics of fouling in WFMF membranes was necessary so as to determine how fast the residual fouling resistance forms.

3.2.4. Contribution of water scouring in the membrane cleaning process

This section seeks to establish the contribution of water scouring in restoring the permeability of fouled WFMF membranes, during the earlier evaluated cleaning regime. The investigation involved comparing membranes that were only water scoured and those that were water scoured, air scoured and backwashed. First, the WFMF membranes were fouled using the method earlier described (see subsection 3.2.2.2(ii)). Thereafter, they were scoured with tap water to remove any visible fouling layer. This was followed by a pure water flux measurement, where the ΔP and flux were recorded. The membranes were then intermittently air scoured and backwashed at the best identified regime in subsection 3.2.3. The pure water flux experiment was then repeated.

A comparison of the pure water flux of the membranes that were only water scoured, and those were water scoured, air scoured and backwashed are shown in Figure 3-8.

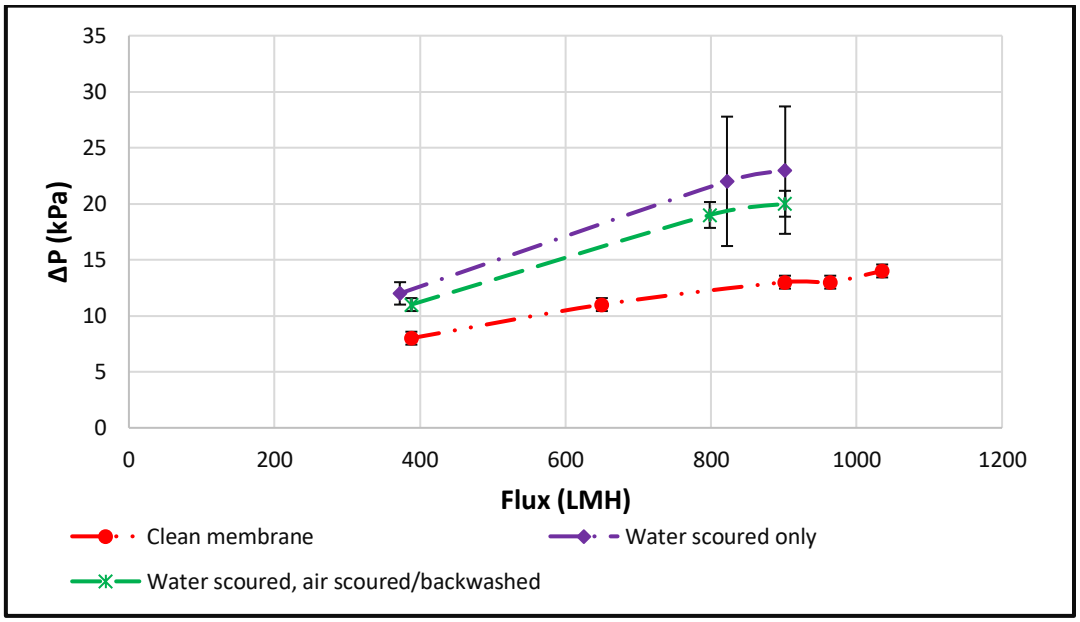

Figure 3-8: Comparison of PWF for membranes that were water scoured only, and those that were water scoured, air scoured and backwashed

(Three repeat runs, average presented with error bars)

From the Figure 3-8, it can be inferred that there was a slight difference between the membranes that were only water scoured, and those that were water scoured, air scoured and backwashed. In

terms of the fouling resistance, water scouring removed about 72% of the fouling layer, while air scouring, and backwash removed the remaining 17%. Hence water scouring contributed approximately 80% of the cleaning effect. Therefore, it can be concluded that water scouring played a major role in the earlier evaluated cleaning process, in removing a majority of foulants deposited on WFMF membranes during the filtration process.

In most membrane filtration systems, water scouring is always combined with other cleaning methods (Bansal *et al.*, 2006; Popović *et al.*, 2009; Wang *et al.*, 2010). This is due to its ineffectiveness in cleaning membranes, when used alone (Bansal *et al.*, 2006; Yang *et al.*, 2011). However, from the findings of this study, the contrary was observed. Water scouring had a major contribution in terms of cleaning the fouled WFMF membranes. It was able to remove around 72% of the deposited foulants. Hence, it can be effective in cleaning WFMF membranes during filtration process; without it being combined with other physical cleaning methods.

The above-mentioned conclusion if implemented will have a positive impact on the development of the WFMF technology. This is because, unlike air scouring and backwash which are used in most commercially available membrane systems, water scouring does not require any major energy input. Furthermore, it is simple in terms of application, as only water from hosepipe, tap or water sparger is needed to clean the membranes. From this section onwards, water scouring would be employed as the physical cleaning method for the WFMF membranes.

3.3. Nature of fouling

3.3.1. The kinetics of fouling

The kinetics of fouling is used in this study to describe how fast the fouling resistance forms on the membranes during filtration process. One of the findings outlined in the previous sections is the presence of a residual fouling layer after any of the employed physical cleaning methods. Therefore, it became imperative to investigate the kinetics of the WFMF membrane fouling so as to establish how fast the reversible and irreversible resistance forms on the membranes over time.

3.3.2. Methodology

3.3.2.1. Experimental procedure

The quantification of the kinetics of fouling in WFMF membranes was done in four stages. The stages included: a pure water flux phase, a fouling experiment, a water scouring phase, and finally a phase

that involved the repetition of the pure water flux experiment with water scoured membranes. The fouling process was done for different filtration durations of 10, 20, 30, 60 and 90 minutes in separate experimental runs. The evaluation of the effect of different filtration durations was randomized to capture any inherent errors. The first pure water flux experiment was used to characterize the initial membrane resistance, while the second one was used to establish the irreversible fouling resistance on the membranes. Water scouring was used to wash away any reversible foulants on the membranes.

3.3.2.2. Determination of filtration resistance

In microfiltration studies, a resistance in series model is commonly used to investigate the fouling characteristics in membranes (Rezaei *et al.*, 2014; Wang *et al.*, 2010). The resistances in this model include intrinsic membrane resistance, reversible fouling resistance and irreversible fouling resistance. The reversible fouling is mostly due to cake layer deposition, while the irreversible is caused by adsorption of foulants in membrane pores. The intrinsic membrane resistance is as a result of the membrane's inherent characteristic. The sum of these resistances is represented by the expression in Equation 3-6.

Equation 3-6

$$R_t = \frac{\Delta P}{\mu J} = R_m + R_r + R_{ir}$$

where R_t is the total membrane resistance (m^{-1}), ΔP is the pressure drop across the membrane (Pa), μ is the permeate viscosity (Pa.s), J is the permeate flux (LMH), R_m is the intrinsic membrane resistance (m^{-1}), R_r is the reversible fouling resistance and R_{ir} is the irreversible fouling resistance (m^{-1}).

As mentioned earlier, the intrinsic membrane resistance can be estimated by the pure water flux of the initial membrane. The reversible fouling was found by the difference between the resistances of the fouled membranes and that of the water scoured membranes. The irreversible fouling on the other hand was estimated by subtracting the resistance of the clean membranes from that of the water scoured membranes.

3.3.3. Results and discussion

In order to establish the kinetics of fouling in WFMF membranes, the different fouling resistances present during filtration process were calculated and plotted. But first, a typical flux-time and ΔP-time profile for a 90-minute membrane filtration process is shown in Figure 3-9. This is used to show

how the flux and ΔP change during a membrane filtration process.

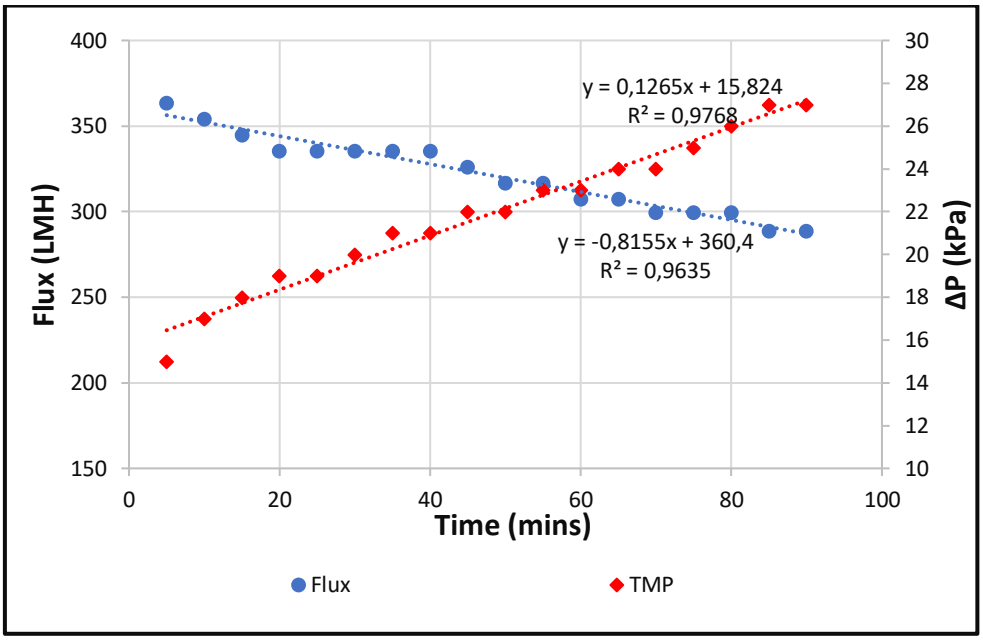

Figure 3-9: Flux and ΔP profile for a 90-minute filtration process

(Three repeats, average shown with best-fit linear trendline)

The resistance profile for the 90-minute filtration process is shown in Figure 3-10.

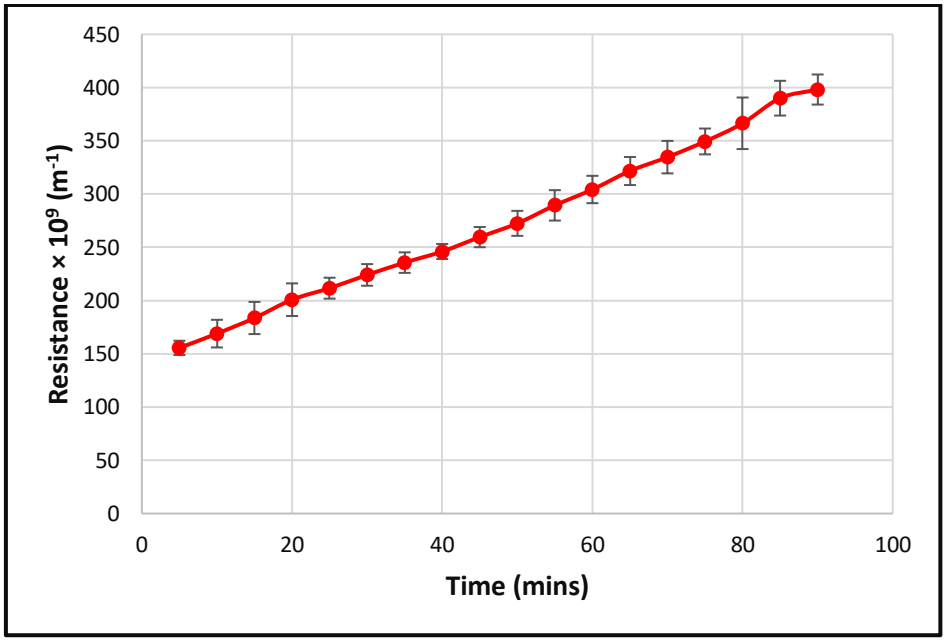

Figure 3-10: Resistance profile for a 90-minute filtration

(Three repeat runs, average presented with error bars)

Consequently, fouling during the other evaluated filtration durations were also indicated using resistance profiles as shown in Figure 3-11. The results presented in the graph are averages of 3 runs.

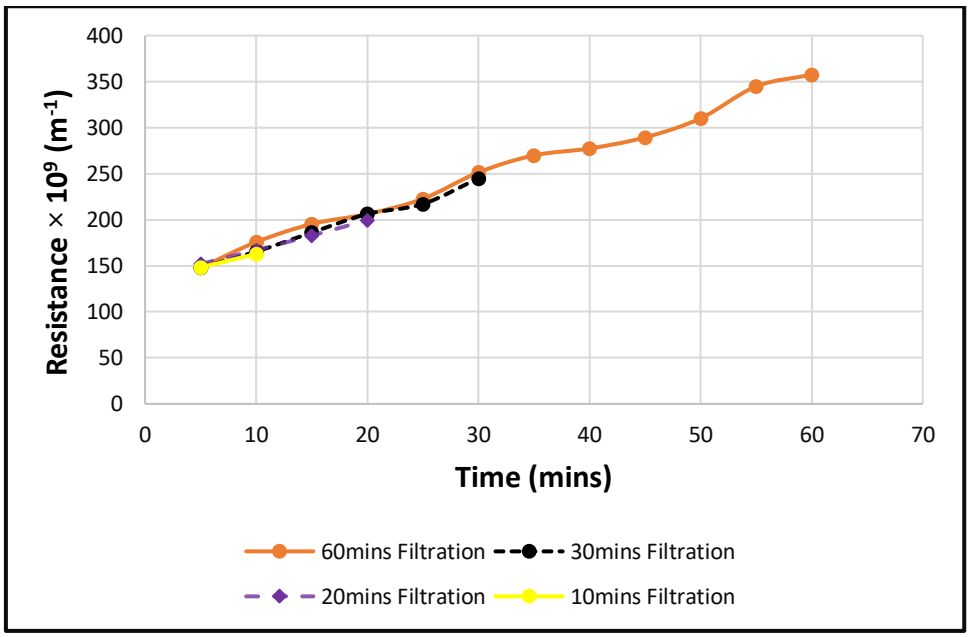

Figure 3-11: Resistance profiles for different filtration durations

From Figure 3-11, it is observed that the total membrane resistance increased with an increase in the filtration time as expected. This is because as time increases, more foulants get deposited and this in turn, increase the fouling resistance. Hence, increasing the total resistance, as illustrated by Equation 3-4.

After each filtration run, the membranes were water scoured, and their pure water flux determined and thereafter presented by a series of charts. The pure water flux curves of the water scoured membranes (after different filtration durations) are presented in Figure 3-12.

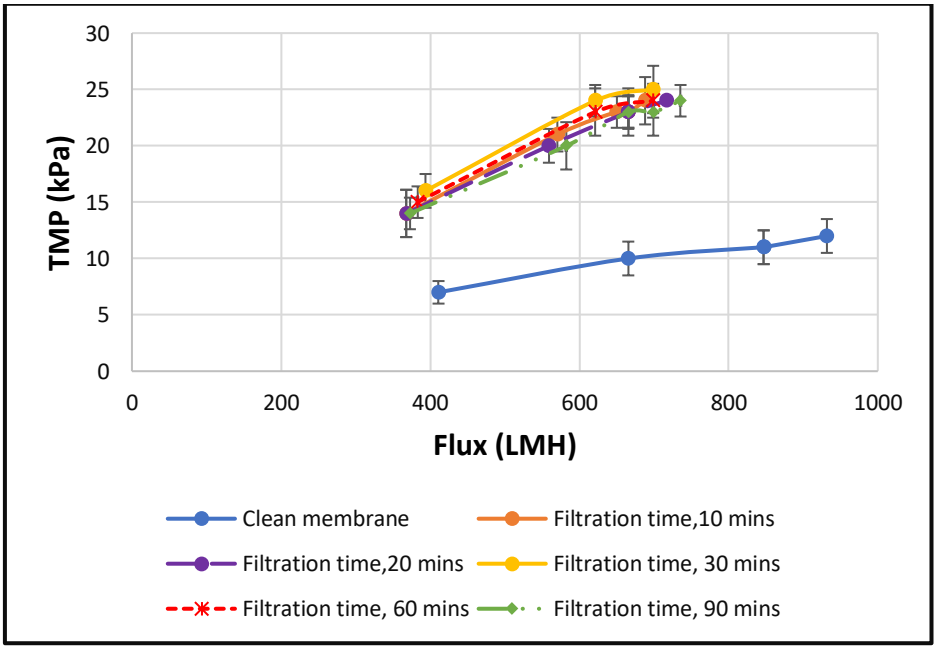

Figure 3-12: PWF results for water scoured membranes after different filtration durations

(Three repeat runs, average presented with error bars)

The pure water flux curves of the water scoured membranes were used to characterize the irreversible fouling in this study. After water scouring the fouled membranes, the irreversible fouling resistance were obtained from the difference between resistances of the water scoured and the initial membranes.

From Figure 3-12, it can be clearly observed that the membranes were not restored to their original permeability, which implies that water scouring did not completely eliminate foulants from the membranes. As it was earlier mentioned, foulants that remain on membranes after physical cleaning are known as irreversible foulants. An interesting thing to note from the result was that there was no significant difference between the pure water fluxes of the water scoured membranes after different filtration durations. This seems to suggest that the irreversible fouling layer appears to occur within the first five to ten minutes of filtration process. This is consistent with the observation made by Wang & Tarabara, where during the early stages of their membrane filtration process, fouling was attributed to the deposition of irreversible foulants in the membrane pores (Wang & Tarabara, 2008). Hence, this finding confirms Pillay *et al.* hypothesis that irreversible fouling resistance could be the cause of permeate flux decline in WFMF membranes at the commencement of the filtration process (Pillay *et al.*, 2016).

Resistance profiles of the clean, water scoured, and fouled WFMF membranes were generated to provide a further insight into their fouling kinetics. The profiles are presented in Figure 3-13.

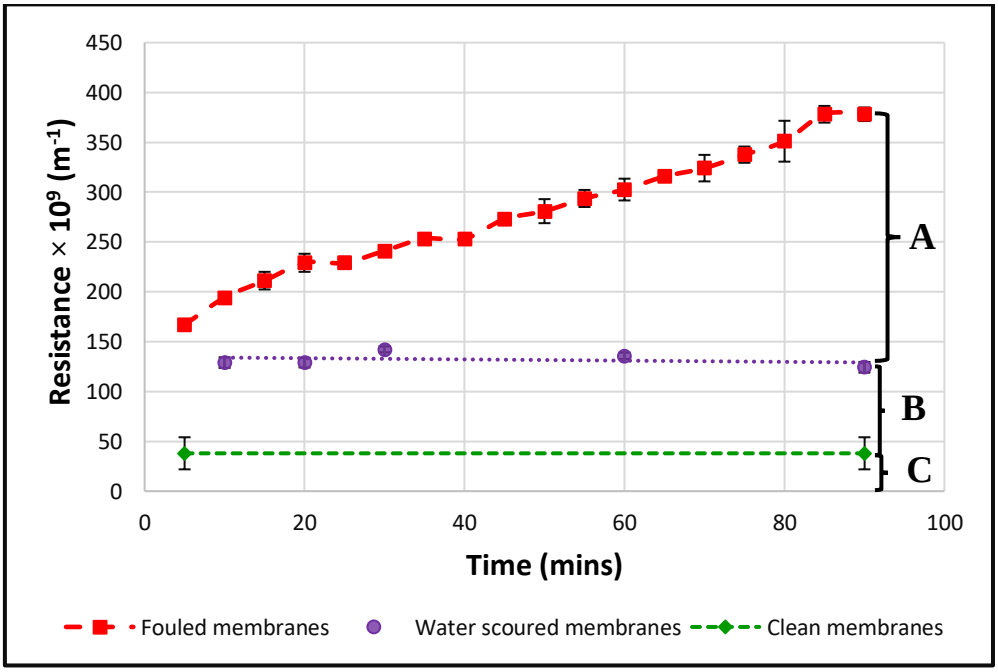

Figure 3-13: Resistance profiles for clean, water scoured, and fouled WFMF membranes

(Three repeat runs, average presented with error bars)

Section A, B, and C represent reversible, irreversible, and initial membrane resistances, respectively. At the end of the 90-minute yeast filtration process, the total resistance on the WFMF membranes was estimated to be around 378 × 10^9 m^{-1} as shown in Figure 3-13. This resistance reduced to 132 × 10^9 m^{-1} after the membranes were water scoured. As was earlier stated in section 3.2.3, the removed fouling layer is referred to as reversible fouling resistance, and it forms as a result of cake layer deposition. The reduction in the fouling resistance represented 65.1% of the total membrane resistance and 72.3% of the fouling layer. Hence, it was considered as the dominant fouling resistance during the filtration process. The remaining fouling layer after water scouring, is known as the irreversible fouling layer, and was estimated to be around 27.7% of the total fouling resistance. The percentage of the irreversible fouling resistance was roughly equal for all the evaluated filtration time intervals. This supports the earlier findings and suggests that the irreversible fouling layer formed within the first five to ten minutes of the filtration process, while the cake layer was deposited later during the filtration process.

Similar observations were also reported in other studies conducted on other types of microfiltration membranes (Blanpain-Avet *et al.*, 1999; Kanani *et al.*, 2008; Nguyen *et al.*, 2010; Sun *et al.*, 2018). In Nguyen *et al.*'s investigation on the treatment of raw activated sludge effluent with microfiltration membranes, it was reported that the sequence of fouling involved adsorption of irreversible foulant into the membrane pores during the first 30 minutes of filtration, followed by cake layer formation (Nguyen *et al.*, 2010). In another study involving the use of microfiltration membrane for soy sauce filtration, fouling was characterized by an initial internal pore clogging followed by a cake layer deposition, and the latter was identified as the dominant fouling resistance (Sun *et al.*, 2018).

Therefore, it can be safely concluded that the kinetics of fouling formation on WFMF membranes is similar to that of other commercial microfiltration membranes. It involves two stages, namely: irreversible layer deposition and cake layer formation. Additionally, the irreversible fouling forms within the first five to ten minutes of filtration process and cannot be cleaned by water scouring. While the cake layer forms later in the filtration process and can be easily removed by water scouring.

3.3.4. Visualization of the WFMF membranes

The persistent occurrence of the residual fouling resistance after water scouring or air scouring/backwash of the WFMF membranes prompted a microscopic observation of the effect of

cleaning on the restoration of WFMF membranes. Images of clean, fouled, and water scoured membranes were taken under a stereo microscope at a magnification of 20x. This was done with a view to gain insight into the membrane blockage mechanisms and to shed more light on the difficulties associated with the irreversible fouling resistance. These microscopic images are shown in Figures 3-14 and 3-15.

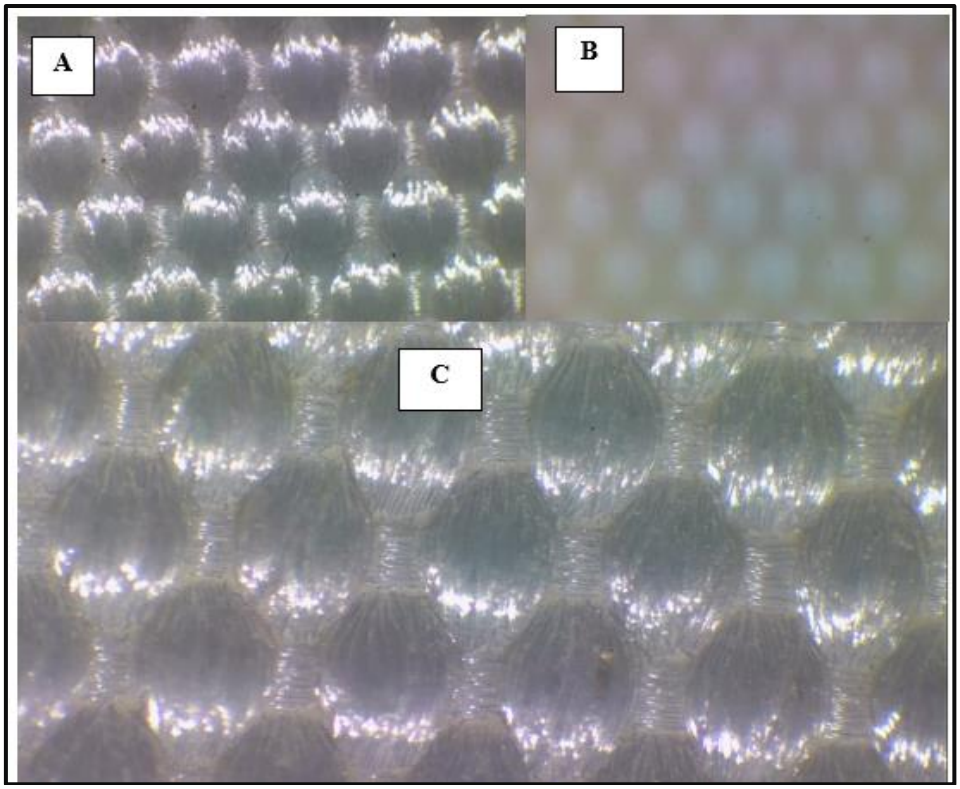

Figure 3-14: Microscopic images of: A-clean, B-fouled and C-water scoured membrane at a magnification of 20x

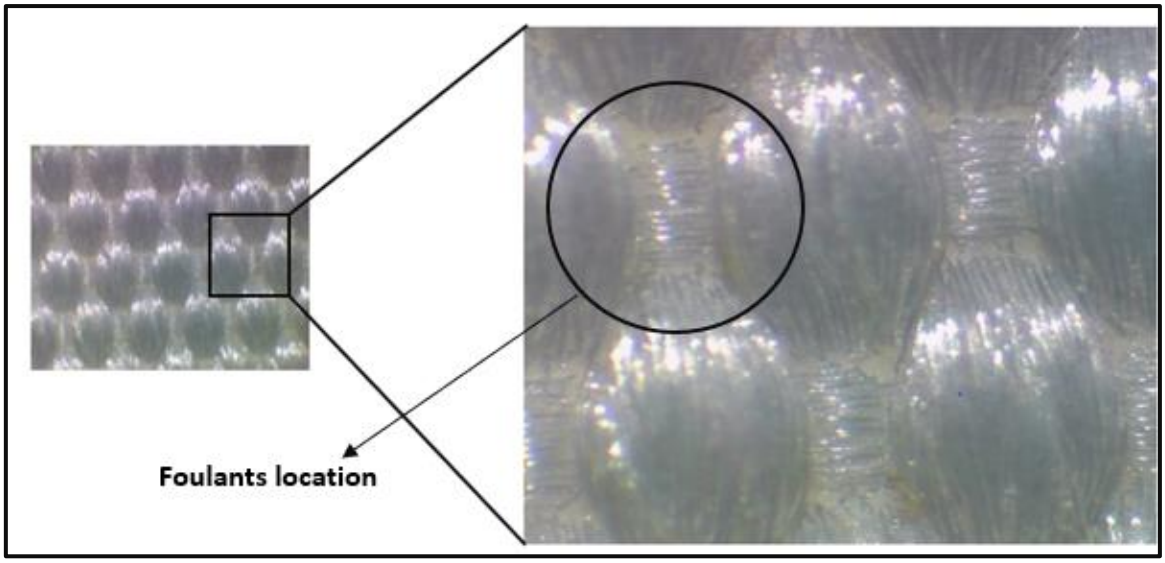

Figure 3-15: An enlarged image of the water scoured WFMF membrane showing the location of the irreversible foulants

From these images, it can be seen that after the filtration process, the membranes were completely covered with a fouling layer. The water scouring process then removed most of these foulants. However, some foulants were still observed at various intersections of groups of fibres (corners), where neither water scouring, nor air scouring was able to reach. This membrane blockage mechanism, which could only be revealed by microscopic images explains why water scouring, air scouring, and backwash were unable to completely restore fouled WFMF membranes.

3.4. Impact of irreversible fouling resistance on the performance of the WFMF membranes

3.4.1. Introduction

It was established in the previous sections that there are two types of fouling layer that occur on WFMF membranes during filtration, namely, reversible, and irreversible fouling. The former layer could be easily removed, while the latter could not be washed away by either water scouring or a combination of water scouring, air scouring and backwash. As was illustrated in Figure 2-12 (see Chapter 2, subsection 2.2.3), the irreversible fouling resistance always tends to progressively build-up with increasing filtration and cleaning cycles in long term membrane processes, thus impacting greatly on the overall performance of membranes.

Therefore, this section sought to:

- establish whether the irreversible fouling resistance that occur on WFMF membranes during filtration process is cumulative in the long run.
- investigate if it was necessary to completely restore the permeability of the fouled membranes during a filtration process.

3.4.2. Methodology

A cyclic filtration and water scouring process was carried out using the laboratory WF-IMF unit shown in Figure 3-1. This involved a pure water flux experiment followed by a 90-minute filtration of 0.5 g/l of fresh yeast. Thereafter, the membranes were water scoured, and the filtration experiment repeated using the cleaned membranes. The filtration and cleaning cycles were repeated 6 times. During the filtration process, the flux and ΔP were recorded at a 5-minute interval. Resistances were then calculated using Equation 3-4.

3.4.3. Results and discussion

Figure 3-16 shows the resistance profiles for the cyclic filtration and water scouring process. From the figure, it is observed that the initial filtration resistance after every water scouring cycle is almost the same for all the cycles. This implies that the original performance of the WFMF membranes is slightly maintained in every cycle. It further indicates that water scouring removes a majority of the fouling layer at the end of every cycle.

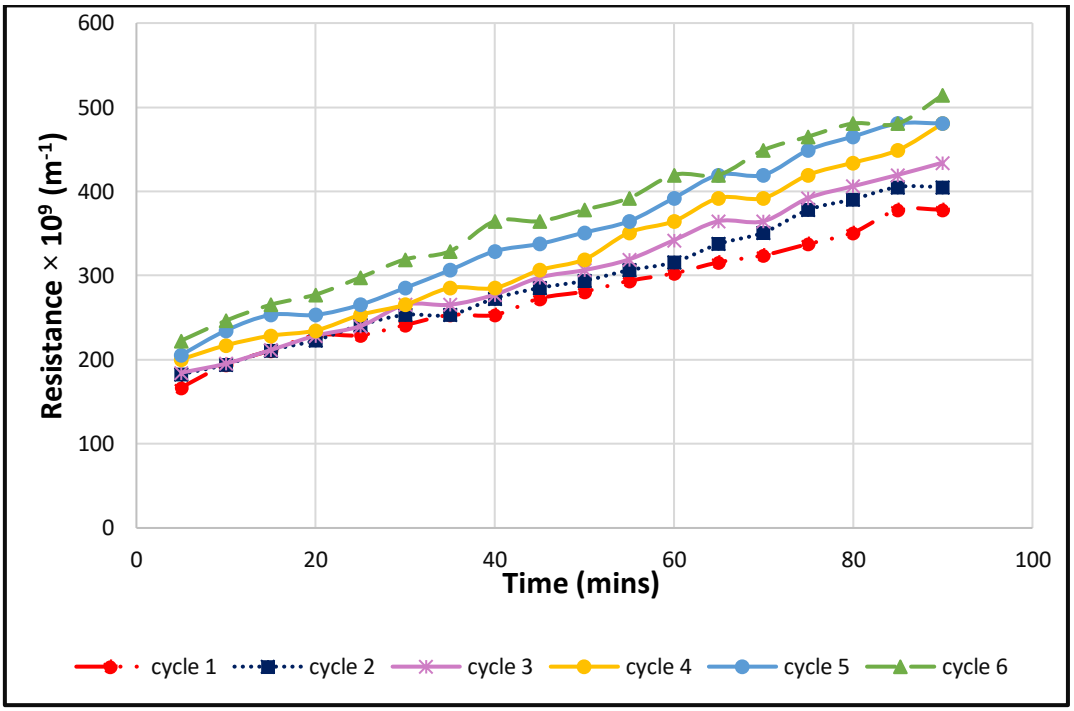

Figure 3-16: Resistance profiles for the cyclic filtration and water scouring process using WFMF membranes

Hence, it would not be necessary to completely restore the initial permeability of the WFMF membranes after every run. The membranes can be run for multicycles before any hard-core cleaning (brushing and hypochlorite soak as indicated in Chapter 2, subsection 2.4.4) is required. This would have a major implication in terms of ease of operation and energy consumption. The ease of operation of the membrane system would be improved through the reduction of the number of stoppages time for complete restoration of the membranes. In addition, the use of water scouring as the main cleaning method results in a relatively low energy consumption as was explained earlier in subsection 3.2.4.

However, it can also be seen from Figure 3-16 that the membranes experienced a gradual increase in fouling resistance with increasing filtration cycle. The increase was low during the first 3 cycles but become significant in the later cycles. At the end of the first cycle, the total resistance recorded

was found to be 378 × 10^9 m^{-1}. This increased to 405 × 10^9 m^{-1} by the end of the second cycle which represents 6.7% increase. However, At the end of the sixth cycle, the total resistance had increased by 26.5%.

The gradual increase in fouling resistance is attributed to the accumulation of irreversible foulants that could not be removed by water scouring (Ma *et al.*, 2019; Verma & Subbiah, 2019). From these results, it can be observed that the effectiveness of water scouring tends to decrease with increasing filtration cycles, as more irreversible foulants accumulate on the membrane surfaces. Therefore, a strategy of repelling the fouling organics before they get deposited within or on the membrane surface is necessary.

3.5. General outcomes of the investigations

Two major outcomes were realized from this investigation:

i) A possible explanation to Pillay *et al*'s anomalous findings

The anomalies reported by Pillay *et al* could be as a result of the difference in the surface structure of the WFMF membranes compared to the normal membranes. Unlike the commercial membrane, the WFMF membrane is neither flat nor smooth. The microscopic images showed that the WFMF membrane has trenches and troughs which are as a result of the intersections of groups of fibres. It is at these intersections that the small fine organics tend to settle during the filtration processes. These locations are not reachable by air scouring. Hence, even at high air aeration rates, the WF-IMBR system tends to experience a significant permeate flux decline.

From the above findings, it is postulated that the trenches and troughs on the WFMF membranes tend to get more exposed during high aeration rates as compared to regimes where air scouring is not applied. This is because air scouring removes the cake layers which always covers these locations, hence resulting in more deposition of irreversible foulants during long term filtration and cleaning processes. This could be the possible reason why Pillay *et al.* observed a high rate of fouling with increasing air scouring rate, but low fouling rate when the system was operated without air scouring, contradicting what had previously been reported in literature.

ii) The contribution of water scouring as a cleaning technique for WFMF membranes

Water scouring was found to play a major role in the cleaning of fouled WFMF membranes. In a combined cleaning strategy that involved water scouring, air scouring and backwash, it was found that water scouring contributed 80% to the whole cleaning process and was able to remove 72% of

the fouling layer. This indicates the key contribution of water scouring in restoring the permeability of fouled WFMF membranes. Given that water scouring is a simple method and does not require any energy input, its application to WFMF systems could have a major impact in terms of ease of operations and energy consumption. This is because, unlike air scouring and backwash, which are used in most commercially available membrane systems, water scouring does not require any major energy input. Furthermore, it is simple in terms of application, as only water from a hosepipe or a tap is needed to clean the membranes.

3.6. Summary

In this chapter, the fouling characteristics of WFMF membranes was investigated. This was achieved by first evaluating the efficiency of different air scouring and backwash regimes and water scouring in restoring the original permeability of WFMF membranes. Thereafter, the kinetics of fouling layer formation on WFMF membranes was established by performing synthetic wastewater filtration and cleaning experiments; where different filtration durations were evaluated. Results from the experiments were used to generate resistance profiles for unused, fouled and cleaned membranes.

From the resistance profiles, it was established that water scouring followed by air scouring and backwash could remove about 89% of the fouling layer but could not restore the membranes to their original permeability. There was always an irreversible fouling that remained on the membrane. In addition, the results indicated that the fouling layer formation on WFMF membranes involves two stages namely: deposition of irreversible foulants and cake layer formation. The irreversible fouling layer forms within the first five to ten minutes, followed by the cake layer deposition in the later stages of filtration. The latter could be easily removed by either water scouring or a combination water scouring, air scouring and backwash, while irreversible foulants were difficult to remove. Microscopic images of water scoured, and air scoured membranes showed that the irreversible foulants settled at the intersections of groups of fibers, where water scouring, and air scouring were unable to reach. From these experiments, it was clearly established that the accumulation of the irreversible foulants on the membranes tend to affect the membranes' performance in the long run. Hence, an alternative strategy of minimizing irreversible fouling in WFMF membranes would be necessary to increase the membrane's usability and performance.

Chapter 4.
Development and characterization of an oleophobic woven fabric microfiltration membrane

Overview

Introduction; Development of an OWFMF membrane; Characterization of the OWFMF membrane; Results and discussion; General outcome of the investigation; Summary.

4.1. Introduction

In Chapter 3, irreversible fouling was established as a major challenge in the filtration of organic suspensions using the woven fabric microfiltration (WFMF) membranes. The irreversible fouling layer could not be removed by either water scouring, air scouring or backwash. Furthermore, the fouling layer accumulated with increasing filtration and cleaning cycles, thus resulting in a decline in permeate flux. Therefore, a strategy for repelling the fouling organics before they get deposited within the membrane pores or on the membrane surface is necessary, to minimize fouling on the WFMF membranes.

Hence, an oleophobic WFMF (OWFMF) membrane that will be able to repel organics, and hence minimize the likelihood of membrane fouling was developed. The membrane was developed through the application of fluorocarbon onto the standard WFMF membrane using the padding process. As was concluded in Chapter 2 subsection 2.5.3.5, this was the best available option for developing the OWFMF membrane. This chapter focuses on the processes that were involved in the development and characterization of this membrane. It is worth noting that this is the first study that has developed an OWFMF membrane that is aimed for sanitation applications.

4.2. Development of an OWFMF membrane

The development of the oleophobic WFMF membrane involved three stages, viz. the optimization of the padding process parameters, the impregnation process, and finally curing and heat setting processes. These stages are discussed in detail in the following sections.

4.2.1. Optimization of the padding process

The optimization of the padding process was done using a response surface methodology (RMS). This methodology has been proven to be an effective technique for evaluating and optimizing processes in which a response of interest is influenced by several variables (Jeirani *et al.*, 2013;

Muhamad *et al.*, 2018; Xu *et al.*, 2016; Zhang *et al.*, 2015). This is because it enables the evaluation of the interaction of various process parameters, which is not possible in the conventional one-factor-at-a time method.

However, before applying the RSM, it is essential to first choose an experimental design. The design helps in defining the experimental runs that are to be carried out during the optimization process (Almeida *et al.*, 2008). In this study, a full factorial design with five centre points was employed. The centre points were used to assess the errors within the experiment runs. The steps that were followed in coming up with the entire experimental design are shown in Figure 4-1.

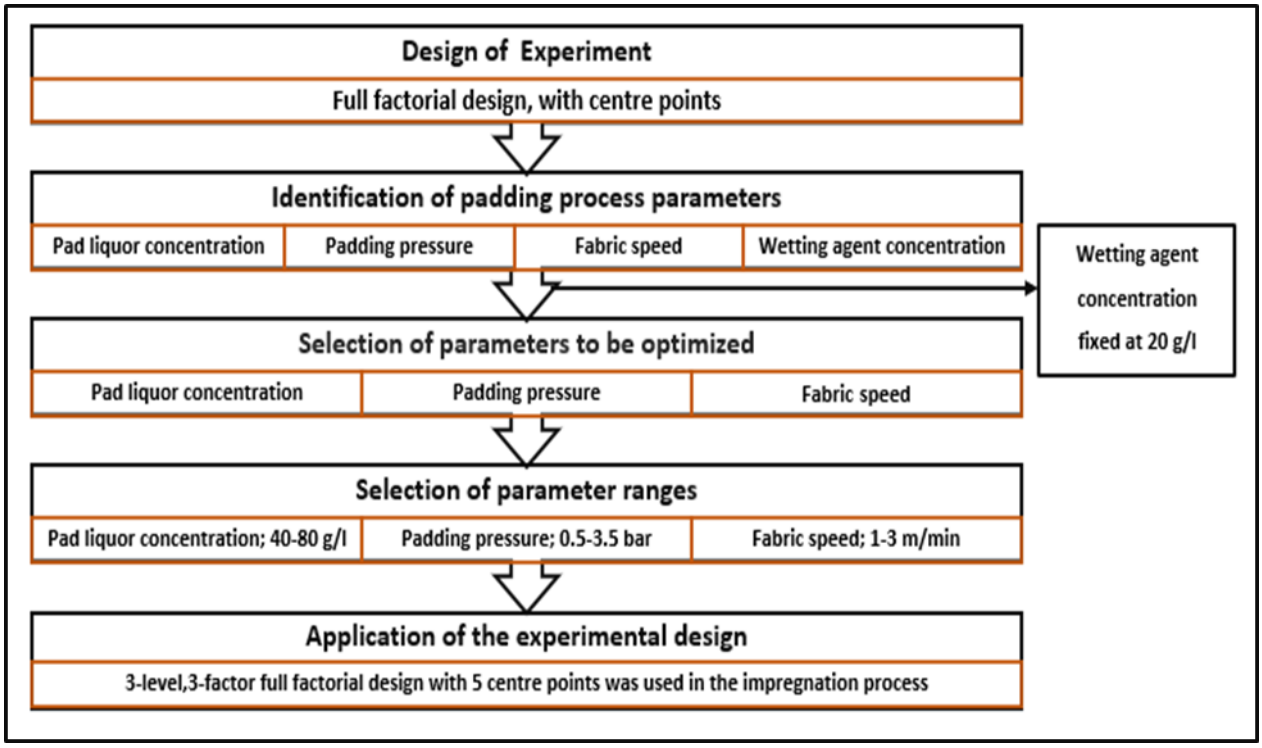

Figure 4-1: Flow chart showing the stages involved in developing an experimental design for the optimization of the impregnation process

First, the factors affecting the padding process were identified through literature review. The factors included fluorocarbon concentration, padding pressure, fabric speed, fluorocarbon temperature, and wetting agent concentration (see Chapter 2 subsection 2.5.4.2). The first three factors were selected for optimization while the fluorocarbon temperature and wetting agent concentration were set at fixed values of room temperature and 20 g/L, respectively. Based on what is reported in literature (Dasdemir & Ibili, 2017) and from consultation with textile experts, the fluorocarbon temperature cannot be changed in a textile industry. In the case of the wetting agent, the concentration was chosen based on the fluorocarbon brochure as seen in Appendix C and also on the account of the preliminary scanning experiments shown in Figure A-1 (Appendix A). Those

results showed that the use of 20 g/L of wetting agent was sufficient.

The next step involved selecting the ranges within which the padding process parameters were to be varied. The padding pressure and fabric speed ranges were selected according to the specification of the padding mangle equipment used for this study and data from literature (Castelvetro *et al.*, 2001; Dasdemir & Ibili, 2017; Shyr *et al.*, 2011; Tang *et al.*, 2017). This information is shown in Table 4-1. Ranges of 0.5-3.5 bar for padding pressure and 1.0-3.0 m/min for fabric speed, were chosen for this investigation.

Table 4-1: Padding pressure and fabric speed ranges from different sources

Process parameters	Padding mangle specifications	Ranges used in different studies
Padding pressure (bar)	0.25-5.5	2.5-3.0[a, b, c]
Fabric speed (m/min)	1.0-5.0	2.0-2.5[b, c, d, e]

[a](Shyr *et al.*, 2011) [b](Dasdemir & Ibili, 2017) [c](Chowdhury, 2018) [d](Tang *et al.*, 2017) [e](Castelvetro *et al.*, 2001)

In the case of the fluorocarbon concentration range, the supplier recommends a concentration of 40 g/L for the textile industry (see Appendix C). However, a higher concentration range of 40-80 g/L was chosen for this study. This is due to the fact that this investigation was targeting a higher oleophobicity than what is standardly required in the textile industry, and higher oleophobicity results from a higher amount of fluorocarbon being deposited on the fabric (Chowdhury, 2018).

Finally, a 3-factor, 3-level full factorial design with 5 centre points was formulated based on the chosen parameters and ranges. These parameters and their ranges are shown in Table 4-2, while the experimental plan is presented in Appendix A (Table A-20). The lower, middle, and higher threshold of the parameter ranges are designated as -1, 0, and 1, respectively.

The impregnation process was then carried out based on the aforementioned experimental design. Subsequently, the oil contact angle of the different membrane samples was measured using the Sessile Drop method. Thereafter, the design matrix together with the experimental results were analysed using the *Statistica* software package. A regression model that would be used to predict the response variable, i.e. the oil contact angle, was generated. In addition, the software was also used to generate response surface plots and to perform a desirability analysis on the experimental results. Through the surface plots and the desirability analysis, optimum conditions for developing the OWFMF membrane were identified. The plots were also used to evaluate the effects of parameters and their interactions on the oil contact angle of the membranes.

Table 4-2: Actual values of the evaluated padding process parameters and their corresponding coded levels

Parameter	Coded Levels		
	-1	0	1
FC concentration (g/L)	40	60	80
Padding pressure (bar)	0.5	2.0	3.5
Fabric speed (m/min)	1.0	2.0	3.5

4.2.2. The impregnation process

As was outlined in Chapter 2 subsection 2.5.4, the impregnation process used in this study was adapted from the textile industry. It involved fabric preparation, pad liquor preparation, and finally the actual padding process. The procedures that were employed in these processes are described in detail in the following subsections.

4.2.2.1. Fabric preparation

Fabric preparation process is usually done prior to the application of any chemical finish. It involves getting rid of any impurities on the fabric that may affect subsequent processes. Different researchers get rid of fabric contaminants through different ways, namely: desizing, scouring and washing (Hashem *et al.*, 2009; Thilagavathi & Kannaian, 2008; Zhou *et al.*, 2016).

In this study, the fabric preparation involved various steps. First, fabric samples of about 80 cm by 25 cm in size were cut from a fabric roll. The samples were then washed and scoured in a washing machine using warm water at 25^{o}C and 5 mL/L of scouring agent for around 30 minutes. Thereafter, they were rinsed completely with water. The scouring agent used was supplied under the trade name Rucogen DFL. This was followed by turbo-drying of the fabric samples and finally, their edges were sealed using a soldering rod. The sealing was done to avoid unravelling of the samples during handling.

4.2.2.2. Pad liquor preparation

The coating used in this study is supplied under the trade name RUCO-GUARD AFR by Rudolf Chemicals Ltd, South Africa. It is a cationic fluorocarbon resin delivered in emulsion form. It has a pH range of 2-5; and it is usually used as water and oil repellent coating on the surface of fabrics in the textile industry.

The pad liquor preparation in this investigation involved mixing distilled water, wetting agent, acetic acid, and the fluorocarbon emulsion in the recommended quantities. The importance of acetic acid is to adjust the pH of pad liquor to around 5 before the addition of fluorocarbon. This is necessary because fluorocarbon emulsions are usually cationic, and therefore stable and effective at this pH level (Sayed & Dabhi, 2014). Based on literature, acetic acid is usually added to the pad liquor at a concentration of 1 g/L (Castelvetro *et al.*, 2001; Chowdhury, 2018; Thilagavathi & Kannaian, 2008). The importance of the wetting agent is to enhance the fabric impregnation. It decreases the marginal interfacial tension between the fibres and the liquor, thereby increasing the saturation rate of the fabric during the padding process (Rouette & Kittan, 1991).

The preparation of the pad liquor involved the addition of 20 g/L of wetting agent to 1 L of water in a beaker. This was followed by an addition of 1 mL of 60% acetic acid. Finally, 40 g, 60 g or 80 g of fluorocarbon (FC) emulsion was added to the mixture and gently stirred to yield 40, 60 and 80 g/L of FC mix, respectively.

4.2.2.3. The padding process

i) Experimental set-up

The padding process was done using a laboratory padding mangle. As shown in Figure 4-2, a padding mangle consists of a deep trough for holding the pad liquor.

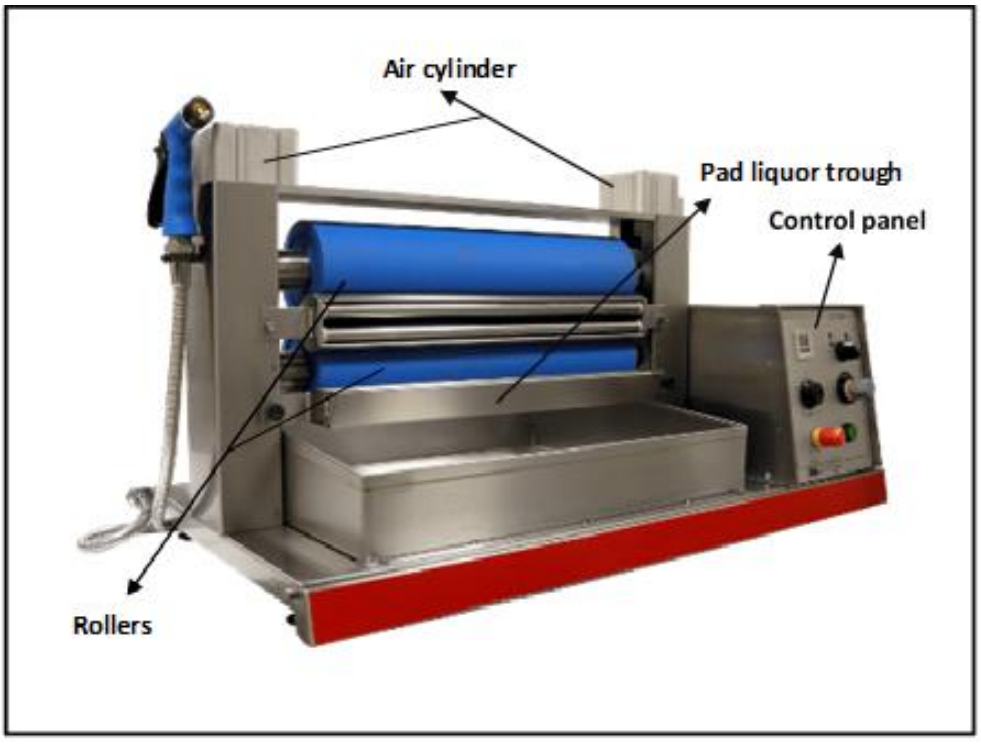

Figure 4-2: Image of a laboratory padding mangle

In addition to the trough, there are two rollers for squeezing the pad liquor into the fibres, a control panel to adjust the padding pressure and fabric speed, and finally air cylinders that control the lifting of the movable roller, which determines the amount of pressure applied for padding. Air is usually supplied from a separate compressor tank.

ii) Application of the fluorocarbon

The washed, scoured, rinsed, and dried fabric samples were impregnated by being immersed in the FC liquor, before being passed between the squeezing rollers. Different combinations of different padding parameter values were used in impregnating the different fabric samples. These combinations are shown in Appendix A, Table A-20.

After the padding process, the padded fabric samples were dried at 100°C for 2 minutes in an oven. The drying process is usually done before the curing process. The aim of this process is to get rid of water in the intermolecular spaces of the membrane fibre. Failure to do this may cause shrinkage of the fibre or imperfect crosslinking of the FC component and the fabric during curing (Maschinenwesen, 2004).

In this work, the drying conditions were chosen based on literature data. In most of the published investigations, a fabric impregnated with fluorocarbon was dried at a temperature range of 100-110 °C for 1-3 minutes (Castelvetro *et al.*, 2001; Chowdhury, 2018; Saffari *et al.*, 2015). A drying condition of 100 °C for 2 minutes was, therefore, chosen for this study.

4.2.3. Curing

After the impregnation and drying process, the different fabric samples were cured in an oven at 180°C for 30, 60 and 90 seconds, respectively. The employed curing conditions were chosen based on the literature (Sayed & Dabhi, 2014), and advice from textile experts.

It was realized during the preliminary experiments that the curing process had a profound effect on the structure of the fabric. It led to the production of fabrics with disorientated fibres. This affected the fabric's permeability properties. Hence, a corrective measure was necessary. The results of these preliminary experiments are presented in section 4.4.2.2.

4.2.4. Curing with simultaneous heat setting

In subsection 2.5.4.3 of Chapter 2, a measure of overcoming the disorientation of fabrics during the curing process was proposed. Heat setting process was identified as a way of maintaining

dimensional stability of the fabrics. This is usually done by applying tension on fabrics at high temperature for a certain period of time. Since the heat setting conditions for a polyester fabric fall within the same range as its curing conditions (see subsection 2.5.4.3), this study concurrently cured, and heat set the padded fabrics.

The different padded fabric samples were cured under tension in an oven at 180°C for 30, 60 and 90 seconds, respectively. The tension on the fabrics was applied through an adjustable stenter frame. A stenter frame (as shown in Figure 4-3(a)) is a square metallic beam with hooks all around it. It applies tension on fabrics by stretching. The stenter frame used in this study had its hooks positioned on the adjustable parts.

Before being put into the oven, the padded fabrics were carefully hooked on the frame as shown in Figure 4-3 (b). During the hooking process, it was ensured that the distance between the adjustable part of the frame and the fixed part is the same all round. This was to ensure that uniform tension is applied all around the fabric during stretching.

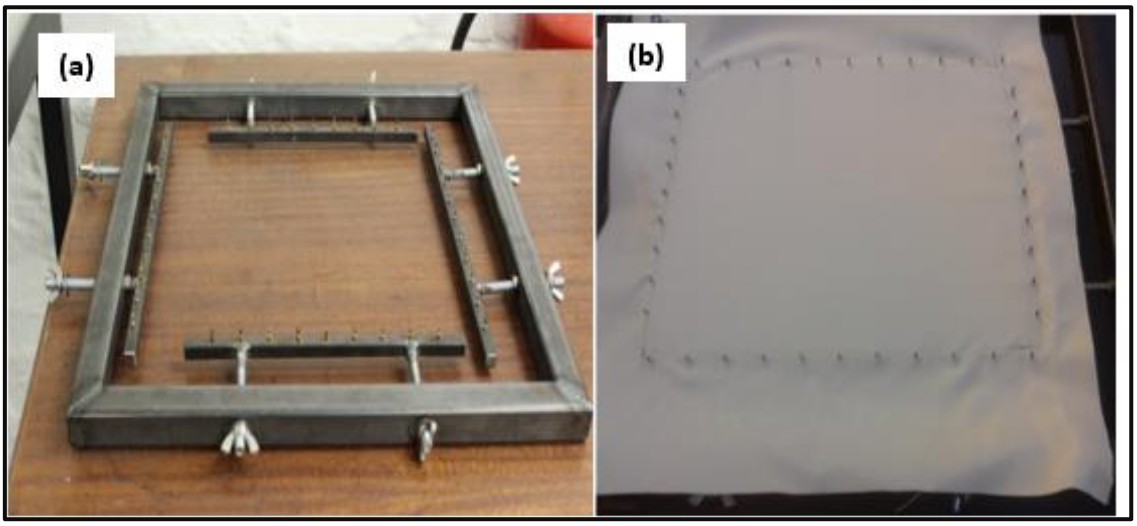

Figure 4-3: An image of: (a) a stenter frame and (b) a fabric on a stenter frame

Three different stretch factors were evaluated during the curing and heat setting process, namely: 2.0, 4.0 and 4.8 %. For this study, the stretch factor was defined by Equation 4-1. The highest stretch factor that could be achieved by the available stenter frame was 4.8 %. Hence, this stretch factor was used as the upper limit range during experimentation.

Equation 4-1

$$\boldsymbol{Stretch\ factor} = \left(\frac{\boldsymbol{l_e}}{\boldsymbol{l_o}} - \mathbf{1}\right) \times \mathbf{100\%}$$

where l_e is the length of the stretched membrane (cm) and l_o is the length of the original membrane (cm).

After the process of curing and heat setting, the tightness of the membranes was assessed. The assessment was done in two ways: (i) by viewing the membranes under a Scanning Electron Microscope; and (ii), by assessing the turbidity removal efficiency of the membranes in a filtration process of 0.5 g/L yeast suspension and comparing it to that of the standard WFMF membranes.

4.3. Characterization of the OWFMF membrane

Two properties of the developed membranes were analysed, namely: the wetting properties of the membrane and the membrane morphology. The procedures for evaluating these two membrane characteristics are outlined in this section.

4.3.1. Membrane surface wetting properties

The aim of characterizing the wetting properties of the membranes was to assess the oleophobic properties of the impregnated membranes as well as determine the optimum conditions for the impregnation process. In addition, the hydrophobicity of the membrane was also evaluated. This is due to the fact that fluorocarbon imparts both oleophobic and hydrophobic properties to the membrane.

The surface wetting properties of the developed membranes were determined by contact angle measurements of different liquids on the membrane surface using the Sessile Drop method. This was done using a Kruss Shape Drop analyser. Prior to the contact angle measurements, the developed membranes were rinsed with distilled water and then left overnight to dry. In determining the oleophobicity of the developed membranes, a 10 µL droplet of hexadecane (oil) was placed on the dry membrane surface using a micro-syringe. The oil droplet image was then captured and analysed by the Kruss Shape Drop analyser to obtain the oil contact angle of the membrane. For each membrane sample, at least 5 measurements of the oil contact angle at different locations of the membrane surface were recorded; and the average value of the measurements was used as the representative oil contact angle of the tested membrane. The procedure was repeated in the evaluation of the membrane's hydrophobicity by using water in the place of hexadecane.

4.3.2. Membrane morphology

The main aim of evaluating the morphology of the developed membrane was to assess if the modification process brought any changes to its surface structure. This was necessary as the change

in the surface structure will inevitably influence its filtration performance.

The membrane morphology was observed through a Scanning Electron Microscope (SEM) at various magnification levels. The membrane samples were dried and sputter-coated with a 10-nm-thick layer of gold before the observation. Both the standard and the oleophobic WFMF membrane were imaged and characterized.

4.4. Results and discussion

4.4.1. The optimization of the padding process

This section presents and discusses the findings of the optimization of the padding process. The experimental design matrix and the results of the optimization process are presented in Appendix A, Table A-20, with the oil contact angle as the response variable.

4.4.1.1. Repeatability of the experimental runs

The repeatability of the experimental runs during the optimization process was assessed from five centre point repeats. These runs were done at a fluorocarbon concentration of 60 g/L, a padding pressure of 2 bar and a fabric speed of 2 m/min. The oil contact angles of the fabrics that were produced during these 5 runs are shown in Figure 4-4.

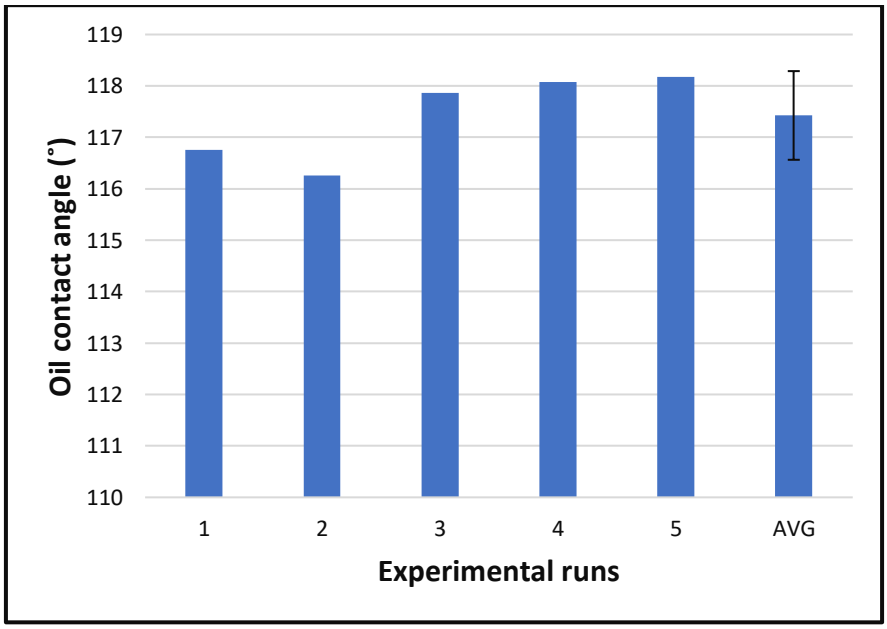

Figure 4-4: Oil contact angles of five repeat runs carried out at a FC concentration of 60 g/L, a padding pressure of 2 bar, and a fabric speed of 2 m/min

From the above figure, it can be seen that the average oil contact angle for the 5 repeat runs was 117.42, with a deviation of ±0.862˚. From this, it can be concluded that the experimental runs of the

optimization process were fairly repeatable.

4.4.1.2. Optimization

In the optimization of the padding process, three parameters were considered: the fluorocarbon concentration (Y_1), the padding pressure (Y_2) and the fabric speed (Y_3). The response variable of the process was in terms of an oil contact angle (Z). Y_1, Y_2 and Y_2 were the independent variables, and Z was the dependent variable. A fourth order polynomial function was fitted to the oil contact angle experimental results using the *Statistica* software, and the model equation shown in Equation 4-2 was obtained:

Equation 4-2

$$Z = 102.2 + 0.043Y_1 + 17.20Y_2 + 8.458Y_3 - 11.46Y_2Y_3 - (1 \times 10^{-4})Y_1^2 - 4.205Y_2^2 - 2.914Y_3^2 + 2.686Y_2^2Y_3 + 2.320Y_3^2Y_2 - 0.536Y_2^2Y_3^2$$

The significance of the various terms in the model was assessed through ANOVA analysis. The analysis is presented in Appendix A, Table A-23. A summary of the results is presented in Table 4-3 for discussion purposes. All terms that had a p-value of less than 0.05 were considered to have a significant effect on the response variable, otherwise the terms were seen to be insignificant. From Table 4-3, it is evident that the linear and the quadratic terms of fluorocarbon (FC) concentration, padding pressure and fabric speed were considered to have a significant effect on the response variable. The analysis also showed that the linear and the quadratic interactions of the padding pressure and fabric speed had a significant effect on the response variables. As a result, all the above-mentioned terms were included in the model equation expressed in Equation 4-2.

Table 4-3: Significance test for the padding process parameter by use of p-values (The ANOVA was carried out at 95% confidence level)

Parameters	P-value	Test of significance (α=0.05)	Significance
(1) FC concentration (L +Q)	0.000055	p<α	Significant
(2) Padding pressure (L+Q)	0.000000	p<α	Significant
(3) Fabric Speed (L+Q)	0.020821	p<α	Significant
1*2	0.439090	p>α	Not significant
1*3	0.998619	p>α	Not significant
2*3	0.003665	p<α	Significant

However, the p-values for the interactive effect of FC concentration and padding pressure, and that of fluorocarbon concentration and fabric speed were found to be higher than 0.05. This shows that

they did not significantly influence the response variable. Hence, these terms were excluded from the model.

Thereafter, the validity of the model in predicting the response variable was assessed. Figure 4-5 shows a graph of the predicted oil contact angle values vs the experimental data. From the Figure, it can be seen that the points as well as the points clusters are aligned closely with the diagonal line. This shows a fairly good agreement between the model and the experimental data. Hence, it can be concluded that Equation 4-2 is a fairly good model for predicting the response variable (oil contact angle) of the padding process.

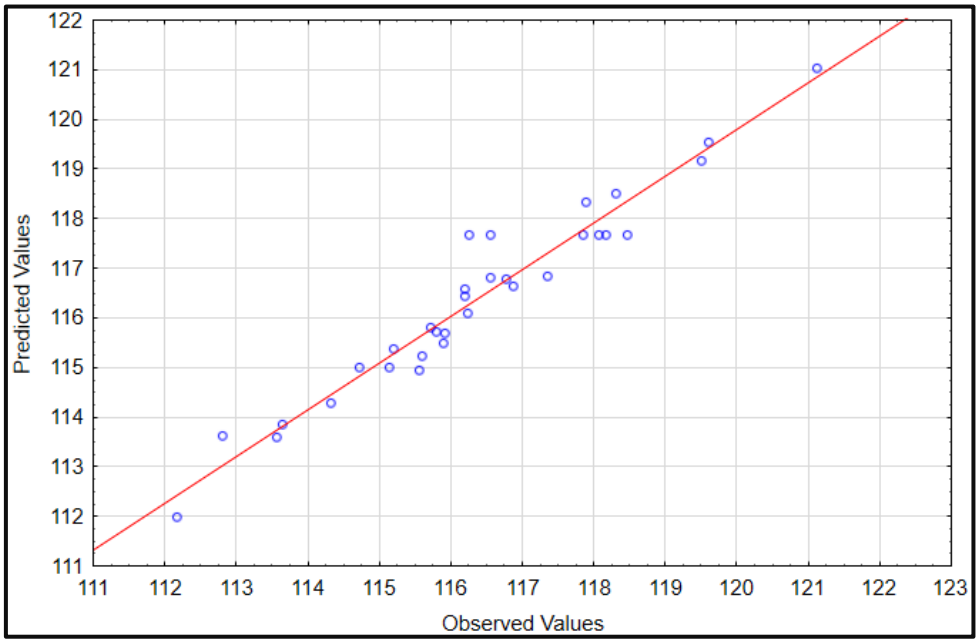

Figure 4-5: Predicted oil contact angle versus experimental oil contact angle values

The value of R^2 also further confirmed that the model is valid. An R^2 value of 0.92 was realized in this study. When the value of R^2 approaches 1, the correlation between the predicted and the experimental values always increases. Hence, this value indicates a fairly good degree of correlation between the predicted and the experimental results.

The model was then used to determine the optimum conditions for the padding process. Solving the model using the experimental data presented in Table A-20 (see Appendix A) revealed an optimum response at the following conditions: concentration 80 g/L, padding pressure 2 bar, and fabric speed 1 m/min, with a predicted oil contact angle of 121.01˚. Similar optimum conditions were also shown by the desirability profile (see Figure 4-6). Therefore, the abovementioned conditions were considered as the optimum conditions for producing the oleophobic WFMF membranes.

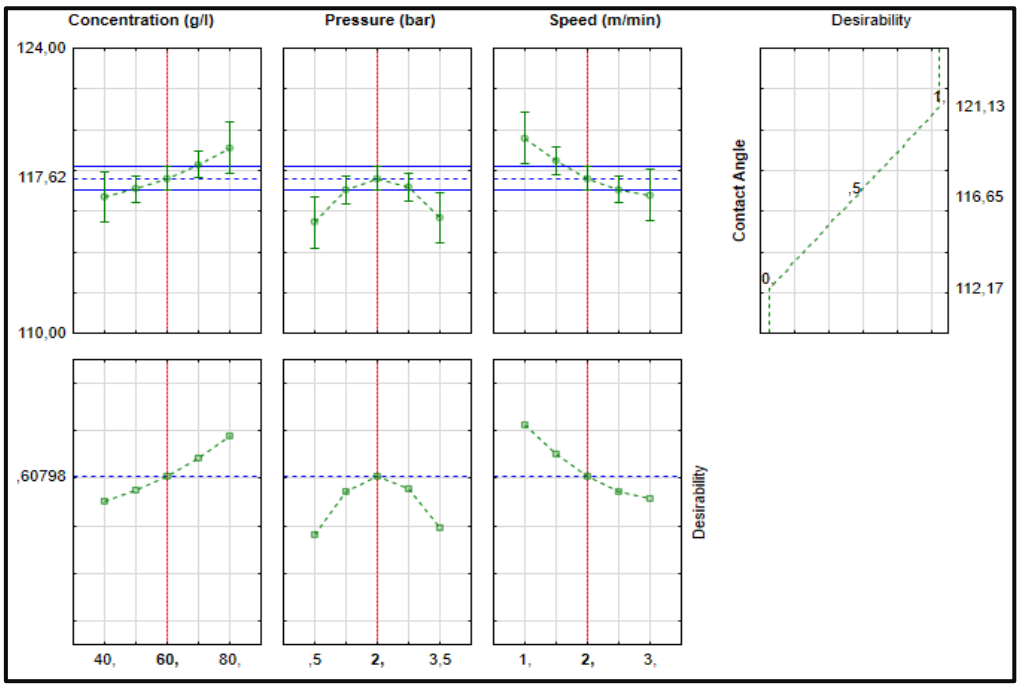

Figure 4-6: The relationship between the oil contact angle and the different independent variables, showing the predicted optimum values based on the experimental results

4.4.1.3. Effects of the padding process parameters

The ANOVA analysis revealed that all the evaluated parameters, including an interaction of the padding pressure and the fabric speed had an effect on the response variable. This section, therefore, outlines how the fluorocarbon concentration, the padding pressure and the fabric speed affect the oil contact angle.

i) Fluorocarbon concentration

Figure 4-7 illustrates the effect of fluorocarbon concentration on the oil contact angle at a padding pressure of 2 bar and a fabric speed of 1 m/min.

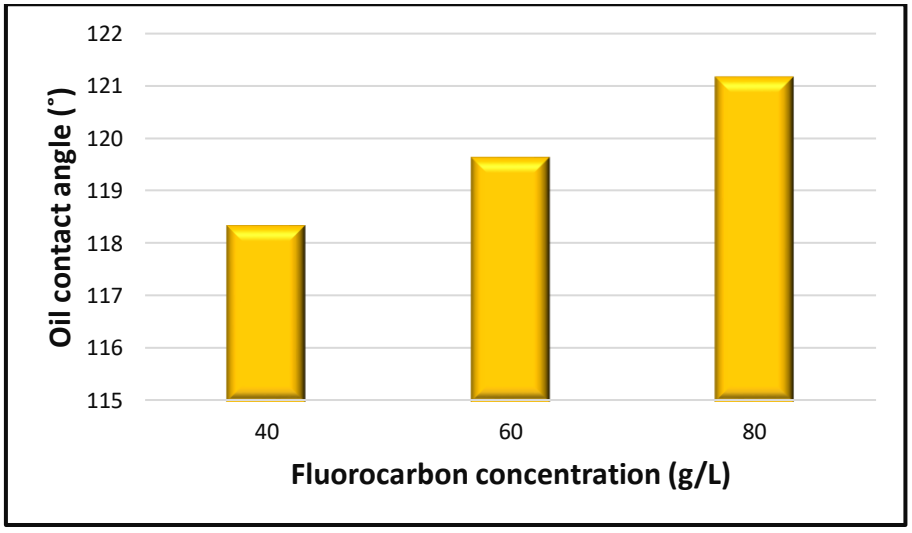

Figure 4-7: Effect of fluorocarbon concentration on the oil contact angle

From the Figure 4-7, it can be observed that the oil contact angle of the membranes increased with an increase in fluorocarbon concentration. The oil contact angle increased from 118.31˚ to 121.13˚ when the fluorocarbon concentration was increased from 40 g/L to 80 g/L. The increase in the oil contact angle is attributed to the additional quantities of fluorocarbon on the membrane surface, which minimizes the surface energy of the membrane. (Chowdhury, 2018; Dasdemir & Ibili, 2017; Thilagavathi & Kannaian, 2008). This results in an increase in the oil contact angle.

ii) Padding pressure and fabric speed

Figure 4-8 shows the interactive effect of padding pressure and fabric speed at constant fluorocarbon concentrations of 40 g/L, 60 g/L and 80 g/L.

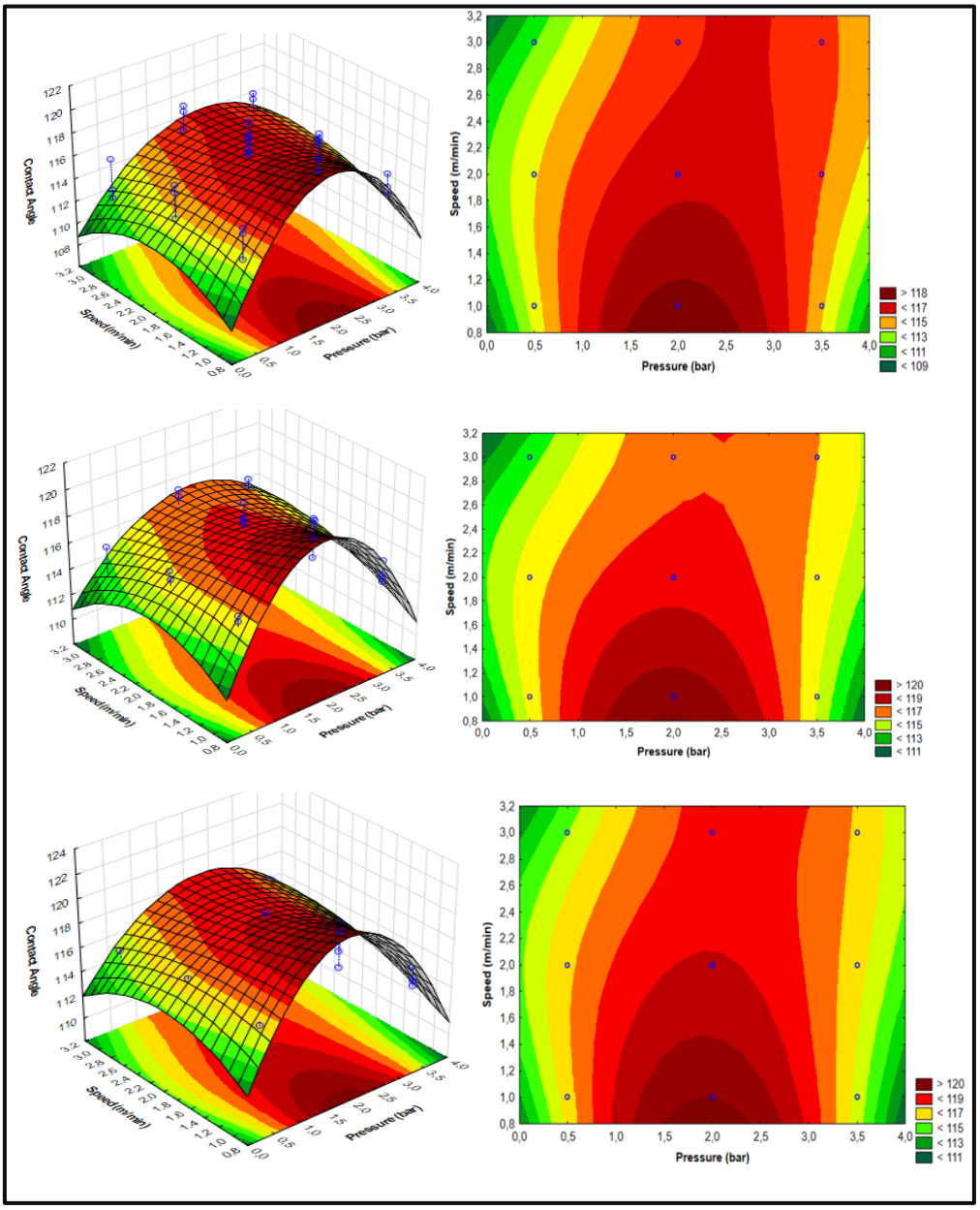

Figure 4-8: Effects of padding pressure and fabric speed on the oil contact angle at FC concentrations of: (a) 40 g/L, (b) 60 g/L and (c) 80 g/L

From the plots, it can be observed that the oil contact angle increased with an increase in padding pressure up to a certain level and then decreased. Furthermore, from Figure 4-8, It can be seen that the oil contact angle decreased with an increase in fabric speed.

The increase in the oil contact angle up to a certain level is attributed to a better penetration of the fluorocarbon (Choudhury, 2006). As the padding pressure is increased the fluorocarbon penetration into the fabric also increased. This in turn increases the oil contact angle of the fabric. However, at very high padding pressures the fluorocarbon (FC) liquor is squeezed out by the rollers, thus reducing the amount of liquor on the fabric. This results in a decrease in the fabric's oil contact angle.

The decrease in the oil contact angle with increasing fabric speed is caused by the decrease in both the immersion time of the fabric in the liquor and, the squeezing time (Speke, 1954). As the fabric speed is increased, the amount of time spent by the fabric in the FC liquor tank is decreased thereby decreasing the amount of fluorocarbon being absorbed by the fabric. Additionally, an increased fabric speed also reduces the squeezing time of the fabric resulting into poor penetration of the fluorocarbon into the fabric. Hence, the oil contact angle generally decreases. Conversely, when the fabric speed is decreased, the opposite will happen.

However, it should be noted that an increase or a decrease in the fabric speed will yield a high contact angle depending on the applied pressure. This is due to the interactive effect of padding pressure and fabric speed, as was indicated by the ANOVA results. From the plots, it can be seen that the membrane had a lower oil contact angle at low pressure and high fabric speed. A similar observation is made at a high padding pressure and low fabric speed. But when the pressure was increased at a constant high fabric speed, the oil contact angle of the fabric increased. Similarly, the oil contact angle increased when the fabric speed was increased at a constant high pressure. This brings out the positive effect of the interaction between the padding pressure and the fabric speed.

4.4.2. Curing and heat setting

In this section, the curing time range that had been selected was evaluated and the optimum curing time chosen. Thereafter, the effect of heat setting was evaluated at different stretch factors.

4.4.2.1. Evaluation of curing parameters

Figure 4-9 shows how the oil contact angle varied with the curing time for membranes impregnated

at a padding pressure of 2 bar and fabric speed of 1 m/min.

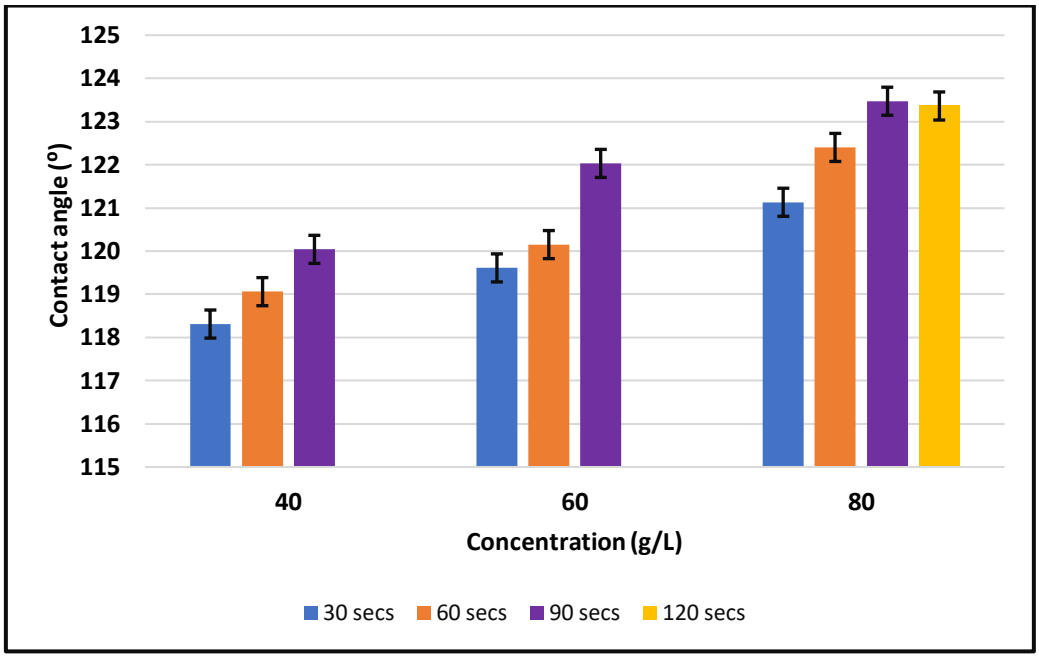

Figure 4-9: Effect of curing time on the oil contact angle at a constant curing temperature of 180°C for membranes padded at 1.5 bar/ 1 m/min

(Three repeat runs, average presented with error bars)

From Figure 4-9, it is observed that an increase of the curing time from 30 to 90 seconds results in an increase in the fabric's oil contact angle. This trend was observed for all the FC concentrations that were investigated. These results conform to findings from similar studies (Hashem *et al.*, 2009). The increase in the oleophobicity performance with an increase in the curing time can be attributed to the increased exposure time of the padded fabric. This in turn allowed for the completion of the chemical reaction between the FC, crosslinking reagent, and the fabric.

An interesting observation from Figure 4-9 is that when the curing time was further increased to 120 seconds (for the 80 g/L FC concentration), no significant change in the oil contact angle was observed. This implies that 90 seconds was enough to fix all the fluorocarbon applied on the fabric. Hence, a curing time of 90 seconds was chosen for the development of the OWFMF membrane.

4.4.2.2. Heat setting

After the curing process, SEM images of both the standard and the developed membranes were taken. This was done to assess if there was any change in the morphology of the developed membranes. Figure 4-10 shows the SEM images of the standard WFMF membrane and that of the OWFMF membrane.

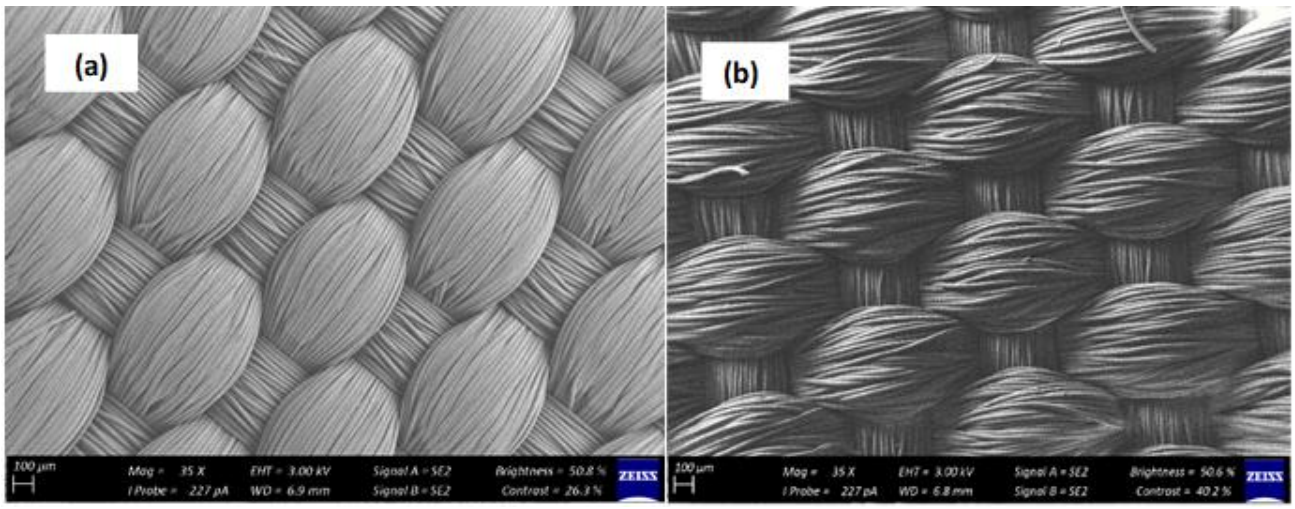

Figure 4-10: SEM image showing: (a) a standard WFMF membrane and (b) an OWFMF membrane

From Figure 4-10, it was observed that the fibres on the OWFMF membrane were slightly distorted when compared to the standard WFMF membrane. According to literature, the distortion is attributed to the exposure of the membrane to a temperature above its glass transition temperature (Huang & Liang, 1996). When a fabric is heated to a temperature above its glass transition temperature, the polymer chains within the fabric become mobile and begin to vibrate, hence making the fibres in the fabric to become distorted. Therefore, in order to avoid this undesirable effect, heat setting was incorporated into the curing process.

Figure 4-11 shows the SEM images of an OWFMF membrane that was only cured, and that which was cured and heat set. From the images, it can be seen that the cured and heat set membrane was fairly tighter than the one that was only cured. Therefore, it can be concluded that the heat setting process was successful in fairly maintaining the dimensional stability of the OWFMF membrane.

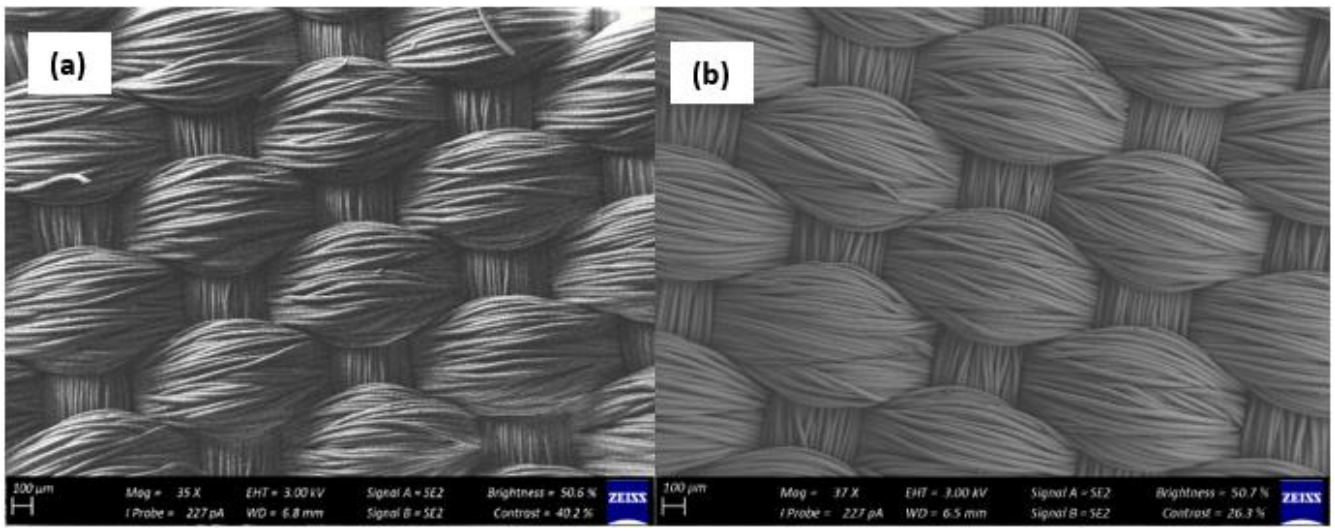

Figure 4-11: SEM images of an OWFMF membrane that was: (a) only cured and (b) cured and heat set

To further confirm this finding, the turbidity removal efficiency of the heat set fabric was compared to that of the membrane that was only cured. The removal efficiencies of these fabrics are presented in terms of permeate turbidity in Figure 4-12.

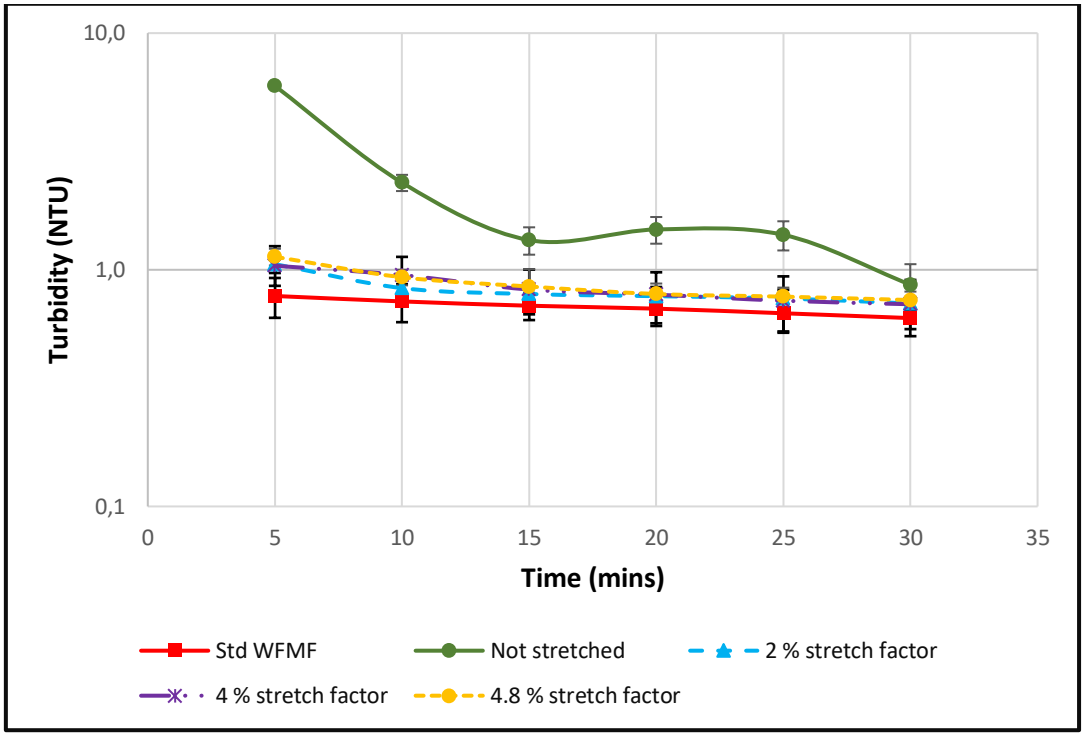

Figure 4-12: Comparison of standard WFMF membranes and OWFMF membranes heat set at different conditions in terms of permeate turbidity

(Three repeat runs, average presented with error bars)

From Figure 4-12, it is clearly seen that all heat set fabric performed better in terms of the permeate turbidity compared to the unset fabric. In addition, their performance was also comparable to that of the standard WFMF membrane. This further confirms the earlier finding. Hence, it can be safely concluded that the incorporation of the heat setting process into the curing process managed to fairly maintain the fabric dimensional stability.

Additionally, it can be observed from the graph that the variation of the stretch factor from 2.0% to 4.8% did not make any significant difference on the tightness of the fabric. The permeate turbidity profiles of all the three fabrics that were heat set under the different stretch conditions, levelled up at the same turbidity of around 0.7 NTU. Therefore, the padded membranes can be satisfactorily heat set at stretch factors between 2.0% and 4.8%.

4.4.3. A summary of the characteristics of the developed OWFMF membrane.

The developed membrane had two distinct characteristics:

4.4.3.1. Oleophobicity

The standard WFMF membrane demonstrated no significant oleophobicity, i.e. a drop of oil immediately wetted and penetrated the membrane. The developed membrane was found to be oleophobic in nature. This was indicated by its oil contact angle which has a value of about 123.5˚. When compared to the standard WFMF, it can be concluded that the developed membrane has a significantly higher degree of oleophobicity. This is illustrated by Figure 4-13, where the standard WFMF seems to be wetted with an oil droplet immediately it lands on its surface.

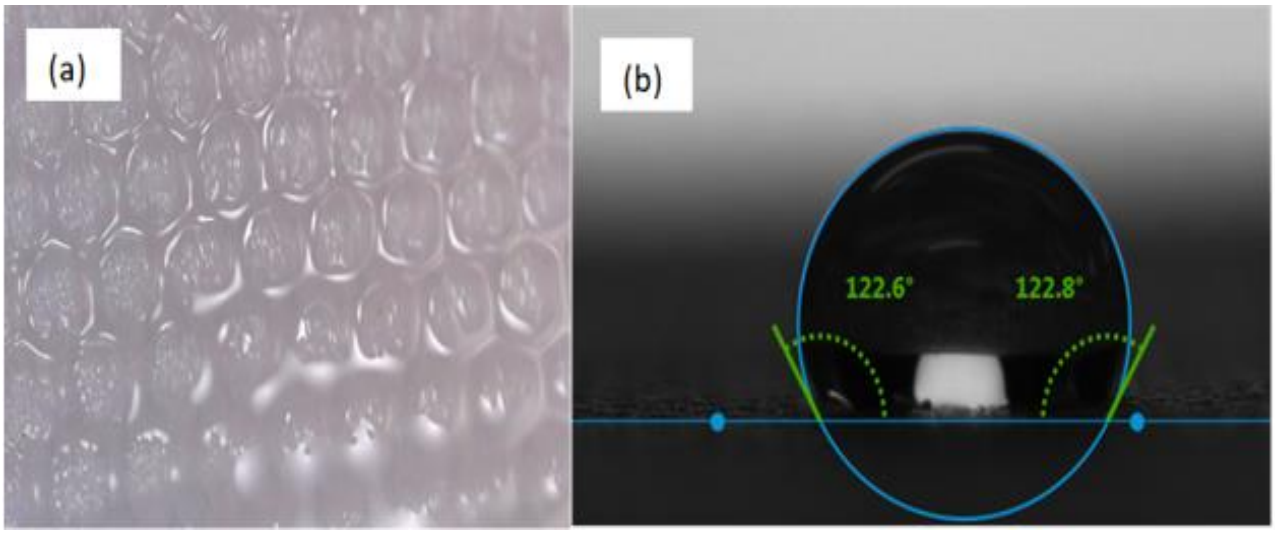

Figure 4-13: Oil contact measurement of: (a)standard WFMF and (b) OWFMF membrane

4.4.3.2. Hydrophobicity

In addition to the oleophobic properties, the developed membrane was found to be hydrophobic. It had a water contact angle (WCA) of approximately 136˚. Its hydrophobicity had increased by 44%. A previous investigation reported the WCA of the standard WFMF membrane to be 76˚ (Mecha & Pillay, 2014). Hence, the application of fluorocarbon did not only make the membrane oleophobic, but it also imparted hydrophobic characteristics to the membrane. Figure 4-14 illustrates the difference in the degree of hydrophobicity between the standard and the OWFMF membrane.

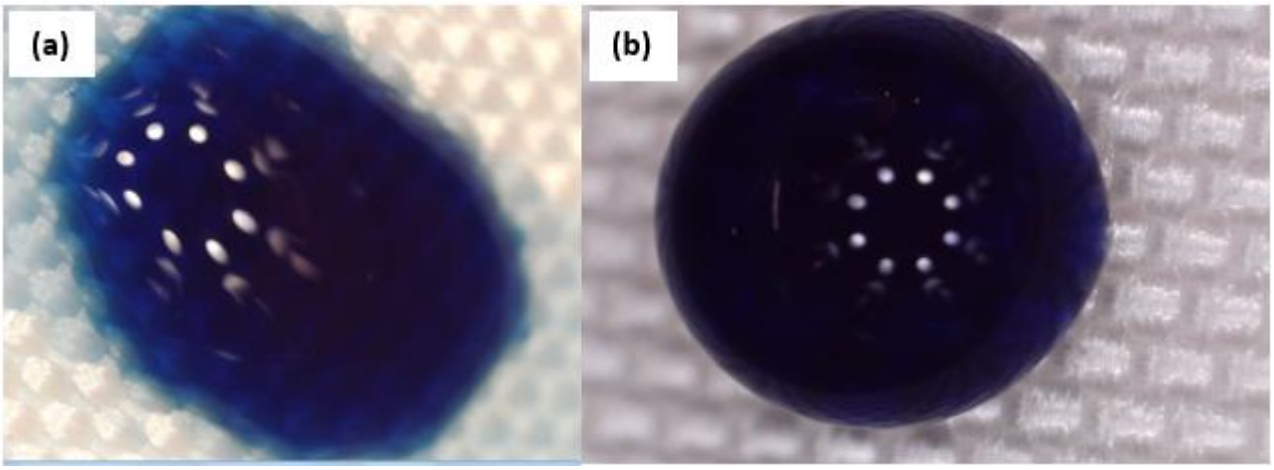

Figure 4-14: Images of a coloured water drop showing the degree of hydrophobicity on: (a)a standard WFMF and (b) an OWFMF membrane

4.5. General outcome of the investigation

The aim of this section was to develop an oleophobic WFMF membrane. The development process involved the application of fluorocarbon on standard WFMF membrane using padding process. After optimizing the process parameters, the membrane was developed at a padding pressure of 2 bar, fabric speed of 1 m/min, fluorocarbon concentration of 80 g/L and curing condition of 180˚ for 90 seconds. The resulting WFMF membrane has an oil contact of 123.5˚, which indicates that the membrane is highly oleophobic. The standard WFMF membrane does not exhibit any oleophobic properties since it becomes wetted immediately it comes in contact with oil droplets. However, the developed membrane showed a high oil contact angle. Hence, the objective of this study was successfully met.

It is also worth noting that the option used in this investigation to develop the OWFMF membrane can easily be done on an industrial scale. This is due to the following factors: - the fluorocarbon compounds are commercially available; the padding process is a well-established process in the textile industry; and finally, it has already been proven that fluorocarbons can get attached to polyesters. Given that this idea can be implemented practically, this investigation will hopefully make a significant contribution to the development of the WFMF technology in sanitation applications.

4.6. Summary

In this chapter, OWFMF membranes were developed by the application of fluorocarbon on standard WFMF membranes. The fluorocarbon application was done through a pad-dry-cure method and the

padding process optimization was carried out using a factorial experimental design. The experimental design involved varying the process parameters such as padding pressure, fabric speed and the fluorocarbon concentration during the padding stage. Thereafter, the parameters were optimized using response surface methodology. Before the optimization of the padding process, a preliminary evaluation of the influence of these parameters was performed by assessing their correlation with the padding process. All the parameters were found to have an effect on the padding process. The optimum condition for padding the fabrics was estimated as 2 bar padding pressure and 1 m/min fabric speed at all the investigated fluorocarbon concentration range. In the case of the investigated fluorocarbon concentration range, 80 g/L gave the highest oleophobic characteristic of around 123.5° OCA at a curing temperature and time of 180°C and 90 seconds, respectively. Additionally, the developed OWFMF membranes were also found to have a hydrophobic characteristic of 136° WCA at the same process conditions.

Chapter 5.
Performance evaluation of the oleophobic woven fabric microfiltration membrane

Overview

Introduction; Methodology; Results and discussion; Limitation of the study; General outcome of the investigation; Summary.

5.1. Introduction

In Chapter 4, a standard woven fabric microfiltration (WFMF) was modified to an oleophobic WFMF (OWFMF) membrane. This was done to improve its fouling resistance, the general performance and the cleanability.

In this chapter, the performance of the developed OWFMF membrane was evaluated and compared to the standard WFMF membrane. This chapter presents the methodology, the analyses of the results, and the conclusions drawn.

5.2. Methodology

The performance evaluation of the oleophobic WFMF membranes relative to that of the standard WFMF membranes was carried out on a laboratory scale, in a series of dead-end filtration experiments. The performance criteria evaluated were the pure water flux, the permeate quality, the fouling characteristics, the ease of cleaning, and the stability of the oleophobic surface.

5.2.1. Experimental set-up

The laboratory experimental set-up that was used in the performance evaluation experiments is similar to that presented and described in Chapter 3, subsection 3.2.1.1. For convenient reference, the set-up is repeated in this section (Figure 5-1). The rig is referred to as a woven fabric immersed membrane filtration (WF-IMF) unit.

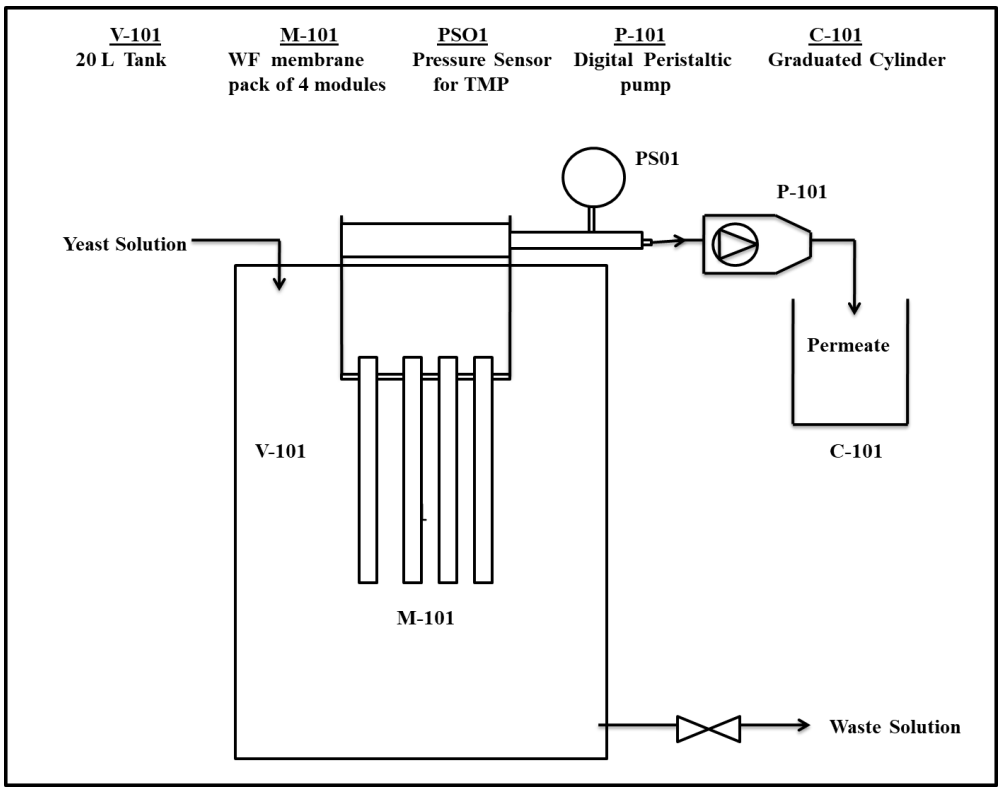

Figure 5-1: A schematic diagram of the laboratory WF-IMF unit (repeated)

5.2.2. Performance evaluation experiments

5.2.2.1. Pure water flux experiments

The pure water flux (PWF) experiments were carried out exactly as the procedure described in Chapter 3, subsection 3.2.2.1. In summary, the procedure was as follows:

- The WF-IMF rig was used to filter pure water only;
- The pump speed was set to 50 rev/min;
- The flow rate and the pressure drop (ΔP) across the membrane were measured and recorded;
- The above procedure was done for pump speeds ranging from 50 to 300 rev/min, at an interval of 50 rev/min.

The flow rate values were then used to calculate the fluxes by employing Equation 5-1. Thereafter, pure water curves were plotted using the calculated flux and the ΔP. Three runs were performed for each pure water flux experiment to ensure reproducibility of the results.

Equation 5-1

$$J_O = \frac{v}{A \times \Delta t}$$

where J_O is the pure water flux (L/m^{2}h or LMH), v is the volume of water collected (L), A is the

effective area of the membranes (m^2), and Δt is the time taken to collect the water (h).

It should be noted that in this study the initial pure water fluxes of the membranes were always restored through brushing and an overnight hypochlorite soak (see Chapter 2, subsection 2.4.4).

5.2.2.2. Filtration experiments

i) Test feed

Yeast suspensions were used as test feeds due to reasons explained in Chapter 3, subsection 3.2.2.2 (i). Both fresh and degraded yeast suspensions of 0.5 g/L were used in this investigation. The fresh and the degraded yeast suspensions represented low-fouling organic and high-fouling organic suspensions, respectively.

The yeast suspensions were prepared using the procedure outlined in Chapter 3, subsection 3.2.2.2 (i). The suspension was referred to as fresh yeast when used immediately, but degraded yeast suspension when left to stand for 72 hours.

ii) Experimental procedure

The procedure used here is similar to that presented in Chapter 3, subsection 3.2.2.2 (ii), and the WF-IMF set-up was used as the rig. The protocol is summarized here for convenience: first, the pure water flux experiments were carried out using the WF-IMF rig; the pump was then set to a constant speed; thereafter, the rig was ran on a fresh yeast suspension for 1 hour; during the filtration process, the permeate turbidity, the permeate volume and the ΔP were measured at a 5-minute interval; the experiment was repeated 3 times, in order to assess the repeatability of the runs. The procedure was then repeated using a degraded yeast suspension.

From the recorded results, flux and membrane resistance were calculated, and the respective graphs were plotted. The filtration flux at every interval was calculated using Equation 5-1 (with J being the permeate flux instead of PWF). While resistance was calculated using Equation 5-2.

Equation 5-2

$$R_t = \frac{\Delta P}{\mu J}$$

where R_t is the total membrane resistance (m^{-1}), ΔP is the pressure drop (Pa), μ is permeate viscosity (Pa.s) and J is the permeate flux (LMH).

The recorded and the calculated results were then used to plot permeate turbidity profiles, a flux

profile, a ΔP profile and finally the membrane resistance profiles.

5.2.2.3. Cyclic fouling and cleaning experiments

The cyclic fouling and cleaning experiment was used to evaluate the ease of cleaning the OWFMF membranes in comparison to the standard WFMF membranes.

The evaluation of the ease of cleaning of the OWFMF membranes was conducted in three stages with five cycles. Firstly, a pure water flux experiment (as described in subsection 5.2.2.1.) was carried out. The membrane resistance was calculated using Equation 5-2 and was denoted as R_m. Next, the membrane modules were used to filter fresh yeast for 1 hour, during which the permeate flowrate and the ΔP were measured and recorded after every 5 minutes. The final resistance at the end of stage 2 was also calculated using Equation 5-2 and was denoted as R_t. Lastly, after the membranes were cleaned, the pure water flux experiment was repeated and the results from the experiment used in calculating the resistance. This resistance was denoted as R_f.

In this investigation, the membranes were cleaned through a simple water scouring method. Water scouring is one of the three options available for cleaning WFMF membranes. Others included air scouring, sodium hypochlorite soak and brushing (as mentioned in Chapter 2, subsection 2.4.4). Water rinsing was considered because of its simplicity and cost effectiveness, yet still efficient in terms of restoring fouled WFMF membranes as was seen in Chapter 3.

The antifouling property and the ease of cleaning the OWFMF membranes in comparison to the standard WFMF membranes was evaluated by analyzing the total fouling resistance and the irreversible fouling resistance after each cycle. The total and irreversible fouling resistances were calculated using Equation 5-3 and Equation 5-4, respectively. Lower fouling resistances indicated better antifouling performance and also an increase in the ease of cleaning.

Equation 5-3

$$\boldsymbol{R_{tf} = R_t - R_m}$$

where R_{tf} is the total fouling resistance (m^{-1}), R_t is the final resistance of the membranes after the 1-hour fresh yeast filtration (m^{-1}) and R_m is the intrinsic membrane resistance (m^{-1}).

Equation 5-4

$$\boldsymbol{R_{ir} = R_f - R_m}$$

where R_{ir} is the irreversible fouling resistance that remains on the membranes after a physical cleaning (m^{-1}), R_f is the total resistance after physical cleaning (m^{-1}) and R_m is the intrinsic

membrane resistance (m^{-1}).

5.2.2.4. Evaluation of the stability of the oleophobic surface

The stability of an oleophobic coating in a modified membrane is regarded as an important feature in long-term membrane filtration processes, since the membrane will not only have to inhibit fouling but will do so while experiencing frequent hydraulic force due to frequent membrane cleaning (Belanger *et al.*, 2019; Guo *et al.*, 2013; Li *et al.*, 2014; Ma *et al.*, 2015). Hence, the stability of the modified membrane will be challenged. This section sought to evaluate the endurance capacity of the oleophobic surface on the OWFMF membranes in resisting the hydraulic force during filtration and membrane cleaning processes.

The stability of the oleophobic surface on the OWFMF membranes was evaluated by analysing the membranes' oleophobicity before and after a certain interval of cyclic filtration and cleaning processes. First, the oleophobicity of the developed membranes were measured. Thereafter, the membranes were used in a cyclic filtration and cleaning process (as described in 5.2.2.3). However, in this case, the cleaning process involved water scouring and intensive brushing of the membranes with tap water. The brushing method was chosen to mimic the most intensive hydraulic force the membranes would experience during a membrane cleaning process. After every four cycles, the membranes were completely cleaned and soaked in a sodium hypochlorite solution to remove any foulants on the membranes. Afterwards, the oil contact angle of the membranes was measured. A total of 16 filtration and cleaning cycles were carried out.

5.3. Results and discussion

This section presents the comparative evaluation between the OWFMF membranes and standard WFMF membranes. The evaluation is presented in terms of pure water fluxes, the permeate quality, fouling characteristics, the ease of cleaning and the stability of the oleophobic surface.

5.3.1. Pure water fluxes

The pure water fluxes of the OWFMF membranes were quantified through pure water flux experiments, and the results were thereafter compared to that of the standard WFMF membranes. The comparison is presented in Figure 5-2.

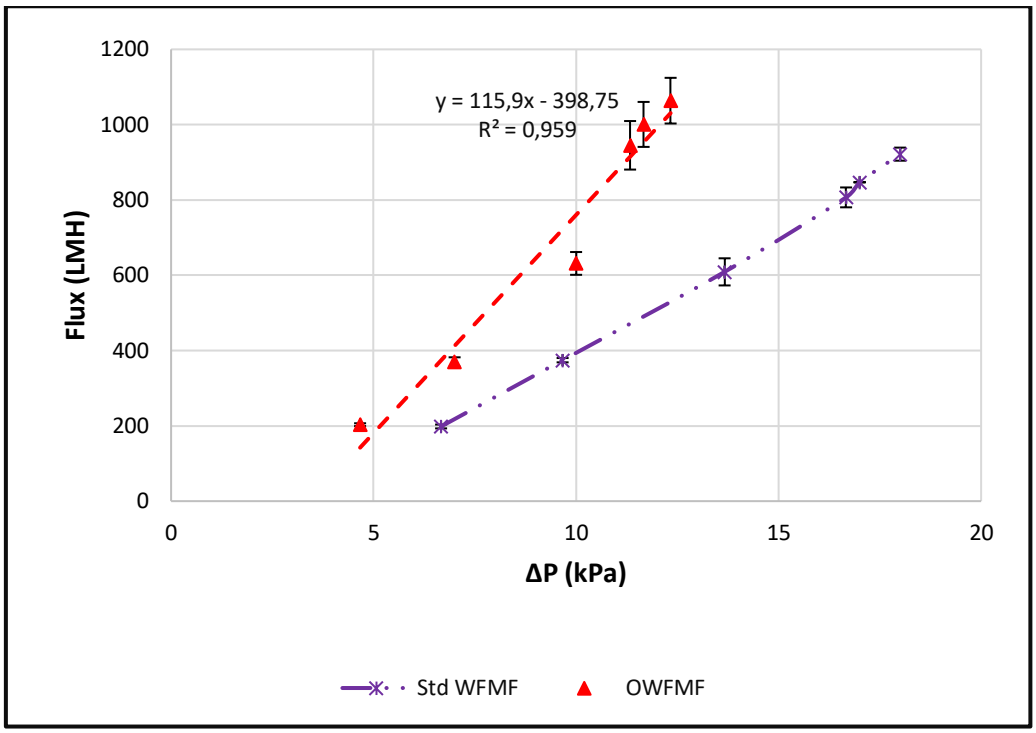

Figure 5-2: Comparison between the pure water fluxes of the OWFMF and that of the standard WFMF membranes

(Three repeat runs, average and error bars shown with best-fit linear trendline)

From Figure 5-2, it can be clearly seen that the OWFMF membranes had slightly higher pure water fluxes as compared to the standard WFMF membranes. This is contrary to what was expected. As was earlier mentioned (Chapter 4, subsection 4.4.3.2), the OWFMF membranes were found to be 44% more hydrophobic than the standard WFMF membranes. Hence, it was expected that their fluxes would be lower, since hydrophobic membranes tend to have low affinity to water resulting in low water fluxes (Zhu *et al.*, 2013).

The unexpected results might be attributed to the slight looseness of the fibers. Although the heat setting process helped in reducing the fabric shrinkage during curing, the process might not have remedied this problem completely. Hence, the original fabric tightness was possibly not 100% retained. Membrane pore sizes have an effect on the flux of a membrane filter (Li *et al.*, 2006). An increase in the pore size results in an increase in the membrane's flux. The space between fibers in WFMF membranes are regarded as its pores. Therefore, the slight looseness of the fibers in the OWFMF membranes resulted to an increase in their pore sizes. This in turn resulted to slightly higher fluxes than that of the standard WFMF membranes.

5.3.2. Permeate quality

The permeate quality was evaluated in terms of permeate turbidities. The permeate turbidities obtained on fresh yeast suspensions are presented in Figure 5-3, and that obtained on degraded yeast suspensions are shown in Figure 5-4.

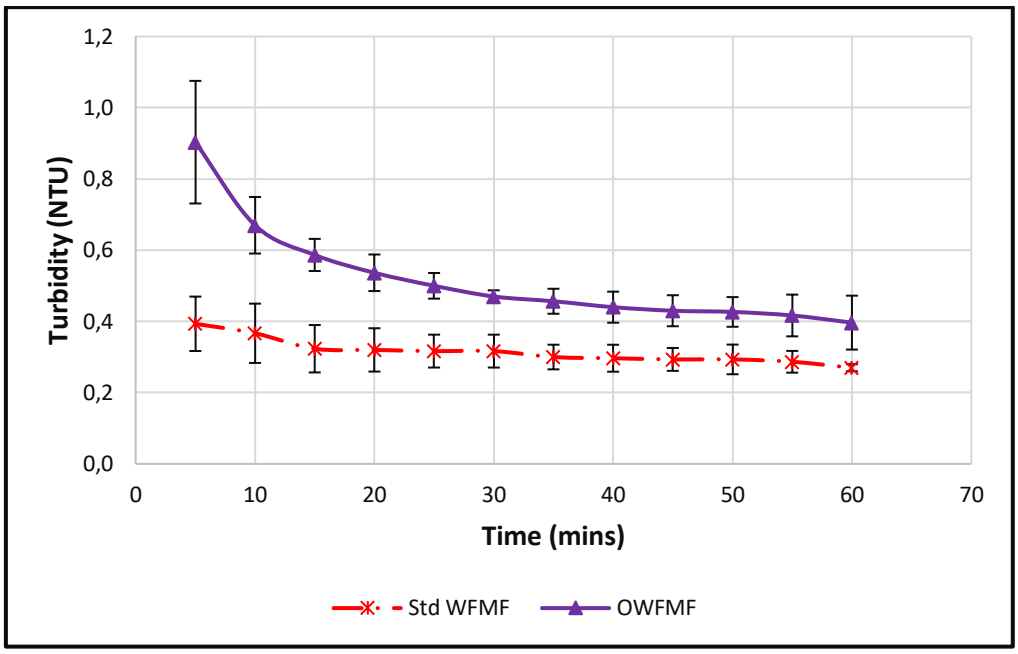

Figure 5-3: Comparison between the permeate turbidities of the OWFMF membranes and that of the standard WFMF membranes in the filtration of 0.5 g/L of fresh yeast suspension

(Three repeat runs, average presented with error bars)

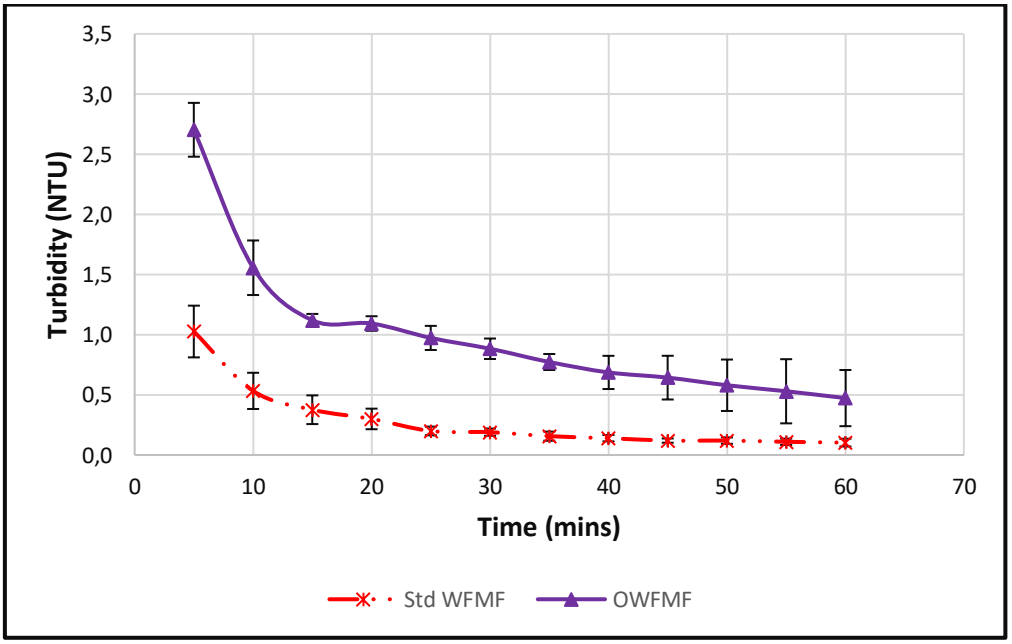

Figure 5-4: Comparison between the permeate turbidities of the OWFMF membranes and that of the standard WFMF membranes in the filtration of 0.5 g/L of degraded yeast suspension

(Three repeat runs, average presented with error bars)

From Figure 5-3 and 5-4, it can be seen that the use of OWFMF membranes in filtering both fresh and degraded yeast feed resulted in a permeate turbidity of 0.5 NTU or below. The initial residual turbidity of the yeast suspension which was around 340-380 NTU, was reduced to around 0.5 NTU in one hour. This performance of the OWFMF membranes in terms of permeate turbidity, is consistent with the results of most commercial membranes used in IMBR system for wastewater treatment, where a permeate turbidity of below 1 NTU is generally obtained (Campo *et al.*, 2017; Hoinkis *et al.*, 2012; Hu & Stuckey, 2006).

However, when the permeate turbidity of the OWFMF membranes was compared to that of the standard WFMF, it was found to be slightly higher. From Figure 5-3, it can be seen that the standard WFMF gave a permeate turbidity that was about 0.1 NTU lower than that of OWFMF membranes when applied to the filtration of fresh yeast. Similarly, from Figure 5-4, it was also observed that the standard WFMF membranes performed slightly better than the OWFMF membranes in the filtration of degraded yeast.

The slightly better performance of the standard WFMF membranes in terms of permeate quality can be attributed to its tighter weave compared to that of the OWFMF membranes. Microfiltration membranes usually treat water based on the sieving mechanism (Li *et al.*, 2006). This mechanism is affected by the membrane's pore sizes. Large membrane pore sizes will allow more contaminants to pass through the membrane, thus resulting in poor permeate quality. On the hand, small pore size will allow less or no contaminants to pass through thereby resulting in excellent permeate quality. As discussed in subsection 5.3.1, the pores size of OWFMF membranes are slightly bigger than those of the standard WFMF due to the looseness of its fibres. This, therefore, explains why the standard WFMF membranes gave better permeate turbidity compared to the OWFMF membranes. However, it should be noted that the permeate quality given by OWMF membranes is still within the recommended quality standard for effluent, and therefore this membrane is suitable for use in the treatment of wastewater.

5.3.3. Fouling characteristics analysis

The fouling characteristics of the OWFMF membranes relative to that of the standard WFMF membranes during the filtration experiments were indicated using resistance profiles. Firstly, a representation of how flux and ΔP changed during the filtration process was plotted. A typical graph showing the changes in flux and ΔP for both the OWFMF and the standard WFMF membranes in the filtration of fresh yeast suspension is shown in Figure 5-5, and the resistance profile calculated from

this data is presented in Figure 5-6. In addition, the resistance profiles comparing the two membranes in the filtration of degraded yeast suspension is shown in Figure 5-7.

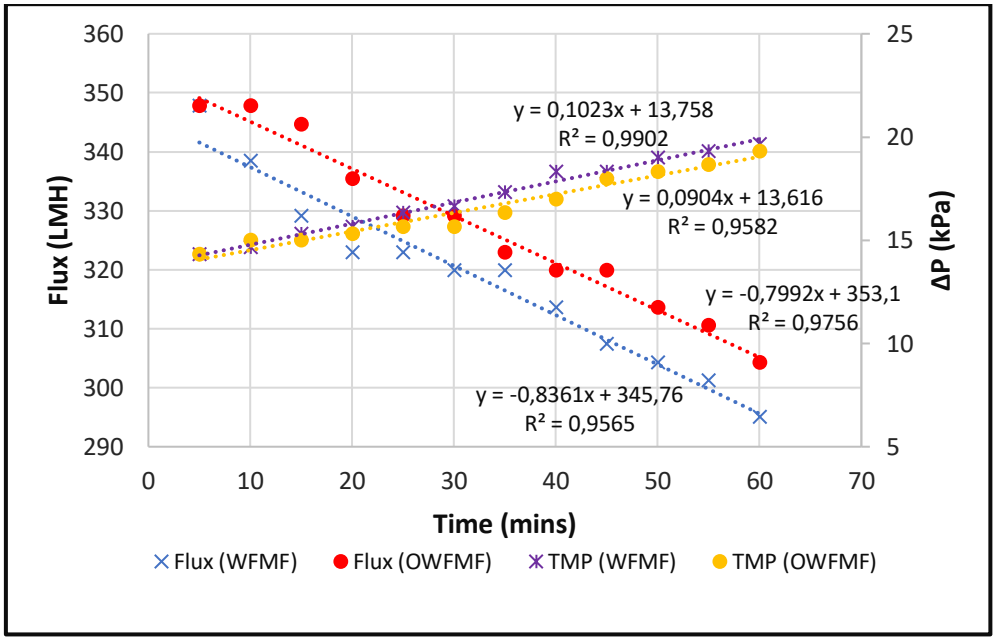

Figure 5-5: A typical flux and ΔP profile for the OWFMF membranes in comparison to that of the standard WFMF in the filtration of 0.5 g/L of fresh yeast solution

(Three repeat runs, average presented with best-fit linear trendline)

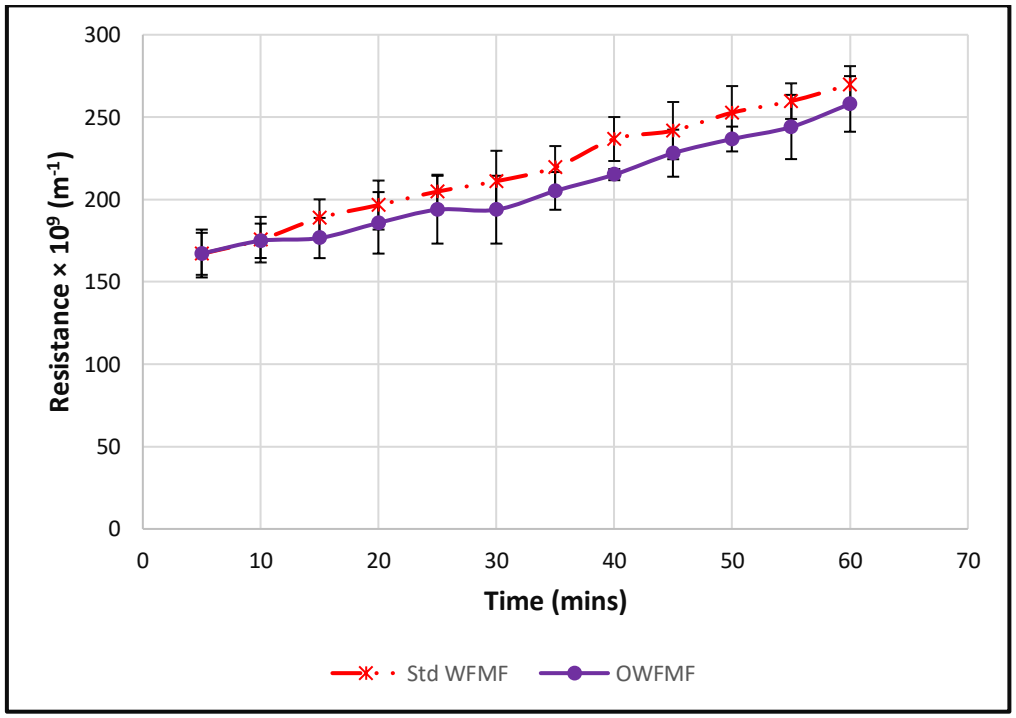

Figure 5-6: The fouling resistance profile for the OWFMF membranes in comparison to that for the standard WFMF in the filtration of 0.5 g/L of fresh yeast suspension

(Three repeat runs, average presented with error bars)

The results of the filtration of fresh yeast suspension presented in Figures 5-6 show that the fouling resistance on the OWFMF membranes was slightly lower than that of the standard WFMF. Similar observations were also made in the filtration of degraded yeast suspension as shown in Figure 5-7.

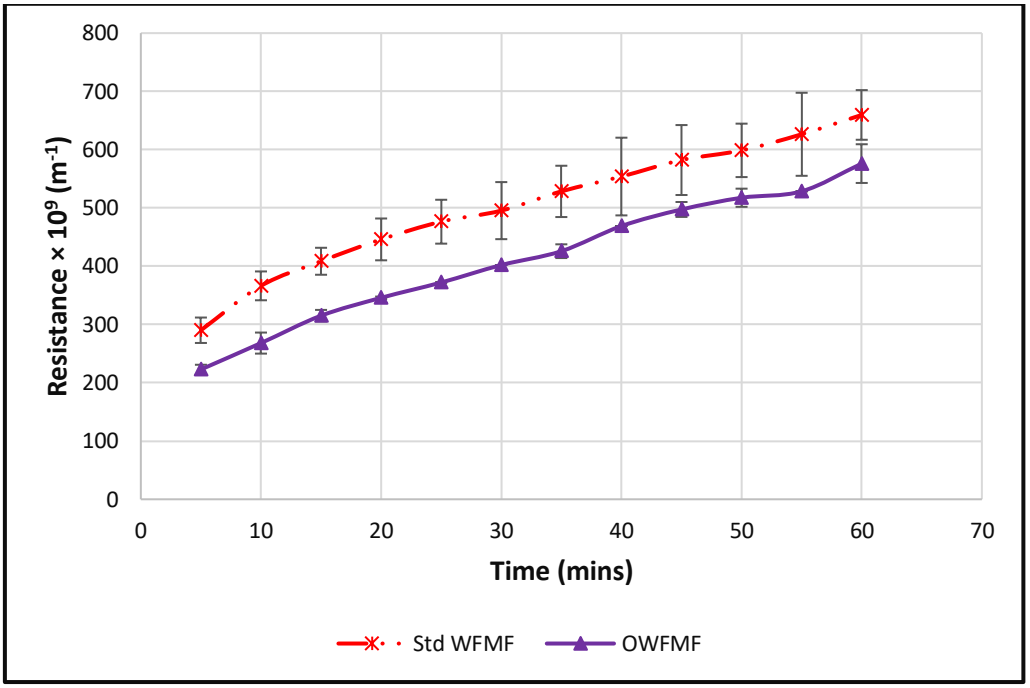

Figure 5-7: The fouling resistance profile for the OWFMF membranes in comparison to that for the standard WFMF in the filtration of 0.5 g/L of degraded yeast suspension

(Three repeat runs, average presented with error bars)

The total resistance of the OWFMF membranes relative to that of the standard WFMF membranes at the end of the filtration process was 4.3% and 12.7% lower with fresh yeast and degraded yeast suspension, respectively. It should be noted that the difference in the total resistance was considered to be significant only in the filtration of degraded yeast suspension as shown by the error bars on the charts.

The slightly lower total resistance of the OWFMF membranes is attributed to the imparted oleophobic properties. Oleophobic surfaces tend to be effective in preventing the adhesion of some organics foulants on the membranes, thus decreasing the total fouling resistance. Similar observations have been reported elsewhere (Ganwei *et al.*, 2019; Zhu *et al.*, 2013), where a membrane surface that was made oleophobic resulted in a decrease in the fouling resistance. Further analysis and discussion of the reduction of the fouling resistance on the OWFMF membranes are presented in the next subsection.

5.3.4. Ease of cleaning and antifouling behavior

The ease of cleaning and the antifouling performance of the OWFMF membranes was evaluated through a five-cycle filtration and cleaning process. The results were then compared to that of the standard WFMF membranes. The resistance profiles of the filtration cycles for the standard WFMF and the OWFMF membranes are shown in Figures 5-8 and 5-9, respectively.

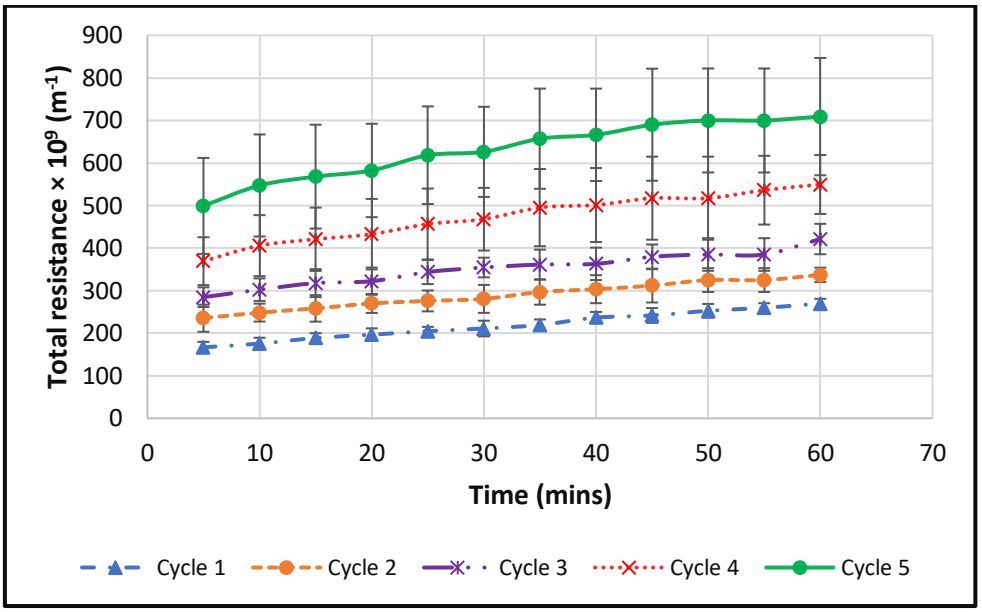

Figure 5-8: The resistance profiles for the standard WFMF membranes in the cyclic filtration of 0.5 g/L of fresh yeast suspension

(Three repeat runs, average presented with error bars)

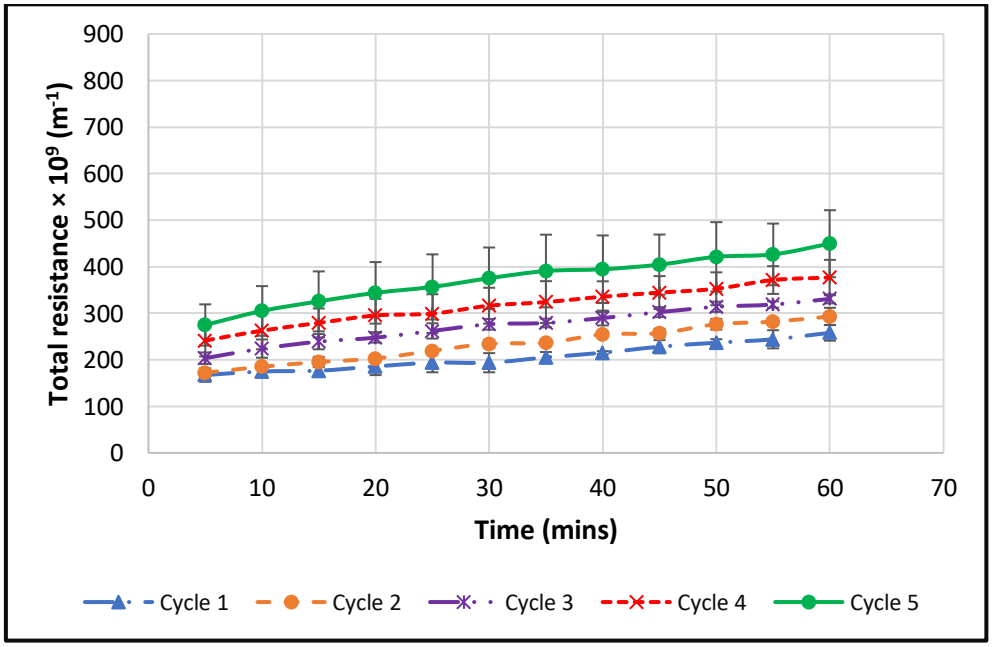

Figure 5-9: The resistance profiles for the OWFMF membranes in the cyclic filtration of 0.5 g/L of fresh yeast suspension

(Three repeat runs, average presented with error bars)

As shown in Figures 5-8 and 5-9, both the standard and the oleophobic WFMF membranes experienced a gradual increase in the fouling resistance with increasing filtration time and cycle. This increase is due to the foulants being deposited on the membrane surfaces, thereby causing an increase in the total resistance. However, from the figures it can be seen that the increase in fouling resistance seems to be significantly lower on the OWFMF membranes as compared to the standard membranes. At the end of the first cycle, both membranes had a total resistance of approximately 250×10^9 m^{-1}. But by the end of the fifth cycle, the total resistance of the OWFMF membranes was 250×10^9 m^{-1} lower than that of the standard WFMF membrane. The relatively low total resistance of the OWFMF membrane is attributed to its oleophobic properties which repel organic foulants, hence reducing the amount of foulants being deposited (Brown & Bhushan, 2015; Ma *et al.*, 2019; Wang *et al.*, 2019).

To further understand the antifouling performance and the ease of cleaning both membranes, a comparison between the standard WFMF and the OWFMF membranes in terms of the total fouling resistance and the irreversible fouling resistance was plotted as shown in Figure 5-10 and 5-11, respectively.

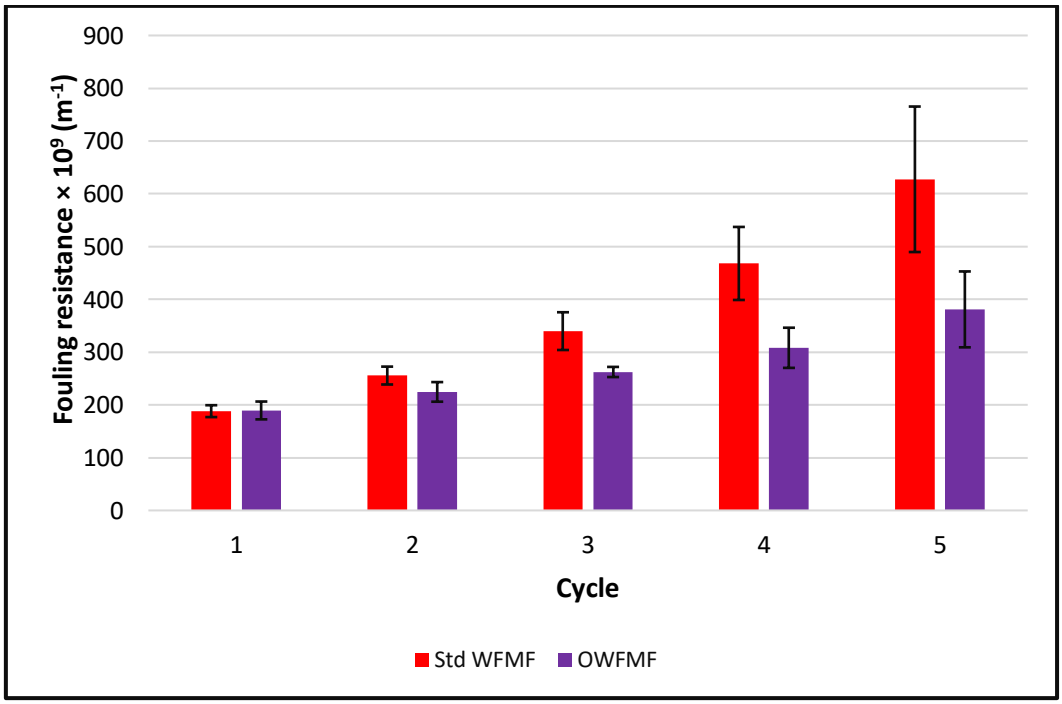

Figure 5-10: The total fouling resistance on the OWFMF membranes relative to that on the standard WFMF membranes at the end of each cycle

(Three repeat runs, average presented with error bars)

From Figure 5-10, it can be observed that the total fouling resistance increase on the OWFMF membranes seemed to be lower than that on the standard WFMF membranes. The fouling resistance which increased with increasing operational cycle, ranged between 24 and 27% for the standard WFMF, while that of the OWFMF membranes was found to be between 14 and 19%. In addition, the amount of foulant deposited on the standard WFMF membranes at the end of the fifth cycle, was found to be 39% relatively higher than that deposited on the OWFMF membranes.

The total fouling resistance comprises of both the reversible and irreversible fouling layer. It is the total resistance on the membrane surfaces at the end of a filtration process, excluding the intrinsic membrane resistance. The relatively low total fouling resistance reported on the OWFMF membranes as compared to that on the standard WFMF membranes is attributed to the excellent capability of the oleophobic surface in repelling most of the organic foulants from the surfaces of the OWFMF membrane (Ma *et al.*, 2019; Zhu *et al.*, 2013). Hence, the OWFMF membranes exhibited a better antifouling behaviour compared to the standard WFMF membranes.

After each filtration cycle, the membranes were water scoured and the fouling resistance that remained on the membrane surfaces after each cleaning cycle is what is referred to as irreversible fouling resistance. Figure 5-11 displays a comparison between OWFMF and standard WFMF membranes in terms of irreversible fouling resistances.

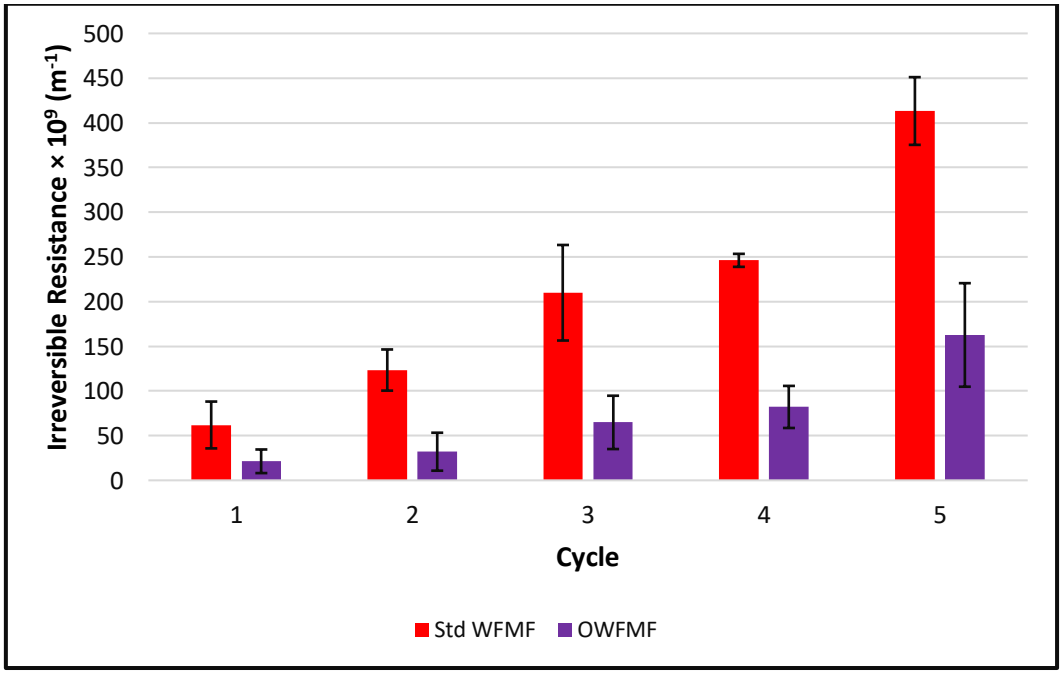

Figure 5-11: Comparison between the irreversible fouling resistance on the OWFMF membranes and that on the standard WFMF membranes at the end of each cleaning cycle

(Three repeat runs, average presented with error bars)

From the results presented in Figure 5-11, it can be seen that there was a remarkable reduction in the cumulative irreversible fouling layer on the OWFMF membranes when compared to the standard membrane. This implies that the OWFMF membranes were easier to clean relative to the standard WFMF membranes. The amount of irreversible foulants that remained on the OWFMF membranes after each cleaning cycle was found to be around 60-74% less than what was left on the standard WFMF membranes. This demonstrated that water scouring could only remove a small portion of the foulants on the standard WFMF membranes but succeeded in removing most foulants on the OWFMF membranes. It also demonstrates that the oleophobic surface on the OWFMF membranes was effective in inhibiting irreversible fouling.

Given that irreversible fouling was considered as the most critical challenge that hampered the further implementation of WFMF technology in wastewater treatment (Pillay *et al.*, 2016), the OWFMF membrane proposed in this study holds a promising prospect on potential application in sanitation systems.

5.3.5. Stability of the oleophobic surface

The stability of the oleophobic surface was evaluated through the measurement of the oil contact angles of the OWFMF membranes before, and after different filtration and cleaning cycles. The oil contact angles are presented in Figure 5-12.

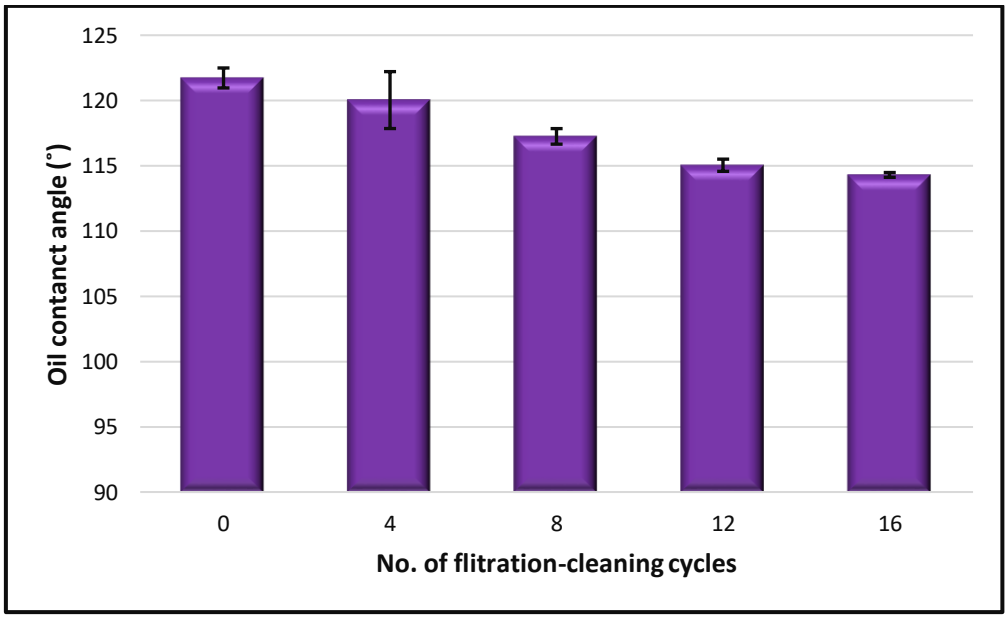

Figure 5-12: The oil contact angles of OWFMF membranes that have undergone different filtration and cleaning cycles

(Three repeat runs, average presented with error bars)

From Figure 5-12, it can be seen that the oil contact angle of the membranes decreased with increasing filtration and cleaning cycles, though with a small margin. There was a 1.40% decrease in the membranes' oil contact angle after 4 filtration and cleaning cycles. This margin of decrease increased to 3.68% and 5.49% for membranes that underwent 8 and 12 cycles, respectively. Thereafter, the oleophobic surface seems to remain stable at an oil contact angle of around 115˚. The minimal decrease in the oleophobicity of the developed OWFMF membranes is attributed to the suction and shear forces experienced during the filtration and cleaning process, respectively (Belanger *et al.*, 2019; Li *et al.*, 2014). This initial decrease in the membrane's oleophobicity is considered normal for any newly modified surface (Belanger *et al.*, 2019).

From the above results, it can be concluded that the oleophobic surface was fairly stable, and only minimal erosion was observed.

5.4. Limitation of the investigation

Despite the success in evaluating the performance of the oleophobic WFMF membranes, this investigation had various limitations. These include:

i) Use of synthetic wastewater

This study was performed on yeast suspension for reasons explained earlier (see Chapter 3, subsection 3.2.2.2), and the results obtained may not accurately represent real wastewater. This is due to the significant difference in the fouling characteristics of real wastewater compared to the synthetic wastewater (Buetehorn *et al.*, 2012; Villain *et al.*, 2014). The difference in fouling characteristics is brought about by the complex and varied composition of real wastewater. Real wastewater is known to contain numerous substances including polysaccharides, proteins, humic acid and inorganic material. While yeast represents only one model foulant. Furthermore, the composition and substance particle size in real wastewater vary from time to time.

ii) Evaluating the performance of the membranes over a short-term filtration period

Due to time constraint, the performance evaluation of the OWFMF membranes was carried in short term filtration experiments. Thus, the long-term stability of the performance of the OWFMF membranes, which is essential in real operation of membrane process, cannot be predicted from the obtained findings.

5.5. General outcome of the investigation

One major outcome that was realized from this investigation was:

The promising potential of the developed OWFMF membrane in sanitation applications

The performance evaluation experiments carried out in this study revealed that the newly developed OWFMF membrane has a promising prospect in sanitation applications. The membrane was able to produce permeates with turbidities of below 1 NTU, which is comparable to that of commercial membranes. Furthermore, when compared to the standard WFMF membrane, the OWFMF membrane showed improved ease of cleaning and excellent capability in resisting organic foulants. With standard 'water scouring' as a cleaning mechanism, the OWFMF membrane showed irreversible fouling that is less than 60% of the standard WFMF membrane. Given that irreversible fouling was considered as the most critical challenge that hampered the further implementation of WFMF technology in wastewater treatment, this finding is considered as a major improvement. Additionally, in terms of stability, the oleophobic surface was reported to be fairly stable and only initial minimal erosion was observed.

With these obtained results, the oleophobic WFMF membrane proposed in this study holds a promising prospect on potential application in sanitation systems.

5.6. Summary

In this work, the performance of the oleophobic WFMF membranes was evaluated. This was done in terms of permeate quality, fouling characteristic, antifouling behavior, and ease of cleaning. The results were then compared to that of the standard WFMF membranes. The evaluation experiments demonstrated that the developed OWFMF membranes were able to provide an acceptable permeate quality with a turbidity of less than 1 NTU. The membranes also had a slightly enhanced pure water flux relative to the standard WFMF membranes. Moreover, when compared to the standard WFMF membranes, the OWFMF membranes showed improved ease of cleaning and excellent capability in resisting organic foulants. The oleophobic surface reduced the reversible and irreversible fouling by approximately 39% and 60%, respectively in a five-cycle filtration and cleaning process. In terms of stability, the oleophobic surface was reported to be fairly stable and only initial minimal erosion was observed. Hence, considering the obtained results, the OWFMF membrane has a great potential for use in decentralized sanitation systems, if further developed.

Chapter 6.
Conclusion and recommendations

Overview

Conclusion; Recommendations

6.1. Conclusion

The overall aim of this study was to develop a woven fabric microfiltration (WFMF) membrane with improved fouling resistance, that could be used in decentralized sanitation systems. To address this aim, three objectives were formulated:

- To investigate the fouling characteristics of woven fabric microfiltration (WFMF) membranes
- To develop and characterize oleophobic woven fabric microfiltration (OWFMF) membranes
- To evaluate the performance of the oleophobic woven fabric membranes in comparison to the standard WFMF membranes

The conclusions drawn from this investigation, in line with meeting the abovementioned objectives are outlined in this section.

6.1.1. Fouling characteristics of the WFMF membranes

The fouling characteristics of the WFMF membranes were investigated on a laboratory scale using a woven fabric immersed membrane filtration (WF-IMF) unit. This was achieved by first evaluating the efficiency of different air scouring and backwash regimes and water scouring in restoring the original permeability of WFMF membranes. Thereafter, the kinetics of fouling layer formation on WFMF membranes was established by performing synthetic wastewater filtration and cleaning experiments; where different filtration durations were evaluated. Results from the experiments were used to generate resistance profiles for unused, fouled and cleaned membranes.

From this investigation, the fouling characteristics of the WFMF membranes were found to be comparable to the fouling characteristics of the standard microfiltration membranes. The evaluation experiments indicated that the kinetics of fouling formation on WFMF membranes involved two stages, namely irreversible fouling, followed by cake layer deposition. In addition, the irreversible fouling occurred within the first five to ten minutes of a filtration process, while the cake layer forms at a later stage. When these findings were compared to standard microfiltration membranes found in literature, it was concluded that in terms of fouling characteristics the WFMF

membranes show a good similarity with the standard microfiltration membranes.

In terms of evaluating the restoration of the fouled WFMF membranes, it was found that the irreversible foulants could not be removed by either water scouring or a combination of air scouring and backwash. From the microscopic images of the cleaned membranes, it was found that the irreversible foulants settled at the intersections of groups of fibres, where water scouring, and air scouring were unable to reach. Hence, it was concluded that this was the reason why either water scouring, or air scouring was unable to restore the original permeability of the fouled WFMF membranes.

Finally, it was also concluded that water scouring can play a major role in cleaning fouled WFMF membranes. In a combined cleaning strategy that involved water scouring, air scouring and backwash; it was found that water scouring contributed 80% to the whole cleaning process and was able to remove 72% of the fouling layer. Given that water scouring is a simple method and does not require any energy input, its application to WFMF systems could have a major impact in terms of ease of operations and energy consumption.

6.1.2. Development and characterization of the oleophobic WFMF membranes

The development and characterization of the oleophobic WFMF membrane involved various stages. First, a literature survey was done to identify the best option for developing the membrane. The surface modification of the standard WFMF membrane through fluorocarbon application using the padding process was found to be the best available option.

The next stage involved developing the membrane using the chosen process, i.e. fluorocarbon application through padding process. The washed, scoured, rinsed, and dried standard WFMF membrane samples were impregnated by being immersed in a fluorocarbon liquor, before being passed between two squeezing rollers. Thereafter, the membranes were dried, cured and heat set in an oven. During the padding process, parameters such as fluorocarbon concentration, fabric speed and padding pressure were optimized using a factorial experimental design. Thereafter, the oleophobicity of the developed membranes was analyzed through the measurement of the membranes' oil contact angles (OCA).

From the development and optimization process, 2 bar padding pressure and 1 m/min fabric speed were estimated as the optimum conditions at all the evaluated fluorocarbon concentration. An

optimum oleophobic WFMF membrane of 123.5˚ OCA was developed at 80 g/L FC concentration at a curing temperature and time of 180˚ and 90 seconds, respectively.

Hence, the objective of this study was successfully met. The investigation demonstrated that it is feasible to develop a highly oleophobic WFMF membrane.

6.1.3. Performance evaluation of the OWFMF membranes

The performance of the OWFMF membranes in comparison to the standard WFMF membrane was evaluated in terms of the following criteria: the pure water flux, the permeate quality, the fouling characteristic, the ease of cleaning, and the stability of the chemical modification. The pure water fluxes of the membranes were determined through the filtration of distilled water using the woven fabric immersed membrane filtration (WF-IMF) unit at increasing pump speeds. The permeate quality and the fouling characteristics were evaluated through a 1-hour filtration of low and high fouling synthetic organic suspensions in separate runs, where the permeate turbidities, volumetric flowrates and pressure drop (ΔP) across the membranes were measured at 5-minute intervals. The results were then used to generate time profiles of permeate turbidity, flux, ΔP, and resistance.

The antifouling property and the ease of cleaning of the OWFMF membranes was evaluated through a five cyclic fouling and cleaning process. Water scouring was used as the cleaning mechanism. During the cyclic runs, fluxes and ΔP were measured and recorded. The data was then used to calculate the reversible and irreversible fouling resistances at the end of each cycle.

Finally, the stability was evaluated through the analysis of the oil contact angle of the membranes. The oil contact angles were measured before and after a certain number of filtration and cleaning cycles. Brushing and water scouring were used as the cleaning methods.

Various conclusions were drawn from this investigation. The evaluation experiments demonstrated that the developed OWFMF membranes were able to provide an acceptable permeate quality with a turbidity of less than 1 NTU. The membranes also had a slightly enhanced pure water flux relative to the standard WFMF membranes. Moreover, when compared to the standard WFMF membranes, the OWFMF membranes showed improved ease of cleaning and excellent capability in resisting organic foulants. The oleophobic surface reduced the reversible and irreversible fouling by approximately 39% and 60%, respectively in a five-cycle filtration and cleaning process.

Hence, considering the obtained results, the OWFMF membrane has a great potential for use in

decentralized sanitation systems, if further developed.

6.2. Recommendations

The OWFMF membrane holds a promising prospect on potential application in sanitation systems. However, this study had various limitations. They include:

- Use of synthetic wastewater;
- Evaluating the performance of the membrane on short-term filtration periods;
- Not optimizing the water scouring cleaning mechanism.

Hence, for the membrane to be implemented, further investigations and development should be done. Future studies should focus on the following:

6.2.1. Evaluating the membrane on real wastewater

This investigation evaluated the performance of the OWFMF membranes on synthetic wastewater due to its reproducibility and ease of use on a laboratory scale. Promising outcomes were realized from this study. However, the results obtained from this evaluation may not accurately represent real wastewater. Hence, to get the actual performance of the OWFMF membranes , the membranes will have to be evaluated on real wastewater.

Ultimately, the OWFMF membranes are aimed for sanitation applications. Therefore, it is recommended that they should be ran on either raw sewage feed or return activated sludge from a membrane bioreactor. Feeds with different concentration should be employed, so as to capture the performance of the membranes in the different feed concentrations. During the evaluation, the following performance criteria should be considered: permeate quality (in terms of turbidity, MLSS and COD), the flux, the fouling characteristics, and the ease of cleaning the membranes.

6.2.2. Evaluating the long-term performance of the membrane

The long-term performance stability of membranes is essential in real operation of membrane processes. In this study, the OWFMF membrane were only evaluated on short-term filtration experiments due to time constraints. Therefore, the long-term performance stability of the OWFMF membranes, cannot be predicted from the obtained results. Hence, it is recommended that:

- Larger OWFMF membrane size should be produced
- Thereafter, commercial size modules should be made

- The membrane modules should then be ran on real wastewater operating conditions for around six months or more, where the stability of the coating and the membrane performance should be evaluated.

6.2.3. Developing an optimal water scouring regime for 'in-situ' cleaning

Water scouring was found to play a major role in restoring the permeability of fouled WFMF membranes. However, this investigation did not optimize its parameters, hence its full efficiency was not realized. Therefore, future research and development should focus on developing an optimal water scouring regime for 'in-situ' cleaning of fouled WFMF membranes. The following water scouring parameters should be considered: water scouring frequency, water scouring duration and lastly, the flux or pressure at which the water for scouring would be released.

References

Akbari, A., Derikvandi, Z. & Mojallali Rostami, S.M. 2015. Influence of chitosan coating on the separation performance, morphology and anti-fouling properties of the polyamide nanofiltration membranes. *Journal of Industrial and Engineering Chemistry*. 28:268–276.

Akhondi, E., Zamani, F., Tng, K.H., Leslie, G., Krantz, W.B., Fane, A.G. & Chew, J.W. 2017. The performance and fouling control of submerged hollow fiber (HF) systems: A review. *Applied Sciences*. 7(8):1–39.

Al-malack, M.H. 2007. Performance of an immersed membrane bioreactor (IMBR). *Desalination*. 214(1–3):112–127.

Alfa, D., Rathilal, S., Pillay, V.L., Pikwa, K. & Chollom, M.N. 2016. Development and evaluation of a small scale water disinfection system. *Journal of Water Sanitation and Hygiene for Development*. 6(3):389–400.

Almeida, M., Erthal, R., Padua, E., Silveira, L. & Am, L. 2008. Response surface methodology (RSM) as a tool for optimization in analytical chemistry. *Talanta*. 76(5):965–977.

Aly, A.S., Hashem, A. & Hussein, S.S. 2004. Utilization of chitosan citrate as crease-resistant and antimicrobial finishing agent for cotton fabric. *Indian Journal of Fibre and Textile Research*. 29(2):218–222.

Aslan, S. & Kapdan, I.K. 2006. Batch kinetics of nitrogen and phosphorus removal from synthetic wastewater by algae. *Ecological Engineering*. 28(1):64–70.

Asquith, J. 2017. Evaluation of a flat sheet woven fabric membrane for use in water treatment processes suited to rural and peri-urban economies. *Department of Process Engineering, Stellenbosch University*.

Audenaert, F., Lens, H., Rolly, D. & Vander Elst, P. 1999. Fluorochemical textile repellents—synthesis and applications: A 3M perspective. *Journal of the Textile Institute*. 90(3):76–94.

Ayyavoo, J., Nguyen, T.P.N., Jun, B.M., Kim, I.C. & Kwon, Y.N. 2016. Protection of polymeric membranes with antifouling surfacing via surface modifications. *Colloids and Surfaces A: Physicochemical and Engineering Aspects*. 506:190–201.

Bansal, B., Al-ali, R., Mercad, R. & Chen, X.D. 2006. Rinsing and cleaning of α-lactalbumin fouled MF

membranes. *Separation and Purification Technology*. 48(2):202–207.

Basile, A., Cassano, A. & Rastogi, N.K. 2015. *Advances in Membrane Technologies for Water Treatment: Materials, Processes and Applications*. Langford lane, UK: Woodhead Publishing.

Belanger, A., Decarmine, A., Jiang, S., Cook, K. & Amoako, K.A. 2019. Evaluating the Effect of Shear Stress on Graft-To Zwitterionic Polycarboxybetaine Coating Stability Using a Flow Cell. *Langmuir*. 35(5):1984–1988.

Di Bella, G. & Di Trapani, D. 2019. A brief review on the resistance-in-series model in membrane bioreactors (MBRs). *Membranes*. 9(24):1–29.

Benedek, A. & Côté, P. 2006. Long Term Experience With Hollow Fibre Membrane Bioreactors. *International Desalination Association BAH03-180*. 1–6.

Besler, N., Gloy, Y.S. & Gries, T. 2016. Analysis of the heat setting process. In Vol. 141 *IOP Conference Series: Materials Science and Engineering*.

Blanpain-Avet, P., Fillaudeau, L. & Lalande, M. 1999. Investigation of mechanisms governing membrane fouling and protein rejection in the sterile microfiltration of beer with an organic membrane. *Food and Bioproducts Processing: Transactions of the Institution of Chemical Engineers, Part C*. 77(2):75–89.

Böhm, L., Drews, A., Prieske, H., Bérubé, P.R. & Kraume, M. 2012. The importance of fluid dynamics for MBR fouling mitigation. *Bioresource Technology*. 122:50–61.

Breite, D., Went, M., Prager, A. & Schulze, A. 2015. Tailoring membrane surface charges: A novel study on electrostatic interactions during membrane fouling. *Polymers*. 7(10):2017–2030.

Brown, P.S. & Bhushan, B. 2015. Mechanically durable, superoleophobic coatings prepared by layer-by-layer technique for anti-smudge and oil-water separation. *Scientific Reports*. 5:8701.

Bruggen, B. Van Der, Vandecasteele, C., Gestel, T. Van, Doyenb, W. & Leysenb, R. 2003. Review of Pressure-Driven Membrane Processes. *Environmental Progress*. 22(1):46–56.

Buer, T. & Cumin, J. 2010. MBR module design and operation. *Desalination*. 250(3):1073–1077.

Buetehorn, S., Carstensen, F., Wintgens, T., Melin, T., Volmering, D. & Vossenkaul, K. 2010. Permeate flux decline in cross-flow microfiltration at constant pressure. *Desalination*.

250(3):985–990.

Buetehorn, S., Brannock, M., Le-clech, P., Leslie, G., Volmering, D., Vossenkaul, K., Wintgens, T., Wessling, M., et al. 2012. Limitations for transferring lab-scale microfiltration results to large-scale membrane bioreactor (MBR) processes. *Separation and Purification Technology*. 95:202–215.

Cabero, M.L., Riera, F.A. & Álvarez, R. 1999. Rinsing of ultrafiltration ceramic membranes fouled with whey proteins: Effects on cleaning procedures. *Journal of Membrane Science*. 154(2):239–250.

Campo, R., Capodici, M., Di Bella, G. & Torregrossa, M. 2017. The role of EPS in the foaming and fouling for a MBR operated in intermittent aeration conditions. *Biochemical Engineering Journal*. 118:41–52.

Castaño, M.A. & Ward, B.B.C.R. 2009. Optical microscope and SEM evaluation of roofing slate fissility and durability. *Materials of construction*. 59(296):91–104.

Castelvetro, V., Francini, G., Ciardelli, G. & Ceccato, M. 2001. Evaluating Fluorinated Acrylic Latices as Textile Water and Oil Repellent Finishes. *Textile Research Journal*. 71(5):399–406.

Cecconet, D., Callegari, A., Hlavínek, P. & Capodaglio, A.G. 2019. Membrane bioreactors for sustainable, fit-for-purpose greywater treatment: a critical review. *Clean Technologies and Environmental Policy*. 21(4):745–762.

Cele, M.N. 2014. Development and Evaluation of woven fabric microfiltration immersed membrane bioreactors on waste water treatment for reuse. *Department of Chemical Engineering, Durban University of Technology.*

Cele, M.N. & Pillay, V.L. 2010. Development and Evaluation of woven fabric microfiltration immersed membrane bioreactors on waste water treatment for reuse. *Water institute of Southern Africa*.

Cele, M., Sibiya, L., Jacobs, E.P. & Pillay, V.L. 2010. Evaluation of a woven fabric immersed membrane bioreactor (WFIMBR) for wastewater treatment. *Water institute of Southern Africa*.

Chan, R. & Chen, V. 2001. The effects of electrolyte concentration and pH on protein aggregation and deposition: critical flux and constant flux membrane filtration. *Journal of Membrane*

Science. 185(2):177–192.

Chang, S. 2011. Application of submerged hollow fiber membrane in membrane bioreactors: Filtration principles, operation, and membrane fouling. *Desalination*. 283:31–39.

Chang, H., Liang, H., Qu, F., Liu, B., Yu, H., Du, X., Li, G. & Snyder, S.A. 2017. Hydraulic backwashing for low-pressure membranes in drinking water treatment: A review. *Journal of Membrane Science*. 540:362–380.

Chen, V., Li, H. & Fane, A.G. 2004. Non-invasive observation of synthetic membrane processes - A review of methods. *Journal of Membrane Science*. 241(1):23–44.

Chen V., Fane A.G., Madaeni S., W.I.G. 1997. Particle deposition during membrane filtration of colloids : transition between concentration polarization and cake formation. *Journal of Materials Science*. 125(1):109–122.

Chollom, M.N., Pikwa, K., Rathilal, S. & Pillay, V.L. 2017. Fouling mitigation on a woven fibre microfiltration membrane for the treatment of raw water. *South African Journal of Chemical Engineering*. 23:1–9.

Choudhury, A.K.R. 2006. *Textile Preparation and Dyeing*. Enfield (New Hampshire), USA: Science Publishers.

Chowdhury, K.P. 2018. Performance Evaluation of Water Repellent Finishes on Cotton Fabrics. *International Journal of Textile Science*. 7(2):48–64.

Chu, H., Zhang, Y., Zhou, X., Zhao, Y., Dong, B. & Zhang, H. 2014. Dynamic membrane bioreactor for wastewater treatment : Operation, critical flux, and dynamic membrane structure. *Journal of Membrane Science*. 450:265–271.

Le Clech, P., Jefferson, B., Chang, I.S. & Judd, S.J. 2003. Critical flux determination by the flux-step method in a submerged membrane bioreactor. *Journal of Membrane Science*. 227(1–2):81–93.

Cuperus, P. 2018. Membrane processes. In 3rd Edition London, New york: Academic Press *Food Process Engineering and Technology*. 261–287.

Dagnew, M., Parker, W. & Seto, P. 2012. Anaerobic membrane bioreactors for treating waste activated sludge: Short term membrane fouling characterization and control tests. *Journal of Membrane Science*. 421–422:103–110.

Dasdemir, M. & Ibili, H. 2017. Formation and characterization of superhydrophobic and alcohol-repellent nonwovens via electrohydrodynamic atomization (electrospraying). *Journal of Industrial Textiles*. 47(1):125–146.

Deelie, M. 2017. Energy Reduction in a Woven- Fabric Immersed Membrane Bioreactor. *Department of Process Engineering, Stellenbosch University*.

Demir, T. 2015. Synthesis and Characterization of Oleophobic Fluorinated Polyester Films. *All Dissertations*. 1580.

Ding, A., Liang, H., Li, G., Derlon, N., Szivak, I., Morgenroth, E. & Pronk, W. 2016. Impact of aeration shear stress on permeate flux and fouling layer properties in a low pressure membrane bioreactor for the treatment of grey water. *Journal of Membrane Science*. 510:382–390.

Drews, A. 2010. Membrane fouling in membrane bioreactors — Characterisation, contradictions, cause and cures. *Journal of Membrane Science*. 363(1–2):1–28.

Ducom, G., Puech, F.P. & Cabassud, C. 2002. Air sparging with flat sheet nanofiltration: A link between wall shear stresses and flux enhancement. *Desalination*. 145(1–3):97–102.

Ebnesajjad, S. 2011. Surface and Material Characterization Techniques. In William Andrew Publishing *Handbook of Adhesives and Surface Preparation*. 31–48.

Ebnesajjad, S. 2016. Introduction to Plastics. In Elsevier Inc. *Chemical Resistance of Commodity Thermoplastics*. xiii–xxv.

Ertekin, G. & Marmarali, A. 2016. The effect of heat-setting conditions on the performance characteristics of warp knitted spacer fabrics. *Journal of Engineered Fibers and Fabrics*. 11(3):64–71.

Field, R.W., Wu, D., Howell, J.A. & Gupta, B.B. 1995. Critical flux concept for microfiltration fouling. *Journal of Membrane Science*. 100(3):259–272.

Gacén, J., Cayuela, D., Maulo, J. & Gacén, I. 2002. Physico-chemical analytical techniques for evaluation of polyester heatsetting. *Journal of the Textile Institute*. 93(1):29–42.

Gander, M., Jefferson, B. & Judd, S. 2000. Aerobic MBRs for domestic wastewater treatment: A review with cost considerations. *Separation and Purification Technology*. 18(2):119–130.

Ganwei, Z., Renbi, B., Shusu, S., Xiaoji, Z. & Yongfu, G. 2019. Hydrophilic and photo-crosslinkable diblock copolymers employed for robust antifouling membrane coatings. *Applied Surface Science*. 464:429–439.

Gao, J. 2016. Membrane Separation Technology for Wastewater Treatment and its Study Progress and Development Trend. In *4th International Conference on Mechanical Materials and Manufacturing Engineering*. 5–8.

Gardiner, J. 2015. Fluoropolymers: Origin, Production, and Industrial and Commercial Applications. *Australian Journal of Chemistry*. 68(1):13–22.

Gkotsis, P.K., Banti, D.C., Peleka, E.N., Zouboulis, A.I. & Samaras, P.E. 2014. Fouling issues in Membrane Bioreactors (MBRs) for wastewater treatment: Major mechanisms, prevention and control strategies. *Processes*. 2(4):795–866.

Guan, D., Dai, J., Ahmar Siddiqui, M. & Chen, G. 2018. Comparison of different chemical cleaning reagents on fouling recovery in a Self-Forming dynamic membrane bioreactor (SFDMBR). *Separation and Purification Technology*. 206:158–165.

Guglielmi, G., Saroj, D.P., Chiarani, D. & Andreottola, G. 2007. Sub-critical fouling in a membrane bioreactor for municipal wastewater treatment: Experimental investigation and mathematical modelling. *Water Research*. 41(17):3903–3914.

Guo, R., Liu, Y., Zhang, Y., Dong, A. & Zhang, J. 2013. Surface Modification by Self-Assembled Coating with Amphiphilic Comb-Shaped Block Copolymers : A Solution to the Trade-Off Among Solubility , Adsorption and Coating Stability. *Macromelecular Research*. 21(10):1127–1137.

Guo, W., Ngo, H.H. & Li, J. 2012. A mini-review on membrane fouling. *Bioresource Technology*. 122:27–34.

Haar, S.J. 2011. Studio practices for shaping and heat-setting synthetic fabrics. *International Journal of Fashion Design, Technology and Education*. 4(1):31–41.

Hashem, M., Ibrahim, N.A., El-Shafei, A., Refaie, R. & Hauser, P. 2009. An eco-friendly - novel approach for attaining wrinkle - free/soft-hand cotton fabric. *Carbohydrate Polymers*. 78(4):690–703.

Hofs, B., Ogier, J., Vries, D., Beerendonk, E.F. & Cornelissen, E.R. 2011. Comparison of ceramic and

polymeric membrane permeability and fouling using surface water. *Separation and Purification Technology*. 79(3):365–374.

Hoinkis, J., Deowan, S.A., Panten, V., Figoli, A., Huang, R.R. & Drioli, E. 2012. Membrane bioreactor (MBR) technology - A promising approach for industrial water reuse. *Procedia Engineering*. 33:234–241.

Hu, A.Y. & Stuckey, D.C. 2006. Treatment of Dilute Wastewaters Using a Novel Submerged Anaerobic Membrane Bioreactor. *Journal of Environmental Engineering*. 132(2):190–198.

Huang, H. & Liu, W. 2006. Polyaniline/poly(ethylene terephthalate) conducting composite fabric with improved fastness to washing. *Journal of Applied Polymer Science*. 102(6):5775–5780.

Huang, Y.J. & Liang, C.M. 1996. Volume shrinkage characteristics in the cure of low-shrink unsaturated polyester resins. *Polymer*. 37(3):401–412.

Hwang, B.K., Lee, W.N., Yeon, K.M., Park, P.K., Lee, C.H., Chang, I.S., Drews, A. & Kraume, M. 2008. Correlating TMP increases with microbial characteristics in the bio-cake on the membrane surface in a membrane bioreactor. *Environmental Science and Technology*. 42(11):3963–3968.

Hwang, K., Chan, C. & Chen, F. 2008. A comparison of hydrodynamic methods for mitigating particle fouling in submerged membrane filtration. *Journal of the Chinese Institute of Chemical Engineers*. 39(3):257–264.

Ibrahim, R.I. 2018. Improving energy efficiency and fouling mitigation for membrane bioreactor in Al-Rustamiyah sewage treatment plant based on hydrodynamics. *International Journal of Environmental Science Technology*. 15(11):2369–2380.

Idumah, C. I. & Nwachukwu, A.N. 2013. Comparative Analysis of the Effect of Heatsetting and Wet Processes on the Tensile Properties of Poly Lactic Acid (PLA) and Poly Ethylene Terephthalate (PET) knitted fabrics. *International Journal of Materials, Methods and Technologies*. 1(4):45–64.

Ivanovic, I., Leiknes, T.O. & Ødegaard, H. 2008. Fouling Control by Reduction of Submicron Particles in a BF-MBR with an Integrated Flocculation Zone in the Membrane Reactor. *Separation Science and Technology*. 43(7):1871–1883.

Jain, A.K., Tesema, A.F. & Haile, A. 2019. Development of shrink resistance cotton using

fluorocarbon. *Fashion and Textiles*. 6(1):1–8.

Jeirani, Z., Jan, B.M., Ali, B.S., Noor, I.M., See, C.H. & Saphanuchart, W. 2013. Journal of Industrial and Engineering Chemistry Prediction of the optimum aqueous phase composition of a triglyceride microemulsion using response surface methodology. *Journal of Industrial and Engineering Chemistry*. 19(4):1304–1309.

Jeon, S., Rajabzadeh, S., Okamura, R., Ishigami, T., Hasegawa, S., Kato, N. & Matsuyama, H. 2016. The effect of membrane material and surface pore size on the fouling properties of submerged membranes. *Water*. 8(12):1–11.

Johnson, D.J., Oatley-Radcliffe, D.L. & Hilal, N. 2018. State of the art review on membrane surface characterisation: Visualisation, verification and quantification of membrane properties. *Desalination*. 434:12–36.

Judd, S. 2008. The status of membrane bioreactor technology. *Trends in Biotechnology*. 26(2):109–116.

Judd, S. 2011. *MBR Book - Principles and Applications of Membrane Bioreactors for Water and Wastewater Treatment (2nd Edition)*. Langford lane, Oxford: Elsevier.

Kanani, D.M., Sun, X. & Ghosh, R. 2008. Reversible and irreversible membrane fouling during in-line microfiltration of concentrated protein solutions. *Journal of Membrane Science*. 315(1–2):1-10.

Khan, S.J. & Visvanathan, C. 2008. Influence of mechanical mixing intensity on a biofilm structure and permeability in a membrane bioreactor. *Desalination*. 231(1–3):253–267.

Kim, J., Chang, I., Park, H., Kim, C., Kim, J. & Oh, J. 2008. New configuration of a membrane bioreactor for effective control of membrane fouling and nutrients removal in wastewater treatment. *Desalination*. 230(1–3):153–161.

Kim, M., Sankararao, B., Lee, S. & Yoo, C. 2013. Prediction and Identification of Membrane Fouling Mechanism in a Membrane Bioreactor Using a Combined Mechanistic Model. *Industrial & Engineering Chemistry Research*. 52(48):17198–17205.

Kimura, K., Hane, Y. & Watanabe, Y. 2005. Effect of pre-coagulation on mitigating irreversible fouling during ultrafiltration of a surface water. *Water Science and Technology*. 51(6–7):93–100.

Kimura, K., Maeda, T., Yamamura, H. & Watanabe, Y. 2008. Irreversible membrane fouling in

microfiltration membranes filtering coagulated surface water. *Journal of Membrane Science*. 320(1–2):356–362.

Kishimoto, S., Wang, Q., Xie, H. & Zhao, Y. 2007. Study of the surface structure of butterfly wings using the scanning electron microscopic moiré method. *Applied Optics*. 46(28):7026–7034.

Kochkodan, V., Johnson, D.J. & Hilal, N. 2014. Polymeric membranes: Surface modification for minimizing (bio)colloidal fouling. *Advances in Colloid and Interface Science*. 206:116–140.

Kong, Y., Wang, Z., Ma, Y., Hou, L. & Yao, W. 2016. Theory investigation on the variation of fouling resistance during water rinsing process of the membrane fouled with sodium alginate. *Journal of the Taiwan Institute of Chemical Engineers*. 66:230–238.

Kong, Y., Wang, Z., Ma, Y., Wang, H. & Khan, B. 2017. Prediction of the instantaneous fouling resistance of sodium alginate during water rinsing. *Chemical Engineering Research and Design*. 122:121–131.

Kraume, M., Wedi, D., Schaller, J., Iversen, V. & Drews, A. 2009. Fouling in MBR : What use are lab investigations for full scale operation? *Desalination*. 236(1):94–103.

Kumar, M. & Ulbricht, M. 2014. Novel ultrafiltration membranes with adjustable charge density based on sulfonated poly(arylene ether sulfone) block copolymers and their tunable protein separation performance. *Polymer*. 55(1):354–365.

Kyllönen, H., Pirkonen, P., Nyström, M., Nuortila-Jokinen, J. & Grönroos, A. 2006. Experimental aspects of ultrasonically enhanced cross-flow membrane filtration of industrial wastewater. *Ultrasonics Sonochemistry*. 13(4):295–302.

Larsen, T.A., Udert, K.M. & Lienert, J. 2015. *Source Separation and Decentralization for Wastewater Management*. London, UK: IWA publishing.

Le-Clech, P., Chen, V. & Fane, T.A.G. 2006. Fouling in membrane bioreactors used in wastewater treatment. *Journal of Membrane Science*. 284(1–2):17–53.

Li, F., Meng, J., Ye, J., Yang, B., Tian, Q. & Deng, C. 2014. Surface modification of PES ultra filtration membrane by polydopamine coating and poly (ethylene glycol) grafting : Morphology, stability, and anti-fouling. *Desalination*. 344:422–430.

Li, J., Sanderson, R.D. & Jacobs, E.P. 2002. Ultrasonic cleaning of nylon microfiltration membranes

fouled by Kraft paper mill effluent. *Journal of Membrane Science*. 205(1–2):247–257.

Li, J., Zhang, X., Cheng, F. & Liu, Y. 2013. New insights into membrane fouling in submerged MBR under sub-critical flux condition. *Bioresource Technology*. 137:404–408.

Li, W., Xing, W. & Xu, N. 2006. Modeling of relationship between water permeability and microstructure parameters of ceramic membranes. *Desalination*. 192(1–3):340–345.

Li, X., Wang, X.X., Yue, T.T., Xu, Y., Zhao, M.L., Yu, M., Ramakrishna, S. & Long, Y.Z. 2019. Waterproof-breathable PTFE nano- and microfiber membrane as high efficiency PM2.5 filter. *Polymers*. 11(4):1–14.

Lim, A.L. & Bai, R. 2003. Membrane fouling and cleaning in microfiltration of activated sludge wastewater. *Journal of Membrane Science*. 216(1–2):279–290.

Lin, H., Peng, W., Zhang, M., Chen, J., Hong, H. & Zhang, Y. 2013. A review on anaerobic membrane bioreactors: Applications , membrane fouling and future perspectives. *Desalination*. 314:169–188.

Lin, H., Zhang, M., Wang, F., Meng, F., Liao, B.Q., Hong, H., Chen, J. & Gao, W. 2014. A critical review of extracellular polymeric substances (EPSs) in membrane bioreactors: Characteristics, roles in membrane fouling and control strategies. *Journal of Membrane Science*. 460:110–125.

Lin, J.C. Te, Lee, D.J. & Huang, C. 2010. Membrane fouling mitigation: Membrane cleaning. *Separation Science and Technology*. 45(7):858–872.

Louie, J.S., Pinnau, I., Ciobanu, I., Ishida, K.P., Ng, A. & Reinhard, M. 2006. Effects of polyether-polyamide block copolymer coating on performance and fouling of reverse osmosis membranes. *Journal of Membrane Science*. 280(1–2):762–770.

Ma, W., Rajabzadeh, S. & Matsuyama, H. 2015. Preparation of antifouling poly(vinylidene fluoride) membranes via different coating methods using a zwitterionic copolymer. *Applied Surface Science*. 357:1388–1395.

Ma, Z., Zhang, S., Chen, G., Xiao, K., Li, M., Gao, Y., Liang, S. & Huang, X. 2019. Superhydrophilic and oleophobic membrane functionalized with heterogeneously tailored two-dimensional layered double hydroxide nanosheets for antifouling. *Journal of Membrane Science*. 577:165–175.

Mahady, K., Sanaei, P., Seric, I., Christov, I., Gizenia, D., Hurwitz, M., Krumwiede, T., Krupp, A., et al.

2015. Effects of membrane morphology on separation efficiency. 1:23–27.

Malaeb, L., Le-Clech, P., Vrouwenvelder, J.S., Ayoub, G.M. & Saikaly, P.E. 2013. Do biological-based strategies hold promise to biofouling control in MBRs? *Water Research*. 47(15):5447–5463.

Maschinenwesen, D.F. 2004. Fundamental investigations on the barrier effect of polyester micro fiber fabrics towards particle-loaded liquids induced by surface hydrophobization. *Technische Universität Dresden*.

Massoud, M.A., Tarhini, A. & Nasr, J.A. 2009. Decentralized approaches to wastewater treatment and management: Applicability in developing countries. *Journal of Environmental Management*. 90(1):652–659.

McAdam, E.J., Cartmell, E. & Judd, S.J. 2011. Comparison of dead-end and continuous filtration conditions in a denitrification membrane bioreactor. *Journal of Membrane Science*. 369(1–2):167–173.

Mecha, C.A. & Pillay, V.L. 2014. Development and evaluation of woven fabric microfiltration membranes impregnated with silver nanoparticles for potable water treatment. *Journal of Membrane Science*. 458:149–156.

Melidis, P., Ntougias, S., Vasilatou, V., Skouteris, G., Azis, K., Diamantis, V. & Alexandridis, A. 2016. Biofouling Aspects and Critical Flux Evaluation in an Intermittently Aerated and Fed Submerged Membrane Bioreactor. *Environmental Processes*. 3:23–33.

Meng, F., Yang, F., Shi, B. & Zhang, H. 2008. A comprehensive study on membrane fouling in submerged membrane bioreactors operated under different aeration intensities. *Separation and Purification Technology*. 59(1):91–100.

Meng, F., Chae, S.R., Drews, A., Kraume, M., Shin, H.S. & Yang, F. 2009. Recent advances in membrane bioreactors (MBRs): Membrane fouling and membrane material. *Water Research*. 43(6):1489–1512.

Meng, F., Zhang, S., Oh, Y., Zhou, Z., Shin, H.-S. & Chae, S.-R. 2017. Review Fouling in membrane bioreactors: An updated review. *Water Research*. 114:151–180.

Middlewood, P.G. & Carson, J.K. 2012. Extraction of amaranth starch from an aqueous medium using microfiltration: Membrane fouling and cleaning. *Journal of Membrane Science*. 411–

412:22–29.

Miller, D.J., Paul, D.R. & Freeman, B.D. 2013. A crossflow filtration system for constant permeate flux membrane fouling characterization fouling characterization. *Review of Scientific Instruments*. 84(035003):1–11.

Miller, D.J., Kasemset, S., Paul, D.R. & Freeman, B.D. 2014. Comparison of membrane fouling at constant flux and constant transmembrane pressure conditions. *Journal of Membrane Science*. 454:505–515.

Miller, D.J., Dreyer, D.R., Bielawski, C.W., Paul, D.R. & Freeman, B.D. 2017. Surface Modification of Water Purification Membranes. *Angewandte Chemie - International Edition*. 56(17):4662–4711.

Mohammad, A.W., Ng, C.Y., Lim, Y.P. & Ng, G.H. 2012. Ultrafiltration in Food Processing Industry: Review on Application, Membrane Fouling, and Fouling Control. *Food and Bioprocess Technology*. 5(4):1143–1156.

Mohammadi, T., Madaeni, S.S. & Moghadam, M.K. 2002. Investigation of membrane fouling. *Desalination*. 153(1–3):155–160.

Muhamad, M.S., Hamidon, N. & Hadibarata, T. 2018. Response Surface Methodology for Modeling Bisphenol A Removal Using Ultrafiltration Membrane System. *Water Air Soil Pollution*. 229(222):1–11.

Murić, A., Petrinić, I. & Christensen, M.L. 2014. Comparison of ceramic and polymeric ultrafiltration membranes for treating wastewater from metalworking industry. *Chemical Engineering Journal*. 255:403–410.

Nady, N., Franssen, M.C.R., Zuilhof, H., Eldin, M.S.M., Boom, R. & Schroën, K. 2011. Modification methods for poly(arylsulfone) membranes: A mini-review focusing on surface modification. *Desalination*. 275(1–3):1–9.

Nakashima, T., Tenjimbayashi, M., Matsubayashi, T., Manabe, K., Fujita, M., Kamiya, T., Honda, T. & Shiratori, S. 2017. Oleophobic/Adhesive Janus Self-Standing Films Modified with Bifurcated Short Fluorocarbon Chains as Transparent Oil Stain-Free Coating with Attachability. *Industrial and Engineering Chemistry Research*. 56(14):3928–3936.

Ndinisa, N. V., Fane, A.G., Wiley, D.E. & Fletcher, D.F. 2006. Fouling control in a submerged flat sheet membrane system: Part II - Two-phase flow characterization and CFD simulations. *Separation Science and Technology*. 41(7):1411–1445.

Ndinisa, N. V, Fane, A.G. & Wiley, D.E. 2007. Fouling Control in a Submerged Flat Sheet Membrane System : Part I – Bubbling and Hydrodynamic Effects. *Separation and Purification Technology*. 41(7):1383–1409.

Ng, C.A., Sun, D. & Fane, A.G. 2006. Operation of membrane bioreactor with powdered activated carbon addition. *Separation Science and Technology*. 41(7):1447–1466.

Nguyen, S.T., Roddick, F.A. & Harris, J.L. 2010. Membrane foulants and fouling mechanisms in microfiltration and ultrafiltration of an activated sludge effluent. *Water Science and Technology*. 62(9):1975–1983.

Nittami, T., Hitomi, T., Matsumoto, K., Nakamura, K., Ikeda, T., Setoguchi, Y. & Motoori, M. 2012. Comparison of polytetrafluoroethylene flat-sheet membranes with different pore sizes in application to submerged membrane bioreactor. *Membranes*. 2(2):228–236.

Nywening, J. & Zhou, H. 2009. Influence of filtration conditions on membrane fouling and scouring aeration effectiveness in submerged membrane bioreactors to treat municipal wastewater. *Water Research*. 43(14):3548–3558.

Ogunbiyi, O.O., Miles, N.J. & Hilal, N. 2008. The effects of performance and cleaning cycles of new tubular ceramic microfiltration membrane fouled with a model yeast suspension. *Desalination*. 220(1–3):273–289.

Osterlund, R & Vingsbo, O. 1979. Scanning electron microscope and optical microscope studies of the topography of some etched steel structures. *Ultramicroscopy*. 4(2):155–162.

Paul, R. 2015. Functional finishes for textiles: An overview. In Woodhead Publishing *Functional Finishes for Textiles: Improving Comfort, Performance and Protection*. 1–14.

Perera, H.A.A.E. & Lanarolle, W.D.G. 2020. Comparative study on the thermal shrinkage behaviour of polyester yarn and its plain knitted fabrics. *The Journal of The Textile Institute*. Article in press.

Perera, A.E., Lanarolle, G. & Jayasundara, R. 2019. Effects of Panel Parameters and Heat Setting

Temperature on Thermal Shrinkage of Heat Cured Polyester Plain Knitted Fabric Panels Statistical Modeling Approach. In IEEE *5th International Multidisciplinary Moratuwa Engineering Research Conference*. 722–726.

Pillay, V.L. 2009. The Development of an Immersed Membrane Microfiltration System for the Treatment of Rural Waters and Industrial Waters. *Water Research Commission*.

Pillay, V.L. & Jacobs, E.P. 2008. Development of a Membrane Pack for Immersed Membrane Bioreactors. *Water Research Commission*.

Pillay, V.L., Cele, M.X. & Deelie, M. 2016. Development of a woven fabric immersed membrane bioreactor (WFIMBR) package plant for decentralized sanitation. *Water Research Commission*.

Pollice, A., Brookes, A., Jefferson, B. & Judd, S. 2005. Sub-critical flux fouling in membrane bioreactors - A review of recent literature. *Desalination*. 174(3):221–230.

Popović, S., Milanović, S., Iličić, M., Djurić, M. & Tekić, M. 2009. Flux recovery of tubular ceramic membranes fouled with whey proteins. *Desalination*. 249(1):293–300.

Radjenović, J., Matošić, M., Mijatović, I., Petrović, M. & Barceló, D. 2008. Membrane bioreactor (MBR) as an advanced wastewater treatment technology. *Handbook of Environmental Chemistry*. 5:37–101.

Rezaei, H., Ashtiani, F.Z. & Fouladitajar, A. 2011. Effects of operating parameters on fouling mechanism and membrane flux in cross-flow microfiltration of whey. *Desalination*. 274(1–3):262–271.

Rezaei, H., Ashtiani, F.Z. & Fouladitajar, A. 2014. Fouling behavior and performance of microfiltration membranes for whey treatment in steady and unsteady-state conditions. *Brazilian Journal of Chemical Engineering*. 31(2):503–518.

Rodgers, M., Wu, G. & Zhan, X. 2008. Nitrogen and Phosphorus Removal from Domestic Strength Synthetic Wastewater Using an Alternating Pumped Flow Sequencing Batch Biofilm Reactor. *Journal of Environmental Quality*. 37(3):977–982.

Rouette H.K & Kittan G. 1991. *Wool fabric finishing*. Ilkley, United Kingdom: Wool Development International Ltd.

Saffari, M., Khoddami, A. & Mallakpour, S. 2015. The effect of a novel booster (bisulfate adduct of

polyisocyanate) on fluorocarbon chain re-orientation and substrate properties: Synthesis and finishing. *Progress in Organic Coatings*. 78:261–264.

Saito, T., Tsushima, Y., Honda, T., Kamiya, T., Fujita, M. & Sawada, H. 2016. Facile creation of modified surface possessing the controlled wettability between superamphiphobic and superoleophobic-superhydrophilic characteristics by using perfluorocarboxamides/calcium carbonate/calcium fluoride nanocomposites: Application to the separation of oil and water. *Journal of Composite Materials*. 50(27):3831–3842.

Sanaei, P. & Cummings, L.J. 2017. Flow and fouling in membrane filters: Effects of membrane morphology. *Journal of Fluid Mechanics*. 818:744–771.

Sayed U. & Dabhi P. 2014. Finishing of Textiles With Fluorocarbons. *International Journal of Advance Science and Engineering*. 1(2):335–352.

Schindler, W.D. & Hauser, P.J. 2004. *Chemical Finishing of Textiles*. Cambridge, England: Woodhead Publishing.

Shen, S. su, Chen, H., Wang, R. hua, Ji, W., Zhang, Y. & Bai, R. 2019. Preparation of antifouling cellulose acetate membranes with good hydrophilic and oleophobic surface properties. *Materials Letters*. 252:1–4.

Shyr, T.W., Lien, C.H. & Lin, A.J. 2011. Coexisting antistatic and water-repellent properties of polyester fabric. *Textile Research Journal*. 81(3):254–263.

Singhania, R.R., Christophe, G., Perchet, G., Troquet, J. & Larroche, C. 2012. Immersed membrane bioreactors: An overview with special emphasis on anaerobic bioprocesses. *Bioresource Technology*. 122:171–180.

Speke, R.W. 1954. Variables in Padding Processes. *Coloration Technology*. 70(6):221–226.

Sun, W., Liu, J., Chu, H. & Dong, B. 2013. Pretreatment and membrane hydrophilic modification to reduce membrane fouling. *Membranes*. 3(3):226–241.

Sun, Y., Qin, Z., Zhao, L., Chen, Q., Hou, Q., Lin, H., Jiang, L., Liu, J., et al. 2018. Membrane fouling mechanisms and permeate flux decline model in soy sauce microfiltration. *Journal of Food Process Engineering*. 41(1):1–10.

Tang, K. po M., Kan, C. wai, Fan, J. tu & Tso, S. leung. 2017. Effect of softener and wetting agent on

improving the flammability, comfort, and mechanical properties of flame-retardant finished cotton fabric. *Cellulose*. 24(6):2619–2634.

Teow, Y.H., Shah, M., Ho, K.C. & Mohammad, A. 2018. A study on membrane technology for surface water treatment: Synthesis, characterization and performance test. *Membrane Water Treatment*. 9(2):69–77.

Thilagavathi, G. & Kannaian, T. 2008. Dual antimicrobial and blood repellent finishes for cotton hospital fabrics. *Indian Journal of Fibre and Textile Research*. 33(1):23–29.

Tian, J., Xu, Y., Chen, Z., Nan, J. & Li, G. 2010. Air bubbling for alleviating membrane fouling of immersed hollow- fiber membrane for ultrafiltration of river water. *Desalination*. 260(1–3):225–230.

Tijing, L.D., Woo, Y.C., Choi, J.S., Lee, S., Kim, S.H. & Shon, H.K. 2015. Fouling and its control in membrane distillation-A review. *Journal of Membrane Science*. 475:215–244.

Trussell, R.S., Merlo, R.P., Hermanowicz, S.W. & Jenkins, D. 2007. Influence of mixed liquor properties and aeration intensity on membrane fouling in a submerged membrane bioreactor at high mixed liquor suspended solids concentrations. *Water Research*. 41(5):947–958.

Tsuyuhara, T., Hanamoto, Y., Miyoshi, T., Kimura, K. & Watanabe, Y. 2010. Influence of membrane properties on physically reversible and irreversible fouling in membrane bioreactors. *Water Science and Technology*. 61(9):2235–2240.

Ueda, T. & Hata, K. 1999. Domestic wastewater treatment by a submerged membrane bioreactor with gravitational filtration. *Water Research*. 33(12):2888–2892.

Vasiljević, J., Gorjanc, M., Tomšič, B., Orel, B., Jerman, I., Mozetič, M., Vesel, A. & Simončič, B. 2013. Surface Modification of Polyester Fibres By Plasma Pre- Treatment and Sol-Gel Finishing. In Dresdan, Germany *13TH AUTEX World Textile Conference*. 1–6.

Verma, V.K. & Subbiah, S. 2019. Fouling resistant sericin-coated polymeric microfiltration membrane. *Journal of Chemical Technology and Biotechnology*. 94(11):3637–3649.

Villain, M., Bourven, I., Guibaud, G. & Marrot, B. 2014. Bioresource Technology Impact of synthetic or real urban wastewater on membrane bioreactor (MBR) performances and membrane fouling under stable conditions. *Bioresource Technology*. 155:235–244.

Visvanathan, C., Ben Aim, R. & Parameshwaran, K. 2000. Membrane separation bioreactors for wastewater treatment. *Critical Reviews in Environmental Science and Technology*. 30(1):1–48.

Vongsayalath, T. 2015. Development of Woven Fiber Microfiltration Membrane System for Water and Wastewater Treatment. *School of Environment, Resources and Development, Asian Institute of Technology*.

Wang, C. 2006. Agent distribution and water remaining of polyester nonwoven fabrics after-treated with polyurethane-citric acid. *Journal of Applied Polymer Science*. 100(1):47–56.

Wang, F. & Tarabara, V. V. 2008. Pore blocking mechanisms during early stages of membrane fouling by colloids. *Journal of Colloid and Interface Science*. 328(2):464–469.

Wang, C., Yang, F., Meng, F., Zhang, H., Xue, Y. & Fu, G. 2010. High flux and antifouling filtration membrane based on non-woven fabric with chitosan coating for membrane bioreactors. *Bioresource Technology*. 101(14):5469–5474.

Wang, K., Hou, D., Qi, P., Li, K., Yuan, Z. & Wang, J. 2019. Development of a composite membrane with underwater-oleophobic fibrous surface for robust anti-oil-fouling membrane distillation. *Journal of Colloid and Interface Science*. 537:375–383.

Wang, Z., Wu, Z., Yin, X. & Tian, L. 2008. Membrane fouling in a submerged membrane bioreactor (MBR) under sub-critical flux operation: Membrane foulant and gel layer characterization. *Journal of Membrane Science*. 325(1):238–244.

Wang, Z., Zhao, S., Liu, F., Yang, L., Song, Y., Wang, X. & Xi, X. 2010. Influence of operating conditions on cleaning efficiency in sequencing batch reactor (SBR) activated sludge process - water rinsing introduced membrane filtration process. *Desalination*. 259(1–3):235–242.

Wang, Z., Ma, J., Tang, C.Y., Kimura, K., Wang, Q. & Han, X. 2014. Membrane cleaning in membrane bioreactors: A review. *Journal of Membrane Science*. 468:276–307.

Wei, L. 2019. Synthesis , Characterization , and Application of Oleophobic Fluorinated Copolymers. *All Dissertations*. 2426.

WHO & UN Habitat. 2016. *Global Report on Urban Health: equitable, healthier cities*. Geneva, Switzerland.

Woltersdorf, L., Zimmermann, M., Deffner, J., Gerlach, M. & Liehr, S. 2018. Benefits of an integrated

water and nutrient reuse system for urban areas in semi-arid developing countries. *Resources, Conservation and Recycling*. 128:382–393.

Wu, Z., Wang, Z., Huang, S., Mai, S., Yang, C., Wang, X. & Zhou, Z. 2008. Effects of various factors on critical flux in submerged membrane bioreactors for municipal wastewater treatment. *Separation and Purification Technology*. 62(1):56–63.

Xia, S., Guo, J. & Wang, R. 2008. Performance of a pilot-scale submerged membrane bioreactor (MBR) in treating bathing wastewater. *Bioresource Technology*. 99(15):6834–6843.

Xiao, K., Shen, Y. & Huang, X. 2013. An analytical model for membrane fouling evolution associated with gel layer growth during constant pressure stirred dead-end filtration. *Journal of Membrane Science*. 427:139–149.

Xiao, K., Liang, S., Wang, X., Chen, C. & Huang, X. 2019. Current state and challenges of full-scale membrane bioreactor applications : A critical review. *Bioresource Technology*. 271:473–481.

XIE, Y. jie, YU, H. yin, WANG, S. yuan & XU, Z. kang. 2007. Improvement of antifouling characteristics in a bioreactor of polypropylene microporous membrane by the adsorption of Tween 20. *Journal of Environmental Sciences*. 19(12):1461–1465.

Xu, E., Pan, X., Wu, Z., Long, J., Li, J., Xu, X., Jin, Z. & Jiao, A. 2016. Response surface methodology for evaluation and optimization of process parameter and antioxidant capacity of rice flour modified by enzymatic extrusion. *Food Chemistry*. 212:146–154.

Yamamura, H., Kimura, K. & Watanabe, Y. 2007. Mechanism Involved in the Evolution of Physically Irreversible Fouling in Microfiltration and Ultrafiltration Membranes Used for Drinking Water Treatment. *Environmental Science and Technology*. 41(19):6789–6794.

Yang, H., Hu, X., Chen, R., Liu, S., Pi, P. & Yang, Z.R. 2013. Fluoropolymer/SiO 2 composite films with switchable superoleophilicity and high oleophobicity for “on-off” oil permeation. *Applied Surface Science*. 280:113–116.

Yang, J., Yin, L., Tang, H., Song, H., Gao, X., Liang, K. & Li, C. 2015. Polyelectrolyte-fluorosurfactant complex-based meshes with superhydrophilicity and superoleophobicity for oil/water separation. *Chemical Engineering Journal*. 268:245–250.

Yang, L., Wang, Z., Sun, Y., Hu, Z., Zhao, S., Wang, X., Li, W., Xi, X., et al. 2011. Influence of various

operating conditions on cleaning efficiency in sequencing batch reactor (SBR) activated sludge process. Part II: Backwash and water rinsing introduced membrane filtration process. *Desalination*. 272:76–84.

Yigit, N.O., Civelekoglu, G., Harman, I., Koseoglu, H. & Kitis, M. 2009. Effects of various backwash scenarios on membrane fouling in a membrane bioreactor. *Desalination*. 237(1–3):346–356.

Zhang, B., Shi, W., Yu, S., Zhu, Y., Zhang, R. & Li, L. 2015. Optimization of cleaning conditions on a polytetrafluoroethylene (PTFE) microfiltration membrane used in treatment of oil-field wastewater. *RSC Advances*. 5:104960–104971.

Zhang, M., Liao, B. qiang, Zhou, X., He, Y., Hong, H., Lin, H. & Chen, J. 2015. Effects of hydrophilicity/hydrophobicity of membrane on membrane fouling in a submerged membrane bioreactor. *Bioresource Technology*. 175:59–67.

Zhang, W., Luo, J., Ding, L. & Jaffrin, M.Y. 2015. A review on flux decline control strategies in pressure-driven membrane processes. *Industrial and Engineering Chemistry Research*. 54(11):2843–2861.

Zhao, Y., Qin, Z., Zhao, Y., Cui, S. & Guo, H. 2019. Evaluating the anti-fouling property of the hydrophilically modified porous PTFE membrane. *Desalination and Water Treatment*. 159:224–231.

Zheng, Y., Zhang, W., Tang, B., Ding, J., Zheng, Y. & Zhang, Z. 2018. Membrane fouling mechanism of biofilm-membrane bioreactor (BF-MBR): Pore blocking model and membrane cleaning. *Bioresource Technology*. 250(November 2017):398–405.

Zhou, C.E., Kan, C.W., Yuen, C. wah M., Matinlinna, J.P., Tsoi, J.K. hon & Zhang, Q. 2016. Plasma treatment applied in the pad-dry-cure process for making rechargeable antimicrobial cotton fabric that inhibits S. Aureus. *Textile Research Journal*. 86(20):2202–2215.

Zhu, X., Loo, H.E. & Bai, R. 2013. A novel membrane showing both hydrophilic and oleophobic surface properties and its non-fouling performances for potential water treatment applications. *Journal of Membrane Science*. 436:47–56.

Zydney, A.L. & Ho, C.C. 2003. Effect of membrane morphology on system capacity during normal flow microfiltration. *Biotechnology and Bioengineering*. 83(5):537–543.

Appendix A
Raw and calculated results

A.1. Fouling characteristics of WFMF membranes

Table A-1: Results of pure water flux (PWF) experiments of clean membranes

Pump settings (rev/min)	Volume(L)	Time (s)			TMP (kPa)			Flux (LMH) Average	TMP (kPa) Average
		Run 1	Run 2	Run 3	Run 1	Run 2	Run 3		
100	0.5	68	76	72	9	10	10	390.91	10
150	0.5	42	47	43	14	14	13	638.86	14
200	0.5	35	36	35	15	16	16	810.15	16
250	0.5	34	34	34	17	16	16	834.34	16
300	0.5	31	31	31	18	17	17	901.62	17

Table A-2: Results of PWF experiment of membranes air scoured at 20 L/min for 5 minutes

Pump settings (rev/min)	Volume(L)	Time (s)			TMP (kPa)			Flux (LMH) Average	TMP (kPa) Average
		Run 1	Run 2	Run 3	Run 1	Run 2	Run 3		
100	0.5	76	78	80	18	16	15	358.34	16
200	0.5	43	45	43	27	26	28	635.23	27
300	0.5	38	42	43	29	28	28	681.71	28

Table A-3: Results of PWF experiments of membranes air scoured at 20 L/min for 15 minutes

Pump settings (rev/min)	Volume(L)	Time (s)			TMP (kPa)			Flux (LMH) Average	TMP (kPa) Average
		Run 1	Run 2	Run 3	Run 1	Run 2	Run 3		
100	0.5	73	73	73	16	16	15	382.88	16
200	0.5	45	44	43	27	26	27	635.23	26
300	0.5	43	39	41	29	27	28	681.71	27

Table A-4: Results of PWF experiments of membranes intermittently air scoured at 20 L/min for 15 minutes

Pump settings (rev/min)	Volume(L)	Time (s)			TMP (kPa)			Flux (LMH) Average	TMP (kPa) Average
		Run 1	Run 2	Run 3	Run 1	Run 2	Run 3		
100	0.5	74	70	75	16	18	14	382.88	16
200	0.5	45	45	45	23	24	23	621.12	23
300	0.5	41	39	43	24	25	24	681.71	24

Table A-5: Results of PWF experiments of membranes air scoured at 30 L/min for 5 minutes

Pump settings (rev/min)	Volume(L)	Time (s)			TMP (kPa)			Flux (LMH) Average	TMP (kPa) Average
		Run 1	Run 2	Run 3	Run 1	Run 2	Run 3		
100	0.5	75	72	77	16	17	16	372.67	16
200	0.5	46	45	48	24	26	25	607.62	25
300	0.5	43	40	44	26	27	26	665.48	26

Table A-6: Results of PWF experiments of membranes air scoured at 30 L/min for 15 minutes

Pump settings (rev/min)	Volume(L)	Time (s)			TMP (kPa)			Flux (LMH) Average	TMP (kPa) Average
		Run 1	Run 2	Run 3	Run 1	Run 2	Run 3		
100	0.5	79	79	79	17	15	16	353.80	16
200	0.5	42	45	45	27	24	25	635.23	25
300	0.5	39	43	41	27	25	27	681.71	26

Table A-7: Results of PWF experiments of membranes intermittently air scoured at 30 L/min for 15 minutes

Pump settings (rev/min)	Volume(L)	Time (s)			TMP (kPa)			Flux (LMH) Average	TMP (kPa) Average
		Run 1	Run 2	Run 3	Run 1	Run 2	Run 3		
100	0.5	74	78	79	17	15	14	362.99	15
200	0.5	40	41	42	26	25	25	681.71	25
300	0.5	36	39	39	27	26	26	735.53	26

Table A-8: Results of PWF experiments of membranes intermittently air scoured at 20 L/min for 15 mins at 40 cm backwash height

Pump settings (rev/min)	Volume(L)	Time (s)			TMP (kPa)			Flux (LMH) Average	TMP (kPa) Average
		Run 1	Run 2	Run 3	Run 1	Run 2	Run 3		
100	0.5	76	74	75	13	12	13	372.67	13
200	0.5	36	36	36	22	22	22	776.40	22
300	0.5	35	36	30	23	23	24	822.07	23

Table A-9: Results of PWF experiments of membranes intermittently air scoured at 20 L/min for 15 mins at 60 cm backwash height

Pump settings (rev/min)	Volume(L)	Time (s)			TMP (kPa)			Flux (LMH) Average	TMP (kPa) Average
		Run 1	Run 2	Run 3	Run 1	Run 2	Run 3		
100	0.5	72	74	70	12	11	13	388.20	12
200	0.5	37	39	38	20	18	20	735.53	19
300	0.5	33	33	33	21	21	22	846.98	21

Table A-10: Results of PWF experiments of membranes intermittently air scoured at 20 L/min for 15 mins at 75 cm backwash height

Pump settings (rev/min)	Volume(L)	Time (s)			TMP (kPa)			Flux (LMH) Average	TMP (kPa) Average
		Run 1	Run 2	Run 3	Run 1	Run 2	Run 3		
100	0.5	73	73	70	11	11	12	388.20	11
200	0.5	36	38	32	20	18	20	798.58	19
300	0.5	31	33	29	21	19	21	901.63	20

Table A-11: Results for evaluating the effectiveness of air scouring/backwash in restoring the original permeability of WFMF membranes, average of 3 repeat runs

Fouling process					Initial membranes	Cleaned membranes
Time (min)	Volume (mL)	Flux (LMH)	ΔP (kPa)	Resistance (m^{-1})	Resistance (m^{-1})	Resistance (m^{-1})
5	2000	372.67	16	1.73663E+11	3.80E+10	7.89E+10
10	1900	354.04	18	2.05653E+11		
15	1900	354.04	19	2.17079E+11		
20	1800	335.40	20	2.41199E+11		
25	1800	335.40	21	2.53258E+11		
30	1800	335.40	22	2.65318E+11		
35	1750	326.09	23	2.85303E+11		
40	1700	316.77	24	3.06464E+11		
45	1700	316.77	25	3.19233E+11		
50	1650	307.45	27	3.5522E+11		
55	1600	298.14	27	3.6632E+11		
60	1600	298.14	29	3.93455E+11	3.80E+10	7.89E+10

Table A-12: Results for evaluating the contribution of water scouring in the restoration of fouled WFMF membranes

Pump settings (rev/min)	Volume(l)	Time (s)			TMP (kPa)			Flux (LMH) Average	TMP (kPa) Average
		Run 1	Run 2	Run 3	Run 1	Run 2	Run 3		
100	0.5	78	71	76	12	11	13	372.67	12
200	0.5	37	31	34	25	15	25	822.07	22
300	0.5	33	28	32	28	17	25	901.63	23

Table A-13: Fouling experiment results of a 20-minutes yeast filtration process, average of 3 repeat runs

Time (min)	ΔP (kPa)	FLUX (LMH)	Resistance (m^{-1})
5	14	372.67	1.5196E+11
10	15	363.35	1.6699E+11
15	16	354.04	1.828E+11
20	17	344.72	1.9948E+11

Table A-14: Fouling experiment results of a 90-minutes yeast filtration process, average of 3 repeat runs

Time (s)	ΔP (kPa)	FLUX (LMH)	Resistance (m^{-1})
5	14.67	372.67	1.55552E+11
10	15.67	365.68	1.68941E+11
15	17.00	363.35	1.83622E+11
20	18.33	356.37	2.00817E+11
25	19.00	354.04	2.11625E+11
30	19.67	349.38	2.24071E+11
35	20.33	344.72	2.35635E+11
40	21.00	344.72	2.4607E+11
45	21.67	337.73	2.59579E+11
50	22.33	330.75	2.72504E+11
55	23.33	328.42	2.89394E+11
60	24.00	321.43	3.04292E+11
65	24.67	314.44	3.21633E+11
70	25.33	307.80	3.3469E+11
75	26.33	305.47	3.4942E+11
80	27.00	300.81	3.66482E+11
85	28.00	293.48	3.9004E+11
90	28.33	291.15	3.98172E+11

Table A-15: Fouling experiment results of a 10-minutes yeast filtration process, average of 3 repeat runs

Time (s)	ΔP (kPa)	FLUX (LMH)	Resistance (m^{-1})
5	14	381.99	1.4825E+11
10	15	372.67	1.6281E+11

Table A-16: Fouling experiment results of a 30-minutes yeast filtration process, average of 3 repeat runs

Time (min)	ΔP (kPa)	FLUX (LMH)	Resistance (m^{-1})
5	15	409.94	1.4801E+11
10	16	391.31	1.6539E+11
15	18	391.31	1.8606E+11
20	19	372.67	2.0623E+11
25	20	372.67	2.1708E+11
30	22	363.36	2.4491E+11

Table A-17: Fouling experiment results of a 60-minutes yeast filtration process, average of 3 repeat runs

Time (min)	ΔP (kPa)	FLUX (LMH)	Resistance (m^{-1})
5	15	409.94	1.4801E+11
10	17	391.31	1.7573E+11
15	18	372.67	1.9537E+11
20	19	372.67	2.0623E+11
25	20	363.36	2.2264E+11
30	22	354.04	2.5135E+11
35	23	344.72	2.6988E+11
40	23	335.41	2.7737E+11
45	24	335.41	2.8943E+11
50	25	326.09	3.1011E+11
55	27	316.77	3.4477E+11
60	28	316.77	3.5754E+11

Table A-18: Resistance of water scoured membranes after different filtration duration, average of 3 repeat runs

Time (min)	Resistance × 10^9 (m^{-1})
0	37.99
10	128.98
20	128.98
30	142.27
60	135.83
120	124.30

Table A-19: Resistance data for WFMF membranes in a cyclic filtration and water scouring process

Time (min)	Resistance (m^{-1})					
	Cycle 1	Cycle 2	Cycle 3	Cycle 4	Cycle 5	Cycle 6
5	1.67E+11	1.83E+11	1.85E+11	2.00E+11	2.06E+11	2.23E+11
10	1.94E+11	1.94E+11	1.95E+11	2.17E+11	2.35E+11	2.46E+11
15	2.11E+11	2.11E+11	2.12E+11	2.29E+11	2.53E+11	2.65E+11
20	2.29E+11	2.23E+11	2.29E+11	2.35E+11	2.53E+11	2.77E+11
25	2.29E+11	2.41E+11	2.40E+11	2.53E+11	2.65E+11	2.98E+11
30	2.41E+11	2.53E+11	2.65E+11	2.65E+11	2.85E+11	3.19E+11
35	2.53E+11	2.53E+11	2.65E+11	2.85E+11	3.06E+11	3.29E+11
40	2.53E+11	2.73E+11	2.77E+11	2.85E+11	3.29E+11	3.65E+11
45	2.73E+11	2.85E+11	2.98E+11	3.06E+11	3.38E+11	3.65E+11
50	2.81E+11	2.94E+11	3.06E+11	3.19E+11	3.51E+11	3.78E+11
55	2.94E+11	3.07E+11	3.19E+11	3.51E+11	3.65E+11	3.92E+11
60	3.03E+11	3.16E+11	3.42E+11	3.65E+11	3.92E+11	4.20E+11
65	3.16E+11	3.38E+11	3.65E+11	3.92E+11	4.20E+11	4.20E+11
70	3.24E+11	3.51E+11	3.65E+11	3.92E+11	4.20E+11	4.49E+11
75	3.38E+11	3.78E+11	3.92E+11	4.20E+11	4.49E+11	4.65E+11
80	3.51E+11	3.91E+11	4.06E+11	4.34E+11	4.65E+11	4.81E+11
85	3.78E+11	4.05E+11	4.20E+11	4.49E+11	4.81E+11	4.81E+11
90	3.78E+11	4.05E+11	4.34E+11	4.81E+11	4.81E+11	5.15E+11

A.2. Development and characterization of an OWFMF membrane

Table A-20: Experimental design matrix and experimental results for the optimization of padding process parameters using a 3-level,3-factor full factorial design

Run	Concentration (g/L)	Pressure (bar)	Speed (m/min)	OCA	WCA
1	40	0.50	1.00	113.58	129.40
2	40	0.50	2.00	113.65	132.87
3	40	0.50	3.00	112.17	132.71
4	40	2.00	1.00	118.31	132.31
5	40	2.00	2.00	116.88	133.88
6	40	2.00	3.00	115.72	134.62
7	40	3.50	1.00	114.32	129.39
8	40	3.50	2.00	115.14	131.39
9	40	3.50	3.00	115.20	132.93
10	60	0.50	1.00	115.60	135.09
11	60	0.50	2.00	115.91	135.22
12	60	0.50	3.00	112.82	129.94
13	60	2.00	1.00	119.61	136.17
14	60	2.00	2.00	118.47	134.64
15	60	2.00	3.00	117.36	131.78
16	60	3.50	1.00	114.73	134.76
17	60	3.50	2.00	115.80	136.41
18	60	3.50	3.00	116.25	133.42
19	80	0.50	1.00	116.20	135.54
20	80	0.50	2.00	116.56	135.70
21	80	0.50	3.00	115.56	135.28
22	80	2.00	1.00	121.13	135.85
23	80	2.00	2.00	119.52	136.10
24	80	2.00	3.00	117.89	134.54
25	80	3.50	1.00	115.92	135.94
26	80	3.50	2.00	116.2	136.13
27	80	3.50	3.00	116.78	135.31
28	60	2.00	2.00	116.76	134.87
29	60	2.00	2.00	116.26	135.59
30	60	2.00	2.00	117.86	133.07
31	60	2.00	2.00	118.08	134.59
32	60	2.00	2.00	118.17	135.12

Table A-21: Effect of curing time on the oil contact angle at a constant curing temperature of 180°C for membranes padded at 1.5 bar/ 1 m/min, average of 5 measurements

FC concentration (g/L)	Curing time (secs)			
	30	60	90	120
40	118.31	119.06	120.40	
60	119.61	120.15	122.03	
80	121.13	122.40	123.47	123.36

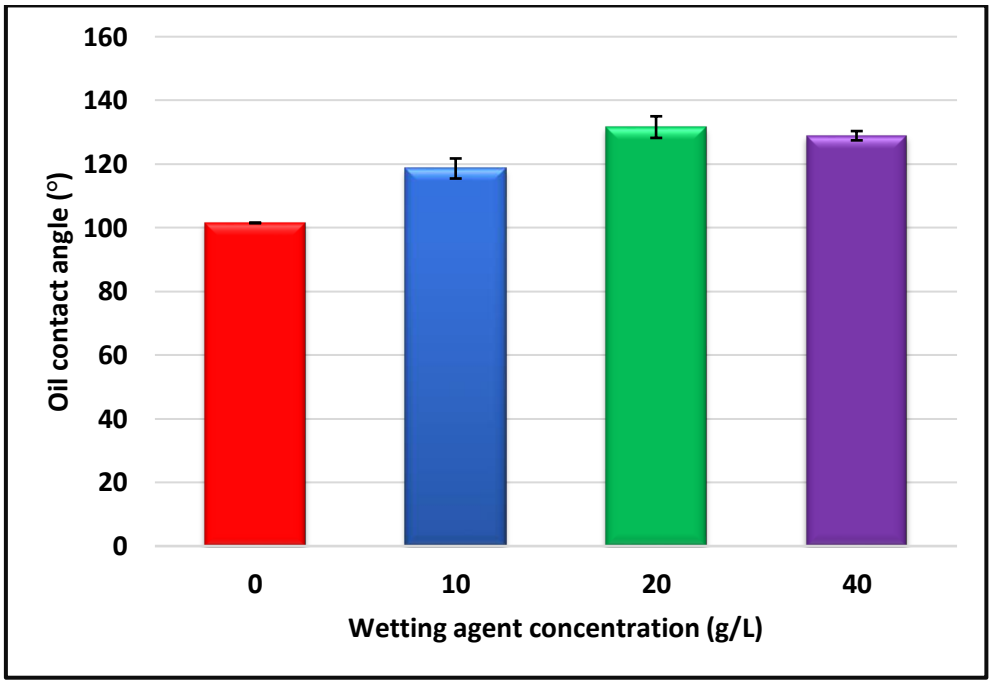

Figure A-1: Effect of wetting agent concentration on oil contact angle at a padding pressure of 1.5 bar and fabric speed of 2.5 m/min, average of 5 measurements.

Table A-22: Regression coefficients for the model used in predicting the oil contact angle for the padding process

Factor	Regr. Coefficients; Var.:**Contact Angle**; R-sqr=,92563; Adj:,89021 (Spreadsheet1) 3 3-level factors, 1 Blocks, 32 Runs; MS Residual=,4289349 DV: **Contact Angle** **Regressn Coeff.**	Std.Err.	t(21)	p	-95,% Cnf.Limt	+95,% Cnf.Limt
Mean/Interc.	102,1793	3,676205	27,79478	0,000000	94,5342	109,8244
(1)**Concentration (g/l)**(L)	0,0428	0,075558	0,56676	0,576884	-0,1143	0,2000
Concentration (g/l)(Q)	0,0001	0,000626	0,19859	0,844490	-0,0012	0,0014
(2)**Pressure (bar)**(L)	17,1965	3,354172	5,12689	0,000044	10,2211	24,1718
Pressure (bar)(Q)	-4,2050	0,815735	-5,15480	0,000042	-5,9014	-2,5085
(3)**Speed (m/min)**(L)	8,4581	3,163690	2,67349	0,014220	1,8788	15,0373
Speed (m/min)(Q)	-2,1355	0,782191	-2,73020	0,012540	-3,7622	-0,5089
2L by 3L	-11,4557	3,662971	-3,12744	0,005090	-19,0733	-3,8382
2L by 3Q	2,4359	0,903554	2,69593	0,013531	0,5569	4,3150
2Q by 3L	2,6857	0,888781	3,02182	0,006490	0,8374	4,5341
2Q by 3Q	-0,5363	0,219196	-2,44686	0,023296	-0,9922	-0,0805

Table A-23: Analysis of variance (ANOVA) for the oil contact angles of fabrics cured for 30 seconds

	ANOVA				
Factor	SS	df	MS	F	p
(1)**Concentration (g/l)** L+Q	24,0154	2	12,00769	22,87309	0,000055
(2)**Pressure (bar)** L+Q	64,0405	2	32,02027	60,99447	0,000000
(3)**Speed (m/min)** L+Q	5,5568	2	2,77841	5,29251	0,020821
1*2	2,1143	4	0,52857	1,00686	0,439090
1*3	0,0525	4	0,01312	0,02500	0,998619
2*3	14,1307	4	3,53267	6,72927	0,003665
Error	6,8246	13	0,52497		
Total SS	121,1158	31			

Table A-24: Permeate turbidity results in evaluating the importance of heat setting in the development of OWFMF membranes, average of 3 repeat runs

Time (min)	**Turbidity (NTU)**				
	Std WFMF	**Not stretched**	**2% stretched**	**4% stretched**	**4.8% stretched**
5	0.78	5.99	1.06	1.04	1.14
10	0.74	2.34	0.84	0.95	0.93
15	0.71	1.34	0.79	0.83	0.85
20	0.69	1.48	0.77	0.79	0.79
25	0.66	1.41	0.76	0.74	0.77
30	0.63	0.87	0.72	0.72	0.75

A.3. Performance evaluation of the OWFMF membrane

Table A-25: Results of the pure water flux experiments for the standard WFMF membranes

Pump settings (rev/min)	Volume(L)	Time (s)			TMP (kPa)			Flux (LMH) Average	TMP (kPa) Average
		Run 1	Run 2	Run 3	Run 1	Run 2	Run 3		
50	0.5	144	137	142	7	7	6	198.23	7
100	0.5	74	74	76	10	10	9	374.33	10
150	0.5	47	43	48	14	15	12	607.62	14
200	0.5	36	34	34	17	17	16	806.26	16
250	0.5	33	33	33	18	17	16	846.98	17
300	0.5	31	30	30	19	18	17	921.44	18

Table A-26: Results of the pure water flux experiments for the OWFMF membranes

Pump settings (rev/min)	Volume(L)	Time (s)			TMP (kPa)			Flux (LMH) Average	TMP (kPa) Average
		Run 1	Run 2	Run 3	Run 1	Run 2	Run 3		
50	0.5	135	140	138	5	5	4	203.03	5
100	0.5	73	78	76	8	7	6	369.39	7
150	0.5	42	46	45	11	10	9	630.46	10
200	0.5	29	32	28	11	12	11	942.15	11
250	0.5	27	30	27	11	13	11	998.23	11
300	0.5	26	28	25	12	14	11	1061.4	12

Table A-27: Permeate turbidity of the standard WFMF and OWFMF membranes in the filtration of fresh yeast suspension

Time (min)	Turbidity (NTU)							
	Standard WFMF				OWFMF			
	Run 1	Run 2	Run 3	Average	Run 1	Run 2	Run 3	Average
5	0.46	0.41	0.31	0.39	1.04	0.71	0.96	0.90
10	0.46	0.34	0.30	0.37	0.64	0.61	0.76	0.67
15	0.40	0.29	0.28	0.32	0.54	0.59	0.63	0.59
20	0.39	0.29	0.28	0.32	0.48	0.58	0.55	0.54
25	0.37	0.29	0.29	0.32	0.46	0.51	0.53	0.50
30	0.37	0.29	0.29	0.32	0.46	0.46	0.49	0.47
35	0.34	0.28	0.28	0.30	0.46	0.42	0.49	0.46
40	0.34	0.28	0.27	0.30	0.46	0.39	0.47	0.44
45	0.33	0.28	0.27	0.29	0.46	0.38	0.45	0.43
50	0.34	0.28	0.26	0.29	0.46	0.38	0.44	0.43
55	0.32	0.28	0.26	0.29	0.46	0.35	0.44	0.42
60	0.28	0.26	0.27	0.27	0.45	0.31	0.43	0.40

Table A-28: Permeate turbidity of the standard WFMF and OWFMF membranes in the filtration of degraded yeast suspension

Time (min)	Turbidity (NTU)							
	Standard WFMF				OWFMF			
	Run 1	Run 2	Run 3	Average	Run 1	Run 2	Run 3	Average
5	1.08	1.21	0.79	1.03	2.55	2.96	2.60	2.70
10	0.61	0.63	0.36	0.53	1.30	1.64	1.73	1.56
15	0.46	0.43	0.24	0.38	1.08	1.18	1.10	1.12
20	0.39	0.29	0.22	0.30	1.03	1.10	1.15	1.09
25	0.23	0.21	0.16	0.20	0.87	1.07	0.98	0.97
30	0.19	0.22	0.16	0.19	0.80	0.88	0.97	0.88
35	0.14	0.20	0.13	0.16	0.79	0.83	0.70	0.77
40	0.12	0.17	0.13	0.14	0.74	0.79	0.53	0.69
45	0.10	0.13	0.13	0.12	0.70	0.79	0.44	0.64
50	0.09	0.13	0.14	0.12	0.65	0.75	0.34	0.58
55	0.09	0.10	0.14	0.11	0.62	0.74	0.23	0.53
60	0.08	0.09	0.14	0.10	0.52	0.68	0.22	0.47

Table A-29: Results of the filtration process of fresh yeast suspension using standard WFMF membranes

Time (min)	Flux (LMH)			ΔP (kPa)			Resistance (m^{-1})			
	Run 1	Run 2	Run 3	Run 1	Run 2	Run 3	Run 1	Run 2	Run 3	Average
5	335.40	363.35	344.72	15	14	14	1.81E+11	1.56E+11	1.64E+11	1.67E+11
10	326.09	354.04	335.40	15	14	15	1.86E+11	1.60E+11	1.81E+11	1.76E+11
15	307.45	344.72	335.40	15	15	16	1.97E+11	1.76E+11	1.93E+11	1.89E+11
20	307.45	335.40	326.09	16	15	16	2.11E+11	1.81E+11	1.98E+11	1.97E+11
25	307.45	335.40	326.09	16	16	17	2.11E+11	1.93E+11	2.11E+11	2.05E+11
30	307.45	335.40	316.77	16	16	18	2.11E+11	1.93E+11	2.30E+11	2.11E+11
35	307.45	335.40	316.77	17	17	18	2.24E+11	2.05E+11	2.30E+11	2.20E+11
40	307.45	326.09	307.45	18	18	19	2.37E+11	2.23E+11	2.50E+11	2.37E+11
45	298.14	326.09	298.14	18	18	19	2.44E+11	2.23E+11	2.58E+11	2.42E+11
50	298.14	316.77	298.14	18	19	20	2.44E+11	2.43E+11	2.71E+11	2.53E+11
55	298.14	307.45	298.14	19	19	20	2.58E+11	2.50E+11	2.71E+11	2.60E+11
60	298.14	298.14	288.82	19	20	20	2.578E+11	2.71E+11	2.80E+11	2.70E+11

Table A-30: Results of the filtration process of fresh yeast suspension using OWFMF membranes

Time (min)	Flux (LMH)			ΔP (kPa)			Resistance (m^{-1})			
	Run 1	Run 2	Run 3	Run 1	Run 2	Run 3	Run 1	Run 2	Run 3	Average
5	335.40	335.40	372.67	14	15	14	1.69E+11	1.81E+11	1.52E+11	1.67E+11
10	335.40	335.40	372.67	15	15	15	1.81E+11	1.81E+11	1.63E+11	1.75E+11
15	326.09	335.40	372.67	15	15	15	1.86E+11	1.81E+11	1.63E+11	1.77E+11
20	316.77	326.09	363.35	16	15	15	2.04E+11	1.86E+11	1.67E+11	1.86E+11
25	298.14	326.09	363.35	16	15	16	2.17E+11	1.86E+11	1.78E+11	1.94E+11
30	298.14	326.09	363.35	16	15	16	2.17E+11	1.86E+11	1.78E+11	1.94E+11
35	298.14	316.77	354.04	16	16	17	2.17E+11	2.04E+11	1.94E+11	2.05E+11
40	298.14	316.77	344.72	16	17	18	2.17E+11	2.17E+11	2.11E+11	2.15E+11
45	298.14	316.77	344.72	18	17	19	2.44E+11	2.17E+11	2.23E+11	2.28E+11
50	298.14	307.45	335.40	18	18	19	2.44E+11	2.37E+11	2.29E+11	2.37E+11
55	288.82	307.45	335.40	19	18	19	2.66E+11	2.37E+11	2.29E+11	2.44E+11
60	279.50	298.14	335.40	19	19	20	2.75E+11	2.58E+11	2.41E+11	2.58E+11

Table A-31: Results of the filtration process of degraded yeast suspension using standard WFMF membranes

Time (min)	Flux (LMH)			ΔP (kPa)			Resistance (m^{-1})			
	Run 1	Run 2	Run 3	Run 1	Run 2	Run 3	Run 1	Run 2	Run 3	Average
5	298.14	335.40	316.77	22	22	24	2.98E+11	2.65E+11	3.06E+11	2.90E+11
10	260.87	298.14	260.87	24	25	25	3.72E+11	3.39E+11	3.88E+11	3.66E+11
15	251.55	270.19	251.55	25	26	27	4.02E+11	3.89E+11	4.34E+11	4.08E+11
20	242.24	260.87	232.92	25	28	28	4.17E+11	4.34E+11	4.86E+11	4.46E+11
25	223.60	260.87	223.60	27	28	28	4.88E+11	4.34E+11	5.07E+11	4.76E+11
30	223.60	251.55	214.29	27	28	29	4.88E+11	4.50E+11	5.47E+11	4.95E+11
35	214.29	242.24	204.97	28	29	29	5.29E+11	4.84E+11	5.72E+11	5.28E+11
40	214.29	232.92	186.34	28	29	29	5.29E+11	5.04E+11	6.30E+11	5.54E+11
45	204.97	223.60	186.34	28	30	30	5.53E+11	5.43E+11	6.51E+11	5.82E+11
50	195.65	214.29	186.34	28	30	30	5.79E+11	5.66E+11	6.51E+11	5.99E+11
55	195.65	204.97	177.02	28	30	31	5.79E+11	5.92E+11	7.08E+11	6.26E+11
60	186.34	195.65	177.02	29	31	31	6.30E+11	6.41E+11	7.08E+11	6.60E+11

Table A-32: Results of the filtration process of degraded yeast suspension using OWFMF membranes

Time (min)	Flux (LMH)			ΔP (kPa)			Resistance (m^{-1})			
	Run 1	Run 2	Run 3	Run 1	Run 2	Run 3	Run 1	Run 2	Run 3	Average
5	354.04	335.40		20	18		2.29E+11	2.17E+11		2.23E+11
10	316.77	316.77		22	20		2.81E+11	2.55E+11		2.68E+11
15	288.82	288.82		23	22		3.22E+11	3.08E+11		3.15E+11
20	279.50	270.19		24	23		3.47E+11	3.44E+11		3.46E+11
25	260.87	260.87		24	24		3.72E+11	3.72E+11		3.72E+11
30	251.55	251.55		25	25		4.02E+11	4.02E+11		4.02E+11
35	242.24	242.24		26	25		4.34E+11	4.17E+11		4.26E+11
40	232.92	232.92		27	27		4.69E+11	4.69E+11		4.69E+11
45	223.60	223.60		28	27		5.07E+11	4.88E+11		4.97E+11
50	214.29	223.60		28	28		5.29E+11	5.07E+11		5.18E+11
55	214.29	214.29		28	28		5.29E+11	5.29E+11		5.29E+11
60	195.65	204.97		29	28		6.00E+11	5.53E+11		5.76E+11

Table A-33: Results of the evaluation of antifouling property and ease of cleaning of the standard WFMF membranes, average of 3 repeat runs

Time (min)	Resistance (m^{-1})				
	Cycle 1	Cycle 2	Cycle 3	Cycle 4	Cycle 5
5	1.67E+11	2.35E+11	2.85E+11	3.69E+11	4.99E+11
10	1.76E+11	2.48E+11	3.02E+11	4.06E+11	5.47E+11
15	1.89E+11	2.58E+11	3.18E+11	4.21E+11	5.68E+11
20	1.97E+11	2.70E+11	3.22E+11	4.33E+11	5.83E+11
25	2.05E+11	2.76E+11	3.44E+11	4.57E+11	6.18E+11
30	2.11E+11	2.81E+11	3.54E+11	4.68E+11	6.26E+11
35	2.20E+11	2.97E+11	3.61E+11	4.95E+11	6.57E+11
40	2.37E+11	3.04E+11	3.63E+11	5.01E+11	6.66E+11
45	2.42E+11	3.12E+11	3.80E+11	5.17E+11	6.90E+11
50	2.53E+11	3.25E+11	3.85E+11	5.17E+11	7.00E+11
55	2.60E+11	3.25E+11	3.85E+11	5.36E+11	7.00E+11
60	2.70E+11	3.37E+11	4.21E+11	5.50E+11	7.09E+11

Table A-34: Results of the evaluation of antifouling property and the ease of cleaning of the OWFMF membranes, average of 3 repeat runs

Time (min)	Resistance (m^{-1})				
	Cycle 1	Cycle 2	Cycle 3	Cycle 4	Cycle 5
5	1.67E+11	1.72E+11	2.03E+11	2.41E+11	2.75E+11
10	1.75E+11	1.85E+11	2.24E+11	2.63E+11	3.05E+11
15	1.77E+11	1.95E+11	2.39E+11	2.79E+11	3.26E+11
20	1.86E+11	2.03E+11	2.48E+11	2.95E+11	3.44E+11
25	1.94E+11	2.19E+11	2.62E+11	2.99E+11	3.57E+11
30	1.94E+11	2.34E+11	2.76E+11	3.16E+11	3.75E+11
35	2.05E+11	2.37E+11	2.79E+11	3.24E+11	3.91E+11
40	2.15E+11	2.55E+11	2.90E+11	3.36E+11	3.95E+11
45	2.28E+11	2.57E+11	3.02E+11	3.44E+11	4.04E+11
50	2.37E+11	2.76E+11	3.14E+11	3.53E+11	4.21E+11
55	2.44E+11	2.82E+11	3.19E+11	3.71E+11	4.26E+11
60	2.58E+11	2.93E+11	3.31E+11	3.77E+11	4.49E+11

Table A-35: Results of total and irreversible fouling resistance on both standard and oleophobic WFMF membranes at the end of each filtration cycle, average of 3 repeat runs

Cycles	Total fouling resistance (m^{-1})		Irreversible fouling resistance (m^{-1})	
	Standard WFMF	Oleophobic WFMF	Standard WFMF	Oleophobic WFMF
1	1.88E+11	1.89E+11	6.19E+10	2.132E+10
2	2.56E+11	2.25E+11	1.23E+11	3.203E+10
3	3.40E+11	2.62E+11	2.10E+11	6.483E+10
4	4.68E+11	3.08E+11	2.46E+11	8.21E+10
5	6.28E+11	3.81E+11	4.13E+11	1.627E+11

Table A-36: Results for the stability analysis of the oleophobic surface

No of cycles	Oil contact angle	Water contact angle	Change in oleophobicity (%)
0	121.73	139.06	
4	120.03	138.45	1.39
8	117.25	138.33	3.68
12	115.04	137.71	5.49
16	114.30	137.50	6.10

Appendix B.
Sample calculations

This section presents sample calculations for various calculations done throughout the different sections in this work.

B.1. Effective membrane area

In this study, a total number of 4 membrane modules were employed for every run. The effective dimensions of a single module were 7 cm by 11.5 cm. The effective surface area of a single module as well as that of an entire membrane pack was calculated as follows;

$$\boldsymbol{A_{s,eff} = 2\ sides \times L_{s,eff} \times W_{s,eff} = 2 \times 7\ cm \times 11.5\ cm \times \left(\frac{1\ m}{100\ cm}\right)^2 = 0.0161\ m^2}$$

$$\boldsymbol{A_{eff,total} = A_{s,eff} \times N_s = 0.0161 \times 4 = 0.0644\ m^2}$$

where $A_{s,eff}$ is the effective area of a single module (m^2), $L_{s,eff}$ is the effective length of the module (m), $W_{s,eff}$ is the effective width of the module (m), $A_{eff,total}$ is total effective area of the membrane pack (m^2), and N_s is the number of modules.

B.2. Flow rate

During the filtration experiments, the cylinder and stopwatch method was used to calculate the volumetric flowrate of the permeate. The volume of permeate collected and time taken to collect the permeate were used to calculate the volumetric flowrate of the permeate as shown below.

$$\boldsymbol{Q = \frac{v}{\Delta t} = \frac{500\ mL}{73\ s} \times \frac{3600\ s}{1\ h} \times \frac{1\ L}{1000\ mL} = 24.7\ L/h}$$

where Q is the volumetric flowrate (L/h), v is the volume of permeate collected, and Δt is the time taken to collect the permeate (h).

B.3. Flux

$$\boldsymbol{J = \frac{Q}{A_{eff,total}} = \frac{24.7}{0.0644} = 383.54\ L/m^2h}$$

where J is the flux (LMH), Q is the volumetric flowrate (L/h), and $A_{eff,total}$ is total effective area of the membrane pack (m^2)

B.4. Resistance

In this investigation, we had three type of resistances, namely: the intrinsic membrane resistance, total resistance, and irreversible fouling resistance. This section outlines how these resistances were calculated.

The intrinsic membrane resistance was characterized through the filtration of distilled, where the flux and ΔP (TMP) were measured. Using flux and ΔP, the membrane resistance was calculated as follows;

$$R_m = \frac{\Delta P}{\mu J_0} = \frac{10\ kPa}{390.91\ {}^{L}/_{m^2 h} \times 0.00089\ Pa.s}$$

$$= \frac{10\ \times 1000\ Pa}{390.91 \times 10^{-3}\ {}^{m^3}/_{m^2 h} \times 0.00089\ Pa.s \times \frac{1\ h}{3600\ s}} = 103.48 \times 10^9\ m^{-1}$$

where R_m is the intrinsic membrane resistance (m^{-1}), ΔP is the pressure drop across the membrane (Pa), μ is the viscosity (Pa.s) and J_0 is the pure water flux (L/m^2h or LMH).

The total resistance is also calculated using the same formula as that of the intrinsic membrane resistance. The only difference being that the feed being filtered is not pure water but is a feed that contains organics. Hence, the flux in this case is the permeate flux instead of pure water flux.

Lastly, the irreversible fouling resistance was calculated by subtracting the intrinsic membrane resistance from the resistance of the membrane that has been physically cleaned.

Appendix C.
Supplier's brochures

C.1. Fluorocarbon brochure

Rudolf GmbH
Altvaterstr. 58 - 64
82538 Geretsried / GERMANY

Telefon +49 81 71 / 53 - 0
Telefax +49 81 71 / 53 - 191
E-Mail pr@rudolf.de
Website www.rudolf.de

RUDOLF CHEMIE

®RUCO-GUARD AFR

COMPOSITION

Fluorocarbon resin, cationic

USES

For the water, oil and soil-repellent finishing of fabrics made from cellulosic fibres or their blends with synthetic fibres; confers excellent resistance to washing and dry cleaning.

PROPERTIES

- Confers resistance to aqueous and oily soilings
- Resistant to washing
- Resistant to dry cleaning
- Confers full handle
- Not suitable for optically brightened white goods
- No high curing temperatures necessary
- Usually highly compatible with many N-methylol compounds
- Compatible with additives
- Readily diluted with cold water
- Liquor preparation with soft water recommended
- Non-flammable
- Free of flammable solvents

TECHNICAL DATA

- Beige emulsion
- Specific gravity at 20°C ca. 1.03 g/cm³
- pH value ca. 2 - 5

APPLICATION

RUCO-GUARD AFR can be used alone or in combination with other finishing agents for the permanent water, oil and soil-repellent finishing of textile goods made from cellulosic fibres or blends with synthetics. Before adding **RUCO-GUARD AFR**, the pH of the liquor should be adjusted with 1 ml/l acetic acid (60 %).

In general, the shear resistance of finishing liquors with perfluorinated compounds is limited. There should therefore be as little liquor turbulence as possible.

Prolonged stirring of the liquor with high-speed impellers produces a creamy foam due to the shearing influence on the emulsion. Such breaking of emulsion components must be avoided. Accumulated foam on the surface of the liquor has to be removed.

The material to be finished has to be thoroughly pretreated and to be free of surface-active residues.

Permanent water and stain repellency

To achieve an excellent permanent stain-repellent finish against oily, fatty and aqueous soilings with a simultaneous water-repellent effect on CO or its blends with synthetic fibres, we recommend

20 - 40 g/l **RUCO-GUARD AFR**

wet pick-up 60 - 80 %
drying under usual conditions
curing 2 min at 140°C
1 min at 160°C

Select curing conditions which will ensure the article is fully cured, ready for further processing.

In case of low curing temperatures

Fluctuations of the curing temperature and time are largely offset by the high reactivity of **RUCO-GUARD AFR**. At the same time, the curing temperature and time can be reduced.

In the case of white goods or pastel shades, curing conditions of 150°C/2 min are sufficient. Higher temperatures may cause yellowing.

In case of penetration problems

In case of penetration problems, we recommend to add

10 - 20 g/l **RUCOWET FN**

to the finishing liquor to ensure a good and uniform liquor pick-up.
The wetting agent must be added before the other liquor components.

It is not recommended to use hydrophobic or softening agents on the basis of silicone in combination with this product, since the stain-repellent effect in particular against oily soilings is reduced.

The product can be combined with many resin finishing agents to obtain easy-care effects. In particular, we recommend the low-formaldehyde type **RUCON FAN**.

RUCO-GUARD AFR is compatible with many cationic and non-ionic finishing agents.

Their suitability has to be established in pretrials.

C.2. Padding mangle brochure

ROACHES

BVHP PADDER

MODEL BVHP

The BVHP model, which can work in either the vertical or horizontal position allowing a conventional liquor trough to be used, or the use of dams in the horizontal position

- Higher performance components allow a greater nip pressure.
- Available with a face width of 350mm or 500mm.
- Includes delivery and wind up rollers, liquour troughs and dam facility as standard.
- Hypalon covered rollers designed to give high loading force per linear cm.
- Digital indication of the nip pressure applied with 0.1 bar resolution for excellent repeatability.
- Spray wash for rapid clean down.
- Constructed from high grade stainless steel.

ROACHES

Key Specifications

Power Supply	110V or 230V, 50-60Hz, 1A, 150W
Speed Range (Adjustable)	1-5 m/min
Pressure Range	0.25 - 5.5 bar (3.5 - 80 psi)
Compressed Air Supply	0-5.5 bar (80 psi)
Cold Water Supply	3 bar (45 psi)
Number of Rollers/Bowls	2 (1 driven as standard)
Hypalon Rubber Hardness	70 ± 5 Shore (Others upon request)

Machine Dimensions

Model EVP 350	890mm (L) x 590mm (D) x 300mm (H)
Model EVP 500	1040mm (L) x 590mm (D) x 530mm (H)
Model EHP 350	890mm (L) x 590mm (D) x 500mm (H)
Model EHP 500	1040mm (L) x 590mm (D) 500mm (H)
Model BVHP 350	890mm (L) x 740mm (D) x 630mm (H)
Model BVHP 500	1040mm (L) x 770mm (D) x 680mm (H)

Optional Extras

- Floor Mounted Stainless Steel Frame
- Castors for ease of moveability
- Gear Wheels for positive drive of both rollers/bowls